

**Preparation, characterisation and application of
carbon black containing electrically conductive
inks for textile printing**

Muhammad Ali

Submitted in accordance with the requirements for the degree of Doctor of Philosophy
in Colour and Polymer Chemistry

**The University of Leeds
Department of Colour Science
School of Chemistry**

July 2013

The candidate confirms that the work submitted is her own, except where work which has formed part of jointly authored publications has been included. The contribution of the candidate and the other authors to this work has been explicitly indicated below. The candidate confirms that appropriate credit has been given within the thesis where reference has been made to the work of others.

The results of some of the letdown stability studies (Section 4.5) were presented in a conference as follows.

1. M. Ali and L. Lin. "Highly conductive inks for screen printing of textile". In *International Istanbul Textile Congress 2013*. 30th -31st May 2013, Istanbul, Turkey.

I was responsible for effectively 95 % of the total contribution in above. The contribution of the other author was 5 % of the work, this being limited to the correction of the draft paper and the provision of relevant advice.

This copy has been supplied on the understanding that it is copyright material and that no quotation from the thesis may be published without proper acknowledgment.

© 2013 The University of Leeds and Muhammad Ali.

The right of Muhammad Ali to be identified as Author of this work has been asserted by him in accordance with the Copyright, Designs and Patents Act 1988.

Acknowledgements

I would like to thank Prof. Long Lin for his valuable guidance, understanding, patience and most importantly his friendship through out my studies.

A special thanks to Mr David Cartridge of the Lubrizol Corporation for sharing his great experience and expertise in the field of printing inks technology.

I would also like to show my gratitude to Prof. Jim Guthrie for his useful tips and thorough feedback.

I am truly indebted to Mr Algy Kazlauciusas for the prompt help in conducting required analyses, carried out in the Colour Science Analytical laboratory and also for his cheerfulness and the motivation he provided time and again.

I gratefully acknowledge the funding received towards my PhD from NED University of Engineering and Technology, Karachi.

Finally, and most importantly, I would like to thank my parents Mr Muhammad Alam, Mrs Nuzhat Alam and my wife Mrs Saman Hina. The generation of this dissertation would not have been possible without their patience and the remarkable encouragement that they have given to me during the course of my studies.

Abstract

In comparison to weaving or other techniques that are employed to embed conductive tracks in textile fabric structure, the obvious advantages of printing the desired conductive pattern are the simplicity of the process and the suitability for low volume production runs as well as high volume production runs. However, the generally inferior durability and poorer electrical performance of conductive inks that have been printed onto a textile fabric give rise to challenges.

In this study, electrically conductive grades of carbon black pigment were used to formulate screen printing inks for use on textiles. On an equal weight basis, electrically conductive grades impart higher electrical conductivity compared to the printing ink grades of carbon black pigment. However, the conductive grades of carbon black are difficult to disperse and stabilise in aqueous media. Therefore in this study, a procedure was devised initially to prepare stable, waterborne dispersions of a number of highly conductive grades of carbon black pigment. The stability of pigment dispersions was characterised by conducting rheological, particle size and accelerated gravitational sedimentation analyses on appropriate formulations.

In order to formulate finished inks from the optimised, stable pigment dispersions, various binders were incorporated in the formulations followed by characterisation of the stability and the electrical properties of the finished inks. Films of the formulated inks were deposited onto various textile substrates. This was followed by testing of the washing and creasing performance of these ink films. It was found that the formulated inks performed considerably better than the tested commercial inks. It was shown that following the ink preparation procedure devised in this study, electrically conductive grades of carbon black pigment can be used to formulate textile printing inks which not only possess very high electrical conductivity but are also durable to withstand washing and creasing of textiles.

Table of Contents

Acknowledgements	iii
Abstract.....	iv
Table of Contents	v
List of Figures	x
List of Tables.....	xvii
List of symbols and abbreviations	xxi
Chapter 1. Introduction	1
1.1 Aims and objectives of the study	1
1.2 E-textiles	2
1.2.1 Applications of e-textiles.....	3
1.2.2 Requirements for e-textiles	4
1.2.3 E-textiles platform.....	5
1.2.4 Wearable e-textiles	6
1.3 Enabling technologies for highly conductive e-textiles.....	8
1.3.1 Techniques based on using conductive filaments or yarns	8
1.3.2 Techniques based on printing/coating conductive materials	15
1.3.3 Summary of the limitations of prior art.....	24
1.4 Performance criteria for printed conductive patterns	25
1.4.1 Electrical performance criteria	25
1.4.2 Durability performance criteria	26
1.4.2.1 Washing durability	26
1.4.2.2 Creasing durability	26
1.5 Printing of electronic devices	27
1.5.1 Flexographic printing of electronic devices	28
1.5.2 Gravure printing of electronic devices.....	28
1.5.3 Offset printing of electronic devices.....	30
1.5.4 Screen printing of electronic devices.....	31

1.5.5	Inkjet printing of electronic devices	32
1.6	Selection of the printing technique.....	33
1.7	Technology of printing inks	35
1.8	Ink preparation processes.....	39
1.9	Pigment dispersion in the ink formulation process	41
1.9.1	Carbon black pigments.....	43
1.9.1.1	Manufacture of carbon black pigments	44
1.9.1.2	The influence of the morphology on the properties of carbon black pigments.....	45
1.9.2	Physico-chemical aspects of pigment dispersion preparation.....	48
1.9.2.1	Pigment Wetting.....	49
1.9.2.2	Breaking down of pigment aggregates/agglomerates.....	51
1.9.2.3	Stabilisation of primary pigment particles	52
1.9.3	Pigment stabilisation mechanisms	52
1.9.3.1	Electrostatic stabilisation.....	54
1.9.3.2	Steric stabilisation	56
1.9.3.3	Other stabilisation mechanisms	57
1.9.4	Classification and selection of dispersing additives	58
1.10	Characterisation of the stability of dispersions.....	63
1.10.1	Sedimentation analysis.....	65
1.10.1.1	Characterisation of sedimentation.....	66
1.10.2	Rheological characterisation of pigment dispersions	68
1.10.3	Particle size analysis	71
1.10.4	Zeta potential studies	73
Chapter 2.	Experimental.....	75
2.1	Materials.....	75
2.1.1	Pigments.....	75
2.1.2	Dispersing additives	75

2.1.3	Binders	77
2.1.4	Defoamer	77
2.1.5	Commercial conductive inks	78
2.1.6	Substrates	78
2.1.6.1	Packaging paperboard.....	78
2.1.6.2	Textile substrates.....	79
2.2	Preparation and characterisation of pigment dispersions	80
2.2.1	Procedure of optimisation of pigment dispersions	80
2.2.2	Sinking test.....	84
2.2.3	Pre-mixing.....	85
2.2.4	Bead milling	85
2.2.4.1	Determination of optimum parameters of bead milling	87
2.2.5	Procedure to establish the repeatability of the pigment dispersion preparation process	88
2.2.6	Analysis and characterisation of pigment dispersions	89
2.3	Let-down of pigment dispersions.....	90
2.3.1	Let-down compatibility tests.....	90
2.3.2	Let-down procedure to formulate finished inks.....	92
2.3.3	Characterisation of finished inks	93
2.3.3.1	Let-down stability	93
2.3.3.2	Electrical characterisation of ink films	93
2.4	The printing and testing of inks.....	94
2.4.1	Preparation of primer coated textile substrates.....	95
2.4.2	Relationship between substrate surface characteristics and the performance of the inks deposits.....	96
2.4.3	Testing of printed textile substrates	96
2.4.3.1	Washing tests of printed textile substrates.....	97
2.4.3.2	Crease resistance testing of printed textile substrates	98

2.4.4	Screen printing of inks onto textile substrates	99
2.4.4.1	Setting up of the screen printer	100
2.4.4.2	Screen printing process parameters	101
2.4.5	Maximum electrical conductivity of ink deposits	102
Chapter 3.	Analytical techniques	103
3.1	Rheometric measurements	103
3.1.1	Test setup for viscosity measurements	105
3.2	Particle size analysis by DLS	106
3.2.1	Test setup for particle size analysis	108
3.3	Zeta potential measurements	109
3.3.1	Test setup for zeta potential measurement	110
3.4	Analytical centrifugation studies	110
3.4.1	Test setup for sedimentation analyses	111
3.5	Electrical conductivity measurements	111
3.6	Surface resistivity measurements	111
3.7	Thermogravimetric analysis (TGA) studies	112
3.7.1	TGA of binders	113
3.7.2	TGA of dispersants	113
3.7.3	TGA of pigment dispersions	114
3.7.4	TGA of commercial ink samples	114
3.8	Scanning Electron Microscopy of textile fabrics	114
3.9	Optical Microscopy	115
Chapter 4.	Results and Discussion	118
4.1	Preparation and optimisation of pigment dispersions	118
4.1.1	Optimisation of Carbon1 (Vulcan XC605) pigment dispersion	118
4.1.2	Optimisation of Carbon2 (Ensaco 250G) pigment dispersion	128
4.1.3	Optimisation of Carbon3 (Ensaco 350G) pigment dispersion	136
4.1.4	Optimisation of the Carbon4 (Printex XE2B) pigment dispersion	145

4.2	Shelf life/Stability of dispersions	153
4.3	Optimisation of the bead milling process.....	158
4.4	Reliability and repeatability of the dispersion preparation process.....	163
4.5	Preparation and characterisation of finished inks.....	177
4.5.1	Selection of pigment dispersions for the let-down stage.....	178
4.5.2	Binder-Dispersant compatibility tests.....	181
4.5.3	Let-down stability of pigment dispersions.....	182
4.5.3.1	Viscosity stability of the inks prepared from the dispersions of Carbon1.	184
4.5.3.2	Viscosity stability of the inks prepared from the dispersions of Carbon2.	189
4.5.3.3	Viscosity stability of the inks prepared from the dispersions of Carbon3.	194
4.5.3.4	Viscosity stability of the inks prepared from the dispersions of Carbon4.	195
4.5.4	Electrical characteristics of finished inks	203
4.6	Printing of formulated inks on textile substrates and subsequent testing.....	208
4.6.1	Selection of binders for the primer coating of textile substrates	208
4.6.2	Electrical characteristics of ink films deposited on textile substrates.....	218
4.6.3	Performance testing of ink films	234
4.6.4	Screen printability of formulated inks	241
4.6.5	Maximum conductivity of formulated inks	243
Chapter 5.	Conclusions.....	245
Chapter 6.	Suggestions for future work	249
Appendices	250
References	253

List of Figures

Figure 1-1: General system configuration for e-textiles.....	6
Figure 1-2: Evolution of Steve Mann’s “wearable computer” invented in 1970s.	7
Figure 1-3: Woven fabric consisting of polyester yarns that are twisted with an insulated copper filament.	8
Figure 1-4: Steps involved in the fabrication of interconnections, (a) woven fabric with orthogonal conductive wires, (b) disconnects made by laser ablation, (c) interconnects formed using conductive adhesive and (d) encapsulation of interconnects.	10
Figure 1-5: The speech-controlled MP3-player demonstrator system designed into a sports jacket.	12
Figure 1-6: Interconnections via conductive ribbons.	13
Figure 1-7: ElexTex touchpads for garments.....	13
Figure 1-8: E-broidery for circuit manufacturing.	14
Figure 1-9: Conductive fabric structure showing the substrate (D), primer layer (C), conductive layer (A) and the insulating layer (B).	16
Figure 1-10: Printed coplanar waveguide lines on Tyvek ® (a) before washing, (b) after washing.	18
Figure 1-11: Laminated printed lines on Evolon 100 GSM; (a) before washing, (b) after washing.	19
Figure 1-12: Gap between printed transmission lines (a) 1 print pass and (b) 10 print passes.....	19
Figure 1-13: Cracking of ink layer after creasing cycles.	20
Figure 1-14: Micrograph of a flexographic printed impression.	28
Figure 1-15: Micrograph of gravure printed ink, showing the “serrated teeth structure” at the edges.	29
Figure 1-16: Capabilities of different printing processes (© Motorola’s Printed Electronics Technology Team).	34
Figure 1-17: An overview of ink production process.....	40
Figure 1-18: Sequence of the development of carbon black structure (© International Carbon Black Association).....	44
Figure 1-19: Structural features of carbon black pigment (© Mitsubishi Chemical Corporation).	46

Figure 1-20: Steps in pigment dispersion preparation.....	48
Figure 1-21: Interfacial energies at solid-liquid-air interface	50
Figure 1-22: Interaction potential between particles as a function of particle separation.	53
Figure 1-23: Mechanism of electrostatic stabilisation	54
Figure 1-24: Mechanism of steric stabilisation	57
Figure 1-25: Classification of dispersants.	59
Figure 1-26: Amphiphilic molecule of a dispersing additive.....	59
Figure 1-27: Adsorption of various types of high molecular weight copolymeric dispersants onto pigment surface - diagrammatic representation.....	60
Figure 1-28: Dispersant selection criteria based on the nature of dispersion medium. .	61
Figure 1-29: Adsorption of anionic dispersant molecules onto the pigment surface.....	62
Figure 1-30: Adsorption of cationic dispersant molecules onto the pigment surface in (a) olephilic medium and (b) aqueous medium.	62
Figure 1-31: Adsorption of non-ionic dispersant molecules onto the pigment surface. .	63
Figure 1-32: Effect of presence of particles on the viscosity of carrier medium.....	69
Figure 1-33: A charged particle dispersed in a fluid medium.	74
Figure 2-1: Scanning electron micrograph of Incada Exel paperboard, (magnification x8000).....	79
Figure 2-2: Scanning electron micrographs of (a) 100% cotton and (b) 100% polyester woven fabrics.....	80
Figure 2-3: Procedure of preparation of pigment dispersions.....	83
Figure 2-4: Dissolver-type stirrer for the high shear mixing of pigment dispersions.	85
Figure 2-5: Schematic of Mini 50 bead mill (Source: Eiger Torrance Limited).....	86
Figure 2-6: Schematic of bead mill and overhead stirrer arrangement for milling of high viscosity dispersions.....	87
Figure 2-7: Design of experiments for the let-down of pigment dispersions.	92
Figure 2-8: Rokuprint SD 05 screen printer	100
Figure 2-9: Vacuum plate with open nozzles only in the area covered by the substrate.	101
Figure 2-10: Arrangement to measure and adjust the squeegee angle. (a) Reference scale fitted coaxially with the squeegee holder, and (b) squeegee holder and scale mounted on the machine.	101
Figure 2-11: Stencil design (scaled down).	102

Figure 3-1: Schematic illustration of cone-plate viscometer geometry.....	103
Figure 3-2: Light scattering by large particles (top) and by smaller particles (bottom).	106
Figure 3-3: Correlation as a function of time.....	107
Figure 3-4: Correlation function for large and small particles.....	107
Figure 3-5: Working principle of LUMiSizer ® Dispersion Analyser (© LUM GmbH).	110
Figure 3-6: Surface resistivity measurement setup.	112
Figure 3-7: Thermograms of the binders used in the study.	114
Figure 3-8: Composite image of a printed textile fabric showing regions of different heights in-focus.	116
Figure 3-9: Optical micrographs recorded in normal mode. (a) Only the ink surface (higher planes) is in-focus and (b) fabric (lower plane) is in-focus.....	116
Figure 3-10: Extent of ink layer cracking observed under (a) normal illumination and (b) combined normal and transmission mode.	117
Figure 4-1: Flow chart of the various steps in this study.....	118
Figure 4-2: Dispersant media observed against an array of LEDs, 72 hours after the addition of Carbon1.....	119
Figure 4-3: Viscosity profiles of control dispersions of Carbon1 pigment.....	120
Figure 4-4: Viscosity profiles of control dispersion, 22 wt% and 26 wt% Carbon1 dispersions.	121
Figure 4-5: Viscosity profiles of dispersions of Carbon1 prepared in Step 3 of optimisation.....	122
Figure 4-6: Viscosity stability of dispersions of Carbon1 prepared using (a) 9%, (b) 12%, (c) 15% and (d) 18% DOWP of Dispersant3.	123
Figure 4-7: Viscosity profiles of dispersions containing 31 wt% Carbon1 and 15% DOWP of the various dispersants.	125
Figure 4-8: Stability of the viscosity of dispersions containing 31 wt% Carbon1 and 15% DOWP of (a) Dispersant1, (b) Dispersant2 and (c) Dispersant3.	126
Figure 4-9: Dispersant solutions after 72 hours of addition of Carbon2.	128
Figure 4-10: Viscosity profiles of dispersions of Carbon2 prepared in Step 2.....	129
Figure 4-11: Viscosity profiles (after milling) of the dispersions containing 28 wt% Carbon2 and various amounts of Dispersant1.	130

Figure 4-12: Stability of the viscosity profiles of dispersions of Carbon2 prepared using (a) 12.5%, (b) 15%, (c) 17.5% and (d) 20% DOWP of Dispersant1.	131
Figure 4-13: Viscosity profiles of dispersions containing 23 wt% Carbon2 and 17.5% DOWP of various dispersants.	134
Figure 4-14: Viscosity profiles of dispersions containing 23 wt% Carbon2 and 17.5% DOWP of (a) Dispersant1, (b) Dispersant2 and (c) Dispersant3.	134
Figure 4-15: Dispersant solutions after 72 hours of addition of Carbon3.	136
Figure 4-16: Viscosity profiles of dispersions of Carbon3 prepared in Step 2.	137
Figure 4-17: Viscosity profiles of dispersions of Carbon3, prepared in Step 3 of the optimisation process.	138
Figure 4-18: Viscosity stability analysis of the dispersions containing 9.25 wt% Carbon3 and (a) 140%, (b) 155%, (c) 170% and (d) 200% DOWP of Dispersant3.	140
Figure 4-19: Viscosity profiles of dispersions of Carbon3 prepared in Step 4.	142
Figure 4-20: Viscosity stability of the dispersions of Carbon3 prepared using 155 %DOWP of (a) Dispersant1, (b) Dispersant2 and (c) Dispersant3.	143
Figure 4-21: Dispersant solutions observed after 72 hours of addition of Carbon4.	145
Figure 4-22: Viscosity profiles of dispersions of Carbon4 prepared in Step 2.	146
Figure 4-23: Viscosity profiles of dispersions containing 9.25 wt% Carbon4 and various amounts of Dispersant1.	147
Figure 4-24: Viscosity stability of dispersions of Carbon4 prepared using (a) 175%, (b) 200% and (c) 225% DOWP of Dispersant1.	148
Figure 4-25: Viscosity profiles of dispersions of Carbon4 pigment prepared in Step 4.	150
Figure 4-26: Viscosity profiles of optimised dispersions of Carbon4 pigment prepared using (a) Dispersant1, (b) Dispersant2 and (c) Dispersant3.	151
Figure 4-27: Transmission profiles recorded during centrifugation of Carbon1 dispersions prepared using (a) Dispersant1, (b) Dispersant2 and (c) Dispersant3.	155
Figure 4-28: Transmission profiles recorded during centrifugation of Carbon2 dispersions prepared using (a) Dispersant1, (b) Dispersant2 and (c) Dispersant3.	156
Figure 4-29: Transmission profiles recorded during centrifugation of Carbon3 dispersions prepared using (a) Dispersant1, (b) Dispersant2 and (c) Dispersant3.	157
Figure 4-30: Milling viscosity of dispersions of Carbon1 prepared using (a) Dispersant1, (b) Dispersant2 and (c) Dispersant3.	159

Figure 4-31: Milling viscosity of dispersions of Carbon2 prepared using (a) Dispersant1, (b) Dispersant2 and (c) Dispersant3	160
Figure 4-32: Milling viscosity of dispersions of Carbon3 prepared using (a) Dispersant1, (b) Dispersant2 and (c) Dispersant3.	161
Figure 4-33: Milling viscosity of dispersions of Carbon4 prepared using (a) Dispersant1, (b) Dispersant2 and (c) Dispersant3.	162
Figure 4-34: TGA thermograms of Dispersants (as-supplied form).	164
Figure 4-35: Viscosity profiles of different batches of Carbon1 dispersions prepared using (a) Dispersant1, (b) Dispersant2 and (c) Dispersant3.....	168
Figure 4-36: TGA thermograms of different batches of dispersions of Carbon1 prepared using (a) Dispersant1, (b) Dispersant2 and (c) Dispersant3.....	169
Figure 4-37: Viscosity profiles of different batches of Carbon2 dispersions prepared using (a) Dispersant1, (b) Dispersant2 and (c) Dispersant3.....	170
Figure 4-38: TGA thermograms of different batches of dispersions of Carbon2 prepared using (a) Dispersant1, (b) Dispersant2 and (c) Dispersant3.....	171
Figure 4-39: Viscosity profiles of different batches of Carbon3 dispersions prepared using (a) Dispersant1, (b) Dispersant2 and (c) Dispersant3.....	172
Figure 4-40: TGA thermograms of different batches of dispersions of Carbon3 prepared using (a) Dispersant1, (b) Dispersant2 and (c) Dispersant3.....	173
Figure 4-41: Viscosity profiles of different batches of Carbon4 dispersions prepared using (a) Dispersant1, (b) Dispersant2 and (c) Dispersant3.....	175
Figure 4-42: TGA thermograms of different batches of dispersions of Carbon4 prepared using (a) Dispersant1, (b) Dispersant2 and (c) Dispersant3.....	176
Figure 4-43: Glass slides deposited with various binder-dispersant mixtures.	181
Figure 4-44: Change in viscosity during four weeks storage of the homogenised batch of the optimised dispersions of Carbon1 pigment.	185
Figure 4-45: Viscosity stability of inks prepared by adding various amounts of Binder1/Binder2/Binder3 in Carbon1-Dispersant1 dispersion.....	186
Figure 4-46: Viscosity stability of inks prepared by adding various amounts of Binder1/Binder2/Binder3 in Carbon1-Dispersant2 dispersion.....	187
Figure 4-47: Viscosity stability of inks prepared by adding various amounts of Binder1/Binder2/Binder3 in Carbon1-Dispersant3 dispersion.....	188
Figure 4-48: Change in viscosity during four weeks storage of the homogenised batch of the optimised dispersions of Carbon2 pigment.	190

Figure 4-49: Viscosity stability of inks prepared by adding various amounts of Binder1/Binder2/Binder3 in Carbon2-Dispersant1 dispersion.....	191
Figure 4-50: Viscosity stability of inks prepared by adding various amounts of Binder1/Binder2/Binder3 in Carbon2-Dispersant2 dispersion.....	192
Figure 4-51: Viscosity stability of inks prepared by adding various amounts of Binder1/Binder2/Binder3 in Carbon2-Dispersant3 dispersion.....	193
Figure 4-52: Change in viscosity during four weeks storage of the homogenised batch of the optimised dispersions of Carbon3 pigment.	195
Figure 4-53: Change in viscosity during four weeks storage of the homogenised batch of the optimised dispersions of Carbon4 pigment.	196
Figure 4-54: Viscosity stability of inks prepared by adding various amounts of Binder1/Binder2/Binder3 in Carbon3-Dispersant1 dispersion.....	197
Figure 4-55: Viscosity stability of inks prepared by adding various amounts of Binder1/Binder2/Binder3 in Carbon3-Dispersant2 dispersion.....	198
Figure 4-56: Viscosity stability of inks prepared by adding various amounts of Binder1/Binder2/Binder3 in Carbon3-Dispersant3 dispersion.....	199
Figure 4-57: Viscosity stability of inks prepared by adding various amounts of Binder1/Binder2/Binder3 in Carbon4-Dispersant1 dispersion.....	200
Figure 4-58: Viscosity stability of inks prepared by adding various amounts of Binder1/Binder2/Binder3 in Carbon4-Dispersant2 dispersion.....	201
Figure 4-59: Viscosity stability of inks prepared by adding various amounts of Binder1/Binder2/Binder3 in Carbon4-Dispersant3 dispersion.....	202
Figure 4-60: Micrographs of 100% polyester fabric padded with Binder1 at various padder pressure settings.	212
Figure 4-61: Micrographs of 100% cotton fabric padded with Binder1 at various padder pressure settings.....	213
Figure 4-62: Micrographs of 100% polyester fabric padded with Binder2 at various padder pressure settings.	214
Figure 4-63: Micrographs of 100% cotton fabric padded with Binder2 at various padder pressure settings.....	215
Figure 4-64: Micrographs of 100% polyester fabric padded with Binder3 at various padding pressure settings.....	216
Figure 4-65: Micrographs of 100% cotton fabric padded with Binder3 at various padding pressure settings.....	217

Figure 4-66: Optical microscope images (Magnification x 300) of drawdowns of inks prepared from Carbon1-Dispersant1 dispersion.....	222
Figure 4-67: Optical microscope images (Magnification x 300) of drawdowns of inks prepared from Carbon1-Dispersant2 dispersion.....	223
Figure 4-68: Optical microscope images (Magnification x 300) of drawdowns of inks prepared from Carbon1-Dispersant3 dispersion.....	224
Figure 4-69: Optical microscope images (Magnification x 300) of drawdowns of inks prepared from Carbon2-Dispersant1 dispersion.....	225
Figure 4-70: Optical microscope images (Magnification x 300) of drawdowns of inks prepared from Carbon2-Dispersant2 dispersion.....	226
Figure 4-71: Optical microscope images (Magnification x 300) of drawdowns of inks prepared from Carbon2-Dispersant3 dispersion.....	227
Figure 4-72: Optical microscope images (Magnification x 300) of drawdowns of inks prepared from Carbon3-Dispersant1 dispersion.....	228
Figure 4-73: Optical microscope images (Magnification x 300) of drawdowns of inks prepared from Carbon3-Dispersant2 dispersion.....	229
Figure 4-74: Optical microscope images (Magnification x 300) of drawdowns of inks prepared from Carbon3-Dispersant3 dispersion.....	230
Figure 4-75: Optical microscope images (Magnification x 300) of drawdowns of inks prepared from Carbon4-Dispersant1 dispersion.....	231
Figure 4-76: Optical microscope images (Magnification x 300) of drawdowns of inks prepared from Carbon4-Dispersant2 dispersion.....	232
Figure 4-77: Optical microscope images (Magnification x 300) of drawdowns of inks prepared from Carbon4-Dispersant3 dispersion.....	233
Figure 4-78: Images of commercial inks printed onto fabrics followed by washing.....	239
Figure 4-79: Optical micrograph (Magnification x100) of the stencil used to print 1 mm wide line on fabric substrate.	241
Figure 4-80: Images of Binder3-containing inks screen printed onto Binder3-coated polyester fabric.	242

List of Tables

Table 1-1: Comparison of properties of typical electronics and textiles.....	5
Table 1-2: Electrical resistance of test samples after washing cycles.	17
Table 1-3: Tests not considered relevant in the present study.....	27
Table 1-4: Characteristics of printing processes (Huebler et al. 2002).	34
Table 1-5: Tests employed for dispersion characterisation	64
Table 2-1: Specifications of carbon black pigments (as provided by the suppliers).....	75
Table 2-2: Dispersants used and their characteristics (as provided by the suppliers). ...	76
Table 2-3: Binders used in the study.	77
Table 2-4: Commercial conductive inks used in the study.	78
Table 2-5: Specifications of paperboard substrate (as provided by the manufacturer). ..	79
Table 2-6: Specifications (provided by supplier) of textile substrates used in the study.	80
Table 2-7: Pigment-dispersant combinations prepared and tested in the study.....	81
Table 2-8: Composition of dispersant solutions prepared for sinking tests.	84
Table 2-9: Specific gravities of the dispersant solutions at 25 °C.....	84
Table 2-10: Analyses carried out on pigment dispersions.....	89
Table 2-11: Loading of dispersants in dispersions and loading of binders in finished inks.	91
Table 2-12: Binder-dispersant combinations tested for compatibility	91
Table 2-13: Conditions for Test number C1S of BS EN ISO 105-C06:1997.	98
Table 2-14: Specifications of Rokuprint screen printer	100
Table 3-1: Parameters for TGA.....	113
Table 4-1: Composition of control dispersions of Carbon1 pigment.....	119
Table 4-2: Composition of the 22 wt% and the 26 wt% Carbon1 dispersions.	120
Table 4-3: Compositions of dispersions containing 22 wt% Carbon1 and various amounts of Dispersant3.	121
Table 4-4: Electrical conductivity and surface resistivity of dispersions of Carbon1 prepared in Step 3.	122
Table 4-5: Results of zeta potential and particle size analyses carried out during storage of the dispersions of Carbon1 prepared in Step 3.	124

Table 4-6: Composition of dispersions containing 31 wt% Carbon1 and 15% DOWP of various dispersants.	125
Table 4-7: Zeta potential and particle size analysis results of dispersions containing 31 wt% Carbon1 and 15% DOWP of various dispersants.	127
Table 4-8: Surface resistivity of K-bar 3 drawdowns of the optimised dispersions of Carbon1 pigment.	128
Table 4-9: Composition of dispersions containing 12.5% DOWP of Dispersant1 and various amounts of Carbon2.	129
Table 4-10: Composition of dispersions containing 28 wt% Carbon2 and various amounts of Dispersant1.	130
Table 4-11: Results of zeta potential and particle size analysis of dispersions of Carbon2 prepared using various dosages of Dispersant1.	132
Table 4-12: Surface resistivity of the drawdowns of dispersions of Carbon2 prepared using various amounts of Dispersant1.	133
Table 4-13: Composition of dispersions of Carbon2 prepared in Step 4.	133
Table 4-14: Average increase in the viscosity of optimised dispersions of Carbon2.	135
Table 4-15: Results of particle size analyses of the dispersions of Carbon2 prepared in Step 4 of optimisation process.	135
Table 4-16: Electrical characteristics of the optimised dispersions of Carbon2.	136
Table 4-17: Composition of dispersions of Carbon3 prepared in Step 2.	137
Table 4-18: Composition of dispersions containing 9.25 wt% Carbon3 and various amounts of Dispersant3.	138
Table 4-19: Results of zeta potential and particle size analysis of the dispersions of Carbon3 prepared using various dosages of Dispersant3.	139
Table 4-20: Electrical characteristics of dispersions of Carbon3 prepared using various dosages of Dispersant3.	139
Table 4-21: Results of particle size analyses of the dispersions containing 9.25 wt% Carbon3 and various amounts of Dispersant3.	141
Table 4-22: Average increase in viscosity of Carbon3 dispersions prepared in Step 3.	144
Table 4-23: Results of particle size analyses carried out on the optimised dispersions of Carbon3.	144
Table 4-24: Electrical characteristics of the optimised dispersions of Carbon3.	145
Table 4-25: Composition of dispersions of Carbon4 prepared in Step 2.	146

Table 4-26: Composition of Carbon4 pigment dispersions prepared in Step 3 of the dispersion optimisation process.	147
Table 4-27: Results of zeta potential and particle size analyses of the dispersions of Carbon4 prepared in Step 3.	149
Table 4-28: Formulations of the dispersions prepared in Step 4 of optimisation of Carbon4 pigment dispersions.	150
Table 4-29: Particle size analysis results of the dispersions of Carbon4 pigment prepared using various dispersants.	152
Table 4-30: Electrical characteristics of optimised dispersions of Carbon4 pigment. ...	153
Table 4-31: Solids contents of dispersants at various temperatures in TGA.	165
Table 4-32: Pigment loading as obtained from the formulation calculations and TGA of the bead milled dispersions.	165
Table 4-33: Electrical conductivity of as-supplied dispersants.	179
Table 4-34: Pigment loading and electrical characteristics of the dispersions used in the let-down stage.	180
Table 4-35: Average increase in the viscosity of Carbon1-Dispersant2-Binder2 and Carbon1-Dispersant3-Binder2 inks.	189
Table 4-36: Change in viscosity of Carbon3 pigment dispersions prepared using Dispersant2/Dispersant3.	194
Table 4-37: Surface resistivity of the films of inks produced from Carbon1 pigment dispersions.	205
Table 4-38: Surface resistivity of the films of inks produced from Carbon2 pigment dispersions.	206
Table 4-39: Surface resistivity of the films of inks produced from Carbon3 pigment dispersions.	207
Table 4-40: Surface resistivity of the films of inks produced from Carbon4 pigment dispersions.	208
Table 4-41: Wet pick up of fabrics at different padding pressures.	210
Table 4-42: Surface resistivity data of the films of inks prepared from the dispersions of low surface area carbon black pigments.	220
Table 4-43: Surface resistivity data of the films of inks prepared from the dispersions of high surface area carbon black pigments.	221
Table 4-44: Change in surface resistivity after washing of Carbon1-/Carbon2-containing ink films deposited onto cotton fabric.	235

Table 4-45: Change in surface resistivity after washing of Carbon3-/Carbon4-containing ink films deposited onto cotton fabric.....	236
Table 4-46: Change in surface resistivity after washing of Carbon1-/Carbon2-containing ink films.	237
Table 4-47: Change in surface resistivity after washing of Carbon3-/Carbon4-containing ink films.	237
Table 4-48: Washing tests results of commercial inks.....	238
Table 4-49: Surface resistivity of inks recorded during crease testing of ink films.	240
Table 4-50: Minimum surface resistivity achieved on Binder3-coated polyester fabric	244
Table 5-1: Final pigment loading and surface resistivity of two layers of inks drawn on coated polyester fabric.....	248

List of symbols and abbreviations

γ_{SV}	-	Interfacial tension between solid and vapour (air)
γ_{SL}	-	Interfacial tension between solid and liquid
γ_{LV}	-	Interfacial tension between liquid and vapour (air)
ζ	-	Zeta potential
Ω/\square	-	Ohms per square area
I_o	-	Intensity of incident light
I_t	-	Intensity of transmitted light
AATCC	-	American Association of Textile Chemists and Colorists
BET	-	Brunauer-Emmet-Teller (surface area determination method)
BOWP	-	Amount of binder on the weight of pigment
DOWP	-	Amount of dispersant on the weight of pigment
DLS	-	Dynamic light scattering
DSC	-	Differential scanning calorimetry
GSM	-	Grams per square meter
LPI	-	Lines per inch
OAN	-	Oil absorption number
OLED	-	Organic light emitting diode
OTFT	-	Organic thin film transistor
RPM	-	Revolutions per minute
SEM	-	Scanning electronic microscopy
SLS	-	Static light scattering
TFT	-	Thin film transistor
TGA	-	Thermogravimetric analysis

Chapter 1. Introduction

1.1 Aims and objectives of the study

The focus of this study was the development of circuitry, which is a common component of any simple or complex e-textile system. One of the more widely reported methods of fabrication of electronic circuitry in textile fabrics is through the use of conductive filaments or threads in the fabric structure. All such methods suffer one or more of the drawbacks that follow.

- High raw material and manufacturing costs
- Lengthy and complicated manufacturing process
- Unsuitability for low or specialised production runs

In contrast to the above mentioned methods, printing is a simple one step process for producing a pattern of almost any level of design complexity. Printing of electronic circuits on textile articles require highly conductive inks that must withstand washing and wearing of textiles throughout the product life cycle. The application of electrically conductive inks by printing is a well-developed technology in the conventional printed electronics industry. However, such inks generally do not possess a very high level of durability to withstand repetitive washing and/or mechanical stress cycles. This is because commercially available conductive inks generally possess poor adhesion to textile substrates and form a brittle ink layer, which fails to withstand multiple washing and creasing cycles. Thus, this study aimed to cover the following aspects of preparation and application of conductive inks on textile substrates:

- Selection of primary conductive filler material
- Selection of printing technique
- A thorough investigation of conductive ink preparation and optimisation process
- Application of formulated inks and performance testing

In this study, it was aimed to formulate, apply and test highly conductive inks for screen printing of textiles. Electrically conductive grades of carbon black pigment were

used as conductive fillers in printing inks while high molecular weight non-ionic dispersants were employed to disperse and stabilise these pigments.

One of aims was to maximise the pigment loading in the binder-free pigment dispersions. This was considered to be crucial to maximise the electrical conductivity of the finished inks. Thus, a two step process was adopted to prepare the inks. In the first step, the formulations of binder-free waterborne dispersions of the pigments were optimised. The pigment dispersions were formulated into finished inks in the next step.

It was aimed to thoroughly characterise the binder-free pigment dispersions and the finished inks. To achieve this objective rheological characterisation, particle size analysis, sedimentation analysis, and electrical characterisation were employed for the characterisation of pigment dispersions and subsequently the finished inks.

1.2 E-textiles

Textiles are in many parts of our day-to-day lives, ranging from micro-engineered textiles such as nanofabrics possessing super hydrophobicity, to large-scale textiles such as geo-textiles. Recent innovations in materials science and engineering have significantly broadened the scope for the uses of textiles. These developments have changed our understanding of textiles, from being passive and simply serving their design purposes of being beautiful and warm, etc., to becoming active or interactive (Karaguzel et al. 2009). The focus of this research is to generate textiles having electronic functionality i.e. electronic textiles or simply e-textiles. The technology of e-textiles creation can be regarded as an intersection between the two seemingly different fields of electronics and textiles. This combination has had limited success to date, as it has not proven easy to combine even the simplest of electronic devices with textiles. However, progress in the fields of electronics and materials science has facilitated rapid developments in integration of textiles and electronics. E-textiles promise the seamless integration of computing elements, sensors, and actuators into familiar forms of textiles such as shirts, hats, parachutes, and blankets, etc. Novel materials and fabrication techniques can be applied to realise both active and passive electronic components onto a conventional textile material (Mattana et al. 2011). There are several

stringent requirements that must be met in order to achieve true integration of electronics and textiles; these requirements are discussed in detail in Section 1.2.2.

There exist several different terms such as 'Wearable electronics', 'Smart fabrics', 'Interactive textiles', 'Functional garments', 'Conductive embroidery' and so on, that are used to represent the technology of integrating electronics and textiles (Andonovska 2009). It must be appreciated that none of these terms encompasses all of the potential applications of this technology.

1.2.1 Applications of e-textiles

The following list provides an overview of application areas for e-textiles in a broader sense and gives examples for envisioned use situations (Stylios 2004), (Stylios 2006). The list is a summary of applications as frequently reported in literature and its comprehensiveness is not claimed.

- **Health monitoring:** Wearable medical monitoring suits, ECG t-shirt, home care and rehabilitation, remote telemedicine, remote monitoring of patients, vital signs monitoring blankets in hospitals.
- **Sport and outdoor:** Wearable monitoring for body functions (respiration rate, breathing frequency, body temperature, ECG shirt), mobile communication ski glove, GPS outdoor jacket, smart jogging shoes, kinaesthetic monitoring for athlete training.
- **Well-being & fun:** Active heating and cooling cloths, wearable gaming console, constant monitoring of vital signs for elderly persons.
- **Fashion & Lifestyle:** Mobile entertainment (MP3 jacket), touch-sensitive shirt, lighting and actuated decoration elements on cloths.
- **Every day life:** Solar cell powered bags, garments and textile switches, etc.
- **Computer-assisted work:** Work flow assistance and surveillance, hands-free human-computer interaction (e.g. wearable motion-capture or speech-controlled systems), location awareness, mobile information exchange.
- **Protective & safety textiles:** Fire fighter cloths, space suits, smart surgery suits.
- **Automotive and aviation industry:** Car upholstery (heated seats, car interior), textile aircraft structures (defect detection).

- **Furniture and interior textiles:** Curtains, wall hangings, carpets, pillows, decoration elements, and carpet embedded guidance systems in buildings.
- **Technical textiles & civil engineering:** Mechanical stress monitoring in technical textiles (buildings), defect detection in textile concrete constructions.
- **Promotion and event industry:** Large size display (luminescent curtains), colour changing textiles.

1.2.2 Requirements for e-textiles

Traditional silicon-based electronic materials do not have much in common with textile materials. Both classes of products are composed of different materials and built in different ways, to serve completely different purposes. Most obviously, electronic products are usually hard and stiff while textiles are normally soft and flexible. Moreover, the texture of electronic devices is usually highly ordered and not meant to change shape during a use phase. In contrast, textiles are foldable, stretchable, compressible, etc. Table 1-1 compares traditional properties of both technologies (Kirstein et al. 2002).

The creation of e-textiles requires the amalgamation of electronic and textile materials, presenting new challenges for developers and designers. Such creation requires radically new design concepts and approaches which are often required to encompass multiple, traditional technological domains. Textile integrated electronic functionality sets unique requirements to the materials composition and device/article construction. Hence, a range of enabling technologies and novel manufacturing technologies are prerequisites for the successful realisation of these new types of products.

From a consideration of the intrinsic properties, it appears evident that electronics in their conventional form are not compatible for integration into textile materials. Textiles, being the platform of e-textiles, should also preserve their classic properties, which make them wearable, comfortable, fashionable, and washable. Embedding electronics must not deteriorate these crucial textile properties. Thus, electronics must become conformable with the properties of the textiles, including attributes such as being soft, flexible, stretchable, and foldable. In addition to the aforementioned requirements, electronics must acquire resistance against mechanical and chemical

impacts if they are to withstand the stresses to which textiles are usually exposed to during use phase (Troster, Kirstein and Lukowicz 2003).

Table 1-1: Comparison of properties of typical electronics and textiles.

Properties	Electronics	Textiles
Mechanical	Hard, stiff	Soft, flexible
	Not stretchable	Stretchable
	Low resistance against mechanical impact	Medium to very high resistance to mechanical impact
	High structural complexity	Low to medium structural complexity
Chemical	Not water proof, not washable	Can be wetted and/or washed
	Can contain hazardous materials	Stringent health and safety requirements must be met
Electrical	Conductive, insulating, semi conductive	Electrically insulating
	Affected by static electricity	Can generate static electricity
Thermal	Often require cooling	Do not generate heat
	Working can be affected by heat	Often employed to dissipate heat
Wear and tear	No physical wear and tear	Designed to withstand severe wearing
	Casing protects against abrasion	Prone to abrasion
	One defective part damages entire device	Defects can be generally tolerated to a high degree
	Often not reusable or repairable	Easy to reuse and/or repair

1.2.3 E-textiles platform

Broadly speaking, e-textiles require innovations in two fields: hardware and software. In the simplest sense, the hardware components of an e-textile system can be said to consist of processing nodes, battery nodes and means of interconnecting the two.

As shown in Figure 1-1 (Tao 2005), the processing nodes consist of various interfaces and functional devices such as displays, sensors, communication devices, data management modules and so on. The circuitry, which is of interest in the present

study, provides interconnections between the processing nodes and the power supply, which furnishes energy needed to run the system.

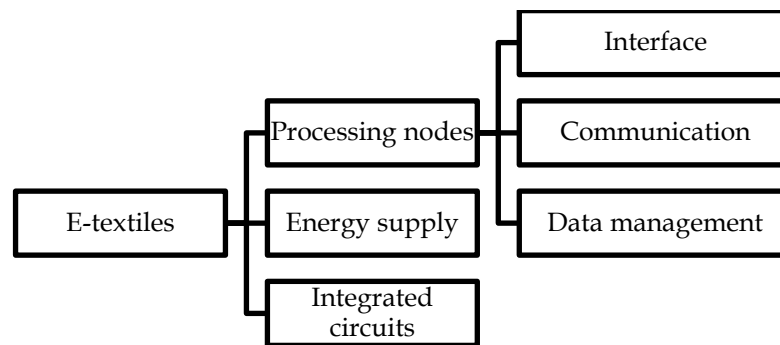


Figure 1-1: General system configuration for e-textiles.

1.2.4 Wearable e-textiles

Among the different product classes of textiles, clothing is potentially the most easily recognised and has the most wide-ranging applications as interactive textiles. Beyond their protective and aesthetic functions, clothes, as our second skin, have the potential to acquire additional functions as a personalised and flexible information platform (Van and Hertleer 2004). Clothing has large panels of fabric which makes the embedding of electronic elements feasible (Marculescu 2003). The large areas that are generally available for embedding components also allow fault-tolerant designs through redundancy. Thus, the term “wearable electronic textiles” refer to a new concept of clothing that combines electronic functionality with the conventional uses of articles of clothing. “Wearable computers”, “smart garments” or “intelligent clothing” are other terms that are used interchangeably for wearable e-textiles. A major challenge in designing wearable e-textiles is that the product design issues arise from a diverse range of sources, including the following (Martin et al. 2003):

- Physical environment;
- Sensor behaviour;
- Human body and motion;
- Motion/draping of clothing;
- Manufacturability (weave and piecework);
- Networking;
- Power consumption and software execution.

The development of wearable electronics technology has been/and is fuelled by the increasing desire for ubiquitous intelligent systems and access to information. Many of the claimed prototypes of interactive electronic textiles are based on integrated wiring to which the devices are attached, adding bulk and weight to the garments which make them uncomfortable and impractical for most of the intended uses. Truly wearable e-textiles require the seamless integration of electronic functionality while maintaining wearing comfort. In other words, the system should ideally be un-obstructive to the user. This unique product design requirement for textile-based wearable electronics differentiates this technology from the concept of simply mounting various electronic systems onto textiles, as shown in Figure 1-2 (Mann 2013).

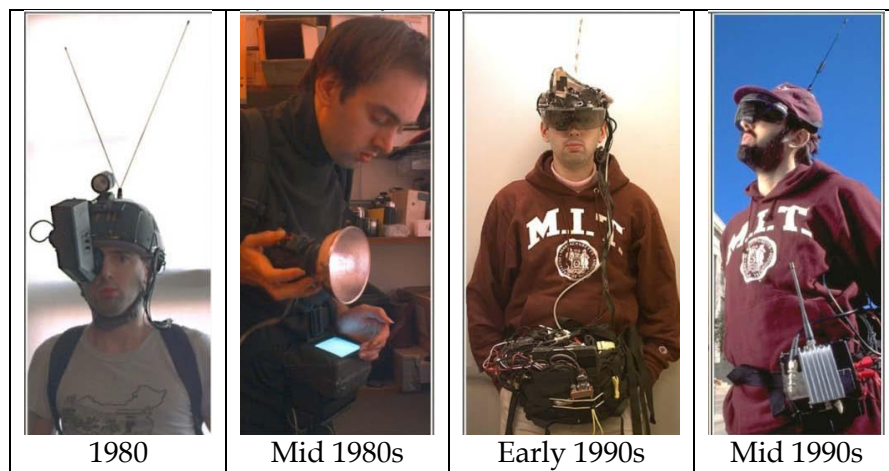


Figure 1-2: Evolution of Steve Mann's "wearable computer" invented in 1970s.

Refinements and new developments in wearable electronic textiles technology have resulted in the identification of many applications in various sectors, some of which are discussed in Section 1.2.1. However, the most common and important issue is the realisation of electrical interconnections. The interconnections between the processing nodes and the power supply are required to perform like a copper trace on a printed circuit board, while paradoxically remaining flexible and durable. It is important to ensure that the hardware integrated into clothing is unobtrusive, washable, and does not impede the garment's ability to conform to body curvatures. Various techniques that can be used to produce circuitry in textile fabrics, while meeting the above mentioned requirements, are discussed in detail in Section 1.3.

1.3 Enabling technologies for highly conductive e-textiles

Several studies describe techniques for achieving electrical conductivity in non-conductive flexible substrates, including textiles. There is an extensive literature base that deals with meeting the criteria for low conductivity applications such as electrostatic charge dissipation or products for which stringent washing and wearing are not required. In the context of the present work, only those studies are discussed in the following sections, in which the reported electrical conductivity was very high. The techniques that are proposed in the relevant studies can be grouped into the following categories:

1. Techniques based on using conductive filaments or yarns; and
2. Techniques based on the printing of conductive inks/coatings.

1.3.1 Techniques based on using conductive filaments or yarns

One of the more widely researched and adopted approaches to achieving conductivity in a textile web is to incorporate electrically conductive filaments (wires) or yarns within the fabric structure, during the fabric manufacturing process. Conductive yarns can be integrated into a knitted fabric structure by employing specialised techniques such as intarsia (Paradiso and Rossi 2006). However, weaving is predominantly used to produce a grid-like pattern of conductive elements in the fabric structure, as shown in Figure 1-3 (Marculescu et al. 2003). Such fabrics, having a plurality of insulated metallic yarns that form a grid of conductive wires in the fabric structure, are commercially available such as the PowerMatrix® system by Sefar.

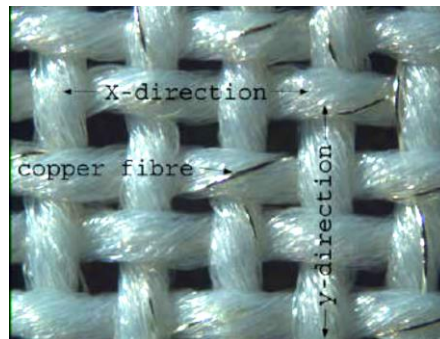


Figure 1-3: Woven fabric consisting of polyester yarns that are twisted with an insulated copper filament.

The required electrical circuit in such a fabric is made by interconnecting the insulated conductive wires. The fabric-based electrical circuits thus formed are flexible and, at the same time, possess a stable structure owing to the intrinsic stability of the structure of the woven fabric. Such fabrics can be produced using the same weaving machinery that is used for the production of conventional textile fabrics. Various weave patterns can be produced on cam, dobby and jacquard mechanisms. Additionally, these fabric-based circuits can be developed in single-layered or multi-layered configurations (Gimpel et al. 2004).

In order to produce the required circuit pattern, various techniques can be employed to selectively connect and disconnect the mutually orthogonal conductive wires. For instance, interconnections in a plain woven fabric, consisting of polyester as the non-conducting thread and steel and copper filaments as the conductive elements, have been produced using resistance welding (Dhawan et al. 2004b). Disconnects were also produced by parallel gap resistance welding in which a large weld current was used to generate thermal melting of the thread between the probes, thereby creating cuts or disconnects. The effectiveness of the resistance welding was evaluated by measuring the DC electrical resistance of the threads forming the cross over point.

A similar approach was used to produce the desired circuit pattern in a woven fabric consisting of polyester monofilaments and copper alloy wires that were coated with a polyurethane varnish, as electrical insulation (Locher and Troster 2008). The circuit manufacturing process that is described in this study is depicted in Figure 1-4. The first step employed was to remove the varnish by laser ablation, using a standard laser for microvia manufacturing. As shown in Figure 1-4(b), this step was followed by the cutting of certain wires to avoid short circuits with the rest of the routing. The cross-over points of the wires filaments were connected using a conductive adhesive (Figure 1-4(c)). The last step was to protect mechanically and electrically, the interconnection by encapsulating it using an epoxy resin, as shown in Figure 1-4(d).

The circuit manufacturing techniques that are summarised in the preceding text utilise woven fabrics that possess isotropic electrical conductivity owing to the conductive wires that are incorporated in both the weft direction and the warp direction. However, fabrics possessing anisotropic electrical conductivity as a result of the fact

that the conductive elements run only in one weave direction were also used to produce circuits, (Post et al. 2001). The conductive fibres served as electrical conduits that were capable of carrying data signals and/or power. It was claimed that the electrical components could be directly soldered onto the substrate. Larger contact areas, for connection to components and terminals, were achieved by arranging the conductive yarns in 'lanes', each lane comprising one or a series of parallel, adjacent conductive fibres. The lanes were separated from each other by non-conductive yarns. The technique was claimed to reduce the density of conductive wires in the fabric structure.

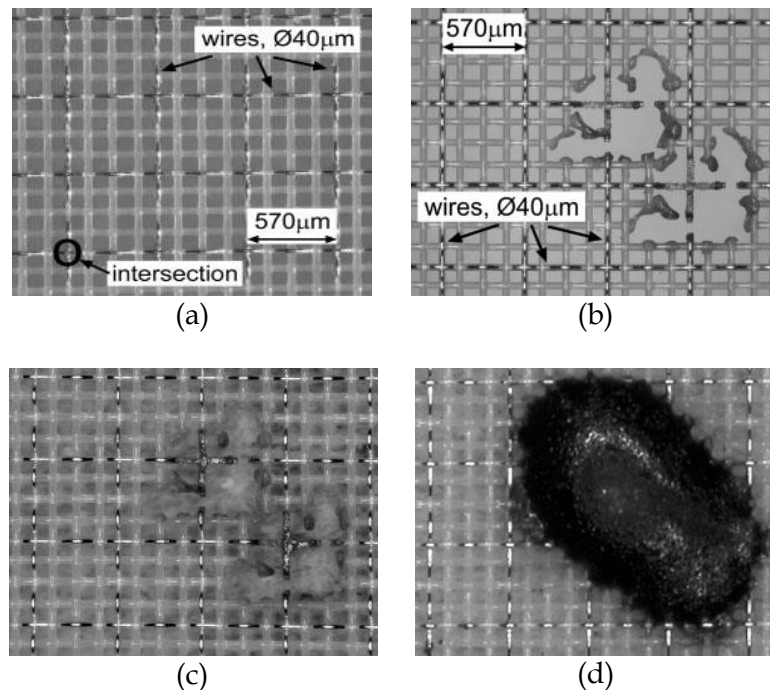


Figure 1-4: Steps involved in the fabrication of interconnections, (a) woven fabric with orthogonal conductive wires, (b) disconnects made by laser ablation, (c) interconnects formed using conductive adhesive and (d) encapsulation of interconnects.

The methods, described above, of embedding electronic components into a textile fabric require individual assembly of each of the components of the electronic system. One approach to overcome this limitation is to assemble a number of electronic components onto a thin plastic stripe followed by insertion of the stripe in weft direction (Zysset et al. 2012). The conductive wires running in the warp direction were suitably spaced to connect the e-stripes with each other and with other components of the electronic system. Fabric was manufactured using a conventional weaving machine. The e-stripes, however, were fabricated using the conventional techniques in the printed electronics industry such as photolithography and flip-chip bonding. Thus,

the e-textile fabrication process on the whole was lengthy and involved complicated steps. Other limitations of this technique are as follows.

- Inability to quickly change the design and layout of the electronic components. This is because the conductive wires which form the required interconnections run in the warp direction and the spacing between adjacent conductive wires could not be changed without changing the warp beam.
- The device size on an e-stripe was limited by the width of the stripe which was 2 mm.
- Washing the e-textile above 40 °C resulted in destruction of the electronic system due to corrosion of copper interconnect lines.

The techniques described above and other similar techniques such as the use of holographic optical fibres, along with conductive filaments to increase the functionality of the textile fabric (Lebby and Jachimowicz 1999), are based on weaving functional (conductive) wires, filaments or threads into the structure to produce a functional textile fabric. The functional threads that are employed for this purpose are expensive as they are designed to meet stringent performance criteria such as high electrical conductivity while, at the same time, having enough durability and flexibility to withstand the stresses that are imparted during fabric manufacturing processes in general and weaving in particular. Once a circuit is developed in such a fabric, it is difficult to control the conductivity and the cross talk noise in the circuit (Dhawan et al. 2004a). Furthermore, the commonly employed weaving techniques do not allow the selective insertion of functional threads that are almost always incorporated in the entirety of the textile web. All of the above mentioned factors contribute to greater overall costs and render these techniques unsuitable for specialised and/or low volume production. In addition, the stiffness and weight of the fabric can increase owing to the presence of metallic threads.

To overcome the limitations of techniques that are based on the incorporation of conductive threads in the fabric structure, the use of flexible conductive leads, which can be stitched to an ordinary non-conductive fabric, has been reported, (Post and Gershenfeld 2002). The conductive leads were stitched to the article to form the required interconnections. It has been claimed that this approach preserves the

character of the final article of use. It should be clearly understood that the manufacturing steps that are involved in such techniques are lengthy and costly.

An example of commercially marketed e-textile product is the Levi's ICD+ jacket, launched in 2000. The technology was based on using electrical "cables" that were claimed to be suitable for incorporation into apparel, clothing accessories, soft furnishings, upholstery and other items (Osborne 1996). Such "cables" consisted of copper filament as the electrical conductor, insulated using a braided, non-conducting textile. It was claimed that these cables are soft and flexible and can be fastened to cloth by stitching and piping or even woven into the base cloth. It was also claimed that the cables could be placed in the washing machine for cleaning with no added risk to the wire, garment or washing machine.

A speech-controlled digital music player system (Figure 1-5), developed by Infineon is another example of commercially available e-textile products, developed using conductive yarns in a fabric structure as means of providing interconnections between the system components (Weber et al. 2003).



Figure 1-5: The speech-controlled MP3-player demonstrator system designed into a sports jacket.

In this system, narrow fabric ribbons of a polyester with several groups of parallel conductive warp threads were used as the electrical interconnects. The conductive thread that was used was copper filament coated with a polyester. As shown in Figure 1-6 (c), an electric module can be directly connected to the conductive wires in the ribbon. Alternately, the contact with an electronic module can be established via a flexible circuit board that is soldered to the ribbon of conductive wires, as shown in Figure 1-6 (d).

Flexible and durable touchpads, which can be integrated into wearable accessories, garments, bags and can be placed in a variety of positions on the item, are available from Eleksen. The textile-based touchpad panels, named as ElexTex, can be integrated into a garment by simple stitching. These panels have no mechanical parts and are claimed to be washable (50 machine washes at a temperature of 60 °C) and durable (key press durability of more than 1,000,000). The conductive elements in these touchpad panels are made using silver thread, as depicted in Figure 1-7.

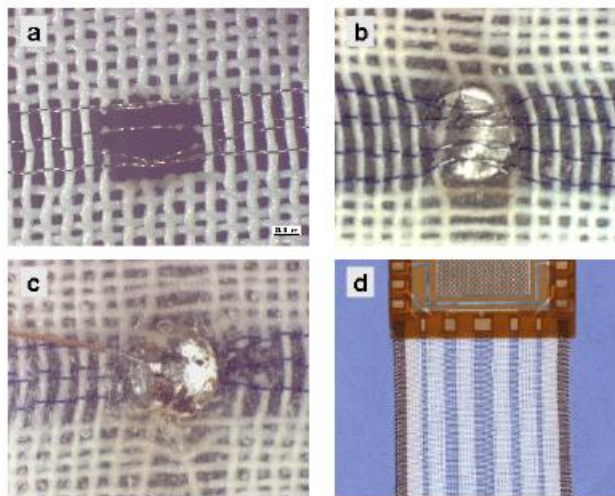


Figure 1-6: Interconnections via conductive ribbons.

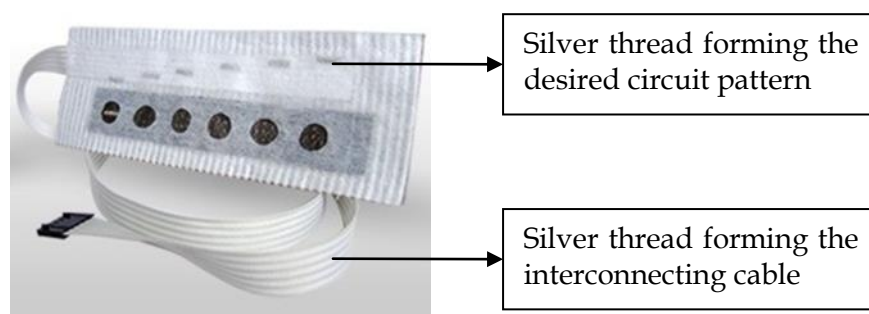


Figure 1-7: ElexTex touchpads for garments.

Techniques employing ribbons, cables or leads of electrically conductive threads, to connect components of an e-textile system, are claimed to be cost effective compared to the methods that are based on forming the desired circuit pattern from a grid of electrically conductive wires that are incorporated in the entirety of the fabric structure. However, one of the major limitations of these techniques is the inability to form

complex circuit patterns, particularly miniature circuits, as this would require the use of multiple cables and difficult-to-fabricate cable-module connections. Furthermore, the selective connection (and possibly disconnection) of conductive threads is also required which increases the number of steps that are involved in preparing a finished product.

Another technique that uses conductive filaments to make durable and flexible electronic circuitry in fabrics is electronic embroidery (or simply e-broidery). E-broidery can be defined as numerically controlled embroidery using a conductive thread to form stitch patterns that define circuit traces, component connection pads or sensing surfaces. The technique allows the fabrication of complex and miniature circuits without involving the need for a number of fabrication steps. One of the examples of product development using e-broidery is the musical jacket with its embroidered keyboard (Post et al. 2000). Figure 1-8 shows a circuit board that was produced by embroidering conductive yarn. The component side of the circuit board is superimposed to show its extent and its connections to the fabric.



Figure 1-8: E-broidery for circuit manufacturing.

The fabric-based keypad was embroidered on 50 jackets. It was found that in all fifty jackets, both the fabric keypad and the interconnections worked reliably and sustained repeated mechanical stresses. The more important considerations in this technology are that the yarns used must be conductive and also strong and flexible enough to be useable in high-speed embroidery processes. A trade-off between the electrical properties and mechanical properties must be made. The resulting circuits were

characterized by high Ohmic losses and were, therefore, limited to lower-speed circuits with low currents. Another limitation of this method is the inherent inability to control the characteristic impedance. Other limitations include the high manufacturing costs for low volume production and difficulties in fabricating the desired conductive patterns over large areas of fabric.

Using conductive wires or filaments in various forms such as yarns, threads, cables or ribbons is the most widely reported method of circuit formation in textile fabrics. A number of the studies that are more relevant to the research theme that this thesis concerns are discussed in the preceding text. Some of these techniques are reportedly used in commercial e-textile prototypes. However, there are limitations. Some techniques restrict circuits to specially prepared fabric. Some require the use of specially prepared electrical components. Others cannot be practically automated or mass produced. In addition, virtually all of the discussed techniques are faced with the complexity of the manufacturing process. In contrast, printing allows the one-step formation of a complex and intricate design on a textile substrate. Thus, printing offers several obvious advantages. This point is discussed in detail in the following section.

1.3.2 Techniques based on printing/coating conductive materials

The manufacturing of flexible electronics is one segment of the printed electronics industry in which new materials are fuelling the development of a variety of functional products and devices. Several producers manufacture electrically functional inks that are frequently employed to develop passive electronic components such as resistors, capacitors, interconnections and so on, as well as the more sophisticated electronic devices such as transistors, displays, etc.

To produce printing inks that possess electrical functionality, conductive elements such as gold, silver, copper and nickel can be used. Also, semi-conductive materials such as carbon, some metallic oxides, conductive polymers and so on, can be incorporated into the ink formulation to achieve a certain level of electrical conductivity. The resulting functional inks can be directly patterned onto various substrates by well developed printing methods, discussed in Section 1.5. It is important to mention here that the substrates commonly used in printed electronics industry generally possess a very

smooth surface. This is important if one is to achieve the desired functionality of the ink deposit. In contrast to the flexible substrates that are commonly employed in the printed electronics industries, for instance polyimide films and polyester films, textile fabrics in general and woven textile fabrics in particular possess a very rough and porous surface. Furthermore, the durability requirements, such as the ability to withstand several washing and wearing cycles, are stringent for inks that are printed onto textile substrates. The aforementioned points and some other factors, mentioned in Section 1.2.2, pose great challenges for successful printing of electronic devices on textiles. A number of research proposals concern various approaches to overcoming the stated problems. Some claim to be novel formulations whereas other focus on physical methods of achieving and maintaining the required functionality in the inks employed. A summary of a number of the studies that are more relevant to the present research problem is now presented.

A detailed method for producing textile fabrics that contain printed, conductive patterns was reported (Park, Cho and Chung 2007). The claimed advantages include washability and being defect-free (free from circuit failure by circuit disconnection). The conductive fabric exhibited satisfactory electrical properties without deteriorating the intrinsic properties of the textile substrate. The conductive fabric structure consisted of a base layer (substrate) on which a primer layer was deposited. The conductive layer was formed on the primer layer and coated, printed or laminated with an insulating material, as shown in Figure 1-9.

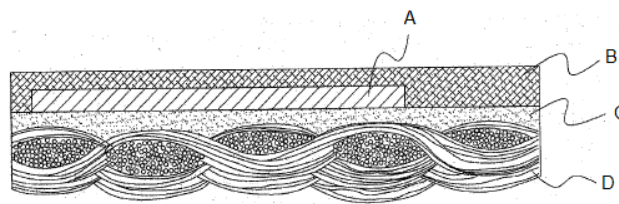


Figure 1-9: Conductive fabric structure showing the substrate (D), primer layer (C), conductive layer (A) and the insulating layer (B).

Several samples were produced on the basis of having different water-repellent primer layers and various ratios of silver-based conductive ink and binder. A liquid silicone rubber was used to form a protective top coat on the ink layer, thus completing the fabrication of conductive fabric. The samples were washed, without a detergent, in a wool programme (57 min.) of a horizontal drum type washer (WD-CR 1010, LG

Electronics Inc.), and dried prior to measuring the electrical resistance of the samples. The results summarised in Table 1-2 clearly indicate that most of the tested samples failed after only one or two wash cycles. However, in some cases (Samples 1, 2, 7 and 8), the increment in the electrical resistance of the test samples was relatively low. It was reported that in the failed samples, cracks were formed on the surface of the conductive layer after only one wash cycle. This impeded the flow of electricity, marked by a sharp increase in the electrical resistance. It was found that the amount of binder had a marked effect on the adhesion between the base layer (primer layer) and the conductive (silver ink) layer

Table 1-2: Electrical resistance of test samples after washing cycles.

	Resistance (Ω) after numerous washing cycles					
	0	1	2	3	4	5
Sample 1	0.83	1.23	2.27	3.21	7.80	13.40
Sample 2	0.69	1.70	3.27	4.50	7.50	10.20
Sample 3	0.84	240.00	590.00	710.37	900.80	10000.00
Sample 4	0.94	56.00	89.65	100.89	788.90	1002.22
Sample 5	1.49	3.20	9.73	62.30	260.70	777.23
Sample 6	1.80	5.20	16.80	59.20	300.00	1900.00
Sample 7	1.70	2.60	3.10	3.52	4.60	5.50
Sample 8	1.26	1.37	3.10	3.42	4.13	4.57
Sample 9	1.44	34.10	1888.00	2777.00	3102.00	5800.00
Sample 10	2.19	54.60	2800.00	5780.00	7880.00	9570.00

Some promising results were achieved in this study but there are limitations. For instance, the samples were tested for up to five washing cycles, without the use of detergent or steel balls, which are usually added to replicate the abrasive action in the laundering of textiles. The stated test conditions did not replicate the washing conditions to which textiles are usually subjected during the product life cycle. Furthermore, the solids content of those inks that performed better in the washing cycles was at least 60 wt%. Such a high loading of expensive conductive filler such as silver results in a high cost for the formulated inks.

In another study, electric interconnections were printed on different non-woven substrates that had various surface characteristics such as roughness (Karaguzel et al. 2009). For this purpose, commercially available silver-based conductive inks of different viscosities and different percentages of silver were used and their performance was studied. It was reported that those substrates having a smoother surface and the use of greater viscosity inks offer the best solution in terms of the electrical properties.

The electrical properties including the DC resistance and characteristic impedance of the printed circuit channels were checked and compared with those of conventional printed circuit boards. The sheet resistance of the printed silver based inks that were used in this study was found to be 42 times greater than that of bulk copper. It was proposed that additional conducting channels could be printed parallel to the main channels, to reduce the power losses that were due to the significantly higher resistance of the printed tracks. The ISO6330 method was followed to test the washing durability of printed inks. The results of this study indicated that only those substrates with a very smooth surface were feasible for use in printing. Even on the substrates with a low degree of surface roughness, the printed inks did not show resistance to washing and wearing. As shown in Figure 1-10, the printed inks began to degrade after only few wash cycles.

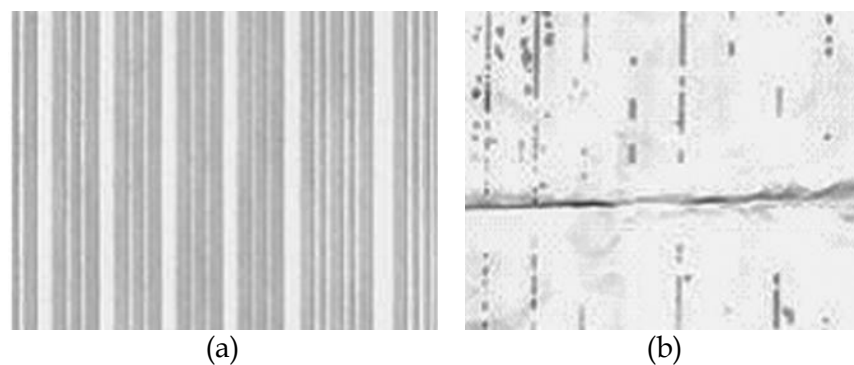


Figure 1-10: Printed coplanar waveguide lines on Tyvek® (a) before washing, (b) after washing.

To improve the washing durability of the screen printed circuit channels, the fabric was laminated using a thermoplastic polyurethane (TPU) melt blown layer. It was found that while the coating prevented the substrates from creasing during laundering, it also protected the ink and kept it sandwiched and in place during deformation.

Figure 1-11 shows the TPU-coated circuit channels before and after washing cycles. It was reported that the TPU-coated circuit channels withstood up to 25 washing cycles.

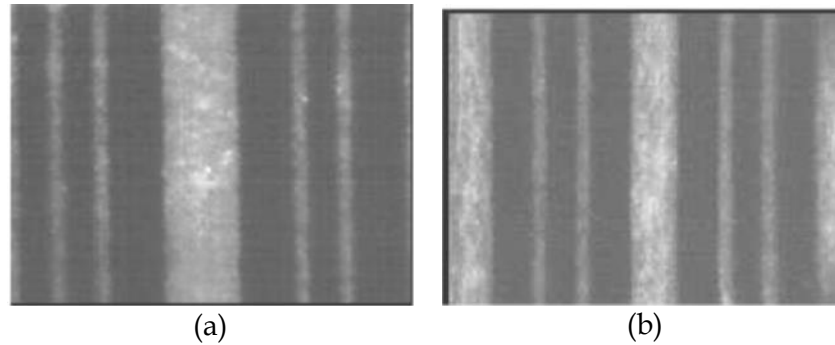


Figure 1-11: Laminated printed lines on Evolon 100 GSM; (a) before washing, (b) after washing.

In another study, conductive tracks were screen-printed onto an acryl-cotton woven fabric (Locher and Tröster 2007). A silver-based conductive ink (75% solids content) was used to print the transmission lines. The variables studied included the curing time and the number of print passes needed to create the conductive tracks. Other factors such as the screen mesh and the viscosity of the paste were also optimised by experimentation. Transmission lines were printed by 1, 5 and 10 print passes and their electrical and mechanical characteristics studied. Figure 1-12 shows the conductive lines that were printed by different numbers of print passes. The major effect of number of print passes was that the gap between adjacent transmission lines decreased as the number of passes was increased.

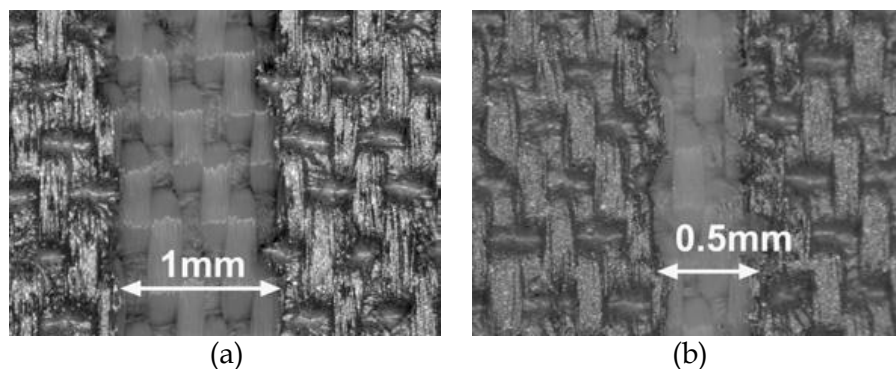


Figure 1-12: Gap between printed transmission lines (a) 1 print pass and (b) 10 print passes.

In this study, a line impedance of close to 50 Ohms was achieved but the samples were not tested for their washing durability. The resistance of the printed transmission lines to mechanical stresses, such as creasing and bending, was also found to be unsatisfactory. The electrical resistance showed a sharp increase after creasing due to the cracking of the printed line. Figure 1-13(a) and Figure 1-13(b) show the cracks that developed in the transmission line after one and after five crease iterations, respectively.

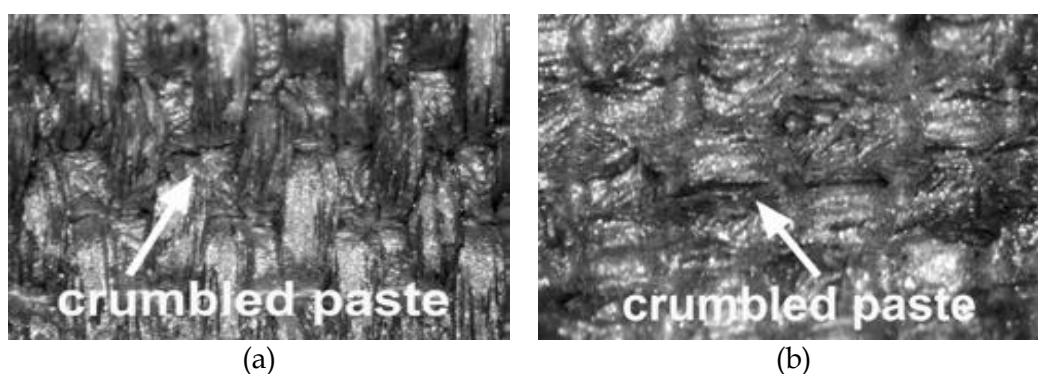


Figure 1-13: Cracking of ink layer after creasing cycles.

Very low surface resistivity ink deposits were produced on a variety of woven textile substrates including cotton, viscose, polyester, polyamide and blends of these (Kazani et al. 2012). For this purpose, Electrodag PF410 and DuPont 5025, which are commercially available silver-based inks, were deposited on fabric substrates by screen printing. The abrasion resistance of printed fabrics was tested using the Martindale method and a considerable increase in the surface resistivity was recorded after 5000 abrasion cycles. The increase in surface resistivity as a result of abrasion was more pronounced in the fabrics which had low absorption capacity and in the case of DuPont 5025 ink which possessed high viscosity and high surface tension. In both cases, it was observed that the ink deposits did not penetrate sufficiently into the fabric structure and thus abraded more easily. The increase in surface resistivity was also recorded at regular intervals during 20 washing cycles as per the ISO 6330:2000. It was found that nearly half of the samples completely lost their conductivity while in the remaining samples, the increase in surface resistivity after 20 washing cycles was very high (minimum 5700% for Electrodag PF410 ink and 15900% for DuPont 5025 ink). Both abrasion and washing tests were performed on printed samples top coated with TPU layer and surface resistivity as low as $0.2 \Omega/\square$ was maintained in some cases.

High loading of metallic fillers such as silver usually renders the ink film brittle and impairs the adhesion with flexible substrates such as textile fabrics. Highly conductive stretchable inks were prepared by adding up to 85 wt% of silver flakes in a polyurethane-based binder (Inoue et al. 2012). The inks that contained 80 wt% silver flakes gave the lowest resistivity value of approximately $10 \mu\Omega\text{cm}$ on glass substrate. The formulated inks, which were deposited onto elastic bands, withstood 10 cycles of 5% elongation, however, the resistance to withstand one or more washing and creasing cycles was not reported.

Another approach to produce a conductive pattern is to deposit a metal precursor followed by a second step in which elemental metal is produced *in-situ* on the substrate by a suitable process such as reduction. This method was used to produce electrically conductive patterns on various substrates including a woven cotton fabric by ink-jet printing (Bidoki et al. 2007). For this purpose, a two step approach was adopted. In the first step, a suitable reducing agent was inkjet printed onto the substrate. This was followed by inkjet printing a metal precursor. Ascorbic acid was found to be the most effective in reducing silver nitrate to elemental silver. Surface resistivity as low as $2.405 \Omega/\square$ was achieved on woven cotton fabric. However, there are limitations. Several layers of both the reducing agent and the metal precursor were required to be printed to form a solid and continuous metal layer on the substrates. Furthermore, the printed conductive patterns were not tested for their durability to withstand washing and creasing cycles.

All of the studies summarised above used inks that contained silver particles as the conductive filler material. Thus, the inks were expensive and an increasing trend in the cost of silver is a major limitation to large scale application of such inks. Furthermore, in a number of cases, washing tests were not carried out and thus the durability of the produced conductive patterns was not established.

The recent discoveries of high performing materials such as graphene have triggered the interest of research community in employing these new materials in numerous applications, including the formulation of electrically conductive inks. Inkjet printable electrically and thermally conductive ink was formulated from nano-graphene

platelets (NGPs) (Jang and Zhamu 2008). It was reported that the surface resistivity of inks formulated from NGPs was considerably lower (on an equal weight basis) in comparison to conductive inks formulated from CNTs, conductive polymer and blends of these. However, the minimum surface resistivity achieved on high gloss photo paper was as high as $75 \text{ k}\Omega/\square$ after five print passes. Furthermore, the durability of such inks to withstand washing and creasing was not reported.

Electrically conductive polymers were discovered in 1970 and hypothetical computations have shown that conductivities of up to 10^7 S/cm , far exceeding that of bulk copper could be obtained if one were truly able to synthesise a conducting polymer with extended conjugation along its entire chain (Tanaka, Murashima and Yamabe 1988). However, the solution processability of such highly conductive polymers is generally very limited (Shirakawa 2001). Several approaches to making conductive polymers that were solution-processable while maintaining the electrical conductivity have been reported. For instance, mixing poly(3,4-ethylene dioxythiophene) with poly(styrene sulfonic acid) was reported to increase the electrical conductivity of PEDOT while making the polymer soluble in aqueous media. This PEDOT:PSS was used to inkjet print circuit patterns on polyester film substrates (Hwang, Son and Lee 2007).

A screen-printable, electrically conductive ink, prepared using poly(3,4-ethylene dioxythiophene):poly(styrene sulphonate) solution (Baytron P, Bayer AG) was reported to produce transparent conductive coating giving a surface resistance of $1000 \Omega/\square$ measured in accordance with DIN IEC 93 (Jonas and Guntermann 1998).

One of the more widely reported methods of producing electrically conductivity textile yarn/fabrics is the in-situ polymerisation of an intrinsically conductive polymer onto a textile material. One such method was reported to produce conductive textiles uniformly coated with doped polypyrrole or polyaniline (Gregory, Kimbrell and Kuhn 1991). Volume conductivity as high as 200 S/cm was estimated from the thickness of the deposited polypyrrole layers. The minimum surface resistivity, however, was $80 \Omega/\square$. This was attributed to the formation of a very thin layer (1 - 2 microns thick) on the individual fibres in the textile fabric. Furthermore, the surface resistivity increased to $6500 \Omega/\square$ after only five domestic washing cycles.

In one study, the generally poor mechanical properties of polyaniline (PANI) were dealt with by adding polyethylene glycol (PEG) during in-situ polymerisation of the conductive polymer onto a polyester fabric (Zhao, Cai and Fu 2011). PEG functioned as a steric stabiliser for PANI. However, blending PANI with PEG was found to considerably reduce the conductivity of the conductive fabric. The minimum electrical resistance that was achieved in this work was 8 k Ω . Furthermore, the effects of washing the conductive fabric were not recorded.

Electrically conductive cotton fabric which was produced using a 'hybrid' coating was found to possess very stable electrical conductivity upon aging and resistance to withstand abrasion (Savitha and Prabu 2013). A maximum weight loss of 2% for coated cotton fabric was recorded after 50 abrasion cycles. The hybrid coating employed in this study was aniline-adsorbed TiO₂. The incorporation of a limited amount of TiO₂ was found to improve the electrical conductivity of the final coating. However, the maximum conductivity achieved was 1.5×10^{-3} S/cm which is very low for applications such as circuit printing.

Some unique materials, such as superconducting ceramics were reported to produce highly conductive screen printing pastes (Jackie and Denise 1991). The suitability of such inks for printing onto textile substrates was not claimed. In one study, a method of producing printed electrical conductors, comprising of a network of fused, interconnected metallic nanoparticles has been reported. The electrically conductive pastes were claimed to be screen-printable and have a resistivity of at least 5X that of the resistivity of bulk metal that was used in the formulation (Vanheusden et al. 2006). The printability of such formulations on textile substrates was not claimed.

A number of the studies that are summarised in the preceding text revealed the use of conductive inks, comprising of different conductive filler materials, in the formation of conductive prints/coatings. Highly conductive printed patterns were achieved in many studies. However, there are limitations. These include there being little or no resistance to mechanical stresses and washing and the very high cost of inks due to the high cost of raw materials, etc. For these reasons, the techniques that have been described lack feasibility for use in printed circuit formations that would be suitable for textile substrates.

1.3.3 Summary of the limitations of prior art

The widely researched and adopted techniques of fabricating electrically conductive textiles are discussed in the preceding section. These methods include the use of conductive yarns or filaments, embedded in the fabric structure, to connect various components of an electronic system. The technical advantages of printing of conductive tracks over other methods of circuit formation such as weaving and embroidering are also summarised above. The existing technologies for printing highly conductive flexible circuit patterns on non-textile substrates are well developed and a number of ink manufacturers offer screen printable pastes based on various conductive filler materials such as silver, carbon, conducting polymers, carbon nanotubes and composite materials (containing combinations of different conductive filler materials), etc. However, these technologies have so far not been found to be fit for printing highly conductive films on textiles. Thus, it was aimed in this project to formulate electrically conductive inks which can be printed on textile substrates.

Prior to presenting a comparison of printing techniques, it is worth mentioning that printing can be used purely as an “additive” process or as part of a “subtractive” process to pattern conductive tracks. In the additive process, the functional material (e.g. conductive ink) is deposited directly in the form of required pattern. In the subtractive process, the functional material is initially uniformly coated on the entire substrate and then removed selectively by different techniques to leave the desired pattern (Adams, Gilpatrick and Gregory 1994). The removal of coated conductive material is referred to as a “transformation” process, (DeAngelis, Child and Green 1997). Limitations such as material loss, the complexity of the process and the fact that textile substrates could be damaged by the strong chemical or physical nature of transformation processes, render the subtractive process technically and commercially unfeasible for developing low cost circuits on textiles.

In the study reported in this thesis, the term ‘printing’ is used to refer to additive processes only. One of the major challenges that arise due to the nature of additive printing processes is the need to ensure that good processability of the functional material can be realised without compromising the performance. Such development should be beneficial in terms of reducing the costs and improving the design reliability for almost every type of product in the e-textiles sector.

1.4 Performance criteria for printed conductive patterns

It is evident from the review of literature presented in the previous section that electrically conductive inks and coatings can be used to produce circuitry. Circuit printing is a process in which either a simple or a complex system of “wires”, in the form of electrically conductive film coatings, are applied to the surface of a dielectric/insulating base material. In the context of present study, the more important performance criteria that must be met for conductive patterns that are printed on textile substrates can be categorised in the following groups.

1. Electrical performance criteria
2. Durability performance criteria

1.4.1 Electrical performance criteria

The electrical performance of a printed conductive pattern is, to a great extent, dependent on the materials used in the ink formulation. However, the printing process parameters and the design of the circuit pattern also have great significance with respect to meeting the electrical specifications. This point is highlighted in the following examples.

- The capacitance between adjacent conductive tracks is greatly influenced by the distance between the tracks, which is limited by the maximum achievable resolution. The maximum capacitance between adjacent conductors must be limited to 27 pF (Membrane Switch and Panel Inc).
- The electrical conductivity of a printed pattern is primarily dependent on the intrinsic electrical conductivity of the conductive filler material. Other components of the ink formulation, such as the binder, the dispersant and so on, also significantly affect the electrical conductivity of ink. In addition, the design of a printed pattern can be altered to adjust the electrical conductivity to a certain extent. The wider and thicker the line, the lower is the resistance (Savage 1976). The width of the conductive tracks of conventional printed circuits ranges between 0.5 - 1.5 mm while the thickness can be up to 75 μm (Kosloff 1981). The thickness of the conductive track can be altered by varying the printing parameters. For instance, one can increase the number of print

cycles to increase the ink film thickness. Thus, the printing process also affects the electrical properties of a conductive ink deposit.

1.4.2 Durability performance criteria

To meet the electrical specifications throughout the product life cycle, the printed conductive pattern must withstand the very severe laundering, creasing, abrasion, dry cleaning and other mechanical and chemical stresses to which textiles are subjected to during their end use (Ghosh, Dhawan and Muth 2006), (Merilampi, Laine-Ma and Ruuskanen 2009). In the research that underpins this thesis, only the washing and creasing durability of inks that were printed onto textile substrates were evaluated. These two tests are the more important durability tests because they must be passed in all cases. A brief description of these tests is presented as follows.

1.4.2.1 Washing durability

In assessing conventional pigment prints, washing tests are conducted to determine the extent of any colour loss associated with respect to the resistance of binder and/or pigment to the combined action of abrasion and detergent, with or without chlorine. If the binder is not present in correct amount or has not been cured properly it may be removed in laundering, due to abrasion. If this happens, the conductive filler may be released into the laundering solution, resulting in marked increase in the electrical resistance of a printed conductive pattern. In this current research study, washing tests were performed according to the BS EN ISO 105:C06 test method, as discussed in detail in Section 2.4.3.1.

1.4.2.2 Creasing durability

Sharp creases are formed in textile articles during their normal end use or during cleaning processes such as washing. Conductive inks that contain a large amount of conductive filler are often brittle. Their electrical performance easily deteriorates after only a few creasing cycles. Thus, the testing of their creasing durability is of prime importance for such applications. In this research study, the ASTM F 2749 - 09 test method was employed to determine any changes in the electrical resistance of conductive ink films during creasing. The procedure is described in detail in Section 2.4.3.2.

Other tests that are frequently carried out on printed textile fabrics, but which are not considered relevant in the present study are listed in Table 1-3.

Table 1-3: Tests not considered relevant in the present study.

Test	Relevance to the study
Light fastness	Printed conductive patterns in most of the anticipated applications are not expected to be exposed to excessive light. Furthermore, the inks contain carbon black pigments which generally possess excellent light fastness. Thus, light fastness testing was not required in the context of present study.
Stiffness	Fabric panels carrying the circuit pattern are likely to be embedded in a multi layer structure (such as a membrane switch) and print-induced stiffness will have negligible effect on the overall stiffness of the assembly. Thus, the stiffness of printed fabrics was not tested.
Fabric hand	<p>This is often considered to be a major limitation of conventional pigment printing but it is not relevant in the present study due to the following reasons.</p> <ul style="list-style-type: none"> • The percentage coverage of print is likely to be small. • The printed fabric panel is not likely to form an outer surface of the article of use.

1.5 Printing of electronic devices

Applications of printing in the electronics industry range from the highly developed technique of printed circuit board manufacturing to novel products such as sensors and transistors (Bao et al. 1997) and other components of intelligent systems (Tymecki, Glab and Koncki 2006). Most of the conventional printing techniques such as flexographic, offset, gravure, screen and inkjet printing can be adopted for the deposition of functional materials (Das 2005). Each printing process has its own characteristics and its suitability needs to be matched to the materials being printed and the required resolution. Despite the advantages that are associated with the fabrication of electronic devices using printing, as highlighted in Section 1.3.2 and Section 1.3.3, there are several challenges. The resolution, accuracy, registration and yield are among the crucial considerations that arise in manufacturing electronics by printing, (Parashkov et al. 2005). In the following sections, various commonly employed printing techniques are discussed in the context of their suitability for the printing of electrically functional inks.

1.5.1 Flexographic printing of electronic devices

As with most printing techniques, the parameters to be considered with regards to printing electronic devices using flexographic printing are resolution, film thickness and accuracy. The printed ink film thickness ranges from 6 to 8 μm with resolutions up to 150 LPI. One limitation of the flexographic printing process is that a pattern is always visible on the edges of the printed areas as shown in Figure 1-14 (Kipphan 2001). This pattern comes from the squashing of the photopolymer plate on the substrate, despite the low pressure applied. Therefore, there will be an irregularity on the edges, which may affect the way printed electronic components work. For instance, in the case of electrical circuits this may cause unequal electrical impedance along the length of the conductive track. The squashing phenomenon may also generate a slight inaccuracy of position, which is not acceptable in case of devices such as transistors. Furthermore, flexographic printing is not known for the printing of textiles substrates.

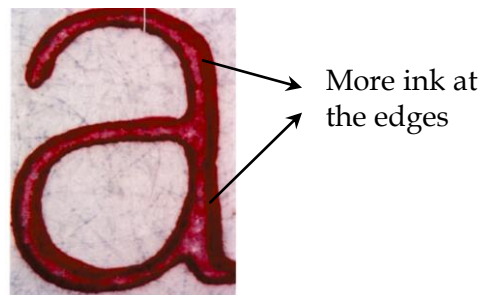


Figure 1-14: Micrograph of a flexographic printed impression.

1.5.2 Gravure printing of electronic devices

Gravure printing is one of the more promising techniques in terms of producing consistent quality for printing electronics. A number of studies have reported that gravure printing is a feasible technique for printing electronic devices of varying complexity and scale. The technique has been used to print particulate (silver) containing polymeric inks onto flexible substrates, such as paper and plastic films/sheets (Sung, de la Fuente Vornbrock and Subramanian 2010). Sheet resistance values as low as $50 \text{ m}\Omega/\square$ were obtained for conductive lines that were 4 - 7 μm in thickness. It was found that the smoothness of the substrate surface also influenced the minimum line resolution and the resistance. Flexible OLEDs (Michels, de Winter and Symonds 2009) and multi-layer devices such as capacitors (Vornbrock et al. 2009) were

developed by employing gravure printing. However, the technique is not without its limitations, some of which are listed as follows.

- The technique is not economically feasible for short production runs, especially in the printing of electronics, which often requires costly engraving methods for high resolution to be achieved.
- The technique cannot respond to a quick pattern change over. This is a drawback because several potential applications of printed electronic circuits on textile fabrics require rather small quantities of panels with different print (circuit) patterns.
- There are some limitations with regard to the printing of flexible and sensitive substrates due to the greater pressures that are involved in the printing.

In gravure printing, the features of engraved cells such as the cell width, the cell depth and the overall cell shape, have the most profound effect on the quality of the print. This is because the ink release from the cells is almost entirely dependent on these features which, in turn, are dependent on the method of engraving the image-carrier cylinder. The advantages and the disadvantages of different engraving techniques, with reference to printing electronic devices, are summarised below.

Electromechanical engraving is the most widely adopted engraving technique in conventional gravure printing. Modern electromechanical engraving units are not optimised for resolutions above 600 LPI. Additionally, all of the cells are constrained to a diamond shape, which makes it difficult to place them close enough for them to print continuous lines. This is one of the more crucial limitations of electromechanical engraving when printing of circuits is concerned. Another important factor to consider is the appearance of “saw tooth” or the jagged edges, due to the geometry of cells. This results in poor line contours, as shown in Figure 1-15 (Kipphan 2001).

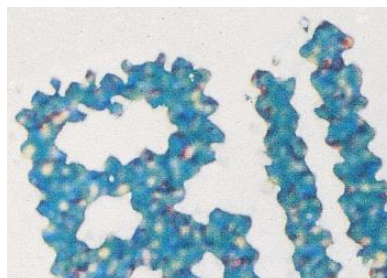


Figure 1-15: Micrograph of gravure printed ink, showing the “serrated teeth structure” at the edges.

Direct laser engraving is another engraving technique. The minimum achievable cell width from direct laser engraving is approximately 20 μm which implies that printing of sub-20- μm lines, which is often required in fabrication of active electronic devices such as transistor gates, is not possible.

With chemical etching, features of approximately 12 μm in width can be etched. The depth of cell, however, is limited to less than 1 μm . This implies that thick ink layers cannot be deposited effectively. The major disadvantages of the chemical etching method, in the context of the printing of electronic devices, are the relatively low uniformity and the inability to pattern small features consistently. This inconsistency is mainly due to the non-uniformities that are imparted during the exposure and development steps of plate development.

The indirect laser engraving method is known to produce more uniform features than the chemical etching method, particularly for small feature sizes. On average, the method produces cells which are smaller and more uniform. Cell widths from 11 - 15 μm have been reported (Subramanian and Sung 2008).

1.5.3 Offset printing of electronic devices

With offset printing, the film thickness ranges between 0.5 to 2 μm and resolution can be down to 10 μm . The low ink layer thickness is advantageous for devices such as transistors. However, printing circuits, for which the main requirement is high conductivity, two or more passes may be necessary in order to print the required thicker layers. Major problems that arise if more than one print pass is required to achieve the operational conductivity include:

- The registration of successive layer(s) must be very accurate. In offset printing, a mechanical accuracy of 2.5 μm is commonly achieved.
- Multiple print passes are not technically feasible when offset printing is done on smaller fabric panels, such as those required for embedded circuits, in a batch type process.

Among the other limitations of this process, as far as the printing of electronics is concerned, is the reality that the technique is not known for printing on textile substrates.

1.5.4 Screen printing of electronic devices

Screen printing can be employed to print on almost any substrate, if the ink can be suitably formulated. It is the most developed and adopted printing technique for the fabrication of electronic circuits. The principle was known as early as 1921 (Kosloff 1981). Screen printing is widely employed in the large scale production of products such as keyboard circuits, flexible circuits in cameras and so on.

Screen printing is particularly suited to the deposition of thick films up to 30 μm or greater. The printing of inks containing large particles is also possible if a suitable screen mesh is used. The ability to deposit thick films, with reasonable accuracy is probably the most important advantage of screen printing. The technique is not known to give very high resolutions. However, continuous developments have enabled its application in novel "high-tech" products such as OTFTs (Gray et al. 2001), sensors (Nilsson et al. 2002) and OLEDs (Lee et al. 2009). There are several other advantages of screen printing, making it one of the more promising techniques for the printing of electronics. These advantages are considered below.

- The process is simple in terms of its control and setup and does not require complicated pre-printing steps, such as the engraving of image carrier cylinder, as required in gravure printing.
- The technique can be employed efficiently for both short runs and long production runs. A wide range of screen printing machine configurations, to suit the needs of the printer, are available. For very small production runs, hand screen printing can be carried out.
- The cost of equipment varies considerably. However, in general, it is possible to employ a low cost setup for commercial products. The running costs are also low, mainly due to the low cost of the image carrier (screen).
- Screen printing is often considered to be the most versatile of all of the printing techniques. This relates to the ability to print a wide variety of substrates in a correspondingly wide variety of ink systems. The technique is widely used for

textile printing and it enables the printer to adjust the characteristics of the print by varying simple process parameters such as the speed of squeegee action, the applied pressure and the number of strokes. For instance, the thickness of the printed ink film can be increased by increasing the number of printing strokes or by decreasing the viscosity of print paste, within acceptable limits.

1.5.5 Inkjet printing of electronic devices

Inkjet printing offers a number of advantages over other printing methods. These include a possible cost reduction and the ability to configure electronic devices of various design complexities. One of the major advantages of inkjet printing is the availability of real-time dynamic alignment, which is critical for the printing of transistors and other multi-layer electronic devices (Hayes et al. 2002).

The piezo and acoustic type inkjet heads are most commonly used for fabrication of organic electronics. Thermal type heads are not used because of potential heat damage to the functional organic material being printed. Simple prototypic devices such as continuous conductive films have been inkjet printed using low surface energy PEDOT:PSS-based ink (Yoshioka and Jabbour 2006). The thickness was controlled through the HSL (hue, saturation and luminosity) function in Microsoft Office Power Point, which shows the ease and simplicity of the process for the stated purpose. The sheet resistivity of the printed films, measured using the 4-point probe method, was found to be approx. $1000 \Omega/\square$. A marked decrease in the resistivity was observed with increasing film thickness. A number of studies report the use of inkjet printing to realise the creation of complex electronic devices such as transistor circuits (Kawase et al. 2001), source and drain electrodes in TFTs and 3D micromechanical systems (MEMS), using nanoparticulate metal colloids (Fuller, Wilhelm and Jacobson 2002). As well as the promising results, inkjet printing has a number of disadvantages that limit the application of this technique for the creation of printed electronics. Some of the major limiting factors are listed below:

- The lateral resolution is relatively low. However, high resolution patterning (up to $5 \mu\text{m}$) has been reported. This was achieved by pre-patterning the hydrophilic substrate with a hydrophobic material which prevented the spreading of water-based ink (Sirringhaus et al. 2000).

- Nozzle clogging is another drawback. This becomes more severe when low boiling solvents are used for organic semiconductors (Kim et al. 2009).
- Low throughput arises because of the slow print speed as opposed to roll-to-roll printing techniques.
- Statistical variations in the droplets can result in the development of a certain degree of process instability.

1.6 Selection of the printing technique

As depicted in Figure 1-16, there is often a significant overlap in the suitability of the different printing techniques. Researchers and industrialists have proclaimed the numerous advantages and disadvantages of each of the printing techniques that were discussed in the previous section. Therefore, the choice of the printing technique is made primarily on the basis of the application requirements. The following factors can be considered as being a general guideline.

- The type of device: Single layer or multilayer in assembly.
- The scale of the device: The maximum resolution that is achievable with a printing technique varies considerably. Therefore, the applications of the technique may be restricted by the dimensions of the device being fabricated.
- The substrate: Not all of the printing techniques can be used for the printing on all types of substrates. For instance, offset printing is not commonly used in the printing of woven textile fabrics.
- Materials: The materials required for the fabrication of electronic devices can be classified broadly as conductors, semi-conductors and insulators/dielectrics. The costs and availability of these materials, in the required form for any given printing technique, are important to consider in the ink formulation stages.
- Quantity: The economic viability of different printing techniques varies with the quantity that is produced.

Review of literature presented in the preceding text indicated that all of the common printing processes can be successfully employed for fabrication of printed electronic devices. Although the initial goal in this work was application oriented, but other aspects such as commercial (e.g. cost of manufacturing) and manufacturing (e.g.

complexity of fabrication) viability of e-textile products were not neglected as they are equally important in the potential future embodiments of this research.

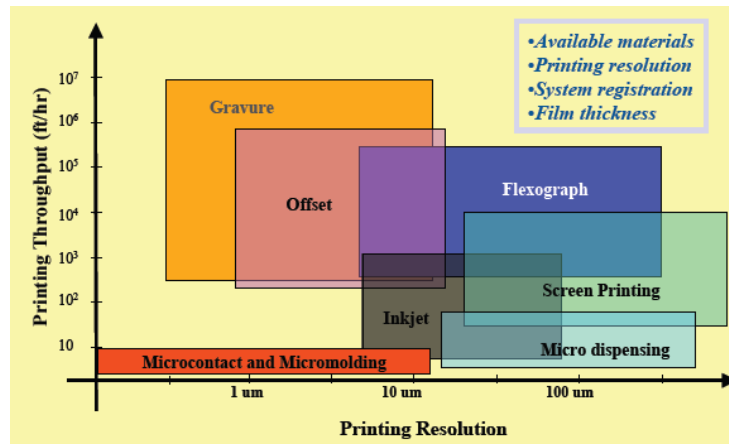


Figure 1-16: Capabilities of different printing processes (© Motorola's Printed Electronics Technology Team).

Table 1-4: Characteristics of printing processes (Huebler et al. 2002).

	Screen	Gravure	Flexography	Offset	Inkjet
Substrates	All substrates	Coated papers and boards, polymers and textiles	Papers, boards, polymers, metals	Papers, boards, polymers, metals	All substrates
Ink film thickness (μm)	0.2 - 100	0.8 - 12	0.8 - 8	0.5 - 2	0.3 - 20
Resolution (μm)	> 100	>15	>40	>15	>50

Based on the discussion presented in Section 1.5 and the characteristics of common printing process summarised in Table 1-4, screen printing was selected as the printing process to be employed in the research that is reported in this. The more important advantages of screen printing are listed below.

- The technique can be applied to produce films from 0.2 μm to 100 μm in thickness. The ability to print thick films is a major advantage when printing highly conductive patterns, such as circuits.

- The technique is well developed and is one of the more widely used printing processes for conventional printing of textiles. Furthermore, screen printing is well known in the conventional printed electronics industry.
- The technique is flexible from the manufacturing point of view. Therefore, it is economical for both short runs and long production runs.
- The attainable resolution from screen printing is sufficient for applications such as circuit printing.

1.7 Technology of printing inks

A review of the literature on the use of electrically conductive inks to create conductive elements on textile substrates is provided in Section 1.3.2. This section deals with the formulation of electrically conductive, water-based, screen printing inks for textile printing. A brief account of the chemistry and technology of such printing inks is provided, followed by a summary of the basic ink/coating production process in Section 1.8. In the present study, a number of grades of carbon black pigment were used to prepare the electrically conductive screen printing inks and thus, it was considered to be relevant to include an overview of carbon black pigment manufacturing processes, as provided in Section 1.9.1. Also considered are the morphology of such pigments and the effects of this on the dispersibility of the carbon black pigment. The preparation of stable, waterborne dispersions of carbon black pigments was considered to be an important target to be achieved in this study. Therefore, pigment dispersion processes, classifications of dispersing additives and the selection criteria for dispersing additives are reviewed in the following sections.

Detailed accounts of the composition of printing inks are available (Todd 1994c), (Laden and Fingerma 1997). There are a number of factors to be considered. These include the printing process employed, the type of printing press, the printing speed, the substrate and the intended use of the printed article, which determine the composition of a printing ink (Todd 1994a). Put simply, a printing ink is a dispersion of a colouring matter or functional material(s) in a vehicle (varnish), formulated into a liquid or a semi-liquid material to produce a pattern on a substrate. The ingredients that comprise an ink system can be listed under one or more of the following broad categories, colourant or functional material, vehicle and additives (Tracton 2006).

The colouring matter can be a dye or a pigment. Currently, approximately 90% of the printing inks that are produced worldwide contain pigments rather than dyes (Kunjappu 2003). As new applications of printing inks are envisaged, increasing numbers of pigments are employed as functional materials in inks (Brenzikofer 2002), (Buxbaum 2002). These functional pigments impart different functionalities to printing inks, including electrical conductivity (Rouse and Klein 2011; Li-Rong, Bin and Xiao 2007; Zhiqing et al. 2010; Harper and Taylor 1983; Azim et al. 2006; Mustonen 2009; Hwang, Son and Lee 2007; Krucińska, Skrzetuska and Urbaniak-Domagala 2011; Li et al. 2009), magnetism (Sambucetti 1980), (Sang-Geun et al. 2011), and so on.

The pigment can be inorganic or organic in nature. This nature helps to determine the ease with which a particular pigment can be dispersed in the vehicle. Generally, inorganic pigments can be dispersed easily by applying a minimal force. However, organic pigments and carbon blacks require special pigment milling techniques to produce an even distribution of pigment particles in the ink vehicle (dispersion medium).

The vehicle in an ink formulation primarily consists of one or more solvents and binders. The major functions of a vehicle are to act as a carrier for the pigment particles and binder and to bring about a reduction in the ink viscosity. The solvents used can be organic, water or monomers depending upon the type of ink i.e., solvent-based inks, waterborne inks or energy curable inks, respectively. It is crucial that the binder and the solvent are compatible, i.e., the binder dissolves satisfactorily in the solvent. Organic solvent-based inks and waterborne inks contain large amounts of solvent to dissolve the high molecular weight polymer(s). Thus, such inks generally have low solids content. On the other hand, solvent-free inks, which are also known as energy curable inks, contain monomeric and/or oligomeric polymer-precursors that can be polymerised *in-situ* after applying the inks to the substrate. It is due to this composition that the solvent-free inks achieve a high solids content. The solvent in an ink also determines the type of drying/curing technology that is employed on the printing press, (Todd 1994b). In a solvent-based ink, the solvent must evaporate to allow the binder to form a film. If the solvent is not readily released from the deposited film, some solvent molecules will remain trapped, thus affecting the film properties, such as

the adhesion and the flexibility. Where a solvent blend is used, it is important to consider the effect that physical interactions between different solvents will have on the evaporation rates and on the overall drying speed of the film (Leach and Pierce 1993). It is also important to note that while fast drying times may be desirable for keeping fast print speeds, this could impact negatively on the ink stability whilst on the press. For example, there may be premature drying of ink in/on the screen mesh in the screen printing process. UV-curable inks require the monomers (acting as a carrier for the pigment) to take part in polymerisation reactions with other formulation components upon exposure of the ink film to a UV radiation source. The number of reaction sites that are available per monomer molecule, referred to as the functionality, has an effect on the rate at which the curing of the liquid film proceeds. Generally, higher functionality monomers will increase the curing speed of an ink film due to there being a greater extent of cross-linking between the polymer chains. However, in this case, the resulting ink film will be less flexible than one where low functionality monomers were present.

The choice of vehicle can also influence the adhesion between the ink film and the substrate. Some solvents and monomers will promote adhesion to selected substrates, either by keying into the surface or by bonding at bonding sites on the surface. It is also possible that the adhesion of an ink can be damaged by introducing solvents that counter the adhesion ability of the binder.

The properties of the wet ink and the final solid ink deposit depend on the choice of pigment(s), the binder(s) and the solvent(s). However, it is not always possible to obtain the desired properties and characteristics simply from these three components of an ink. A multitude of properties, often conflicting ones, is required of the inks. These include, but are not limited to, the required print quality, light fastness, opacity, flexibility, adhesion, drying in air, shear stability, gloss, slip, tinctorial strength, water resistance, rubbing fastness, and other functionalities (e.g., electrical conductivity and magnetism.)

Alterations of the composition to improve one characteristic can have a detrimental impact on another characteristic. Often additives are introduced into an ink formulation either to have a positive impact on one or more of the characteristics or to

impart a particular property to the ink. Sometimes, additives are used to control any detrimental impact on ink properties that is brought about by another component. A wide range of additives is available. The more common types include dispersants, surfactants, rheology modifiers, defoamers/anti-foaming agents, pH modifiers, humectants and biocides (Todd 1994c), (Kunjappu 2003).

Among the two major variations of solvent-borne inks, waterborne inks are generally considered to be more environmentally friendly than organic solvent-based inks. A detailed discussion of the advantages and disadvantages of waterborne inks is beyond the focus of this study. The reader is directed to other sources that provide a comprehensive account of the historical, legislative and technical developments that drive the rapid growth of the waterborne inks sector (Leach and Pierce 1993; Shapiro and Sagraves 1997; Todd 1994e; Hartschuh et al. 1997; Warnon 2004). The present study deals with the formulation of electrically conductive waterborne inks, designed to be used for the screen printing of textile substrates. As with other printing inks, the requirements for screen inks are dictated primarily by the printing process. The requirements for screen inks have been summarised as follows (Barker 1993).

- The vehicle must not be too volatile. This is important to ensure that the ink does not start to dry while it is held on/in the screen.
- The solvent(s) must not damage the squeegee. With rubber squeegees, damage to the squeegee refers to the swelling and cracking of the rubber blade. In the case of steel blades, the primary damage that is caused by an unsuitable solvent is the corrosion of the metal.
- The ink must meet the stringent viscosity requirements that are imposed by the printing process. During the screen printing process, the ink is subjected to a shear rate ranging from 500 s^{-1} during the flood stroke, to up to 10000 s^{-1} when the ink is being forced out of the screen mesh (Abbott 2008). Thus, the ink must possess a sufficiently low viscosity to pass through the screen mesh during printing. At the same time, the ink must quickly regain the viscosity once it is transferred onto the substrate, to ensure proper print definition.
- After printing, the ink layer must dry at a reasonable rate when it is subjected to the available drying process.

The ink preparation process also plays a crucial role in achieving the desired ink properties. This point is discussed in detail in the following section.

1.8 Ink preparation processes

The property requirements for various ink systems (e.g., screen inks, offset inks, and so on) are often significantly different from one another. Thus, the technological aspects of various inks and the corresponding ink production processes are also different. There are huge varieties of ink manufacturing equipment that are designed to meet specific requirements of a particular ink manufacturing process. The selection of equipment and the sequence of the steps that are involved in ink preparation are primarily dependent on the type of ink and the quantities of inks being manufactured. The main target is to achieve a proper blend of all the ink components, in general, and an optimal dispersion of the pigment, in particular. Ink manufacturing processes can be said to have three steps, namely pre-mixing, milling and let-down.

Figure 1-17 provides a view of an ink production process. During the pre-mixing stage, various wet ingredients and dry ink ingredients are mixed together. The mixture of the ink's ingredients, at this stage, is often referred to as the 'pre-mix'. Pre-mixing is aimed at achieving key benefits, e.g., reduced milling times during the later stages of ink production. Pre-mixed dispersions are often prepared by using an overhead stirrer that is fitted with a serrated or saw-toothed mixer, also termed as a high speed disperser or open impeller. The primary action of the high speed disperser is providing mechanical shear. The mode of transmission of energy to the ink mixture involves adhesion between the saw-tooth blade and ink vehicle, cohesion within the ink vehicle and adhesion between the ink vehicle and particles to be dispersed (Lin 2003). The full benefits of pre-mixing can be achieved only if the process is carried out carefully. The viscosity of the pre-mix has the most significant effect on the effectiveness of the pre-mixing process (Todd 1994d). A pre-mix viscosity that is greater than 10000 mPa s will probably result in a doughnut-shaped surface during mixing if a serrated or saw-toothed stirrer blade is used. This can be considered as an indicator of the presence of high pigment-shearing action. At viscosities that are lower than 10000 mPa s, the shearing action is reduced. The ink formulator can overcome this problem by initially holding out part of the solvent to achieve higher pre-mix viscosity. Other factors

governing the efficiency of pre-mixing process include the stirrer geometry, in conjunction with the size of the vessel in which pre-mixing is carried out (Schak 1997).

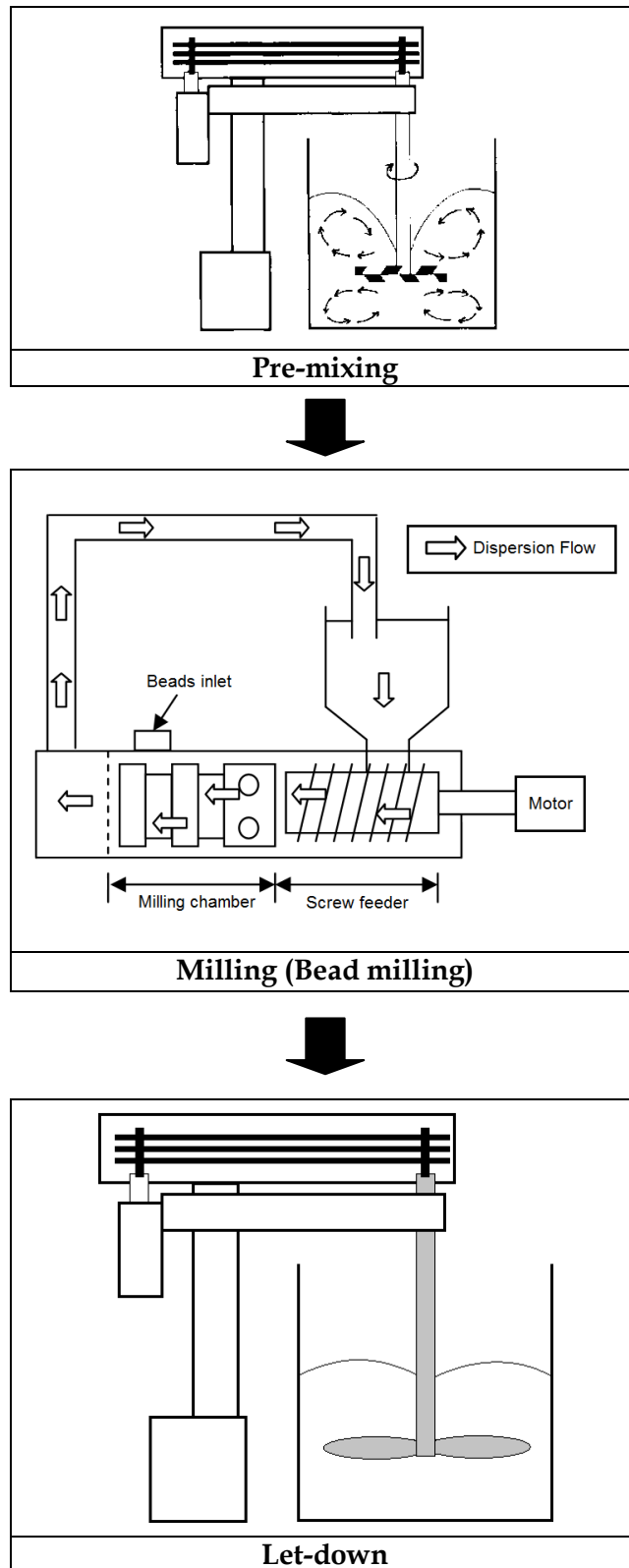


Figure 1-17: An overview of ink production process.

The second stage in production of inks is that of milling (Figure 1-17(b)). Milling is more severe process than pre-mixing. It is during this stage that the pigment particles are broken down into primary particles and distributed homogeneously in the ink vehicle. Organic pigments and carbon blacks are generally very difficult to disperse, particularly in aqueous media. This difficulty can be primarily attributed to the non-polar surfaces of such pigments. Conversely, ionically constructed inorganic pigments possess varying degrees of surface polarity and are relatively easy to disperse. There are, of course, many types and variations of milling machine. The selection of a particular milling process is dependent on many factors, including the viscosity of the premix, the ink vehicle, the solids content in the formulation, the pigment hardness, temperature limitations, aeration tendencies and so on. Some of the more common milling units include triple-roll mills, bead/sand mills and ball mills. Depending upon the design of milling equipment, single or multiple passes through a mill may be required to achieve the required ink characteristics. It is important to note that the main manufacturing cost in ink preparation is associated with the cost of pigment milling which has two components. One is the cost that is associated with the duration of the milling. The other component of cost is associated to the wear and tear on the milling equipment. Important aspects of the pigment dispersion preparation process, in the context of present study, are discussed in Section 1.9.

The last stage in the preparation of inks is known as the let-down. In this step, the proportions of ink components, (vehicle, binder and additives) that were left out of the pre-mixing and milling stages, are added. Mixers and dispersers of rather simple design, as depicted in Figure 1-17(c), are usually employed in this stage.

1.9 Pigment dispersion in the ink formulation process

In the process of ink formulation, the dispersion preparation is a vital step, if ready-made pigment dispersions are not employed. The pigment is wetted, dispersed and stabilised in the dispersion medium during the milling process. The traditional approach is to incorporate a polymeric binder as a 'grinding aid', to achieve one or more of the above mentioned purposes of milling and also to control some of the qualities of the finished ink. Maximising the pigment content during the milling stage offers economic benefits. However, special pigment wetting and dispersing additives

are usually required to significantly increase the pigment loading without generating adverse effects such as an increase in the viscosity of the dispersion during milling, strong thixotropy and a reduction in the gloss of the printed ink. For binder-containing pigment dispersions, relatively low dosages in the range of 1 - 3 % of wetting and dispersing additive(s) can produce impressive results. However, there are limitations. One of the major limitations of the more common carboxyl-functionalised acrylic and styrene-acrylic binders in solution is the limited compatibility of the resulting pigment dispersions with a wide range of let-down binders.

To tackle the limitations of binder-containing pigment dispersions, one approach is initially to prepare binder-free pigment dispersions followed by a separate let-down step in which the binder solution is added to produce the finished ink. An ideal binder-free pigment dispersion would consist of the pigment(s), the solvent(s), and dispersing additive(s) only. In practice, other auxiliary ingredients such as defoamers and preservatives are included in the formulation. The preparation of pigment dispersions without a binder puts pressing demands on the wetting and dispersing additives. Thus, the use of such additives is essential if one is to ensure that the required performance-related characteristics of the pigment(s) are achieved. Binder-free pigment dispersions are generally considered to be costly compared to binder-containing dispersions. This difference can be attributed primarily to the significantly large amounts of wetting and dispersing additives that are required for optimal formulation. However, with improvements in dispersant technology, it is now widely accepted that binder-free dispersions are not always more expensive than those in which a binder is added in the pigment milling stage (Cowley and Walsh 1997).

The current study has a focus on carbon black-containing, waterborne, electrically conductive inks. For this, aqueous binder-free pigment dispersions were produced in the first phase. The following characteristics were considered to be the necessary properties of the pigment dispersions.

- High pigment loading.
- Low viscosity for easy incorporation of binder during the let-down stage.
- Good storage stability without pigment sedimentation or increase in viscosity.
- Excellent compatibility with the let-down binders being used. This means that no re-flocculation should occur during or after let-down with binder.

- High electrical conductivity

A brief description of the properties of carbon black pigments, followed by an account of the various steps in their dispersion preparation processes are provided in the following sections.

1.9.1 Carbon black pigments

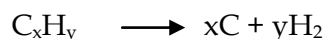
CI Pigment Black 7; CI No 77266; CAS No. 1333-86-4 (Clayton 1993)

Carbon blacks are considered to be a separate class of pigments because of their very small particle size and their structural complexity in relation to most of the other pigment types. More than 90% of current carbon black production is for the rubber industry. The plastic processing, printing ink and paint industries collectively form the market for the remaining 10% of worldwide production (Schumacher 1997). Besides their use as black pigments and UV protectors in composites, carbon black is widely used as conductive filler in insulating polymer systems (Bourrat 1993), (Zhang, Dehghani-Sanij and Blackburn 2007). The present study concerns the use of carbon black pigments as electrically conductive filler materials to impart conductivity to an essentially insulating matrix. Therefore, the important aspects of carbon black pigments are considered in the context of the electrical conductivity of carbon-containing composite systems.

Carbon black pigments are considered to be inorganic although they are primarily made up of elemental carbon. The primary particle size of carbon black pigments is typically the smallest of all pigments. The particle size range of the carbon black pigments that are used in inks is about 10-30 nm. Carbon black is not soot or black carbon, the two most common generic terms applied to various unwanted carbonaceous by-products that result from the incomplete combustion of carbon-containing materials, such as vegetable oils, fuel oils, coal, paper, rubber, plastics and waste material. Soot and black carbon also contain large quantities of dichloromethane extractable and toluene extractable materials. Such carbons can exhibit an ash content of 50% or more (Medalia, Rivin and Sanders 1983). Most types of carbon black pigment contain greater than 97% of elemental carbon, arranged as an aciniform (grape-like cluster) particulate. On the contrary, typically less than 60% of the total particle mass of soot or black carbon is composed of carbon.

1.9.1.1 Manufacture of carbon black pigments

Carbon black is a particulate form of industrial carbon that is produced by the thermal cracking or thermal decomposition of a hydrocarbon-based raw material. At high temperatures, that are usually achieved by incomplete combustion (limited oxygen supply), a hydrocarbon can be dissociated by the rupture of C-H bonds, as shown below:



The formation of elemental carbon is the first step in the formation of carbon black pigments. Following this “cracking” stage, the carbon and the aromatic radicals react to form a planar lattice of hexagonal carbon rings. These “layer planes” then stack together forming bundles, several layers thick, termed crystallites. Subsequently, these crystallites combine to form spherical primary particles. The primary particles further fuse forming the primary aggregates that are the characteristic of carbon black. Figure 1-18 shows the steps in the growth of the carbon black structure. The size and structure of carbon black can be controlled by controlling the reactor conditions. Some of the more widely used manufacturing processes are briefly discussed in the following text.

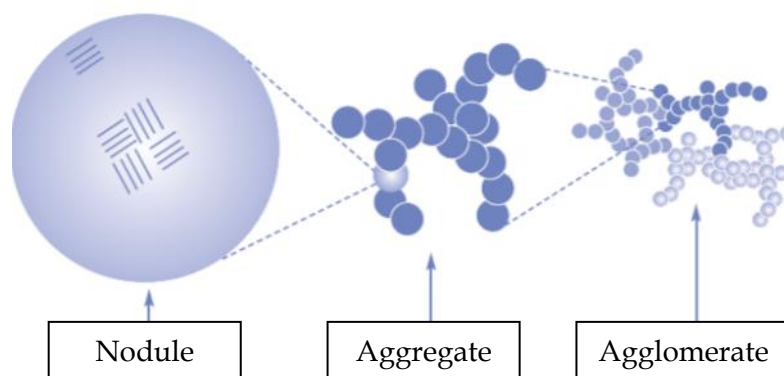


Figure 1-18: Sequence of the development of carbon black structure (© International Carbon Black Association).

a. Furnace Black Process

This method forms carbon blacks by blowing petroleum oil or coal oil as raw material into high-temperature gas flame to combust them partially, followed by quenching. This method is suitable for mass production due to its high yield, and allows ample control over carbon black properties such as particle size or structure. This is currently

the most common method used for manufacturing carbon black accounting for over 90% of the current worldwide production.

b. Channel Process

The channel process forms carbon black by bringing partially combusted fuel, often natural gas, in contact with cooled, U-shaped steel channels and then collecting the carbon black which deposits on the channels. There are yield issues and environmental issues around this method. Because of these points, this method has lost the leading role as a mass production process. However, the channel process provides carbon black particles that have various functional groups on the surface. Such grades of carbon black are used in applications that require excellent dispersibility, such as in printing inks.

c. Acetylene Black Process

This process produces carbon black by the controlled thermal decomposition of acetylene gas. It provides carbon black with higher structures and higher crystallinity. Such carbons are mainly used in applications where electrical conductivity is of prime interest.

d. Lampblack Process

Here carbon black is produced by collecting soot from the fumes that are generated by burning oils or pine wood. This is the oldest known method of producing carbon blacks and it is not amenable to mass production. Furthermore, there is virtually no control over the process parameters and, therefore, the properties of pigment.

1.9.1.2 The influence of the morphology on the properties of carbon black pigments

Non-conductive polymer composites can be made electrically conductive by the addition of a sufficient quantity of carbon black. Such conductivity is dependent on the polymer matrix, the type and loading of the carbon black and the distribution of the carbon black during and after the application of the composite. Conductivity is observed because of the formation of a continuous path for the flow of electrons. This continuous path is referred to as the percolation network. The formation of the percolation network is governed primarily by the quantity of carbon black which, in

turn, depends on the morphology of carbon black (Ehrburger-Dolle, Lahaye and Misono 1994). Any structural feature, such as porosity, which increases the specific volume of pigment, will also increase the possibility of closer contact between the adjacent carbon units (Ambrosetti et al. 2009). Figure 1-19 shows the morphology of a typical furnace carbon black. The major features having a significant effect on properties of a carbon black such as the blackness, the dispersibility and the electrical conductivity, are the particle size, the structure and the surface chemistry (Lahaye and Ehrburger-Dolle 1994).

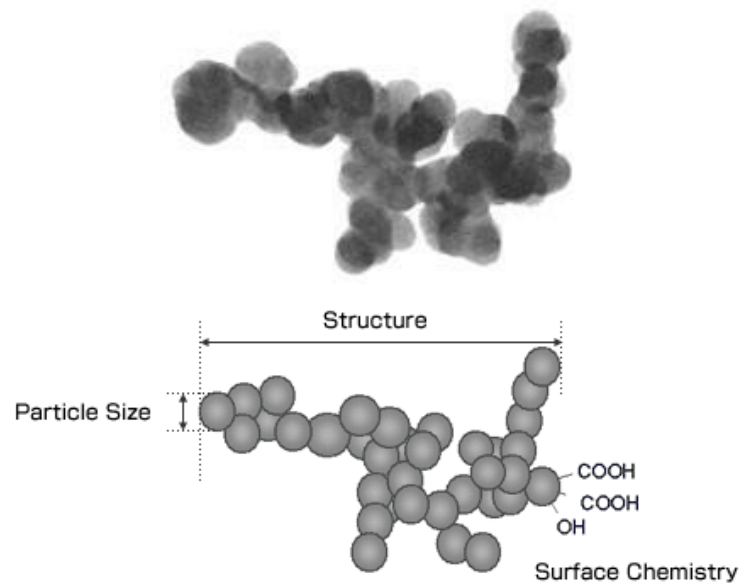


Figure 1-19: Structural features of carbon black pigment (© Mitsubishi Chemical Corporation).

a. Particle size

The particle size of carbon black is often used to represent the diameter of the particle that makes up the primary aggregates of the pigment. Since the surface area is expressed per unit mass, the greater the surface area per unit mass, the smaller would be the particle size (assuming the use of standard low porosity grades). The smaller the carbonised droplets or nodules that comprise the carbon black aggregates are, the tighter is the packing ability of the aggregates. Tighter packing results in smaller gaps between the conductive carbon units and a closer resemblance to a continuous conductive medium. This point is especially important for good conductivity to be achieved.

b. Structure

A carbon black pigment whose primary aggregates are composed of many primary particles, with considerable branching and chaining, is referred to as a high-structure black. If the primary aggregates consist of relatively few primary particles that form a more compact unit, the carbon black is referred to as low-structure carbon black.

Low-structure carbon blacks allow greater pigment loadings to be used and impart greater gloss because of their lower vehicle demand. Low-structure blacks have less occluded air and, thus, are easier to wet-out than are the high-structure blacks. However, because of the closer packing of the aggregates, they are more difficult to disperse (Liang and Yang 2007). At a given weight loading, the probability of closer contact between the adjacent carbon black aggregates increases with an increase in the structure of the carbon black aggregates. It is believed that for good conductivity, the adjacent carbon black aggregates must be within about 5 nm, so that electron transfer by tunnelling mechanisms can occur (Jager et al. 2001).

c. Surface chemistry

Carbon blacks of the same particle morphology may vary considerably in their ease of dispersion. Such differences in dispersibility can be attributed to the amount of chemisorbed complexes which, in turn, depends on the manufacturing method and on the raw materials used. The term "volatile content" is used in the industry to quantify the chemisorbed complexes, since these complexes can be driven off by heating the carbon black to 960 °C. Besides sulphur, nitrogen and small amounts of trace metals, oxygen-complexes are also present on the pigment surface. It is known that the oxygen on the surface of a carbon black particle influences the technical use this material more than does any other type of chemisorbed complex. The more important oxygen atom sources are carboxyl groups (acidic), lactol groups (acidic), phenol groups (acidic), quinoid carbonyl groups (acidic) and pyrone groups (basic) (Schumacher 1997).

It should be noted that the concept of the volatile material content does not include absorbed moisture. The polar chemisorbed oxygen sources increase the wettability of the carbon black surface by polar solvents and resin precursors. The increased wettability results in the better and faster dispersion of the carbon black in a polar dispersion medium (Boehm 1994), (Okazaki and Tsubokawa 2000). To chemically

modify the surface, carbon blacks are subjected to a variety of techniques (Papirer, Lacroix and Donnet 1996). While a high volatile content is generally desired by the coating/ink producer, it increases the surface resistivity because the oxygen-containing fractions act as an electrically insulating layer on the surface of the carbon black aggregates. The increase in volatile content creates a dramatic increase in the surface resistivity for both the large surface area/high structure grades and for the small surface area/low structure grades of carbon black (Pantea et al. 2001).

1.9.2 Physico-chemical aspects of pigment dispersion preparation

As shown in Figure 1-20, the process of pigment dispersion preparation involves physico-chemical actions as well as the use of mechanical forces to break down and to distribute homogeneously the pigment particles in the ink vehicle.

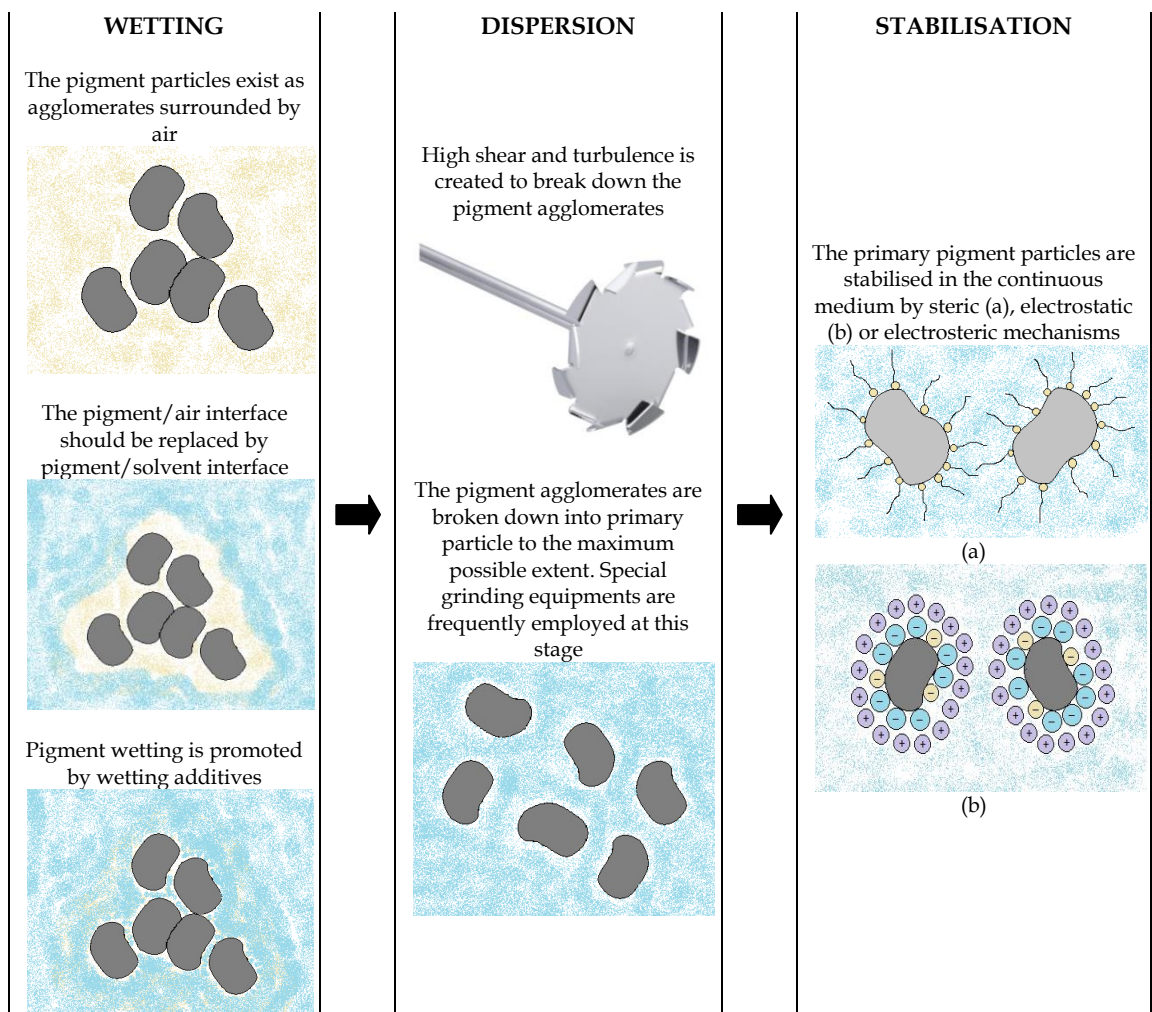


Figure 1-20: Steps in pigment dispersion preparation.

In general, the required physico-chemical actions are achieved by the addition of one or more chemically compatible wetting and dispersing additives that are incorporated into the formulation. These interact with the pigment particles and stabilise them by various mechanisms, as discussed in detail in Section 1.9.3. The use of effective dispersion preparation equipment furnishes the mechanical forces that are required to breakdown the particle assemblies and to distribute the pigment particles. Each of the steps, i.e., pigment wetting, break down of agglomerates and stabilisation of dispersed particles should be efficiently performed with the aid of either physico-chemical interactions or the application of mechanical force or both. A more detailed account of the pigment dispersion process is given in the following sections.

1.9.2.1 Pigment Wetting

In powder form, pigment particles exist as agglomerates that are surrounded by air. In a pigment agglomerate, the edges and corners of the primary particles are in contact. Thus, such structures are relatively easy to break. In the case of carbon black pigments, the tendency of the primary particles to agglomerate is more pronounced due to the large surface area that is generally associated with these pigments. Consequently, a large amount of air can be trapped in a given volume of pigment powder. During the pigment wetting stage, air surrounding the pigment particle surface is replaced by the dispersion medium, i.e., the solvent (with or without the binder). Thus, the wetting process involves three phases; the solid phase, the liquid phase and the vapour phase. The wetting of a pigment particle surface depends on the interactions between these three phases and can be correlated to the velocity of penetration of a liquid (vehicle or binder solution) into the pigment powder. The Washburn equation (Equation 1) can be used to represent the velocity of penetration, ignoring the effects of gravity, in such a system.

$$V = \frac{dl}{dt} = \frac{r}{2l\eta} \gamma \cos \theta \quad \text{Equation 1}$$

In Equation 1,

V = Speed of wetting

l = Depth of penetration

t = Time

r = Radius of capillary

η = Viscosity of dispersion medium

γ = Surface tension of dispersion medium

θ = Contact angle

During dispersion preparation, there is virtually no control over the factors represented in Equation 1. The term $\gamma \cos \theta$ is an exception. This can be altered in a controlled way by incorporating a wetting additive. An understanding of the interfacial free energies that are involved when a solid, a liquid and/or air are brought into contact, can help to provide an explanation of how wetting additives can improve pigment wetting.

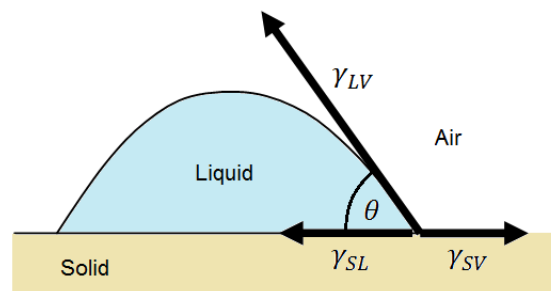


Figure 1-21: Interfacial energies at solid-liquid-air interface

Figure 1-21 shows the geometry of a small amount of liquid on a solid surface. If the liquid is in equilibrium with its vapour, the Young-Dupre equation (Equation 2) can be used to describe the equilibrium relationship.

$$\gamma_{SV} = \gamma_{SL} + \gamma_{LV} \cos \theta \quad \text{Equation 2}$$

In Equation 2,

γ_{SV} = Interfacial free energy of solid/air

γ_{SL} = Interfacial free energy of solid/liquid

γ_{LV} = Interfacial free energy of liquid/air

θ = Equilibrium contact angle between the solid and liquid phases

The use of wetting agents reduces both γ_{SL} and γ_{LV} . As a result, θ is reduced. This implies that there will be improved wetting of the pigment surface. It is important to note that addition of wetting agents will reduce both γ_{LV} and θ . Of the two, a low value for the contact angle θ is the more important. The wetting of the pigment particles initiates breakdown of the pigment flocculates and of most of the agglomerates. This is beneficial in reducing the energy and the time required for dispersion preparation.

Depending on the molecular structure of the dispersant that is used, a wetting additive may or may not be required during the pigment wetting stage. If the dispersant possesses an interfacially active molecular structure, it will migrate to the pigment-solvent interface where it will function as a wetting additive by altering the surface tension of the solvent.

1.9.2.2 Breaking down of pigment aggregates/agglomerates

After the pigment agglomerates have been wetted out by the dispersion medium, mechanical energy is used to break down the pigment agglomerates. The milling machines that are used for wet comminution belong to one of the six categories; Impeller mills, ball mills, small media mills (sand and bead mills), vibratory mills, roll mills and ultrasonic dispersers (Conley 1996). De-agglomeration is brought about by shearing and comminution. The mechanical energy furnished by the milling equipment must be efficiently transmitted to the pigment particles to ensure proper milling (Lin 2003). An ideal dispersion is achieved when all of the agglomerates are broken down into primary particles and no further particle size reduction is possible. One needs to be aware of the possibility of subsequent particle re-agglomeration, after milling.

The effects of particle size, structure and surface chemistry on the dispersibility of carbon black pigment were considered, in detail, in Section 1.9.1.2. Smaller particles result in a larger surface area to be wetted. A closer packing of the aggregates occurs in the low-structure blacks thus making such carbon blacks difficult to disperse. Carbon black having a high volatile content gives better dispersibility than that possessed by a carbon black of similar particle size but lacking the surface complexes. In general, carbon blacks are difficult to disperse and require the input of very high energy to break up the agglomerates. For this purpose, several variations of pigment milling equipment are employed, depending upon a number of factors such as the premix viscosity, the type of pigment, the required level of milling and the required finished ink characteristics.

1.9.2.3 Stabilisation of primary pigment particles

The broken pigment particles must be stabilised in the dispersion medium if one wishes to achieve the required characteristics for the dispersion. The stabilisation of the pigment particles must be maintained during storage and application. It is during the pigment milling stage that the dispersant molecules interact (adsorb) onto the pigment surface and maintain proper spacing between the dispersed pigment particles, providing stabilisation by a number of different mechanisms, as discussed in the following section.

1.9.3 Pigment stabilisation mechanisms

A common phenomenon that occurs as a result of dispersion instability in ink/coating systems is flocculation. Flocculation is a process in which smaller particles join together to form large clusters that possess lesser interfacial free energy than the smaller particles. Flocculation occurs as a consequence of the random Brownian motion of the particles, which results in collisions of the particles. Collisions of particles also occur as the particles move under the influence of gravity. The influence of gravity is more important generally for coarser pigment particles, having average particle sizes that are greater than 1 micron (Bieleman 2000).

The Brownian motion of particles is greatly influenced by the temperature and the viscosity of the continuous phase or the dispersion medium. Besides the kinetic energy of the particles, attractive and repulsive inter-particle forces also act, the stability of a dispersion being governed by the resulting interactions. For example, the collision of particles due to Brownian motion is likely to allow short range van der Waals forces to bind the particles, if a means of restricting such collisions is absent. These intermolecular interactions are of great relevance to the current study because it was crucial to ensure that the conductive grades of carbon black pigment are dispersed effectively and stabilised in the dispersion medium. Examples of the intermolecular forces include:

- London - van der Waals forces are the dominant attractive forces in colloidal dispersions resulting from interactions between the dipoles in the particles. These attractive forces are weaker than ionic forces or covalent bonds. Usually the strength of this force is proportional to the particle size and inversely

proportional to the distance between the particles. As the inter-particle distance decreases, the attractive effect increases rapidly to a maximum.

- Electrostatic attractive or repulsive forces act in accordance with Coulomb's law, as expressed in Equation 3. In case of colloidal dispersions, the Coulombic forces arise due to the charges on the pigment surfaces. In Equation 3, F is the electrostatic force, k is the Coulomb's constant, q_1 and q_2 are the magnitude of interacting charges and r is the distance between the charged species.

$$F = k \frac{q_1 q_2}{r^2} \quad \text{Equation 3}$$

- Hydrogen bonding, for which the strength is greater than those of London - van der Waals forces. However, the attractive effect acts over a shorter range.
- Repulsive forces (e.g., in the cases of steric hindrance) or attractive forces (e.g., in the cases of polymer bridging between particles) as generated by layers of surfactants and/or polymers that are adsorbed onto the pigment surface.

The dispersion stability can be established by using a 'Potential energy curve', as shown in Figure 1-22. The potential curve of a colloidal system relates the particle-particle separation to the attractive potential energies, to the repulsive potential energies and to the resulting overall interactions. In general, a dispersion is considered to be stable if certain conditions for intermolecular interactions are satisfied. These are that the net repulsive force is greater than the net attractive force between the particles and that the magnitude of net repulsive force is several orders of magnitude greater than the thermal energy of particles (Marmur 1979).

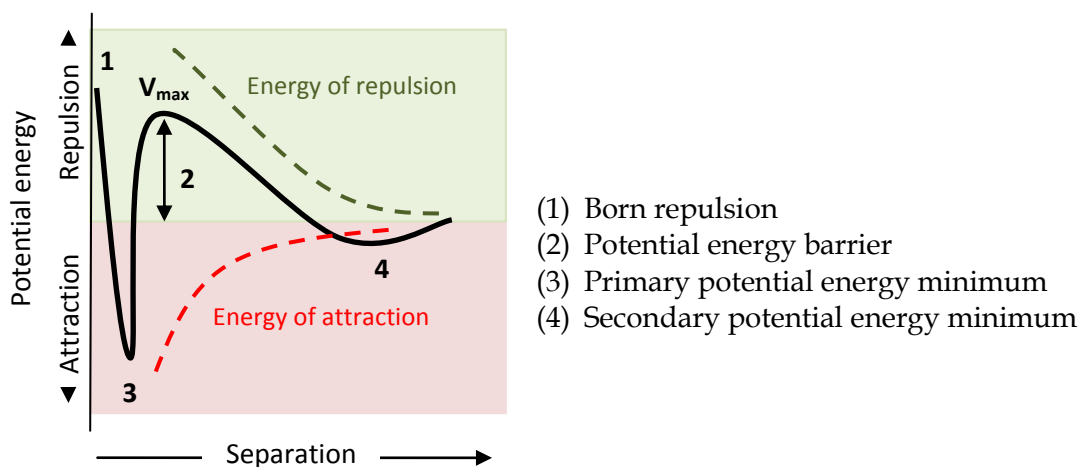


Figure 1-22: Interaction potential between particles as a function of particle separation.

In Figure 1-22, (1) represents very strong repulsion when particles are extremely close to each other. This strong repulsion is generally attributed to orbital overlap. At the primary minimum (3), the attraction between particles is maximum and results in spontaneous aggregation. To achieve a desired level of stability, various mechanisms of repulsion can be employed to increase the potential barrier, V_{\max} (2), to a level at which it cannot be overcome by the pigment particles at the expense of their kinetic energy, i.e., $V_{\max} \gg kT$. The repulsive forces between the pigment particles can be furnished by the compression of the electrical double layer around the particles, by polymer chain compression, by osmotic pressure effects and from the presence of any non-adsorbed polymer. The means of particle-particle repulsion, and their combinations thereof, are grouped in different categories of stabilisation mechanisms, as discussed in the following sections.

1.9.3.1 Electrostatic stabilisation

Pigment particles that are in a liquid medium can have electrically charged surfaces. The surface charge appears because of preferential adsorption of certain ions, of charged organic molecules or through the dissociation of ionic groups on the surface of the pigment. In electrostatic stabilisation, the dispersant increases the magnitude of the surface charge and also creates an equivalent charge on all the pigment particles. Thus, stabilisation of the particles results from Coulombs electrostatic repulsion forces, as shown in Figure 1-23.

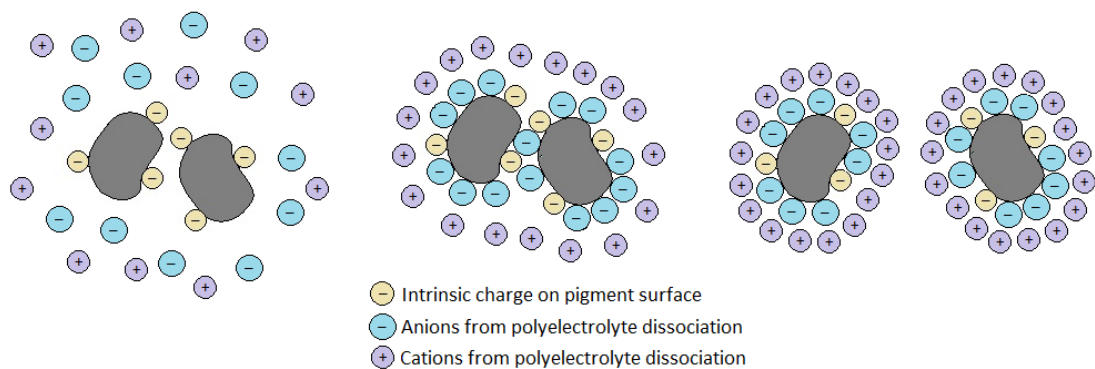


Figure 1-23: Mechanism of electrostatic stabilisation

The dispersant that create electrostatic repulsion between pigment particles are often referred to as polyelectrolytes (polyanions, polycations, polyampholytes) or polysalts. These are high molecular weight products that contain a multitude of charged groups in the polymer side chains. In aqueous media, the groups in the side chains dissociate, rendering the polymer charged. The charged polymer adsorbs and transfers its charge to the pigment surface. Counter ions in the vicinity accumulate around the charged pigment particle, forming an electric double layer. Flocculation is prevented by the compression of electrical double layer and by the electrostatic repulsive forces that act as two pigment particles approach close to each other. The stability of the particles is proportional to the thickness of electrical double layer which, in turn, is sensitive to the type and amount of electrolytes in the dispersion medium. The electrostatic stabilisation mechanism is effective in media that possess high dielectric constant, such as water. This mechanism of stabilisation is practically of lesser importance because most industrial aqueous formulations contain significant amounts of one or more electrolytes.

The DLVO theory, proposed independently by Derjaguin and Landau and Verwey and Overbeek, describes the interaction between London - van der Waals attraction forces and electrostatic repulsive forces. The DLVO theory is generally applied to aqueous systems in which the effect of steric/entropic stabilisation is negligible and the net interaction (V_{total}) between particles that results is only due to the ionically adsorbed dispersing additives. The DLVO theory has been extended to non-aqueous systems and/or non-polar systems in which the medium possesses intermediate dielectric constants (McGown and Parfitt 1966).

In case of aqueous dispersions, the potential curve (V_{total} as a function of particle-particle separation) always contains two minima, as shown in Figure 1-22. As discussed in preceding text, the first minimum corresponds to spontaneous aggregation while the second minimum corresponds to presence of flocculates that can be broken by shaking or by other means of providing relatively small energy input.

Sufficient electrostatic stabilisation is achieved when surface charge is great, which increases the potential barrier. Two of the conditions that reduce V_{max} and thus destabilise the dispersion, are as follows.

- Low magnitude of surface charge due to the presence of only few dispersant molecules on the surface of pigment.
- High concentration of electrolytes which can neutralise the charge on the pigment surface.

A good measure of electrostatic stabilisation is the zeta potential. This is the potential at the hydrodynamic slipping plane. In effect, it is the potential across the diffuse layer of ions surrounding a charged colloidal particle (Section 1.10.3). Zeta potential in the range of -50 mV to -100 mV indicates a stable dispersion in the case of aqueous systems. The zeta potential is the main component of surface potential and it can be calculated using data from electrophoresis studies or other means of measuring the mobility of the suspended particles in an electric field. Equation 4 relates the zeta potential to other factors in such measurements.

$$\zeta = 4\pi\eta U/H\varepsilon \quad \text{Equation 4}$$

In Equation 4,

ζ = Zeta potential

η = Viscosity of dispersion medium

U = Electrophoretic mobility

H = Electrical intensity of the externally applied electric field

ε = Dielectric constant of the dispersion medium

1.9.3.2 Steric stabilisation

The work of Napper and co-workers (Napper 1970) has provided a foundation for the current understanding of the steric stabilisation mechanism. For steric stabilisation, the dispersants employed are polymeric species that consist of one or more pigment-affinic groups and one or more binder and/or solvent-compatible chains in the structure. Polymeric dispersants possessing interfacially active molecular structure also function as wetting additives. The pigment affinic groups in sterically stabilising dispersant molecules anchor strongly onto the pigment surface while the binder-compatible hydrocarbon chains extend into the medium, as shown in Figure 1-24. As two particles approach close to one another, the polymeric chain segments are compressed. This thermodynamically unfavourable compression (decrease in entropy) of the polymer

chains results strong repulsion between the particles, thus providing the required potential barrier for stabilisation. In addition, as the polymeric chains overlap, the dispersion medium is forced out from this region of increased polymer concentration. This localised increase in polymer concentration results in an osmotic pressure that tends to force the medium back between particles, thus maintaining separation between the particles.

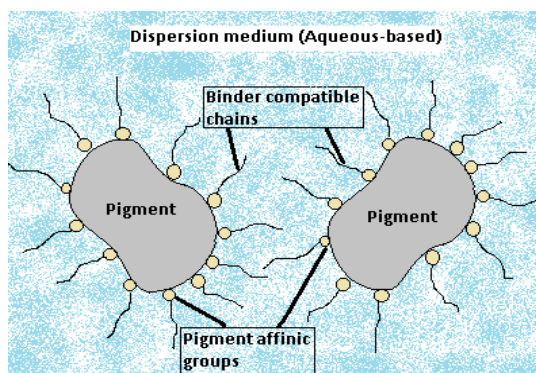


Figure 1-24: Mechanism of steric stabilisation.

Certain conditions, listed below and discussed in more detail in Section 1.9.4, need to be fulfilled for effective steric stabilisation (Jerome 1992).

- Dispersant molecules must completely cover the pigment surface.
- Strong anchoring of the dispersant molecule onto the pigment surface. This is crucial to avoid desorption of dispersant molecule during the dilution of the dispersion.
- Sufficient thickness of the adsorbed layer to ensure that the London - van der Waals forces do not overcome the repulsion forces that are furnished by the segments of dispersant molecules the dangle in the dispersion medium.
- The polymeric chains that dangle in the solvent must be fully solvated so that the chains are in a stretched form, in order to build up the maximum layer thickness.

1.9.3.3 Other stabilisation mechanisms

Besides electrostatic and steric stabilisation, other mechanisms, such as electrosteric and depletion stabilisation, also exist (Shi 2002). Several newly marketed dispersants are claimed to provide robust stabilisation of dispersed pigments by electrosteric

stabilisation, in which the dispersant furnishes both steric hindrance and electrostatic repulsion between the pigment particles. The depletion mechanism of stabilisation, which is of lesser importance, requires the pigment particles to force out non-adsorbed polymers as the particles approach close to each other.

1.9.4 Classification and selection of dispersing additives

A classification of dispersing additives on the basis of their chemical composition and their structure is shown in Figure 1-25 (Kissa 1999e). Inorganic dispersants are of no interest in the present study and hence these are not discussed. Organic dispersants are physico-chemically amphiphilic substances i.e., they possess polar-apolar duality, as shown in Figure 1-26. One part of the dispersant molecule is polar and contains heteroatoms such as O, S, P or N. The polar segment exhibits strong affinity for polar media such as water. The other part of the molecule is a non-polar hydrocarbon chain of the alkyl type or of the alkylbenzene type and exhibits hydrophobicity. It is due to this surfactant type of structure of the molecule that the dispersants are interfacially active materials. In some cases, however, the same effect of selective adsorption and solubilisation in a single molecule can be achieved by covalently bonding the soluble polymer directly to the particle (Laible and Hamann 1980).

Higher molecular weight polymeric dispersants are more effective in stabilising a pigment than are low molecular weight dispersants, especially in situations where the conditions for effective stabilisation, as described in Section 1.9.3, have to be fulfilled. The number of adsorption contacts per molecule that are offered by high molecular weight dispersants is large compared to that from low molecular weight dispersants. Therefore, for high molecular weight dispersants, the total sum of adsorption energies per molecule is very great, which results in strong binding of the dispersant molecule onto the pigment surface. In contrast, for a low molecular weight dispersant, which furnishes a small number of adsorption contacts, for example, one linkage per molecule, the chances of complete desorption are statistically great (Bieleman et al. 2000). Important factors to consider in the use of high molecular weight dispersants are the nature of stabilising polymeric chain and the configuration of dispersant molecule.

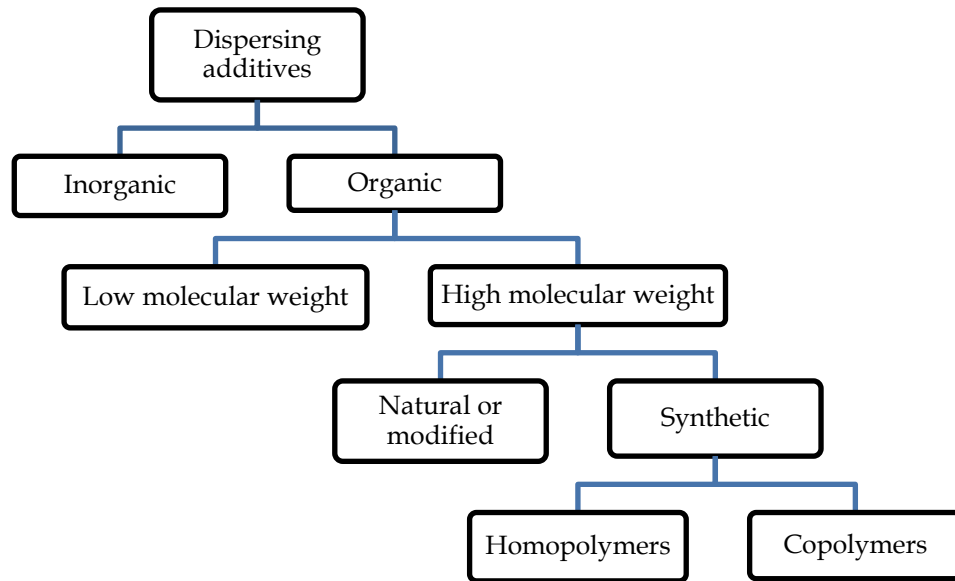


Figure 1-25: Classification of dispersants.



Figure 1-26: Amphiphilic molecule of a dispersing additive.

The binder and/or solvent-compatible chain in a dispersant molecule is the stabilising part of the molecule. The dispersant molecules should form a sufficiently thick layer on the pigment surface to prevent van der Waals forces of attraction from overcoming the repulsive forces that are furnished by the polymeric chains dangling into the solvent. A layer thickness of 5 – 20 nm is considered sufficient to stabilise pigment particles that have an average size of 0.1 – 10 μm , (assuming that the interaction between polymeric layers is purely repulsive), (Schofield 1987). The factors influencing the thickness of protective barrier provided by the stabilising polymeric chains include the molecular weight of dispersant molecules and the solubility of the polymeric chains. Thus, the molecular weight of dispersant molecule should be great enough to provide polymeric chains of sufficient length. For example, in case of block copolymers, stabilisation is possible with chains of molecular mass in the range of 1000 – 15000 g/mol (Jerome 1992). However, the effectiveness of a dispersant molecule ceases to exist over an optimum length of the polymeric chain. Also, the stabilising polymeric chains in a dispersant molecule should be solvated enough to be completely mobile in the liquid phase. If the solubility is decreased, the thickness of protective barrier around the

pigment particles also decreases. Thus, the stabilisation effect is reduced. During drying of the ink/coating later, the pigment may flocculate, if the solubility of the polymeric chains is reduced.

In polymeric dispersants, both homopolymer and copolymer molecular configurations can be used. A homopolymer molecule can be regarded as the simplest molecular configuration for a dispersant. A homopolymeric dispersant will preferentially interact with either the solvent/dispersion medium or with the pigment surface. Furthermore, it has been shown that the high free energy of even strongly adsorbed polymer drives slow desorption from the pigment surface (Russel, Saville and Schowalter 1989). Thus, the effectiveness and robustness of stabilisation provided by homopolymer dispersants is limited. Several copolymeric molecular configurations are also possible for dispersants (Jakubauskas 1986). For industrial applications that involve the preparation of concentrated suspensions, copolymeric dispersants are considered to be the most effective (Barrett 1973).

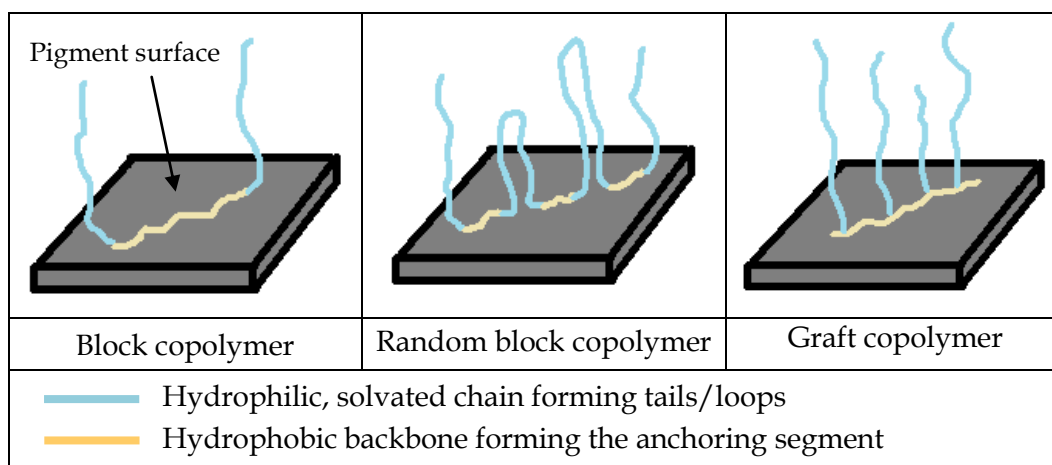


Figure 1-27: Adsorption of various types of high molecular weight copolymeric dispersants onto pigment surface – diagrammatic representation.

Figure 1-27 depicts, schematically, the adsorption of different copolymeric dispersant molecules onto the surface of a pigment. Depending upon the distribution of the monomeric segments in the polymeric chain, copolymeric dispersants can be subdivided further into three categories.

1. Mass or block copolymers - the pigment affinic groups (A) and the solvent compatible chains (B) are arranged into blocks. Common configurations are A-B, A-B-A and B-A-B.
2. Statistical/Random block copolymers - the pigment affinic groups (A) and the solvent compatible chains (B) are distributed arbitrarily in the polymer chain.
3. Graft copolymers - such polymers usually consist of a linear homopolymer backbone, on which side chains of other monomer blocks are grafted. However, in some instances, the polymer backbone may be a block copolymer.

The ionic nature of the dispersant molecule, the type of pigment (organic or inorganic) and the nature of the continuous medium (aqueous based or non-aqueous based) are the major factors that one needs to consider in the selection of dispersants.

As shown in Figure 1-28, the stabilisation mechanism in action depends to a great extent on the continuous medium. For organic solvent-based systems, steric stabilisation is usually the main stabilisation mechanism while, for aqueous-based systems, electrostatic, hybrid or steric mechanisms occur, depending on the characteristics of the particular dispersion.

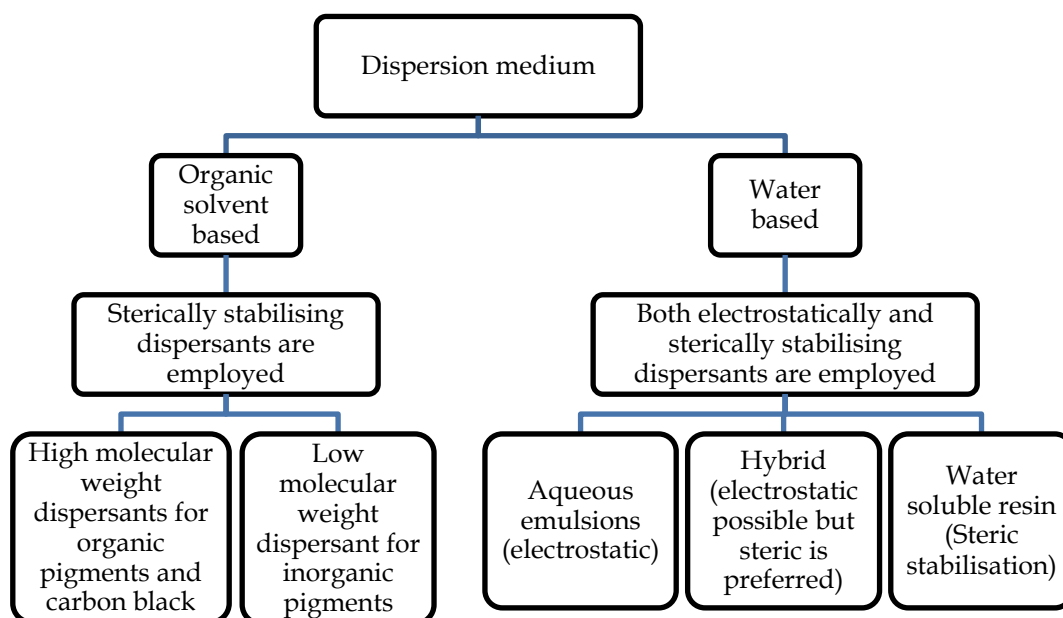


Figure 1-28: Dispersant selection criteria based on the nature of dispersion medium.

On the basis of the dissociation of polar groups in water, dispersants can also be classified as being one of anionic, cationic, amphoteric and non-ionic in character. In

conjunction with the nature of the dispersion medium, the ionic nature also dictates the stabilisation mechanism that is furnished by a dispersant. Anionic dispersing additives dissociate in aqueous media into an amphiphilic anion and a cation. The hydrophobic segment of the anion adsorbs onto the pigment surface while the negatively charged polar segment extends into the dispersion medium (aqueous), as depicted in Figure 1-29. Thus, the pigment particles acquire an overall negative charge and are electrostatically stabilised. Di-alkyl sulphosuccinates and lignosulphonates are examples of anionic wetting and dispersing additives.

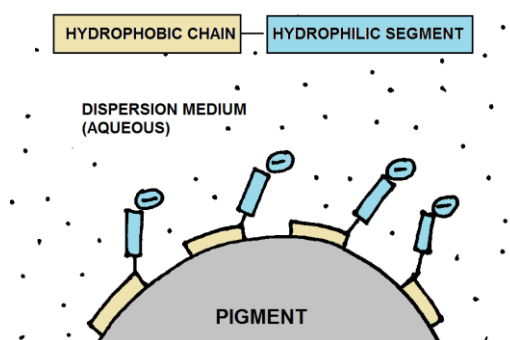


Figure 1-29: Adsorption of anionic dispersant molecules onto the pigment surface.

Cationic dispersing additives, which dissociate into a cationic amphiphile and an anion, are suitable for oleophilic media that contain negatively charged particles. The hydrophilic cationic segment of the ionised molecule adsorbs onto the pigment surface and the hydrophobic segment protrudes into the dispersion medium, as shown in Figure 1-30. Cationic dispersing additives suffer two major limitations. These are their high cost and their sensitivity to pH changes in the aqueous medium.

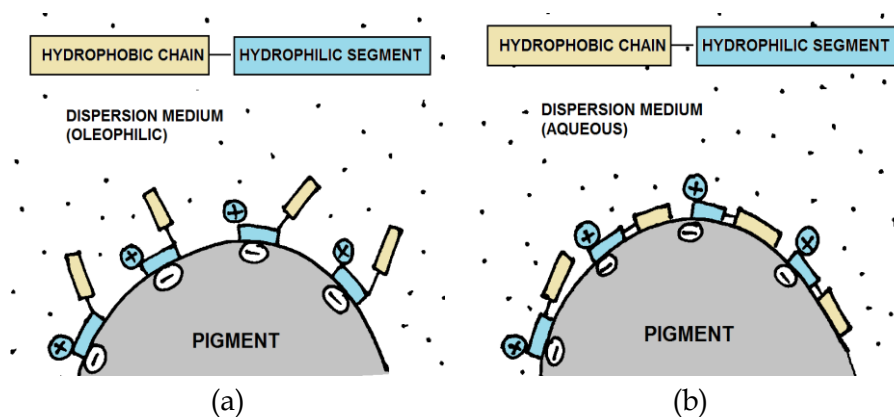


Figure 1-30: Adsorption of cationic dispersant molecules onto the pigment surface in (a) oleophilic medium and (b) aqueous medium.

Non-ionic dispersants do not dissociate into charged species when added into the dispersion medium. In most cases, hydrophilic steric stabilising chains are usually based on alkoxy chemistry (based on for example, polymers of ethylene or propylene oxide). Thus, such dispersants are often referred to as polyethoxylated, non-ionic dispersants. The hydrophobic segment in non-ionic dispersants is an alkyl type or alkylbenzene type, for instance, acrylic and styrene-acrylic polymers. The pigment attachment is due to the hydrophobic nature of the backbone, as shown in Figure 1-31. Non-ionic dispersants are very effective, especially for pigments with non-polar surfaces, such as carbon blacks. Moreover, the functioning of this type of dispersants is not affected by pH changes.

Practically, there are other factors such as the interactions between dispersants when more than one type is used, the effects of co-solvents and the application related factors, such as the pH stability, which should be considered in the selection of dispersants. In the light of the review of the literature that is presented here, a number of high molecular weight non-ionic polymeric dispersants were selected for use in this research programme for the preparation of binder-free waterborne pigment dispersions of various grades of carbon black pigment.

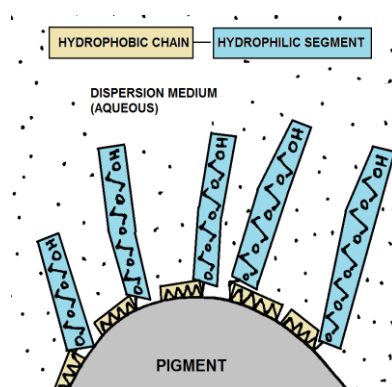


Figure 1-31: Adsorption of non-ionic dispersant molecules onto the pigment surface.

1.10 Characterisation of the stability of dispersions

The stability of a pigment dispersion has to be established before the dispersion can be formulated into an ink or a coating system. This is because an unstable dispersion is likely to result in an under-performing finished ink/coating. For instance, in the

context of the present study, maintaining the dispersed state of pigment is important for there to be high electrical conductivity with the final ink deposit. The pigment particles should maintain their state of dispersion during storage, during ink preparation processes and even after application.

Dispersion evaluation methods can be broadly categorised into qualitative methods, semi-quantitative methods and quantitative methods. The more common characterisation methods that are applied to dispersions are listed in Table 1-5 (Kissa 1999b).

An “ideal” pigment dispersion is one in which the pigment particles exist in the form of primary particles, i.e., particles that cannot be broken down into smaller entities. In an unstable pigment dispersion, the number of pigment particles per unit volume of the dispersion medium decreases during storage for a specified time period. This is because the dispersed primary pigment particles are constantly acted upon by several forces that cause the particles to join together to form larger particles; a process generally referred to as aggregation. The forces acting on a dispersed particle include the gravitational force, the Brownian force and particle-particle interactions. The effects of these forces are considered in Section 1.9.3. Dispersion characterisation techniques are designed according to the different phenomena that operate due to these forces acting on the particle. Below, relevant dispersion characterisation techniques are discussed.

Table 1-5: Tests employed for dispersion characterisation

Characterisation method	Analysis type
Qualitative microscopy	Qualitative
Fineness tests	Qualitative
Sedimentation tests	Semi-quantitative and Quantitative
Viscosity	Qualitative and quantitative
Solids content	Quantitative
Particle size distribution	Qualitative and quantitative
Electrical properties	Quantitative

1.10.1 Sedimentation analysis

The gravitational force can cause the pigment particle to settle to the bottom in the vehicle, a process known as sedimentation. The rate of sedimentation, i.e., the amount of settled particles per unit time, is directly proportional to the density of particles and inversely proportional to the viscosity of continuous phase (Kissa 1999d). This implies that in a poly-disperse pigment dispersion, the settling/sedimentation rate varies for the dispersed pigment particles. As a dispersed pigment particle falls down in the continuous phase, it may collide with other slowly descending particles and form an aggregate. As in case of individual pigment particles, the gravitational force increases as the weight of an aggregate of particles increases. The resistance to settling, however, increases as the size of aggregate increases. Stoke's law, expressed by Equation 5 below, can be used to define the sedimentation behaviour of an isolated particle.

$$\frac{dx}{dt} = \frac{2r^2}{9\eta}(\rho_p - \rho_c)g \quad \text{Equation 5}$$

In Equation 5 above,

$\frac{dx}{dt}$ = sedimentation rate

r = effective radius of the particle

η = Viscosity of the continuous phase

ρ_p = Density of the dispersed particle

ρ_c = Density of the continuous phase

g = acceleration due to gravity

Stokes law is valid if certain assumptions are met. One is that the dispersed particle is spherical. In case of non-spherical particles, the application of Stokes law yields the Stokes diameter, which is "the effective particle size corresponding to the size of a sphere that would fall at the same velocity" (Hostomský et al. 1986). Another assumption is that the settling of dispersed particles is unhindered, i.e., no interactions occur between the dispersed particles and between the dispersed particles and the walls of the vessel. To exclude interactions between the dispersed particles, the maximum particle loading is limited to 0.2% to 1.0% in solids. BS 3046 recommends a loading of 0.1% by volume. In case of the hindered settling of particles, the mechanisms involved are very complex. Thus, the Stokes law cannot be applied (Doheim, Abu-Ali and Mabrouk 1997). A further assumption is that the movement of dispersed particles is that of free fall under laminar flow conditions.

From Equation 5, it is evident that no dispersion is truly stable. However, the sedimentation rate can be controlled in one or more of the following ways.

- Reducing the particle size (r) exponentially decreases the sedimentation rate.
- Increasing the viscosity of continuous phase reduces the sedimentation rate. The viscosity of the continuous phase can be increased by using an appropriate rheology modifier (thickener). In most cases, the viscosity of the dispersion increases as the pigment loading is increased, which is an advantage.
- Aggregation of dispersed particles can be prevented by using particle stabilisation entities, generally referred to as 'dispersants'. Dispersants and their role in stabilising pigment particles are discussed in detail in Section 1.9.3 and Section 1.9.4.

1.10.1.1 Characterisation of sedimentation

The characterisation techniques applied to study sedimentation process can be grouped into the following categories.

- Gravitational sedimentation
- Centrifugal sedimentation
- Electrophoretic sedimentation

In sedimentation, the parameters that influence the sedimentation process, in the dispersion being studied, are the sedimentation rate, sedimentation volume, particle size distribution during settling and the stability of the dispersions to sedimentation (i.e., the time required for a given amount of sediment to develop).

In this study, centrifugal sedimentation was used in the stability analyses of dispersions. The advantage of this technique is that strong centrifugal forces accelerate sedimentation and, thus, it is possible to complete the required analysis in a reasonable time (Jansen, de Kruif and Vrij 1986). Particularly for a carbon black pigment which generally exists as sub-micrometre size particles (0.5 - 1 μm), very lengthy settling times are required. Therefore, centrifugal methods are more practical compared to gravitational methods (Allen and Baudet 1977).

Among the various types of centrifuge that can be employed for the analysis of dispersions are laboratory centrifuges, ultracentrifuges and disk centrifuges. Conventional laboratory centrifuges can be conveniently used to assess the stability of a dispersion qualitatively. The technique, however, is not applicable if particle size analysis is required or if the required distinct layers in the dispersion are not clear enough for visual assessment, i.e., if the dispersion is very stable.

The ultra-centrifuge was developed by Svedberg and co-workers (Svedberg and Rinde 1924). With the advent of low cost computers and sophisticated electronic feedback circuits, the technique has become popular for dispersion analysis. The test sample is contained in a transparent cell and rotated in the horizontal plane at speeds up to 100,000 RPM. In most of the modern analytical centrifuges, the radial movement of dispersed particles, under the action of extreme gravitational forces, is measured using a detection system that is generally based on recording the effects of the dispersed particles on the light that is transmitted through the dispersion. The mathematical relationship, represented by Equation 6, is provided by the light scattering theory (Bohren and Huffman 2004).

$$I_t = I_o \exp(-\alpha_{ext}L) \quad \text{Equation 6}$$

In Equation 6,

- I_o = Intensity of incident light
- I_t = Intensity of transmitted light
- α_{ext} = Attenuation coefficient (turbidity)
- L = Length covered by light through the suspension (dispersion)

The instrument design provides the values of I_o and L while the light detectors measure I_t . On-board computers calculate α_{ext} which is then used to estimate the number of dispersed particles and/or particle size, as described below.

α_{ext} is related to the number concentration of particles per unit volume (N) and the extinction cross section (C_{ext}) of the particle.

$$\alpha_{ext} = NC_{ext} \quad \text{Equation 7}$$

The extinction efficiency of a particle of cross section (A) is given by Equation 8.

$$E_{ext} = \frac{C_{ext}}{A} \quad \text{Equation 8}$$

Substituting the value of C_{ext} and area of particle A into Equation 8, gives Equation 9, which gives the diameter of the particle.

$$\alpha_{ext} = NE_{ext} \frac{\pi d^2}{4} \quad \text{Equation 9}$$

Using the Mie theory of light scattering, E_{ext} is calculated from the refractive index of the dispersed particle, its size and shape, the state of the polarisation, the wavelength of the scattered light and the refractive index of the continuous phase.

Centrifugation is a reliable method for the determination of a particle size distribution (Lange 1995). However, in this study, the primary aim was to analyse the extent of sedimentation in undiluted pigment dispersions. Modern analytical centrifuges allow the simultaneous analysis of up to twelve different samples. The details of analytical centrifuge and the associated analysis parameters are discussed in detail in Section 3.3.

1.10.2 Rheological characterisation of pigment dispersions

Rheology is the study of deformation of a material under the action of an applied external force. Flow is an irreversible form of deformation which is hindered by the internal friction in the flowing material. This internal resistance to flow is referred to as the viscosity, given by Equation 10.

$$\eta = \frac{\text{Shear stress}}{\text{Shear rate}} \quad \text{Equation 10}$$

The viscosity of a fluid increases as the molecular weight of the molecules of the fluid, or other polymeric species present in the fluid, increases. This is because larger molecules experience more 'friction' during flow. In addition, the presence of particles such as those of a pigment, influences the viscosity of the carrier medium.

As shown in Figure 1-32, a particle that is dispersed in a fluid consumes some of the energy that is needed to move the fluid layers, thus increasing the total amount of energy required to cause the flow, i.e., the viscosity. The effect of the presence of particles on the viscosity of the medium containing the particles is magnified if the interaction between particles is strong or if a large number of particles is present.

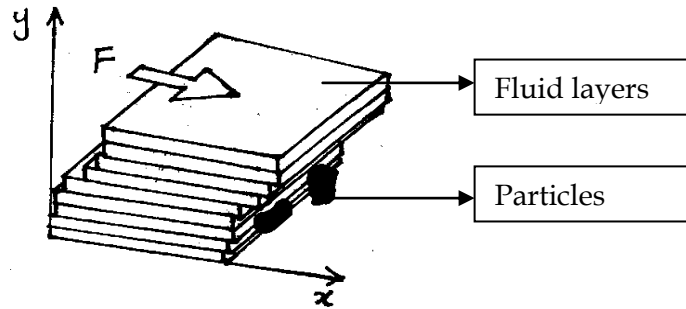


Figure 1-32: Effect of presence of particles on the viscosity of carrier medium.

The viscosity of dispersion is related to the concentration of dispersed particles by Equation 11 (Mills 1995).

$$\eta = \eta_o(1 + [\eta]\Phi) \quad \text{Equation 11}$$

In Equation 11,

η = Viscosity of the dispersion

η_o = viscosity of the continuous phase

$[\eta]$ = Intrinsic viscosity of the particle

Φ = Volume fraction of the particle in the dispersion

The ratio η/η_o can be referred to as the relative viscosity η_r and Equation 11 can be rewritten as follows.

$$\eta_r = 1 + [\eta]\Phi \quad \text{Equation 12}$$

Equation 12 is applicable to dilute dispersions and excludes particle size and particle size distribution. Mathematical relationship which relates viscosity and particle size is given in Equation 13.

$$\eta_r = \left(1 + \frac{1.25 \Phi}{1 - (\Phi/\Phi_{max})}\right)^2 \quad \text{Equation 13}$$

In Equation 13,

Φ = Volume fraction of the particle in the dispersion

Φ_{max} = Maximum volume fraction to which particles can pack

The volume fraction of particles (Φ) will increase if the effective particle radius increases as in case of adsorption of high molecular weight polymeric dispersants onto the surface of pigment. If the thickness of adsorbed dispersant layer is δ , the actual radius of particle is R , then the actual volume fraction (Φ) is related to the effective volume fraction (Φ_e) by Equation 14 (Goodwin and Ottewill 1991).

$$\Phi_e = \Phi \left[1 + \left(\frac{\delta}{R}\right)^3\right] \quad \text{Equation 14}$$

The effective volume fraction is also affected in case of electrostatically stabilised pigment particles. This is due to the electro-viscous effects of the charged 'environment' in which the particle moves (Mewis and Haene 1993).

In general, the viscosity of pigment dispersion depends on the applied deformation force, the amount of pigment dispersed in the continuous phase (vehicle), the solubility of pigment in the vehicle, temperature, particle-particle interactions and the state of particles aggregation (Kissa 1999b).

Practically, only the state of particle aggregation can be altered during the dispersion preparation process. All of the other factors listed above are governed by the uses, the application processes involved or by the intrinsic characteristics of the pigment.

A change in the viscosity of the dispersion is observed as structural changes occur in the dispersed pigment particles, during the milling process (Lubrizol 2011). Rheological measurements are very helpful in providing insight into the degree of dispersion at various stages during the milling of the pigment. Furthermore, the viscosity of a pigment dispersion can be reliably used to evaluate the state and the stability of the dispersion (Biddle, Walldal and Wall 1996). Rheological analyses are

useful for concentrated systems which cannot be characterised, without introducing a degree of uncertainty, as seen in other methods, such as radiation scattering and sedimentation analysis. Another advantage of rheological characterisation is that 'time' can be involved as another dimension.

In this study, a cone-and-plate rheometer was employed. The working principles of the rheometer and the analysis parameters are described in detail in Section 3.1. There are several advantages of using cone and plate rotational rheometry for determination of rheological characteristics of a fluid. The more important benefits are listed below.

- A minimal amount of test sample, generally on the order of 0.1 cm³, is required for testing purposes.
- The peripheral edge effects can be neglected for general testing purposes.
- Any heat generated in the sample is quickly dissipated due to the extremely thin film of the test fluid that is used.
- The temperature of sample can be adjusted very easily and quickly if an arrangement for effective temperature control is provided in the horizontal flat plate.
- The instrument is easy to setup, run and clean.
- The geometry of the system is such that the shear stress, shear strain rate and the viscosity can be related by meaningful theoretical relationships. This point is further elaborated in Section 3.1.

1.10.3 Particle size analysis

Evaluations of the size, shape and size distribution of pigments and fillers as components of an ink or coating formulation are very important. This is because, besides the properties and performance, the environmental impact of the coating is also considerably dependent on the size, shape and size distribution of its particulate ingredients. In ink formulation studies of conductive inks, it is crucial to breakdown the conductive pigment agglomerates if one is to achieve the formation of a percolation network through the electrically insulating vehicle (dispersion medium) and binder bulk. Thus, it is important to analyse the state of dispersion of particles after dispersion preparation and after storage.

The effect of changes to the particle size distribution and the loading can be used as measures of inherent dispersion stability. Since these changes can be monitored by recording the light scattered by the dispersed particles, techniques based on light scattering can be employed to estimate the stability of dispersions (Barringer, Novich and Ring 1984).

A simple description of the working principle of light scattering methods is as follows. Light incident upon a small particle is scattered by the particle in all directions. The scattering pattern depends on the size of the particle and therefore, established theories can be used to estimate the particle size from the scattering pattern obtained. Depending on the nature of dispersion and the required analysis, various light sources such as white light, lasers and X-rays can be used. The light scattering theories dealing with various particle size ranges are briefly described as follows (Kissa 1999c).

- Rayleigh theory of light scattering.

This is applicable to light scattering by a very small sphere having diameter $D < \lambda/10$. The scattering intensity I is expressed with the Equation 15 below.

$$\frac{I}{I_o} = \frac{8 \pi^4 (1 + \cos^2 \theta)}{\lambda^4 d^2} \left(\frac{\alpha}{4\pi\epsilon_o} \right)^2 N \quad \text{Equation 15}$$

In Equation 15,

I = Intensity of incident light

I_o = Intensity of scattered light

θ = Scattering angle

α = Particle polarizability

λ = Wavelength of incident light

d = Detection distance from the sample

ϵ_o = Dielectric permittivity of free space

- Rayleigh-Gans-Debye (RGD) theory of light scattering.

This theory is applicable to light scattering by a particle having diameter $\lambda/20 < D < \lambda$. As the particle size increases, the intensity of light scattered in the forward direction ($\theta \leq 90^\circ$) increases. Thus, the ratio of the intensity of forward

scattered light (I_{45°) to the intensity of back-scattered light (I_{135°) can be used to estimate the particle size.

- Mie theory.

This theory applies to light scattering by a particle having diameter $D \geq \lambda$. In this case, the scattering pattern is complex and the scattered light intensity is different at various scattering angles. It is important to note that the Mie regime ($D \geq \lambda$) is very useful for determination of particle size distribution in polydisperse systems such as most practical dispersions (Schnablegger and Glatter 1993).

Light scattering methods can be grouped into the following categories.

1. Static light scattering (SLS) - Measures time averaged intensity of scattered light.
2. Dynamic light scattering (DLS) or Photon correlation spectroscopy (PCS) - Measures time dependent fluctuations in the intensity of scattered light.

It is important to note that both SLS and DLS have their advantages and limitations if compared with each other or with other techniques of analysing particles, such as microscopy. The main advantage of DLS is that it is the fastest technique available for routine particle sizing. In this study Malvern Zetasizer Nano ZS, the working principle of which is based on DLS, was used for pigment particle size analysis. This is described in detail in Section 3.2.

1.10.4 Zeta potential studies

As depicted in Figure 1-33, an electric double layer exists around a particle that acquires a net surface charge in a fluid medium. The electrical double layer can be said to have two regions; a Stern layer (A) and an outer diffuse layer (B). Counterions that are within the Stern layer are strongly bound while the counterions in the diffuse layer are less firmly attached to the surface of the charged particles. The counterions within the diffuse layer, which are at a certain distance from the surface of the particle move when the particle moves, for instance due to gravity. Thus, there exists a notional boundary outside which the counterions do not travel with the particle. This boundary

is called the hydrodynamic shear plane or the slipping plane and the electrostatic potential that exist at this boundary is called zeta potential.

Since the magnitude of zeta potential is a qualitative measure of the electric charge on the particle, it is used practically as an indication of the potential stability of the particles (Clayton 1997), (Kissa 1999a). For instance, if the particles in a dispersion possess a large, negative zeta potential, there will be a significant negative charge density around the particles. This results in stronger electrostatic repulsion between the particles as they approach each other, thus stabilising the particles. This is described in detail in Section 1.9.3.1.

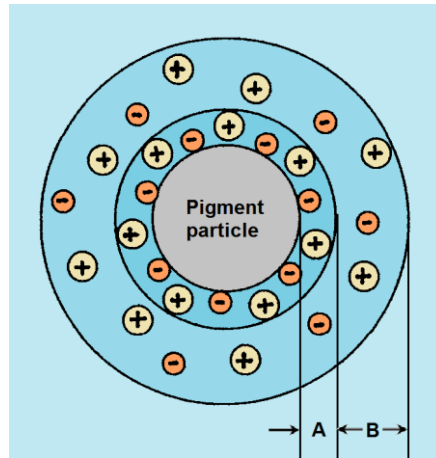


Figure 1-33: A charged particle dispersed in a fluid medium.

For this study, the zeta potential of appropriate dispersions was determined using a Zetasizer Nano ZS from Malvern Instruments. The working principle of the instrument and the test parameters are described in Section 3.3.

Chapter 2. Experimental

2.1 Materials

2.1.1 Pigments

On the basis of a consideration of the properties, electrically conductive grades of carbon black pigment that contained low volatile matter content were selected for the preparation of binder-free, waterborne dispersions and subsequently, appropriate screen printing inks. Two low surface area and two very high surface area grades were selected in order to establish that the dispersion preparation procedure that was devised in this study can be successfully employed to produce stabilised (optimised) dispersions of these difficult-to-disperse grades of carbon black pigment. Furthermore, this selection allowed us to compare the properties of inks that contained a large amount of low surface area pigment with the properties of inks that contained a very small amount of high surface area pigment. Data related to the main characteristics, as provided by the suppliers of the selected carbon black pigments, are shown in Table 2-1. Throughout this document, these commercial pigments are referred to as Carbon1, Carbon 2 and so on, as specified in Table 2-1.

Table 2-1: Specifications of carbon black pigments (as provided by the suppliers).

Pigment (Code)	Supplier	BET Surface area (m ² /g)	OAN (cm ³ /100g)	Volatile content (%)
Vulcan XC605 (Carbon1)	Cabot	59	148	< 0.1
Ensaco 250G (Carbon2)	Timcal	62	191	0.2
Ensaco 350G (Carbon3)	Timcal	840	336	0.3
Printex XE2B (Carbon4)	Orion Engineered Carbons	1000	420	< 0.1

2.1.2 Dispersing additives

For the preparation of waterborne dispersions of carbon black pigments, high molecular weight non-ionic wetting and dispersing additives are generally

recommended. The advantages in the use of such dispersants are discussed in Section 1.9.4. Three different dispersants, selected on the basis of their supplier recommendations for the intended application, were used to prepare stable dispersions of a pigment. The optimised dispersions were then formulated into finished inks. The dispersants possess a hydrophobic backbone (that could be for example, polyurethane, styrene-acrylic, etc.) and hydrophilic steric stabilising chains that are usually based on alkoxy chemistry (based on for example, polymers of ethylene oxide or propylene oxide). The hydrophobic backbone is grafted with hydrophilic stabilising chains resulting in a comb-type molecular structure. Thus, in aqueous media, these dispersants attach to the pigment due to the hydrophobic nature of the molecule's backbone.

The more important characteristics of the selected dispersants are provided in Table 2-2. For each of the dispersants, the weight loss profile as a function of temperature was recorded using TGA, as described in Section 3.7.2. As discussed in Section 4.4, the solids content in the dispersant samples corresponded with the active matter content specified by the suppliers. Throughout the discussion, the dispersants are referred to as Dispersant1, Dispersant2 and Dispersant3, instead of using the commercial names.

Table 2-2: Dispersants used and their characteristics (as provided by the suppliers).

Dispersant (Code)	Supplier	Description	Density (g/cm³)	Water solubility	Active Matter %
Solsperse 44000 (Dispersant1)	Lubrizol	Not disclosed	1.67	Soluble	50
BYK-190 (Dispersant2)	BYK Chemie	Solution of a high molecular weight block copolymer with pigment affinic groups	1.06	Completely miscible	40
Tego Dispers 760W (Dispersant3)	Evonik Tego	Aqueous preparation of surface active polymers	1.03	> 500 g/L	35

2.1.3 Binders

In this study, polymeric binders were used for one or more of the following: to prepare control dispersions during the pigment dispersion optimisation process; for the let-down of optimised pigment dispersions; and in the primer coating of textile substrates.

Three polymeric binders, which represent the types commonly used in inks/coatings for textiles, were selected. The available details for these binders are provided in Table 2-3. In order to calculate the amount of binder that was required to formulate the finished inks from the optimised pigment dispersions, the solid content of each of the four binders was determined using thermogravimetric analysis, as described in Section 3.7.1.

Table 2-3: Binders used in the study.

Binder (code)	Supplier	Description	Applications
Impranil DLC-F (Binder1)	BASF	Anionic polycarbonate ester polyurethane dispersion	Suitable for the formulation of textile coatings for use as finish and top coat in outer wear, bags/luggage, fashion shoe uppers, technical articles and upholstery.
Impranil LP GHG 519 (Binder2)	BASF	Anionic aliphatic polyester-polyurethane dispersion	Suitable for the formulation of textile coatings.
Printofix Binder 83 liquid (Binder3)	Clariant	Aqueous dispersion of a styrene-acrylic copolymer	Suitable for fixation of printing inks onto textile substrates.
Glascal HN2 (Binder 4)	BASF	Sodium salt of an acrylic copolymer cross linked with melamine formaldehyde	Not specified

2.1.4 Defoamer

The generation of a foam, due to the presence of surface active compounds such as dispersants, is possible specially in waterborne pigment dispersions. This problem becomes more pronounced when large amount of a dispersant is present (Hobisch and Tsang 2009). Foaming can result in the entrapment of air in the dispersion during the

initial pigment wetting-out phase. Air bubbles can act as shock absorbers for the energy that is provided to break the pigment particle assemblies, during pigment dispersion process. Thus, one of the more important ingredients of a pigment dispersion is a defoamer or an anti-foaming additive (Schak 1997). To eliminate any foaming that might occur during the early phase of pigment milling, organo-modified siloxane defoamers are known to be very effective. Tego Foamex 805, which is described by the supplier as a modified poly-siloxane defoamer, was used in the preparation of pigment dispersions.

2.1.5 Commercial conductive inks

The surface resistivity and the durability (resistance to washing and creasing) of the inks that were formulated in this study were compared against two commercially available highly conductive carbon-based inks, listed in Table 2-4. The surface resistivity values that are shown in Table 2-4 relate to a 25 microns thick ink layer deposited on a polyimide film. The solids content of these inks was determined using thermogravimetric analyses, as described in Section 3.7.4.

Table 2-4: Commercial conductive inks used in the study.

Product	Supplier	Description	Surface resistivity (Ω/\square)
C2030519P4 Carbon/Graphite ink	Gwent Electronic Materials Ltd	Carbon sensor paste	13 -20
SD 2843 HAL	Peters GmbH	Carbon conductive ink	10

2.1.6 Substrates

2.1.6.1 Packaging paperboard

Iggesund Incada Exel packaging paperboard, the specifications of which are given in Table 2-5, was used as the substrate for electrical characterisation of the formulated pigment dispersions and inks. The substrate, the micrograph of which is shown in Figure 2-1, is coated with a calcium carbonate clay to make the surface smooth and to absorb the printing ink uniformly in demanding processes such as half tone gravure printing and offset lithography. Thus, this substrate was considered to be suitable for electrical characterisation of pigment dispersions and printing inks. This is because in

these experiments, it was crucial to minimise any variations in the electrical conductivity of the deposited dispersion/ink layer, which might be caused by substrate surface roughness and/or non-uniform absorption.

Table 2-5: Specifications of paperboard substrate (as provided by the manufacturer).

Product name	Incada Exel
Type	Standard packaging paperboard
Grammage	240 g/m ²
Thickness	400 μm

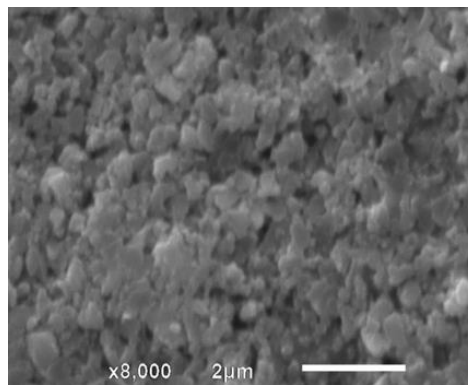


Figure 2-1: Scanning electron micrograph of Incada Exel paperboard, (magnification x8000).

2.1.6.2 Textile substrates

The substrates on which the printing of electronic circuits was targeted in this study were textile fabrics. There are number of physical and chemical properties of a textile fabric that might influence the resultant print quality and, in turn, influence the performance/behaviour of the printed circuit patterns. These include the surface smoothness, the absorbency, the surface energy, the fabric construction (weave design, warp and weft count in case of woven fabrics), the GSM, the porosity (related to fabric construction and GSM) and the resistance to acidic/alkaline media. The aforementioned substrate-dependent variables are important. None-the-less this study was focused on achieving high electrical conductivities in ink formulations. Thus, the testing of substrate-related variables was beyond the scope of this study.

In this study, 100% cotton and 100% poly(ethylene terephthalate) (elsewhere referred to as polyester) woven fabrics, which are the two more commonly used woven textile

fabrics, were selected as the substrates on which to test the performance of the inks. These fabrics were obtained from Whiley-Bradford Limited, UK.. Figure 2-2(a) and Figure 2-2(b) show the micrographs of the 100% cotton and 100% polyester fabrics, respectively. The specifications of the fabrics are provided in Table 2-6.

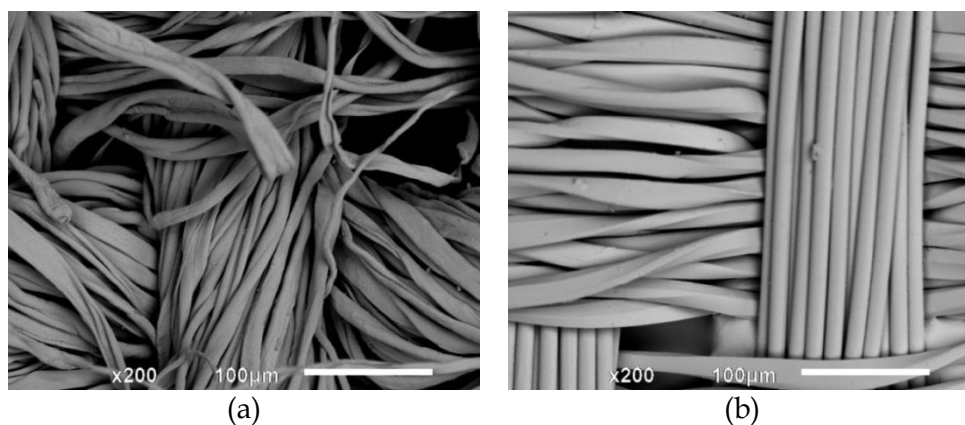


Figure 2-2: Scanning electron micrographs of (a) 100% cotton and (b) 100% polyester woven fabrics.

Table 2-6: Specifications (provided by supplier) of textile substrates used in the study.

Substrate	Weave	GSM (g/m ²)
100% cotton	1 x 1 plain	80
100% polyester	1 x 1 plain	55

2.2 Preparation and characterisation of pigment dispersions

2.2.1 Procedure of optimisation of pigment dispersions

In this study, waterborne dispersions of four different carbon black pigments (Table 2-1) were prepared using three different dispersants (Table 2-2). Thus, twelve pigment-dispersant combinations, represented as Dispersion 1 - Dispersion 12 in Table 2-7, were optimised and tested.

The procedure adopted in this study was closely related to the 'minimum viscosity method' for the optimisation of pigment dispersions. A major limitation of the minimum viscosity method is that it can give lower estimates of the optimum dispersant dosage (Clayton 1997). In the present study, one of the major characteristics of interest was the electrical conductivity of the pigment dispersions. Thus, 100% coverage of the pigment surface by the dispersant molecules was not targeted and

dispersions which remained stable for up to four weeks were considered to be sufficiently stable. Furthermore, the optimum dispersant dosage was determined by preparing and analysing a ‘ladder series’ of dispersions containing dispersant amounts, calculated around the theoretical dispersant dosage (Cowley and Walsh 1997). To overcome the limitations of ‘minimum viscosity method’, rheological studies, sedimentation analysis, photoextinction studies and zeta potential measurements were carried out to characterise the optimised formulations of the binder-free pigment dispersions. A 4-step procedure, as described in detail in the following text, was devised to “optimise” the dispersions of the carbon black pigments.

Table 2-7: Pigment-dispersant combinations prepared and tested in the study.

		Dispersants		
		Dispersant1 (Solsperser 44000)	Dispersant2 (BYK-190)	Dispersant3 (Tego 760W)
Pigments	(Carbon1) Vulcan XC605	Dispersion 1	Dispersion 2	Dispersion 3
	(Carbon2) Ensaco 250G	Dispersion 4	Dispersion 5	Dispersion 6
	(Carbon3) Ensaco 350G	Dispersion 7	Dispersion 8	Dispersion 9
	(Carbon4) Printex XE2B	Dispersion 11	Dispersion 10	Dispersion 12

Dependent upon the surface area of pigment, an optimal amount of dispersant is generally needed to form a monomolecular layer on the pigment surface. The use of the correct dispersant dosage is crucial if one is to achieve the required level of dispersion stability without compromising the properties of the final ink film. A viscosity minimum is generally observed at the optimum dispersant dosage. This minimum has been shown to correspond to approximately 2 mg of dispersant for 1 m² of the pigment surface area as measured by the BET nitrogen adsorption number method (Cowley and Walsh 1997). Thus, in the first step of dispersion preparation, the theoretical amount of dispersant (100% dispersant active matter on the weight of pigment, referred to as %DOWP) was calculated using the empirical formula given as Equation 16.

$$\%DOWP = \frac{BET \text{ surface area}}{5} \quad \text{Equation 16}$$

The maximum loading of carbon black pigment in dispersion depends on a number of physical and chemical properties of the pigment, as discussed in detail in Section 1.9.1. The carbon black pigments used in this study can be categorised into low surface area grades (Carbon1 and Carbon2) and very high surface area (Carbon3 and Carbon4) grades. The volatile matter content, as stated by the suppliers, is well below 0.5 wt% for all of the pigments studied. The BET surface area (m^2/g of pigment), oil absorption number and other characteristics of a pigment can be used as tools to predict the maximum amount of pigment that can be dispersed provided effective calibration is carried out. However, it is important to note that aqueous media present greater challenges in the dispersion of non-polar carbon pigments and it is impossible to furnish an exact value of the maximum pigment loading in such formulations. Thus in Step 2 of the dispersion optimisation process, the maximum amount of pigment that could be dispersed using the theoretical %DOWP was determined. This was achieved by comparing the characteristics of 'control' pigment dispersion with a ladder series of dispersions. The control dispersion was prepared without a dispersing additive and the pigment dispersion was achieved with the aid of the Glascol HN2 acrylic resin. A ladder series of pigment dispersions was prepared such that each dispersion contained a known, specific amount of pigment and a corresponding theoretical %DOWP of dispersant, calculated as described in Step 1. The pigment dispersion possessing a similar viscosity profile to that of the control dispersion was selected for the next step.

In the third step, the optimum amount of dispersant was determined. This was achieved by preparing a series of pigment dispersions, each containing the maximum pigment amount, that was determined in the previous step, but different amounts of dispersant. Using the cumulative results from viscosity determination, particle size analysis, zeta potential measurements and electrical property characterisation, the dispersions that were prepared in Step 3 were compared and the optimum dispersant dosage was determined.

In Step 4, dispersions of a pigment were prepared using each of the three dispersants considered in the study. Since these dispersions were prepared using the optimum %DOWP, they are referred to as the 'optimised dispersions'. As discussed in Section 2.2.6, the properties that were characterised to compare the different optimised dispersions of a pigment included the viscosity, the dispersion stability and the

electrical conductivity. In this step, the pigment loading was maximised while maintaining the optimum pigment:dispersant ratio. The major advantages of maximising the pigment loading in the dispersion are listed below.

- Since the electrical conductivity of the dispersion of a conductive pigment and the ink prepared from the dispersion are strongly dependent on the amount of pigment, increasing the pigment loading considerably increases the electrical conductivity.
- Increasing the pigment loading increases the viscosity of dispersion which is beneficial in stabilising the dispersed particles, as discussed in Section 1.10.1.

The long milling duration to prepare a pigment dispersion limited the number of samples that could be bead milled. Therefore, the optimisation process described above could not be performed for each of the twelve pigment-dispersant combinations shown in Table 2-7. Thus, for each pigment, the optimum dispersant dosage (%DOWP) was determined using only one of the dispersants, followed by the use of the optimised formulation to prepare pigment dispersions using the other two dispersants. The selection of a particular dispersant, to determine the optimum dispersant dosage for a particular pigment, was made on the basis of the results of a 'sinking' test, as described in Section 2.2.2. Figure 2-3 shows the sequence of the addition of the formulation ingredients and the steps involved in the preparation of the pigment dispersions. This procedure was followed for the preparation of all of the dispersions.

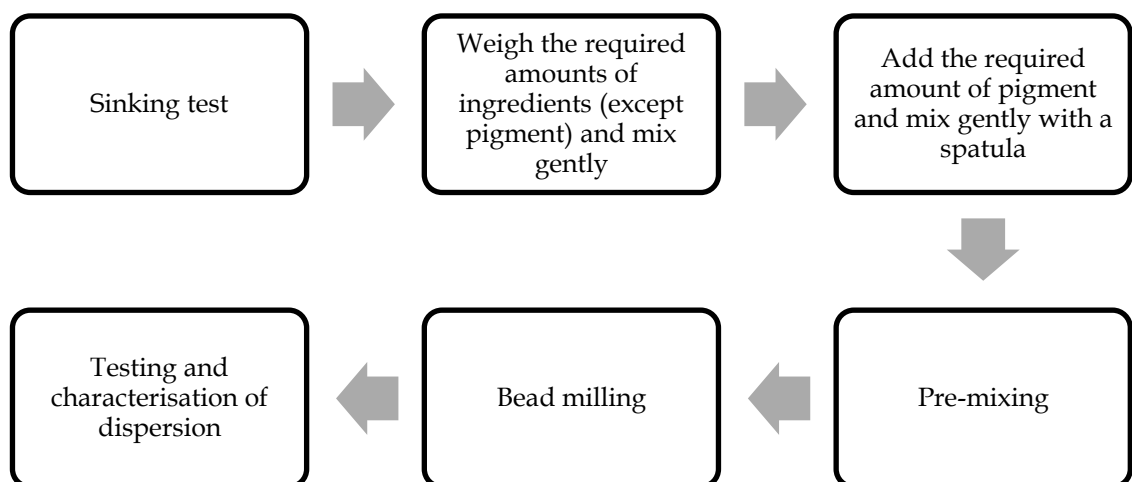


Figure 2-3: Procedure of preparation of pigment dispersions.

2.2.2 Sinking test

Preliminary information on pigment-dispersant compatibility can be obtained by qualitative or semi-quantitative testing (Bernhardt 1988). In this study, a 'sinking' test was performed for qualitative assessment of the effectiveness of a dispersant in dispersing a particular pigment. For this purpose, aqueous solutions of the three dispersants were prepared. As shown in Table 2-8, the amount of a dispersant was such that the percentage of active matter of the dispersant in the test solution was 5 wt%.

The specific gravity of the aqueous dispersant solutions was calculated using a 10 mL density bottle. This was required to establish that the observed differences in the opacity of mixtures after the addition of pigment and the amount of settled pigment were not merely due to differences in the densities of the dispersant solutions. It was found, as shown in Table 2-9, that there was no significant difference in the specific gravities of the 5 wt% (active matter content) dispersant solutions.

Table 2-8: Composition of dispersant solutions prepared for sinking tests.

Dispersant name	Active matter in as-supplied form (wt %)	Dispersant amount (g)	D.I. water (g)	Total solution (g)	Active matter in solution (wt %)
Dispersant1	50	1	9	10	5
Dispersant2	40	1.25	8.75	10	5
Dispersant3	35	1.43	8.57	10	5

Table 2-9: Specific gravities of the dispersant solutions at 25 °C.

Dispersant	Specific gravity (g/cm ³)	pH
Dispersant1	1.008	6
Dispersant2	1.008	6
Dispersant3	1.006	6

To perform the sinking test, equal amounts of a pigment were added to each dispersant solution contained in a test tube that was then left at ambient temperature (22 - 25°C) without agitation. The dispersant mixtures were observed after 24 hours, 48 hours and 72 hours of addition of pigment and the dispersant which gave the best

results, i.e., minimum sedimentation of pigment and maximum opacity of the mixture, was selected for the optimisation of dispersion of the tested pigment.

2.2.3 Pre-mixing

In the present study, pre-mixing was achieved using a high speed over-head stirrer (Model: IKA Eurostar digital). The stirrer can be operated in the range from 5 RPM to 2000 RPM. A dissolver type stirrer blade, as shown in Figure 2-4 (© IKA® Werke GmbH & Co.), was employed. Such a stirrer provides radial flow, thus drawing the material that is to be mixed from the top and the bottom of the vessel containing the mixture. The stirrer creates high turbulence, high shearing forces and promotes particle size reduction.

The radius of the stirrer used in this work was 2 cm which provided a peripheral speed of 4.19 m/s at 2000 RPM. During pre-mixing, the dispersion was mixed at 800 RPM for 5 minutes followed by mixing at 2000 RPM for 25 minutes. This initial mixing at the lower speed is important to achieve a high level of pigment wetting and to prevent any compaction of pigment agglomerates. The compaction of agglomerates is possible if the pigment is subjected to strong impact forces when the pigment surface is not properly wetted-out.



Figure 2-4: Dissolver-type stirrer for the high shear mixing of pigment dispersions.

2.2.4 Bead milling

To create improved dispersions, the pre-mixed dispersion of a pigment was bead milled. In this study, the bead mill was a Mini 50 Motormill (Model No: MK11.M50.VSE.EXD.DI), manufactured by Eiger Torrance Limited. A schematic diagram of the horizontal recirculating bead mill is shown in Figure 2-5. The milling

chamber of the bead mill has an empty volume of 50 mL and it needed to be filled between approximately 65% (32.5 mL) and 85% (42.5 mL) with grinding beads. The size of the zirconium oxide beads used as grinding media was approximately 1 – 1.25 mm and the bead loading was maintained between 30 – 35 mL. It was estimated, in some trial experiments, that a minimum volume of approximately 75 mL was required to ensure proper recirculation of the dispersion in the mill. Based on the recommendations of the bead mill manufacturer, the milling time was typically 3 hours and the milling speed was 3750 – 4000 RPM. The optimum duration of milling was validated by recording reduction in the viscosity of a number of dispersions, as described in Section 2.2.4.1.

It was considered to be important to ensure proper recirculation of the dispersions during bead milling. This was difficult to achieve in the case of high viscosity dispersions (as in the present case) because such dispersions were likely to ‘sit’ in the inlet funnel of the bead mill. To overcome this problem, an overhead stirrer was used in conjunction with the bead mill. As shown in Figure 2-6, the overhead stirrer blade was placed in the inlet funnel of the bead mill and rotated at 400 – 500 RPM while milling a viscous dispersion. This facilitated the continuous flow of dispersion in the milling chamber through the feed zone.

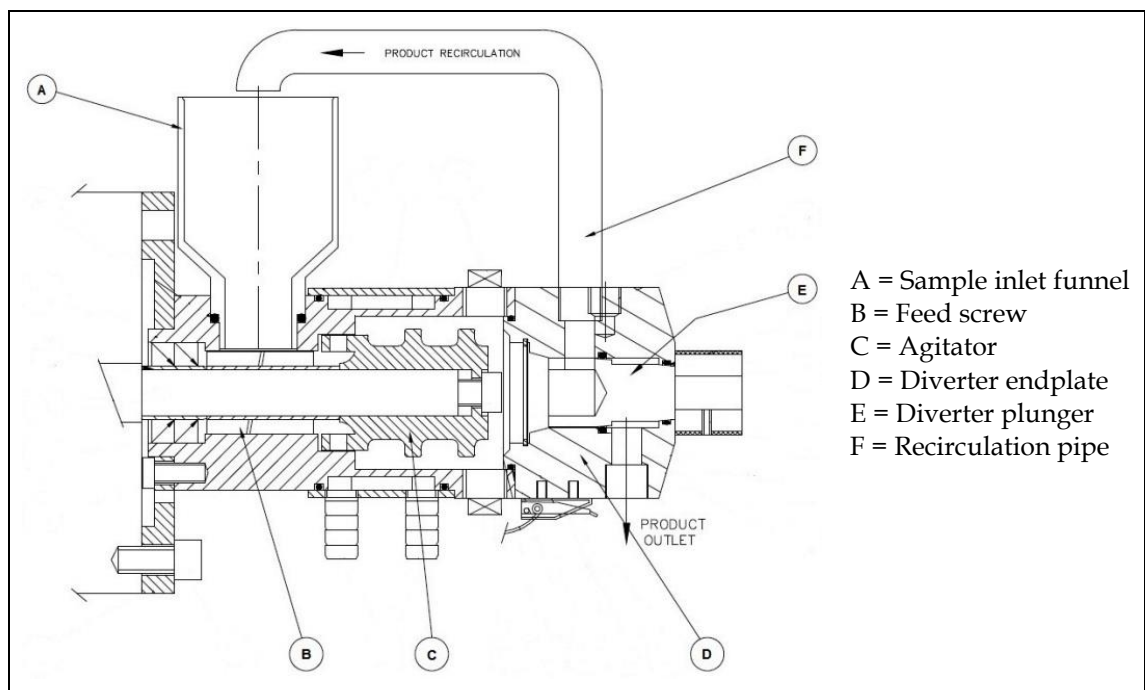


Figure 2-5: Schematic of Mini 50 bead mill (Source: Eiger Torrance Limited)

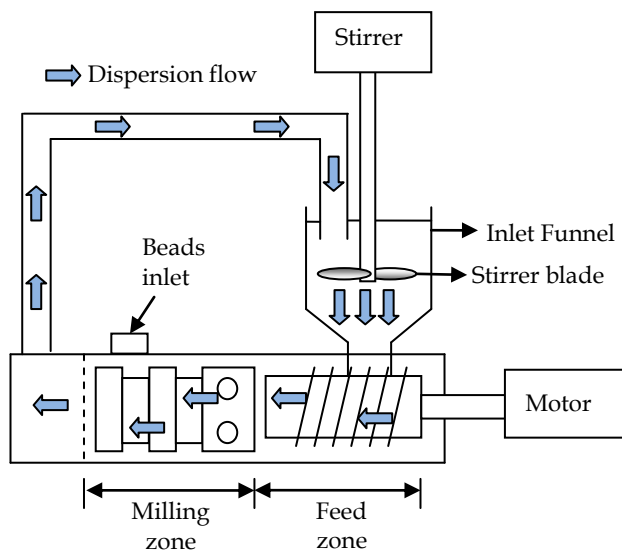


Figure 2-6: Schematic of bead mill and overhead stirrer arrangement for milling of high viscosity dispersions.

2.2.4.1 Determination of optimum parameters of bead milling

The optimum milling process parameters, i.e., the milling time and the milling speed, to prepare pigment dispersion depends on a number of factors including the pigment hardness, the pigment aggregate size, the solubility of pigment in the dispersion medium, the design of the milling equipment and the effectiveness of the dispersant(s).

As discussed in Section 1.9.1, carbon black pigment is generally difficult to disperse. It is even more challenging to disperse and to stabilise a carbon black pigment in polar solvents such as water. The carbon black grades that are used in printing inks generally have a high proportion of chemisorbed oxygen-containing complexes which improve the dispersibility of these pigment grades in hydrophilic media. In this study, however, electrically conductive grades of carbon black, which have very low volatile matter content, were employed. Thus, it was considered to be important to establish the optimum milling process parameters to ensure that pigment milling was done effectively.

Initially, the milling process parameters were set on the basis of recommendations of the bead mill manufacturer. These process parameters are discussed in Section 2.2.4. After the optimum dispersant dosage for each of the four pigments was determined, the effects of the milling duration were studied to establish confidence in the effectiveness of the milling process. In some trial experiments, it was observed that a

milling speed in the range of 3750 – 4250 RPM resulted in improved recirculation of dispersions of both low surface area as well as high surface area pigments. Below 3750 RPM, it was found difficult to recirculate the high viscosity pre-mixed dispersions that contained large amounts of low surface area pigments or the highly thixotropic dispersions of high surface area pigments. Above 4250 RPM, the milling chamber of the bead mill started to heat up rapidly. Thus, the milling speed was maintained between 3750 – 4000 RPM, which is also in line with the bead mill manufacturer recommendations to minimise any wear and tear of the equipment.

The effect of the milling duration was studied for all of the 12 optimised pigment-dispersant combinations. The viscosity profiles were recorded following the procedure described in Section 3.1.1. A decrease in the viscosity can be considered as being a direct indication of the reduction in particle-particle interactions (Lubrizol 2011). The viscosity profiles of samples, exposed to a shear rate range of 1 – 1000 s⁻¹, were recorded at regular intervals during milling. The milling duration after which no significant decrease occurred in the viscosity of the dispersions was considered to be the optimum milling duration. The process was repeated for all of the optimised pigment dispersions, thus providing enough data for the determination of the optimum milling process parameters that are generally applicable to a range of dispersion formulations. The results of this study are discussed in Section 4.3.

2.2.5 Procedure to establish the repeatability of the pigment dispersion preparation process

In attempts to achieve greater electrical conductivity from the finished inks, the pigment loading was maximised in the binder-free pigment dispersions. In most cases, the pre-mixed dispersions were very viscous and it was difficult to ensure proper recirculation, especially during the initial several minutes of bead milling. This created potential chances of losing some of the pigment in the form of accumulations in various sections of the mill, particularly between the feed screw and the agitator where the dispersion is forced through small holes in the agitator. Thus, it was considered to be important to establish that the measures taken, as described in Section 2.2.4, ensured that the dispersion formulations after bead milling were not significantly different

from the starting point formulations in terms of pigment loading and that the dispersion preparation procedure was repeatable.

For the let-down stage, at least two batches of each of the 12 optimised pigment dispersions were prepared. The solids content and the viscosity profiles of the different batches of each of the optimised dispersions were compared with each other in order to establish the reliability and repeatability of the dispersion preparation procedure. The results of various analyses carried out for this purpose are presented in Section 4.4.

2.2.6 Analysis and characterisation of pigment dispersions

The particle size distribution, zeta potential, electrical conductivity, viscosity, dispersion stability and solids content of the pigment dispersions, prepared and optimised in the first phase of this study, were characterised. Table 2-10 provides a summary of the purposes and the techniques employed for the various analyses that were carried out on the pigment dispersions. The results of these analyses are discussed in detail in Sections 4.1, 4.2 and 4.4. In summary, the following information was obtained from these analyses.

- Optimum dispersant dosage for each of the carbon black pigments used in the study.
- Stability of pigment dispersions.
- Electrical conductivity and surface resistivity of dispersions.
- Repeatability and reliability of the experimental procedure devised in the study.

Table 2-10: Analyses carried out on pigment dispersions.

Characteristic studied	Analyses employed
Optimum dispersant dosage	Particle size analysis, zeta potential, viscosity and electrical conductivity.
Stability of pigment dispersions	Viscosity, particle size analysis and centrifugal sedimentation.
Electrical characteristics	Surface resistivity of drawdowns and conductivity of dispersions.
Repeatability and reliability of procedure	Rheology for comparison of different batches and TGA for formulation correctness.

2.3 Let-down of pigment dispersions

The pigment dispersions that were prepared and optimised, following the procedure as described in Section 2.2.1, were formulated into finished inks by incorporating the binder(s). In an initial study, it was shown that the surface resistivities of the drawdowns of the 12 optimised pigment dispersions were similar. Therefore, all of these dispersions were formulated into finished inks, the stability and the electrical characteristics of which were tested. The following sections present the sequences and the detailed procedures of the let-down studies, carried out on the optimised pigment dispersions.

2.3.1 Let-down compatibility tests

To establish any incompatible binder-dispersant combinations, compatibility tests were carried out before the pigment dispersions were let-down with binders. For this purpose, various amounts of binder(s) and dispersant(s) were mixed together and visually assessed for any signs of binder-dispersant incompatibility, such as precipitation of either the dispersant or the binder or both. The mixtures were also deposited onto glass slides and qualitatively analysed for the film opacity, cloudiness, clarity, adhesion and cracking of film after air drying for 48 hours at ambient temperature and also after heating at 70 °C for 1 hour.

The design of experiments for compatibility tests was such that lesser amounts of binders were tested with greater amounts of dispersants and vice versa. This is because, in the let-down stage, the amount of binder was calculated on the weight of pigment. The dispersions of high surface area pigments contained low pigment loading (approximately 11 wt% as a maximum) and very high dispersant dosage. On the other hand, the dispersions of low surface area pigments contained large amounts of pigment (up to 31 wt%) dispersed using low dispersant dosage.

As shown in Table 2-11, the loading of dispersants (in as-supplied form) was in the range between 8.05 wt% to 13.28 wt% and between 34.10 wt% to 61.07 wt% in the dispersions of the low surface area pigments and the high surface area pigments, respectively. In the let-down stage, inks were formulated to contain 100%, 150% and 200% binder solids on the weight of pigment (referred to as %BOWP). However, to

achieve binder-dispersant mixtures that were clear enough to visually detect precipitation and other signs of incompatibility, only 100% BOWP of binder loading was tested. In such case, the maximum loading of a binder (in as-supplied form) was 43.66 wt% and 21.5 wt% (of the weight of finished ink) in the inks formulated from the dispersions of the low surface area pigments and the high surface area pigments, respectively.

Table 2-11: Loading of dispersants in dispersions and loading of binders in finished inks.

	Dispersant loading (%wt of dispersion)			Binder loading (%wt of finished ink)
	Dispersant1	Dispersant2	Dispersant3	Binder1/2/3 100% BOWP
Carbon1 inks	9.30	11.63	13.28	43.66
Carbon2 inks	8.05	10.06	11.50	36.50
Carbon3 inks	34.10	42.63	48.71	21.50
Carbon4 inks	42.75	53.44	61.07	19.19

Table 2-12: Binder-dispersant combinations tested for compatibility

		Dispersants					
		Dispersant2		Dispersant3		Dispersant1	
Binders		10% (A)	40% (B)	10% (E)	40% (F)	10% (I)	40% (J)
Binder3 (Printofix Binder 83)	10% (A)		AB		AF		AJ
	20% (B)		BB		BF		BJ
	30% (C)	CA		CE		CI	
	50% (D)	DA		DE		DI	
Binder1 (Impranil DLC-F)	10% (E)		EB		EF		EJ
	20% (F)		FB		FF		FJ
	30% (G)	GA		GE		GI	
	50% (H)	HA		HE		HI	
Binder2 (Impranil LPGHG519)	10% (I)		IB		IF		IJ
	20% (J)		JB		JF		JJ
	30% (K)	KA		KE		KI	
	50% (L)	LA		LE		LI	

Legend: The first letter representing a binder-dispersant combination refers to the binder while the second letter refers to the dispersant.

On the basis of the calculations provided in Table 2-11, solutions of 10 wt% of various dispersants were mixed with suspensions of 30 wt% and 50 wt% of various binders. On the other hand, solutions of 40 wt% of various dispersants were mixed with suspensions of 10 wt% and 20 wt% of various binders. These binder-dispersant combinations are represented by the highlighted boxes in Table 2-12. The selected dispersant loading and binder loading for preparation of mixtures for binder-dispersant compatibility tests represented most of the inks that were formulated to contain 100% BOWP. The results of these compatibility tests are presented in Section 4.5.2.

2.3.2 Let-down procedure to formulate finished inks

The selected pigment dispersions were let-down with the binders after establishing the compatibility of various binder-dispersant combinations. For let-down, 10 g of a pigment dispersion was weighed in a 25 mL beaker and the required amount of binder was added drop-wise using a pipette while the mixture was continuously stirred using a magnetic stirrer. The beaker containing the ink was sealed using parafilm to avoid evaporation and mixing was continued for 10 minutes after addition of the required amount of the binder. The ink was then collected in a glass vial that was sealed with a PTFE sealed cap to avoid exposure to the air and to prevent evaporation of water. Each of the 12 optimised pigment dispersions was let-down with Binder1, Binder2 and Binder3. As depicted in Figure 2-7, inks were formulated to contain 100%, 150% and 200% binder solids on the weight of pigment (referred to as %BOWP). The relevant calculations are provided in Appendix A. A total of 108 inks (12 pigment dispersions x 3 binders x 3 loading levels of each binder) were prepared and characterised.

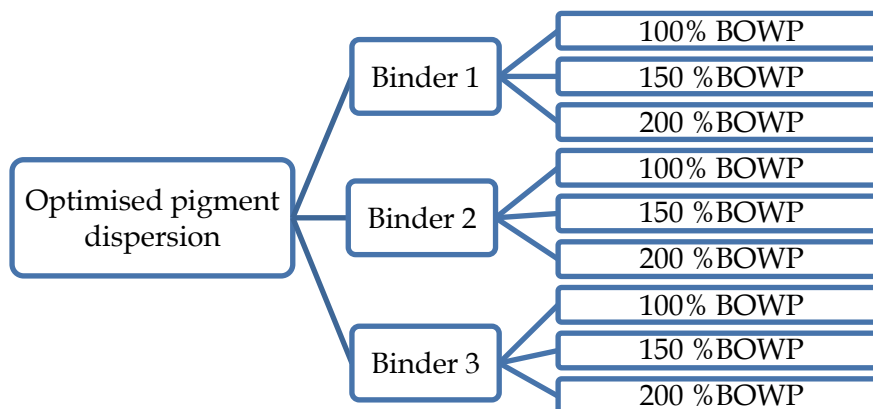


Figure 2-7: Design of experiments for the let-down of pigment dispersions.

2.3.3 Characterisation of finished inks

The finished inks that were formulated from the optimised pigment dispersions were tested for their viscosity stability and electrical conductivity (surface resistivity), as described in the following sections.

2.3.3.1 Let-down stability

The viscosity of the finished inks was determined by following the procedure outlined in Section 3.1. The change in viscosity profile after the incorporation of a binder was recorded and compared against the viscosity profile of the corresponding binder-free pigment dispersion and the viscosity profile of the as-supplied binder. The inks were stored in sealed vials at ambient temperature (22 – 25 °C) for four weeks. A significant change in the viscosity profile of an ink after 4 weeks of storage was considered as an indication of the instability of the ink. The results of this study are discussed in Section 4.5.3.

2.3.3.2 Electrical characterisation of ink films

Drawdowns of each of the finished inks were prepared on paperboard substrate and the surface resistivity was recorded, as described in Section 3.6. It was observed in trial experiments that the deposition of a single, very thick layer of ink using K bar 9 (having wire diameter of 1.5 mm producing a wet film deposit of 120 µm) resulted in a significant deformation of the paperboard substrate. This made it difficult to obtain a stable measurement of surface resistivity. Thus, test samples for surface resistivity measurements were produced with three ink layers deposited on top of each other using K-bar 3 (having wire diameter of 0.31 mm producing a wet film deposit of 24 µm). The ink layers were air dried at ambient temperature for one hour and the surface resistivity was recorded between successive ink depositions. After deposition of the third ink layer, the printed substrates were oven dried at 60 °C for 30 minutes followed by conditioning at ambient temperature for one hour before the surface resistivity was recorded. The data thus obtained provided the electrical characteristics of single layer and multiple layers of the formulated inks. The results are discussed in Section 4.5.4.

2.4 The printing and testing of inks

As described in Section 2.3, the optimised pigment dispersions were formulated into finished inks and tested for their storage stability. The results of this study indicated that most of the formulated inks either possessed stable viscosity profiles or the change in viscosity of ink was in line with the change in the viscosity of corresponding binder-free dispersion. The surface resistivity of the drawdowns of these inks was also measured and the results indicated clearly that the electrical conductivity considerably decreased as the amount of binder was increased in the inks.

The testing of the finished inks on different, commonly used woven textile substrates (100% cotton and 100% polyester), with and without a binder primer layer, was considered to be important to establish the general applicability of the conclusions drawn from this study. Thus, there were practical limitations to the number of samples to be prepared and tested if all of the aforementioned variables were to be included in a single set of experiments. To deal with this problem, further testing was continued only on inks containing 100% BOWP. Inks containing higher amounts of binder were not tested because it was shown that the electrical conductivity decreased considerably as the amount of binder was increased in the ink. The procedure, summarised in the following text and described in detail in the following sections, was devised to ensure comprehensiveness of the study.

- A design of experiments was devised (Section 2.4.1), to assist the selection of the most suitable binder for the primer coating of the textile substrates and also to establish the optimum padding process parameters for each of the two types of textile substrates that were used in this study.
- The formulated inks were then printed onto the binder-coated fabrics and the uncoated fabrics, in order to give a basis for selecting the most suitable substrate for further testing of the formulated and the commercial inks. This procedure is described in Section 2.4.2.
- For the washing and creasing tests of the formulated and commercial inks, K-bar drawdowns were produced on fabric substrates instead of screen printing the inks. The aim at this stage was to establish whether or not the use of 100% BOWP loading resulted in the required level of durability of the printed ink layers. The experimental procedure is described in Section 2.4.3.

- The inks selected on the basis of the results of washing and creasing tests, were tested for their screen printability onto the two textile substrates. The procedure devised for the printability tests is described in Section 2.4.4.

2.4.1 Preparation of primer coated textile substrates

In this study, the effect of the binder primer coating on the electrical conductivity of the inks that were printed onto textile fabrics was investigated. Coating a textile fabric with a suitable primer coating results in a smoother surface for printing (Park, Cho and Chung 2007). These effects occur due to the events that occur with such a primer layer. The first of these concerns the blocking and/or covering of the pores and capillaries in the fabric structure. This is particularly important in case of woven fabrics in which pores can run through the thickness of fabric. The second involves the masking of the short fibres and other irregularities on the surface of the substrate, thus reducing the overall roughness of the surface.

One objective of this study was to establish whether or not, besides the above mentioned effects, depositing an ink layer on top of uncured binder primer layer could result in the development of improved adhesion of the ink layer with the substrate, without significantly needing to increase the amount of non-conducting binder in the ink layer. In order to study this effect, the formulated inks were printed onto the woven textile fabrics with and without a binder primer layer. The surface resistivities were then measured and the results compared.

Primer-coated fabric substrates were prepared using a Mathis laboratory dye padder. Binder1, Binder2 and Binder3 were tested for their suitability as a primer coat. This was done by varying the padding pressure to control the uptake and penetration of binder in the fabric structure. The padded substrates were air dried at ambient temperature (22 - 25°C) for 2 hours followed by curing at 100°C for 10 minutes. The primer layers were then characterised using SEM. The coated fabrics were washed following the BS EN ISO 105:C06 test method which is summarised in Section 2.4.3.1. The primer layers were also analysed after washing and the smoothness of a primer layer before and after washing and the resistance to washing were used as criteria for the selection of the most suitable binder for the primer coating of the textile substrates.

The effects of the padding process parameters on the morphology of primer layer were also studied. The aim was to identify the most appropriate primer layer morphology in terms of the layer thickness, the surface smoothness and the penetration of binder into the fabric structure. These are important because an excessively thick primer layer can result in a stiffer fabric, poor washing and poor wearing resistance, due to film cracking. On the other hand, a very thin primer layer is unlikely to cover the pores and surface irregularities completely. The results of the experiments that were carried out to determine the most suitable binder and the associated padding process parameters are discussed in Section 4.6.1.

2.4.2 Relationship between substrate surface characteristics and the performance of the inks deposits

It was thought that the substrate's surface smoothness might affect the print quality which, in turn, would directly affect the required functionality of the ink deposit. Since one of the major aims of this study was to achieve highly conductive prints on textile substrates, the inks selected, following the procedure described in Section 2.3.3, were printed onto various selected substrates. This was done in order to establish that which substrate and surface form (coated or uncoated) would be the most suitable if one wished to maximise the electrical conductivity of the cured ink deposit. For this purpose, K bar drawdowns were produced on coated fabrics and on uncoated fabrics. As discussed in Section 4.5.4, the surface resistivity of all of the formulated inks decreased sharply when multiple ink layers were deposited on top of each other. Thus, in order to deposit a single very thick layer of ink, K bar 9 was used in this study. The surface resistivity of each sample was measured following the procedure described in Section 3.6. The ink layer topography was also analysed using a high resolution optical microscope, as described in Section 3.9. The results of these analyses are discussed in Section 4.6.2.

2.4.3 Testing of printed textile substrates

On the basis of the results of the preceding study, the uncoated 100% cotton fabric and Binder3-coated 100% polyester fabric were selected as substrates for the further testing of inks. The formulated inks containing 100% BOWP and the two commercial conductive inks were tested for their surface resistivity and their resistance to washing

and creasing. Two sets of printed samples were prepared using the K-bar 9 in order to deposit a thick layer of ink onto uncoated 100% cotton and Binder3-coated 100% polyester fabrics. The printed samples were air dried at ambient temperature (22 – 25°C) for one hour, followed by curing at 120 °C for 20 minutes. The curing conditions were set according to the supplier's recommendations to ensure proper curing of the binders. The cured samples were then conditioned at ambient temperature (22 – 25°C) for 48 hours before further tests were performed, as described in the following sections.

2.4.3.1 Washing tests of printed textile substrates

From one of the sets of printed substrates, prepared as described in the preceding section, swatches were cut out for washing tests which were performed according to the BS EN ISO 105-C06:1997 test method. This test method is used to determine the colour fastness of a textile material to domestic washing and commercial laundering. In the context of present study, however, the test was carried out to determine the effects of washing on the surface resistivity of the conductive inks deposited onto textile substrates. For this purpose, the surface resistivity of the test samples was recorded before and after the washing test. On the basis of the results of the washing tests, increasing the amount of binder was proposed only if an ink failed to withstand a single washing cycle, as indicated by the occurrence of a significant increase in the surface resistivity and/or the cracking of the ink film, in such cases. The test procedure is summarised as follows.

- The washing tests were carried out on a Mathis Washtester Model WT, which complies with the requirements for a suitable mechanical device, as specified in the standard test method.
- The AATCC Reference Detergent 1993 (Without Optical Brightener) was used in all the tests.
- For each test specimen, two suitable single-fibre adjacent fabrics, complying with the sections F01 to F08 of ISO 105-F:1985, were used.
- The test number C1S, for which the test conditions are provided in Table 2-13, was performed.

Table 2-13: Conditions for Test number C1S of BS EN ISO 105-C06:1997.

Temperature	60 °C
Liquor Volume	50 mL
Available chlorine	None
Sodium perborate	None
Time	30 minutes
Number of steel balls	25
pH	10.5 ± 0.1

2.4.3.2 Crease resistance testing of printed textile substrates

Tests to determine the creasing durability of the selected inks were carried out on the second set of printed substrates, prepared as described in Section 2.4.3. Creasing tests were performed according to the ASTM F 2749 - 09 test method, which specifies the procedure, without specifying the precision and bias of the procedure, for the creasing of any part of a membrane switch with conductive circuits. The method defines 'crease' as a ridge or groove made by folding and pressing. A crease cycle is defined as a 180° crease, followed by straightening of the crease.

In this study, compression conductor testing was carried out according to the modified procedure summarised as follows.

- The surface resistivity of the specimen was recorded following the procedure described in Section 3.6.
- One end (Static end) of the specimen was clamped to the test fixture while the unsecured end (dynamic end) was looped underneath the static end.
- A smooth steel roller measuring 1 inch in diameter was used to apply a constant load of 20 N while it was rolled from the clamped end towards the end of the loop at a speed of approximately 25 mm/s.
- The roller was rolled completely off the loop creating a crease.
- The creased specimen was opened immediately and straightened, followed by recording the surface resistivity.
- Five creasing cycles were performed and the surface resistivity of the specimen was recorded between successive cycles.

2.4.4 Screen printing of inks onto textile substrates

Besides the properties of ink, there are a number of printing press related variables which affect the quality of ink deposits. In case of screen printing, these variables can be categorised as follows.

1. Screen variables

- i. Mesh material
- ii. Mesh count
- iii. Mesh filament diameter
- iv. Mesh weave
- v. Mesh tension
- vi. Mesh filament direction
- vii. Emulsion type
- viii. Emulsion thickness
- ix. Pattern direction

2. Machine variables

- i. Squeegee attack angle
- ii. Squeegee hardness
- iii. Squeegee edge shape
- iv. Squeegee pressure
- v. Squeegee traverse speed
- vi. Flood blade setting
- vii. Volume of ink on the screen

A detailed study of the above mentioned printing parameters and their optimisation was considered to be beyond the scope of this research programme. After a number of formulated inks possessing high electrical conductivity and durability on textile fabrics had been produced, the objective was to investigate whether or not these inks might be suitable for screen printing onto textile substrates. The following sections describe the procedure. The results of the printability tests are discussed in Section 4.6.4.

2.4.4.1 Setting up of the screen printer

A Rokuprint SD05 screen printer, with a flat screen attachment was used in the experiments to test the printability of the inks that were selected after performance (wash and crease) testing. The equipment specifications are provided in Table 2-14. The screen printer, as shown in Figure 2-8, is provided with a vacuum plate attachment which was used to hold down the samples during printing. In order for the vacuum plate to work, the area of plate not covered by the substrate had to be sealed. This was done using a sheet of impervious cellulose acetate film, as shown in Figure 2-9.

Table 2-14: Specifications of Rokuprint screen printer

Manufacturer/Model	Rokuprint SD 05
Printing size (max)	320 x 220 mm (12.5 x 8.5 inch)
Useful screen size	600 x 300 mm (23.5 x 11.5 inch)
Squeegee speed	Stepless adjustment
Printing attachment	Pneumatic squeegee mechanism with separately adjustable printing squeegee and pre-squeegee
Driving system	Controlled D.C. motors

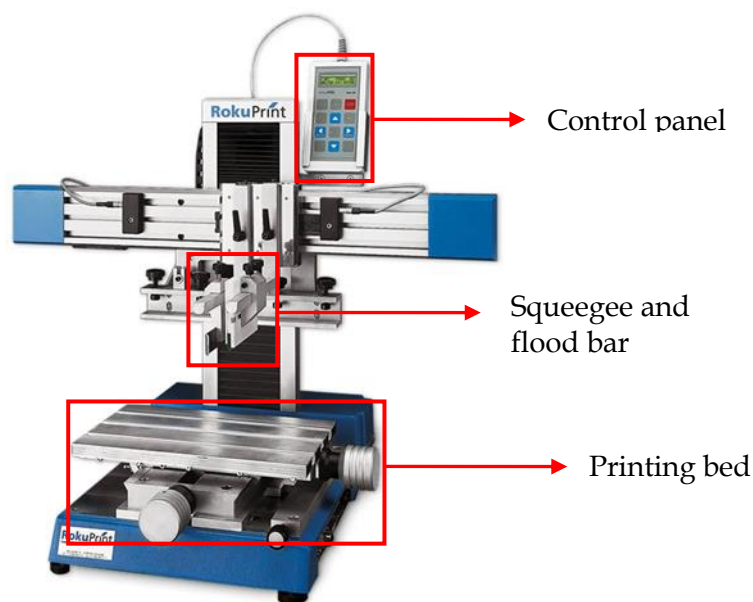


Figure 2-8: Rokuprint SD 05 screen printer

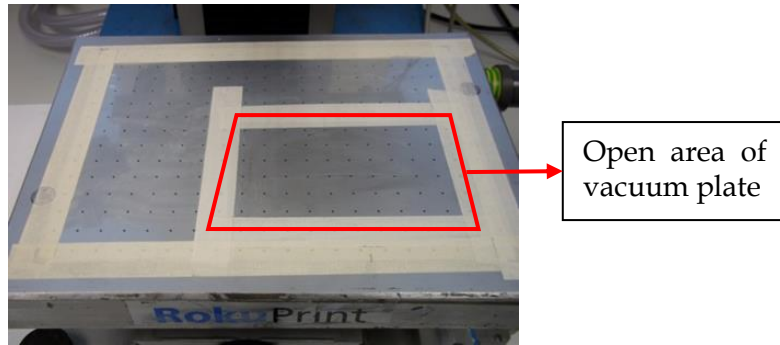


Figure 2-9: Vacuum plate with open nozzles only in the area covered by the substrate.

The screen printer was not provided with a means of measuring the squeegee angle. To overcome this problem, a reference scale was designed and fitted coaxially with the squeegee holder. This arrangement, as shown in Figure 2-10, provided a means of adjusting the squeegee angle quickly and accurately.

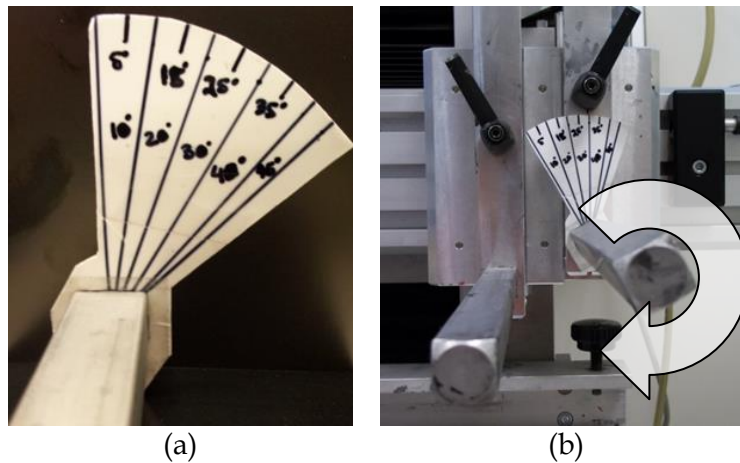


Figure 2-10: Arrangement to measure and adjust the squeegee angle. (a) Reference scale fitted coaxially with the squeegee holder, and (b) squeegee holder and scale mounted on the machine.

2.4.4.2 Screen printing process parameters

The screen printing process parameters that were employed in the printability tests are discussed in this section. A square-edged polyurethane squeegee of 80 shore hardness was used to draw the inks across the screen. A stainless steel plain woven mesh screen having 32 microns thread diameter and 56 microns aperture size was used and the snap-off height was set at approximately 1 mm. The stencil emulsion thickness was approximately 20 microns. The design shown in Figure 2-11, which is a set of parallel lines of different widths, was printed. This was followed by evaluation using an optical

microscope in order to establish the quality of prints. The results of this study are considered in Section 4.6.4.

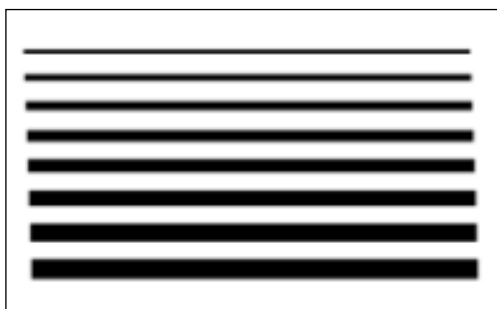


Figure 2-11: Stencil design (scaled down).

In trial runs, it was observed that squeegee pressure that was below 300 – 350 kPa was insufficient to move the squeegee holder down to the print position. On the other hand, the pressurised air supply connected to the machine provided a maximum of 500 kPa. Thus, for the squeegee pressure an intermediate parameter value of 400 kPa was maintained. The squeegee angle was set at 30° (from vertical axis) in accordance with the machine manufacturer's recommendations.

2.4.5 Maximum electrical conductivity of ink deposits

After the screen printability of formulated inks was evaluated, a study was conducted to estimate the minimum surface resistivity which could be achieved using the formulated inks. In this study, Binder3-coated polyester fabric was selected as substrate on which to print the inks. This is because the results of a previous study showed that the surface resistivity of a formulated ink was generally lower on the Binder3-coated polyester fabric, compared to that obtained on other substrates and/or surfaces. To achieve a thick ink deposit, K bar 9 was used to draw one layer of ink, followed by air drying for 1 hour before another ink layer was deposited on top of the dried ink layer. The ink layer was cured at 120 °C for 20 minutes followed by conditioning at 22 – 25 °C for one hour before the surface resistivity was recorded. The results of surface resistivity and thickness of printed ink layers are considered in Section 4.6.5.

Chapter 3. Analytical techniques

3.1 Rheometric measurements

In order to determine the rheological character, the viscosity profiles of the formulated pigment dispersions and finished inks was measured using TA Instruments AR-1500 EX rheometer. A cone-and-plate configuration, as shown in Figure 3-1, was employed.

In a cone-and-plate arrangement, the angle between the cone and the plate is very small (on the order of $0.2^\circ - 4.0^\circ$). The test fluid is filled in the wedge-like space between the cone and the plate. Almost always, the horizontal flat plate is stationary while the cone is rotated about its axis.

The measurement principle of rotational viscometer lies in measuring the torque required to rotate the cone at a particular speed of rotation. The mathematical relationship between the viscosity of test fluid and the torque can be derived by considering a differential volume dV of the test fluid held between the cone and the plate, as shown in Figure 3-1.

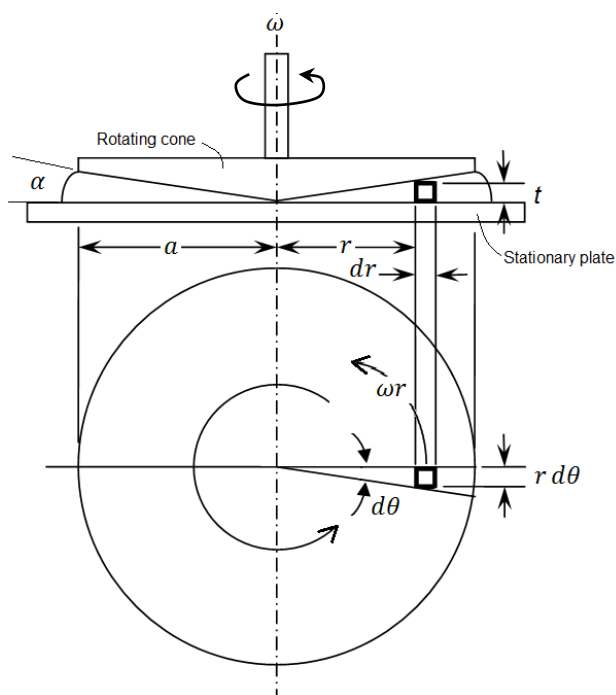


Figure 3-1: Schematic illustration of cone-plate viscometer geometry

From Figure 3-1, the differential area of the fluid is given by Equation 17.

$$dA = rd\theta \times dr \quad \text{Equation 17}$$

From Figure 3-1, the thickness t of fluid segment can be calculated using trigonometry as follows.

$$\sin \alpha = \frac{t}{r} \quad \text{Equation 18}$$

For small angles $\sin \alpha \approx \alpha$. Substituting the value of $\sin \alpha$ in Equation 18 gives the following relationship.

$$\alpha = \frac{t}{r}$$

$$t = r\alpha$$

Since the top surface of the differential volume is in contact with the cone rotating at an angular velocity ω , the linear velocity of the surface of test fluid in contact with the plate can be given by Equation 19.

$$v = r\omega \quad \text{Equation 19}$$

Thus, the shear rate to which the differential volume of the test fluid is subjected can be given by Equation 20.

$$\text{Shear rate} = \frac{\text{Velocity of top layer of test fluid}}{\text{thickness of the fluid layer}} \quad \text{Equation 20}$$

$$\text{Shear rate} = \frac{r\omega}{r\alpha}$$

$$\text{Shear rate} = \frac{\omega}{\alpha}$$

Equation 20 shows that the shear rate for the differential volume of test fluid is independent of r , it follows that the shear rate is constant over the entire volume of the test fluid. It also follows that the shear stress τ must be constant for any given angular velocity ω . Shear stress τ is related to Torque T by Equation 21 below.

$$\text{Torque} = \text{Shear stress} \times \rho \times A \quad \text{Equation 21}$$

Where, ρ is the distance from the axis of cone to where the shear stress is acting, and A is the area of test fluid on which the shear stress is acting. In case of differential volume

of test fluid, the total torque T is equal to the cumulative torque contributions from various differential areas, as given in Equation 22.

$$T = \int_A \tau \rho dA \quad \text{Equation 22}$$

From Figure 3-1, $\rho = r$ and $dA = r d\theta \times dr$. After substituting the values of ρ and dA , Equation 22 can be solved to obtain the value of shear stress, as follows.

$$\begin{aligned} T &= \int_0^{2\pi} \int_0^a \tau r^2 dr d\theta \\ T &= \tau \frac{2\pi a^3}{3} \\ \tau &= T \frac{3}{2\pi a^3} \end{aligned}$$

The viscosity η of a fluid is the ratio of shear stress to the shear rate to which the fluid is subjected.

$$\begin{aligned} \eta &= \frac{\text{Shear stress}}{\text{Shear rate}} \\ \eta &= \left(T \frac{3}{2\pi a^3} \middle| \frac{\omega}{a} \right) \\ \eta &= \frac{T}{\omega} \frac{3\alpha}{2\pi a^3} \quad \text{Equation 23} \end{aligned}$$

Inertial forces can be neglected relative to the viscous forces when the angle between the cone and the plate is small (Slattery 1961). Thus, in commercial instruments, Equation 23 defines the underlying mathematical relationship used to calculate viscosity of the test fluid.

3.1.1 Test setup for viscosity measurements

ASTM D4287 - 00(2010), which is the standard method for measuring the high shear viscosity using a cone-and-plate viscometer, was followed for the rheological characterisation of the formulated dispersions and inks. Prior to measurement, each sample was gently shaken for 10 seconds and then left at ambient temperature (22°C - 25°C) for five minutes. The instrument air-bearing and zero-gap of the geometry were calibrated each time the instrument was turned on. A 60 mm stainless steel cone with 1° taper angle and 27 μm truncation gap was used. Each test sample was equilibrated on the instrument for two minutes at 25°C and measurement was made without pre-

shearing the sample. A continuous ramp test was employed and the viscosity profile was recorded over a shear rate range of 1 s^{-1} to 1000 s^{-1} . 70 data points were recorded in the specified shear rate range. Each sample was tested at least twice to establish confidence in the data obtained. Between successive tests, the cone geometry was removed from the spindle and cleaned following the procedure recommended by the instrument manufacturer.

3.2 Particle size analysis by DLS

In the present study, a Zetasizer Nano ZS (Malvern Instruments) was used to analyse pigment particle size distribution in the waterborne dispersions that were prepared. The principle of particle size measurements, using dynamic light scattering, as performed by the instrument, is described below.

Light incident upon a small particle is scattered by the particle in all directions. If the particle is stationary, the scattering pattern will also be stationary. Particles suspended in a liquid constantly undergo Brownian motion and due to this motion, the constructive and destructive interference of the scattered light results in fluctuation of the intensity of scattered light. The rate of intensity fluctuation depends on the velocity of particle which in turn depends on its size, as shown in Figure 3-2. Thus, fluctuation in the intensity of scattered light can be used to estimate the particle (scatterer) size.

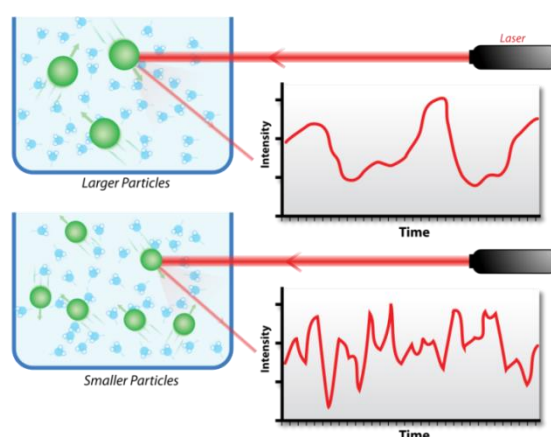


Figure 3-2: Light scattering by large particles (top) and by smaller particles (bottom).

The scattered light intensity signals are recorded over very short time intervals (in the order of nanoseconds). A digital correlator measures the degree of similarity between

two signals to give an overall correlation function against time, as shown in Figure 3-3. In case of large particles which move slowly, the correlation function decays slowly. For small particles which move quickly, however, the correlation function decays rapidly as shown in Figure 3-4.

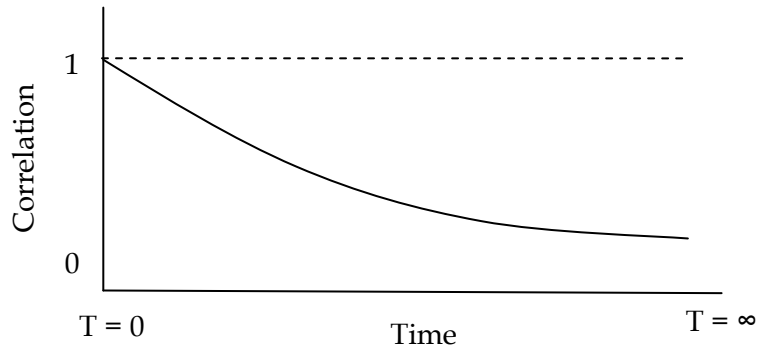


Figure 3-3: Correlation as a function of time

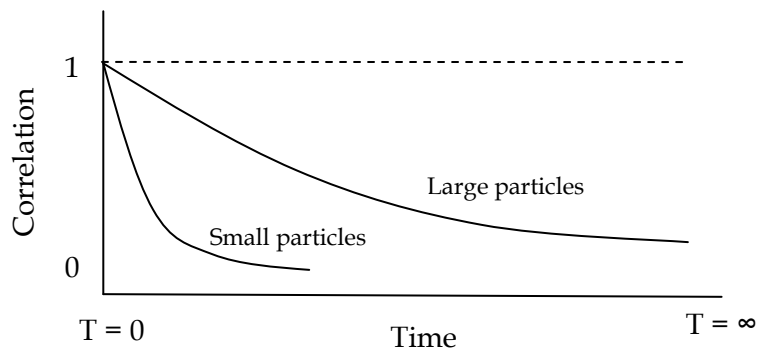


Figure 3-4: Correlation function for large and small particles

After determining the decay rate of the correlation function, the instrument software compares it with the decay rates for a number of size classes to produce a size distribution.

Mean size of the dispersed particle is obtained from the correlation function by using various algorithms. This is done by fitting a single exponential to the correlation function to obtain the mean size and an estimate of the width of the distribution, which are referred to as the z-average particle size and polydispersity index, respectively. This approach is called the Cumulants analysis and is defined in ISO13321:1996 E. The Cumulants analysis is actually a 3rd order fit of a polynomial to the log of the G1 correlation function.

$$\ln[G1] = a + bt + ct^2$$

The value of b is known as the second order cumulant, or the z -average diffusion coefficient. This is converted to a size using the dispersant viscosity and some instrumental constants. Only the first three terms a, b, c are used in the standard analysis to avoid over-resolving the data. The coefficient of the squared term, c , when scaled as $2c/b^2$ is known as the polydispersity, or polydispersity index (PDI) (Malvern 2008).

3.2.1 Test setup for particle size analysis

For particle size analysis by DLS, the recommendation is to have a solids content of below 0.1% in the sample (Kissa 1999c). Thus, samples were prepared by diluting 0.25 g of pigment dispersion with 50 grams of deionised water and subjecting the diluted sample to ultra-sonication for five seconds. The default values of 1.675 for the refractive index and 1.00 for the absorption of the pigment were set in the instrument software. Due to the extent of dilution, water was selected as dispersant in the test SOP, for which the default values of 1.330 and 78.5 were used for refractive index and dielectric constant, respectively. The test sample was equilibrated at 25 °C for 60 seconds prior to recording the data. A disposable sizing cuvette (Malvern reference: DTS0012) was used for the size analyses.

The instrument uses a monochromatic and coherent He-Ne laser beam (wavelength 632.8 nm) to illuminate the test sample. In the size analyses, backscatter detection was applied. Backscatter detection has several advantages over forward (90°) detection optics. These include the reality that greater loadings of pigment in the sample can be used. This is because light has to pass through a shorter path length of the sample. Also, the effects of multiple scattering are reduced because the incident beam does not have to travel through the entire sample. It should be noted that contaminants in the sample, such as large dust particles, are likely to scatter in the forward direction. Therefore, backscatter detection significantly reduces the effects of contaminants on the acquired data.

3.3 Zeta potential measurements

A charged particle in an electric field exhibits a number of electrokinetic effects such as electrophoresis, electroosmosis, streaming potential and sedimentation potential. The Zetasizer Nano ZS measures the zeta potential of pigment particles that are dispersed in an aqueous medium by performing an electrophoresis experiment. In this experiment, the velocity of a particle relative to the dispersion medium is determined. Electrophoresis can be defined as the movement of a charged particle under the influence of an electric field applied across the liquid in which the particle is suspended. Such a movement of the particle is opposed by the viscous forces that are inherent in the liquid. When an equilibrium is achieved between these two opposing forces, the particle attains a constant velocity, known as the electrophoretic mobility. Henry's equation (Equation 24) described the mathematical relationship among the various factors influencing the electrophoretic mobility (Malvern 2008).

$$V_E = \frac{2\varepsilon\zeta f(Ka)}{3\eta} \quad \text{Equation 24}$$

In Equation 24,

V_E = Electrophoretic mobility

ε = Dielectric constant of the dispersion medium

ζ = Zeta potential

$f(Ka)$ = Henry's function

η = Viscosity of the dispersion medium

The value of Henry's function $f(Ka)$ depends on the nature of continuous phase, the particle size and the electrolyte type and concentration.

- For particles larger than about 0.2 microns, dispersed in aqueous media containing moderate electrolyte concentration (typically more than 10^{-3} moles of a suitable salt), the Smoluchowski approximation ($f(Ka) = 1.5$) is used.
- Huckel's approximation provides the value of Henry's function ($f(Ka) = 1.0$) in the case of small particles that are dispersed in a low dielectric constant medium (non-aqueous media).

3.3.1 Test setup for zeta potential measurement

The test samples that were prepared for particle size analysis, as described in Section 3.2.1, were used for zeta potential measurements as well. A disposable zeta cell (Malvern reference: DTS1060C) was employed.

3.4 Analytical centrifugation studies

Centrifugation is a widely used technique for characterising de-mixing phenomena such as sedimentation, flotation and/or consolidation. An analytical centrifuge is an instrument which evaluates the stability of a colloidal system by accelerated gravitational settling, as discussed in Section 1.10.1.

A LUMiSizer ® dispersion analyser was used in this study to analyse the tendency to sedimentation of pigment in the optimised, waterborne pigment dispersions. The working principle, as depicted in Figure 3-5, is described in the following text.

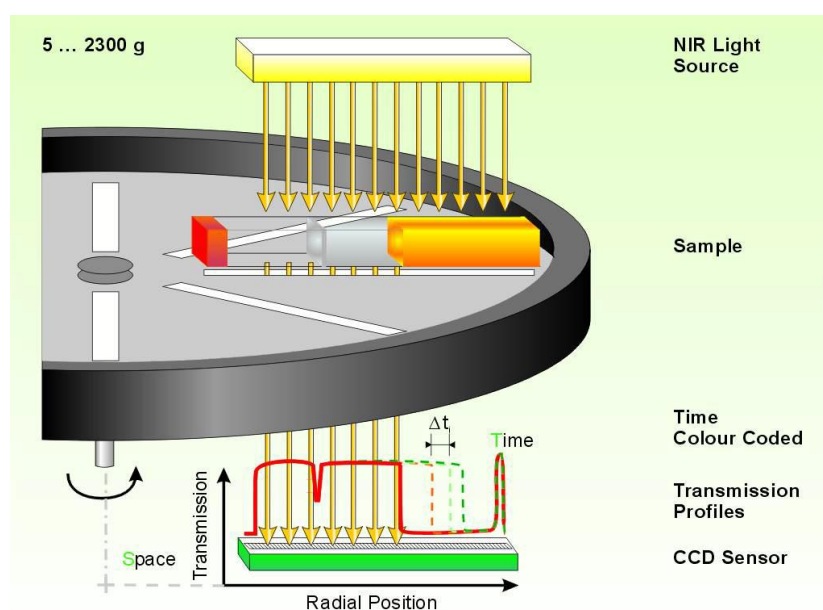


Figure 3-5: Working principle of LUMiSizer® Dispersion Analyser (© LUM GmbH).

The dispersion sample to be analysed is contained in a suitable cell and secured horizontally in the instrument. Near infrared light (wavelength 870 nm) of known intensity (I_0) illuminates the entire sample. The intensity of transmitted light (I) through the sample is recorded by a detector consisting of 2048 CCD elements. The

transmission profile recorded by the detectors is converted into space- and time-resolved extinction profiles over the entire sample length. The instrument is also capable of particle size analysis but in this study, it was employed only for accelerated gravitational sedimentation analysis.

3.4.1 Test setup for sedimentation analyses

An attempt was made to characterise the sedimentation that occurred in the optimised pigment dispersions, without diluting the dispersions. For this purpose, the pigment dispersions were tested for their six months storage stability. Due to their very high viscosity, the dispersions of Carbon4 pigment could not be placed in the LUM 2 mm polycarbonate cell. Thus these dispersions were not tested in this way. Little or no change in the transmission profiles of the dispersions occurred during the six months stability test. The results are considered in detail in Section 4.2.

3.5 Electrical conductivity measurements

The electrical conductivity of the pigment dispersions was recorded using a Mettler Toledo portable conductivity meter (Model: FG3-Kit FiveGo™) fitted with a Mettler Toledo LE703 conductivity electrode. To measure the conductivity of a dispersion, the conductivity electrode was submerged in the dispersion and stirred gently to ensure that air was not trapped inside the cell. The cell was left immersed in the dispersion until a steady reading of the conductivity was obtained.

3.6 Surface resistivity measurements

The surface resistivity was the most important electrical characteristic of interest in this study and it was measured at several stages in the work, as listed below.

- During preparation and optimisation of pigment dispersions. At this stage, the aim was to identify the dispersions which possessed high surface resistivity.
- After the let-down of pigment dispersions. This was done on the basis that only those inks would be used for further tests which possessed low surface resistivity.

- After printing the formulated inks onto various substrates, surface resistivity measurements were done to evaluate the durability of the inks. The minimum surface resistivity that could be achieved using these inks was also measured.

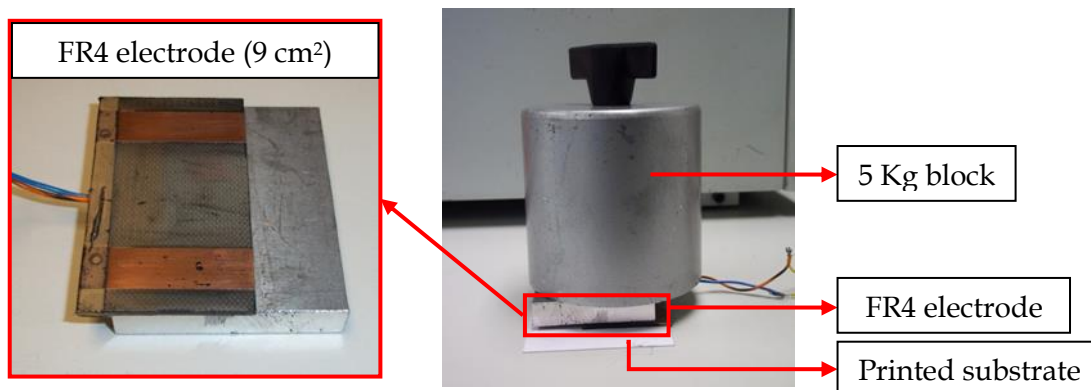


Figure 3-6: Surface resistivity measurement setup.

The surface resistivity was recorded using a Keithley digital multimeter (Model 2100). An electrode, as shown in Figure 3-6, was designed to record the surface resistivity of a 30 mm x 30 mm printed area. A standard 5 kg weight block was used to press the electrode onto the printed substrate, thus helping to ensure that intimate contact between the electrode and the test surface was achieved.

3.7 Thermogravimetric analysis (TGA) studies

Thermogravimetric analyses were performed using a TA Instruments TGA Q50, on samples of binders (as-supplied) and dispersants (as-supplied), on the optimised pigment dispersions and on the commercial ink samples. The parameters for the above-mentioned analyses are tabulated in Table 3-1 while the objectives of these analyses are described in the following sections.

This space is deliberately left blank due to pagination.

Table 3-1: Parameters for TGA.

TGA parameter	Material analysed			
	Binders	Dispersants	Pigment dispersions	Commercial inks
Heating method	Ramp	Ramp	Ramp - Isothermal for 10 minutes at end temperature	Ramp - Isothermal for 10 minutes at end temperature
Heating rate (°C/min)	10	10	10	10
Start temperature (°C)	25	25	25	25
End temperature (°C)	500	500	800 - 825	800
Test atmosphere	Nitrogen purge	Nitrogen purge	Nitrogen purge	Nitrogen purge
Balance purge flow (mL/min)	40	40	40	40
Sample purge flow (mL/min)	60	60	60	60

3.7.1 TGA of binders

Thermogravimetric analysis was carried out to determine the solids content of the binders used in this study. This was required because the amount of binder solids in a finished ink was calculated on the weight of pigment in the dispersion as discussed in Section 2.3.2. As shown in Figure 3-7, the solids content for Glascol HN2 was found to be 30 wt% while for Binder1 (Impranil DLC-F), Binder2 (Impranil LP GHG 519) and Binder3 (Printofix Binder 83) the solids content in the curing temperature range was found to be approximately 40 wt%.

3.7.2 TGA of dispersants

TGA of the dispersants (in as-supplied form) was carried out to determine the temperatures at which evaporation and decomposition occurred. The relevant thermograms are presented and discussed in Section 4.4.

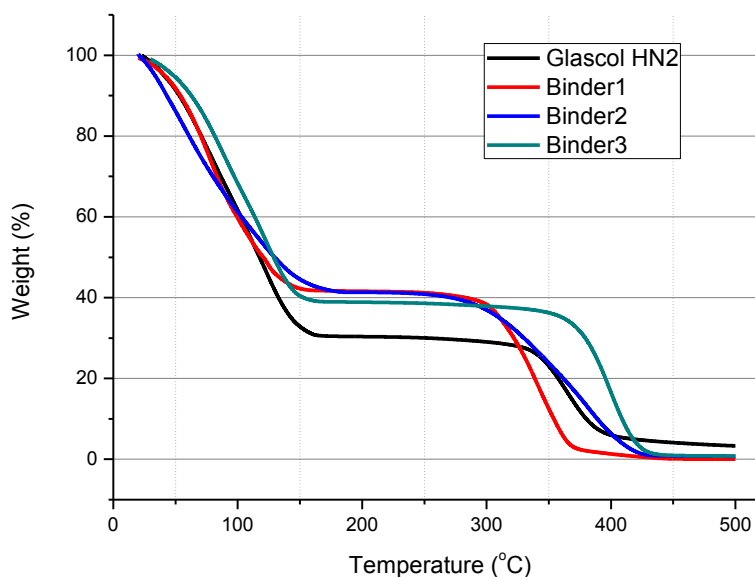


Figure 3-7: Thermograms of the binders used in the study.

3.7.3 TGA of pigment dispersions

TGA of an optimised pigment dispersion was carried out to determine and compare the pigment loading in different batches of the dispersion. This was used as a diagnostic tool to establish the correctness of formulations and repeatability of the dispersion preparation process, as described in Section 2.2.5.

3.7.4 TGA of commercial ink samples

One of the more important investigations in this study was the electrical performance comparison of the formulated and the selected commercially available conductive inks. Since the electrical conductivity of an ink depends, to a great extent, on the amount of conductive pigment in the ink, the solids content in the commercial inks samples was determined using TGA and it was found to be 40 wt% and 73 wt% for the Gwent conductive carbon ink C2030519P4 and for the Peters SD 2843 HAL carbon ink, respectively. These results were then compared with those relating to the amount of pigment in the formulated inks, as discussed in Section 4.6.3 and Section 4.6.5.

3.8 Scanning Electron Microscopy of textile fabrics

Scanning electron microscopy is one of the more commonly employed surface characterisation techniques. In this study, SEM was used primarily to establish aspects

of the morphology of the binder primer layers that were deposited on the various textile fabrics.

In the scanning electron microscopy, a finely tuned electron beam is scanned over the sample surface. The beam undergoes a variety of interactions leading to emission of electrons of different energies, X-rays and light. The image is produced by the detection of low energy secondary electrons. The scanning electron microscope has a depth of field some 10 – 100 times greater than that of an optical microscope at the same magnification, while the resolution of SEM is also considerably better. Any charging of insulating materials is overcome by applying a 30 – 50 nm of a conductive coating, deposited by a vapour deposition procedure, prior to SEM analysis. The steps involved in obtaining SEM micrographs of a sample were the coating of the sample with a 30 – 50 nm thick layer of conductive materials such as gold. Then the samples were placed in a vacuum chamber to exclude any possible interactions of the electron beam with the particles in air. The focus was then adjusted and the image was recorded.

For SEM analysis, the deposited thin layer of gold was achieved using a Bio-Rad SC500 diode sputter coating unit. The SEM used was a Jeol JSM-6610LV.

3.9 Optical Microscopy

In the optical microscopic evaluations, a Keyence VHX-2000E digital optical microscope, fitted with a VH-Z100UR lens, was used. The analyses consisted of ink layer topography, ink film cracking and an assessment of the print quality on textile substrates.

For ink layer topography evaluations and the ink film cracking study, composite images were recorded. These composite images were compiled by the instrumental software, by superimposing images that were recorded at different focal planes. Thus, the final image was in-focus from the lowest to the highest plane. This allowed improved visualisation of the extent of any ink cracking in a sample, as shown in Figure 3-8.

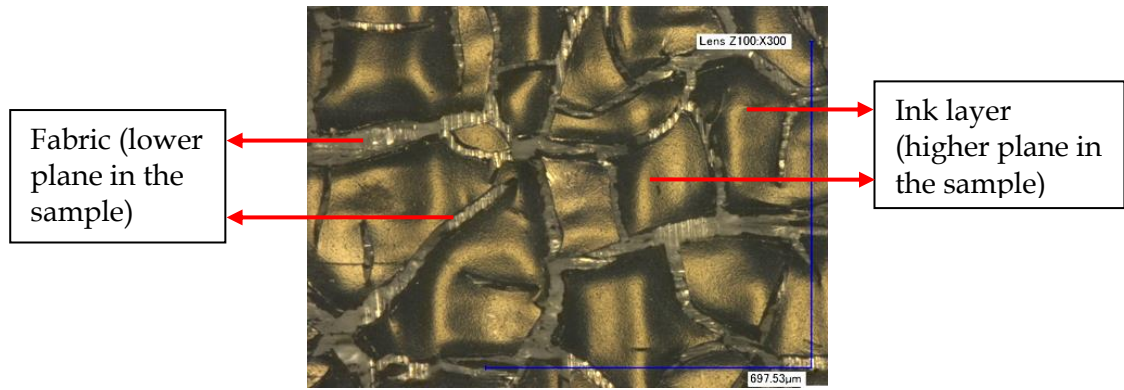


Figure 3-8: Composite image of a printed textile fabric showing regions of different heights in-focus.

In contrast to a composite image compilation, in the normal mode of recording the images, only one of the focal planes was recorded at a time. Thus, in the resulting image, either the lower or the higher planes in an uneven target were in-focus, as shown in Figure 3-9.

It was also observed that the use of the microscope in combined normal (light incident on the sample surface) and transmission modes resulted in better visualisation of cracks in an ink layer. This approach was found to be particularly useful for samples having a lesser extent of cracking of the ink layer, as shown in Figure 3-10. Thus, all the images for the evaluation of the ink layer cracking were recorded in this combined mode of illumination.

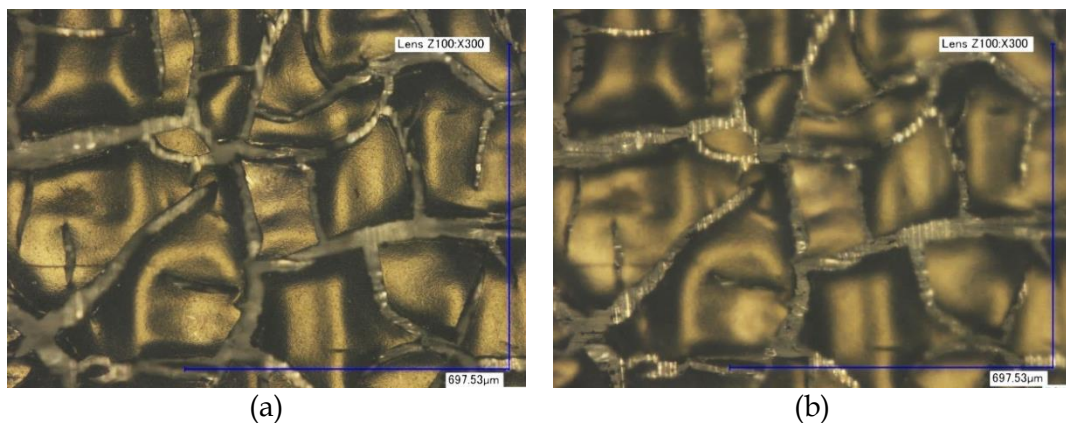


Figure 3-9: Optical micrographs recorded in normal mode. (a) Only the ink surface (higher planes) is in-focus and (b) fabric (lower plane) is in-focus.

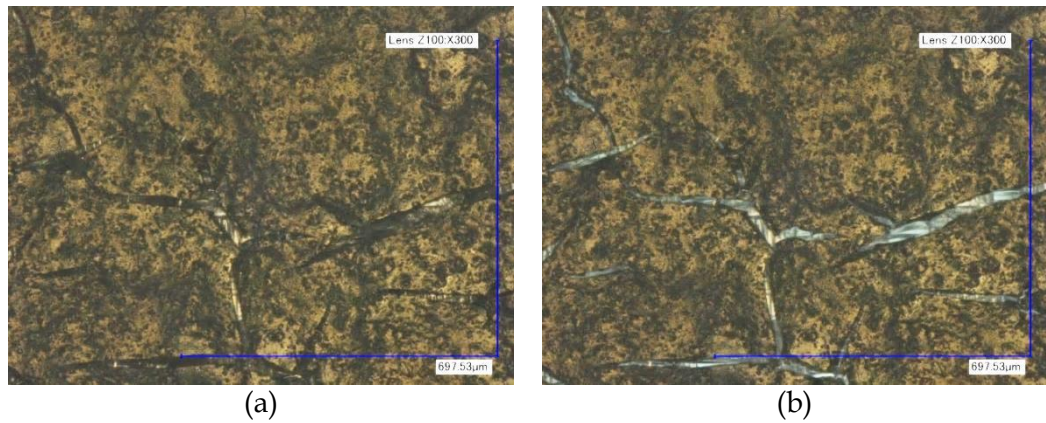


Figure 3-10: Extent of ink layer cracking observed under (a) normal illumination and (b) combined normal and transmission mode.

In order to evaluate the quality of the prints, images of a 1mm wide line, printed onto the Binder3-coated 100% polyester fabric, were recorded using the microscope in a normal illumination mode. The instrument software allowed real-time measurement of the width of the printed lines. The results of these analyses are discussed in Section 4.6.4.

Chapter 4. Results and Discussion

Figure 4-1 depicts the sequence in which the results of experiments carried out in this study are presented and discussed.

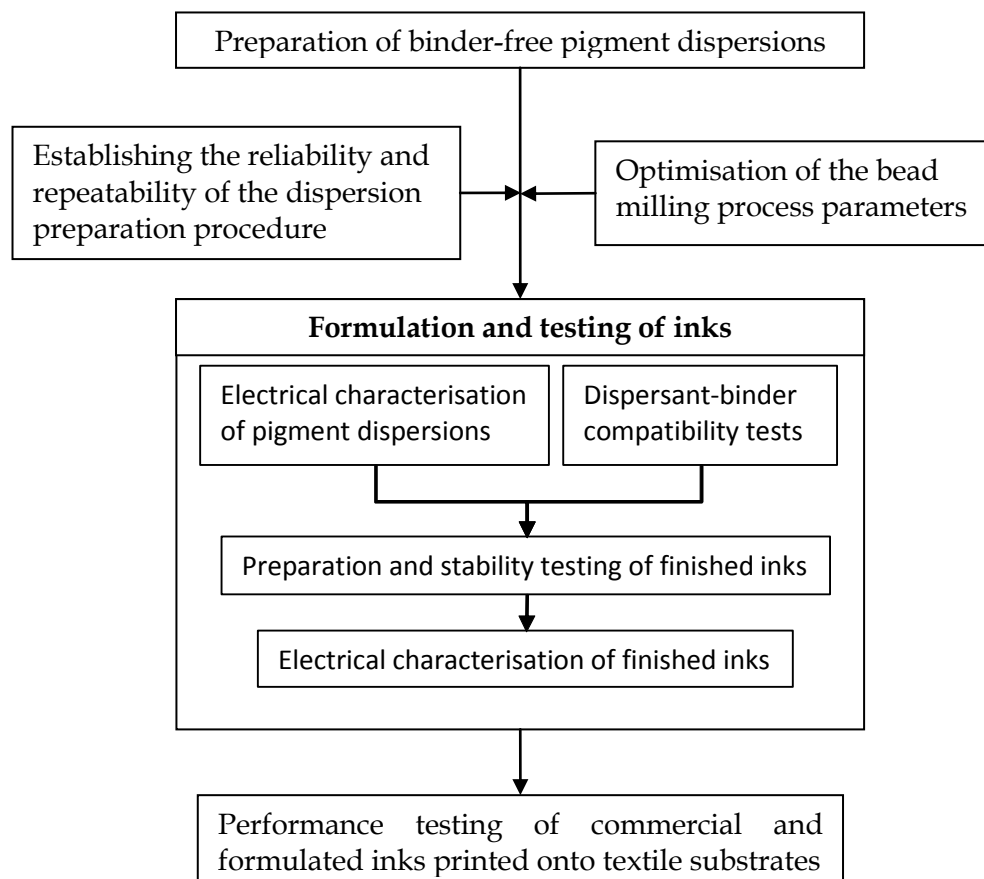


Figure 4-1: Flow chart of the various steps in this study.

4.1 Preparation and optimisation of pigment dispersions

4.1.1 Optimisation of Carbon1 (Vulcan XC605) pigment dispersion

In the sinking test carried out for Carbon1, 0.170g of the pigment was added gently to each dispersant solution that was contained in a test tube. Images were recorded 24 hours, 48 hours and 72 hours after the addition of the pigment. Figure 4-2 shows the dispersant media that were collected from the top of test tubes after 72 hours of pigment addition. It was found that the opacity of the mixture that was prepared in Dispersant3 (760W) solution was significantly greater than that of any of the other mixtures. Thus, Dispersant3 was used to optimise the dispersion of Carbon1 pigment.

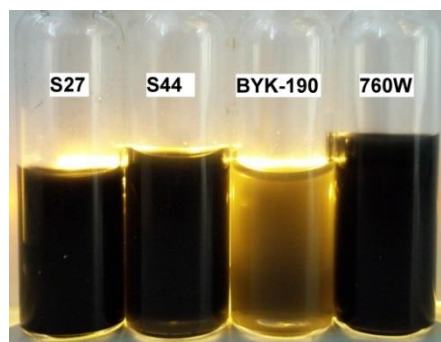


Figure 4-2: Dispersant media observed against an array of LEDs, 72 hours after the addition of Carbon1.

Using Equation 16, the theoretical dispersant dosage for the Carbon1 pigment was calculated to be 12% DOWP (approx.). A series of control dispersions, the composition of which is given in Table 4-1, was prepared.

Table 4-1: Composition of control dispersions of Carbon1 pigment.

Control dispersion composition	Carbon1 (g)	Foamex 805 (g)	Glascal HN2 solution (g)	Total (g)
Carbon1 18 wt%, Glascal HN2 3 wt% solids	18	1	81	100
Carbon1 15 wt%, Glascal HN2 10 wt% solids	15	1	84	100

The viscosity profiles, as shown in Figure 4-3, indicated that the dispersion containing 15 wt% of the Carbon1 pigment and 10 wt% of binder solids was suitable for use as control dispersion. This is because the viscosity profile of the control dispersion containing 3 wt% of Glascal HN2 binder solids indicated that the amount of binder was not sufficient to result in the satisfactory stabilisation of the pigment particles.

This space is deliberately left blank due to pagination.

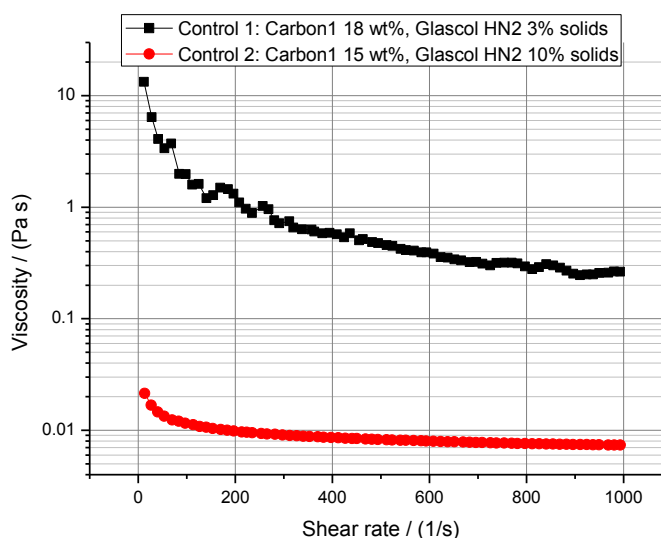


Figure 4-3: Viscosity profiles of control dispersions of Carbon1 pigment.

Using 12% DOWP of Dispersant3, a dispersion containing 26 wt% of the Carbon1 pigment was prepared and the viscosity profile was compared with that of the Control 2 dispersion. It was found that the pigment loading had to be decreased to match the viscosity profile of the Control 2 dispersion. Thus, a dispersion containing 22wt% Carbon1 was prepared. The compositions of dispersions containing 26 wt% and 22 wt% Carbon1 are given in Table 4-2.

Table 4-2: Composition of the 22 wt% and the 26 wt% Carbon1 dispersions.

Dispersion composition	Carbon1 pigment (g)	Dispersant3 (35% active) (g)	Foamex 805 (g)	D.I. water (g)	Total (g)
Carbon1 26 wt%, Dispersant3 12 % DOWP	26	8.91	1	64.08	100
Carbon1 22 wt%, Dispersant3 12 % DOWP	22	7.54	1	69.45	100

The viscosity profile of the dispersion containing 22 wt% Carbon1 matched the viscosity profile of the Control 2 dispersion, as shown in Figure 4-4. Thus in the next step, the dispersant dosage was optimised for 22 wt% loading of Carbon1 pigment in aqueous dispersion.

Table 4-3 provides compositions of the dispersions containing 22 wt% Carbon1 pigment and different amounts of Dispersant3 calculated around the theoretical

dispersant dosage. The viscosity profiles are presented in Figure 4-5 and the electrical characteristics of the dispersions are tabulated in Table 4-4.

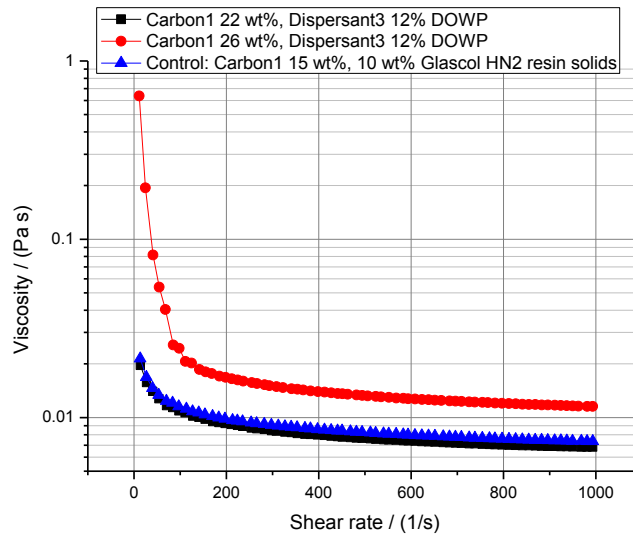


Figure 4-4: Viscosity profiles of control dispersion, 22 wt% and 26 wt% Carbon1 dispersions.

Table 4-3: Compositions of dispersions containing 22 wt% Carbon1 and various amounts of Dispersant3.

Dispersion Composition	Carbon1 pigment (g)	Dispersant3 (35% active) (g)	Foamex 805 (g)	D.I. water (g)	Total (g)
Carbon1 22 wt%, Dispersant3 9% DOWP	22	5.66	0.8	71.54	100
Carbon1 22 wt%, Dispersant3 12% DOWP	22	7.54	0.8	69.66	100
Carbon1 22 wt%, Dispersant3 15% DOWP	22	9.43	0.8	67.77	100
Carbon1 22 wt%, Dispersant3 18% DOWP	22	11.31	0.8	65.89	100

As shown in Figure 4-5, the viscosity profiles of the dispersions containing 15% DOWP and 18% DOWP of Dispersant3 were only very slightly different from each other. However, the viscosities were lower than those of the dispersions containing 9% DOWP and 12% DOWP of Dispersant3. This indicated that the greater dispersant dosage resulted in an improved dispersion of the Carbon1 pigment.

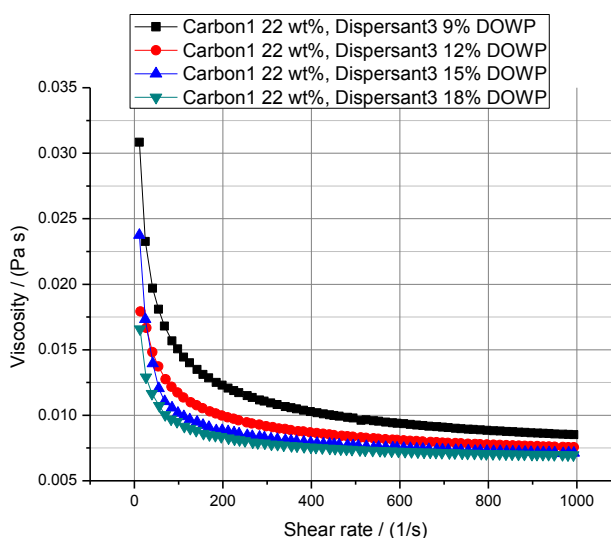


Figure 4-5: Viscosity profiles of dispersions of Carbon1 prepared in Step 3 of optimisation.

The results of electrical characterisation, as summarised in Table 4-4, of the dispersions that were prepared to determine the optimum dispersant dosage, also indicated that increasing the amount of dispersant improved the electrical conductivity. This can be attributed to improved dispersion of the pigment upon increasing the dispersant dosage.

Table 4-4: Electrical conductivity and surface resistivity of dispersions of Carbon1 prepared in Step 3.

Dispersion composition	Conductivity ($\mu\text{S/cm}$)	Surface resistivity (Ω/\square)
Carbon1 22 wt%, Dispersant3 9% DOWP	119.4	426
Carbon1 22 wt%, Dispersant3 12% DOWP	134.3	357
Carbon1 22 wt%, Dispersant3 15% DOWP	152.2	350
Carbon1 22 wt%, Dispersant3 18% DOWP	163.4	330

The stability of the pigment dispersions was considered to be crucial in the context of this study. Therefore, the viscosity profiles (Figure 4-6), the zeta potential values and particle size parameters (Table 4-5) of the dispersions prepared in Step 3 of the optimisation, were also determined after storage. As shown in Figure 4-6(a), the deviation from shear thinning behaviour after 10 days and after four weeks of storage, indicated clearly that the dispersion containing 9% DOWP was developing structure

and there was probably some aggregation of the pigment. The dispersions containing 12%, 15% and 18% DOWP of Dispersant3, however, showed a stable, shear thinning rheology throughout the time of ageing, as shown in Figure 4-6 (b - d). Table 4-5 shows that the zeta potential of dispersion containing 15% DOWP of Dispersant3 was relatively stable compared to the other dispersions in the ladder series. The average particle size increased considerably in the dispersions containing 9% DOWP and 12% DOWP of Dispersant3. Both the average particle size and PDI remained relatively stable for dispersions containing 15% DOWP and 18% DOWP of Dispersant3.

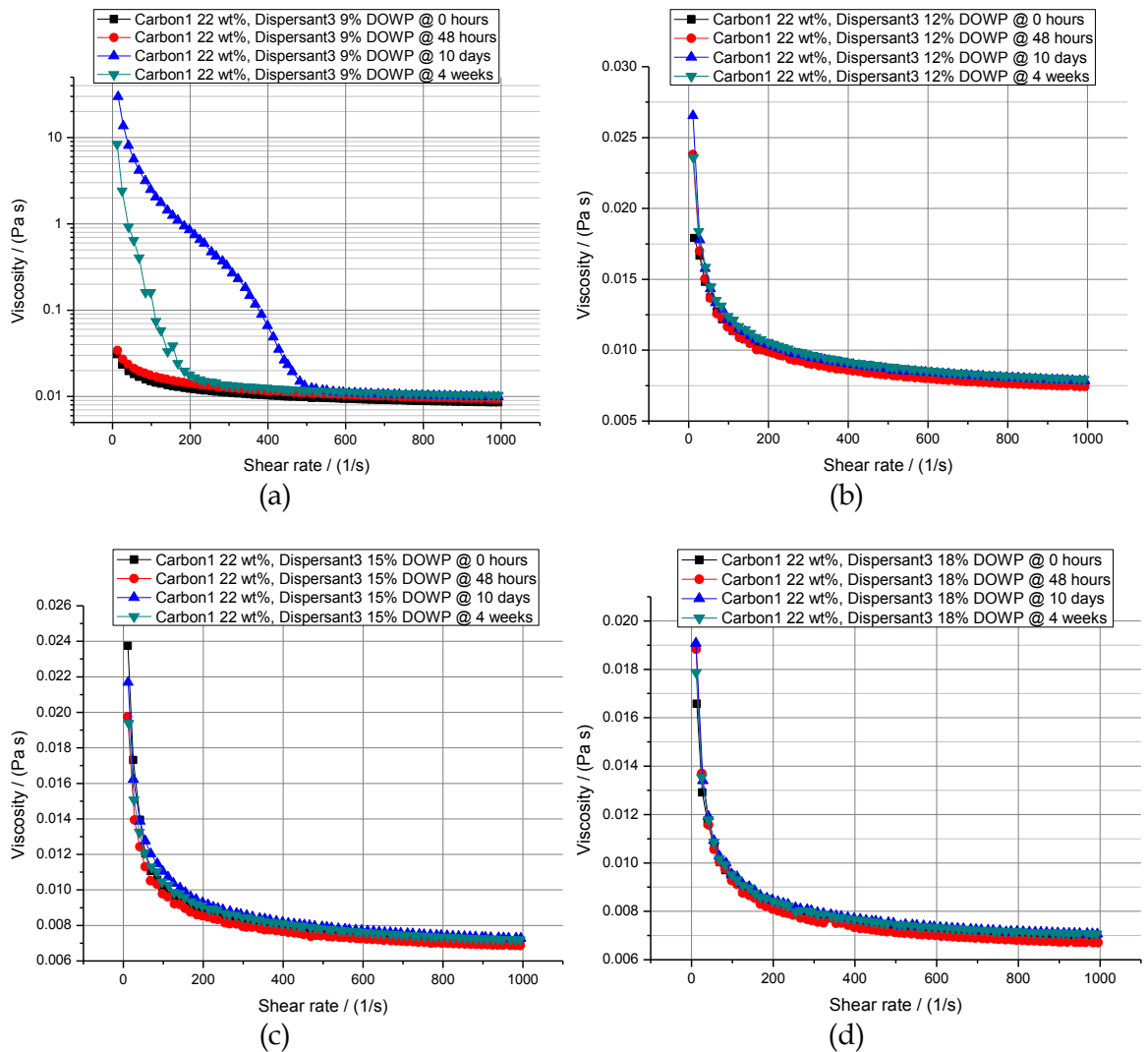


Figure 4-6: Viscosity stability of dispersions of Carbon1 prepared using (a) 9%, (b) 12%, (c) 15% and (d) 18% DOWP of Dispersant3.

This space is deliberately left blank due to pagination.

Table 4-5: Results of zeta potential and particle size analyses carried out during storage of the dispersions of Carbon1 prepared in Step 3.

Dispersion composition	Time	ζ (mV)	Z-avg (nm)	PDI	Peak 1 (nm)	Peak 2 (nm)	Peak 1 area (%)	Peak 2 area (%)
Carbon1 22wt%, Dispersant3 9% DOWP	0 hours	-25.9	224	0.14	252	0	100	0
	48 hours	-27.0	223	0.17	249	0	100	0
	10 days	-34.1	223	0.18	231	5027	97.7	2.3
	4 weeks	-16.9	335	0.28	504	0	100	0
Carbon1 22wt%, Dispersant3 12% DOWP	0 hours	-16.3	224	0.19	233	5213	98.6	1.4
	48 hours	-23.2	227	0.12	262	0	100	0
	10 days	-15.4	227	0.15	263	0	100	0
	4 weeks	-22.0	415	0.21	555	0	100	0
Carbon1 22wt%, Dispersant3 15% DOWP	0 hours	-25.4	296	0.28	366	4420	95.9	4.1
	48 hours	-22.3	238	0.21	276	5011	98.3	1.7
	10 days	-12.4	233	0.18	259	4807	98.1	1.9
	4 weeks	-27.4	292	0.32	367	5034	97.8	2.2
Carbon1 22wt%, Dispersant3 18% DOWP	0 hours	-16.4	220	0.11	250	0	100	0
	48 hours	-21.0	246	0.22	275	4832	97.2	2.8
	10 days	-32.2	229	0.14	268	0	100	0
	4 weeks	-19.1	222	0.20	239	4687	96.7	3.3

In the aforementioned analyses, the difference between the dispersions containing 15% DOWP and 18% DOWP of Dispersant3 was not found to be significant in terms of the viscosity, the electrical conductivity and the average particle size. Generally, a lower dispersant dosage is likely to result in superior finished ink characteristics. Thus, based on the analyses carried out immediately after the preparation of dispersions and after four weeks of storage, it was concluded that 15% DOWP was the optimum dosage of Dispersant3 for the preparation of stable dispersions of the Carbon1 pigment.

Using the optimum dosage, i.e. 15 %DOWP, it was attempted to maximise the Carbon1 loading in binder-free dispersions. For this purpose a dispersion containing 35 wt% Carbon1 pigment and 15% DOWP of Dispersant3 was prepared initially. However, the viscosity was found to be too high for bead milling. Thus, the amount of pigment was reduced to 31 wt% by adding a calculated amount of de-ionised water. Consequently, dispersions containing 31 wt% of Carbon1 pigment were prepared using 15% DOWP of Dispersant1 and Dispersant2. Table 4-6 gives the exact formulations of the dispersions prepared in Step 4 of the optimisation process.

Table 4-6: Composition of dispersions containing 31 wt% Carbon1 and 15% DOWP of various dispersants.

Carbon1 Pigment (g)	Dispersant name	Dispersant Amount (g)	Foamex 805 (g)	D.I water (g)	Total (g)
33	Dispersant1	9.9	0.8	62.80	106.5
33	Dispersant2	12.38	0.8	59.95	106.13
33	Dispersant3	14.14	0.8	58.18	106.13

Figure 4-7 shows the viscosity profiles of the dispersions containing 31 wt% Carbon1 pigment and 15% DOWP of the various dispersants. In comparison to Dispersant2 and Dispersant3, Dispersant1 resulted in a considerably lower viscosity of the pigment dispersion which can be attributed to the larger amount of vehicle, i.e. water, in this formulation. As illustrated in Figure 4-8(b), the deviation from shear thinning rheology after storage was most pronounced in the dispersion prepared using Dispersant2. However, it was noticed that this event occurred only in the low shear rate range of 0 – 300 s⁻¹ (approx.). Thus, it is speculated that probably easy-to-break flocculates of the dispersed pigment formed in this dispersion during storage. The average increase in the viscosity of the dispersion prepared using Dispersant3 was approximately 18.18% (SD=0.88) after storage. In contrast, the viscosity of dispersion containing Dispersant1 remained virtually unchanged with the average increase being 6.48% (SD=1.58) after four weeks of storage, as shown in Figure 4-8(a).

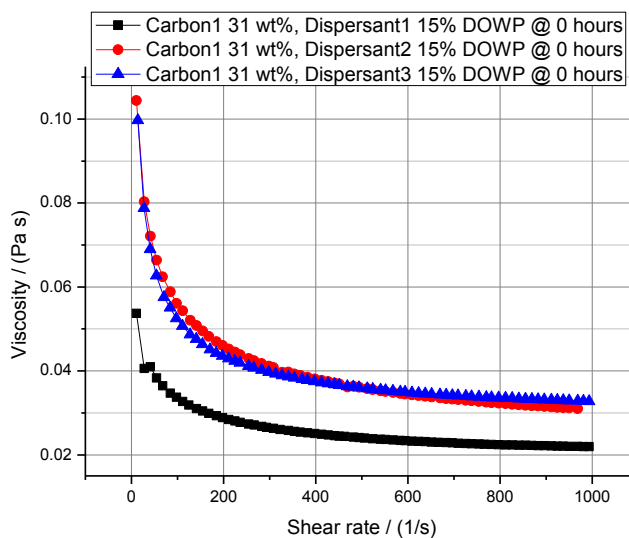


Figure 4-7: Viscosity profiles of dispersions containing 31 wt% Carbon1 and 15% DOWP of the various dispersants.

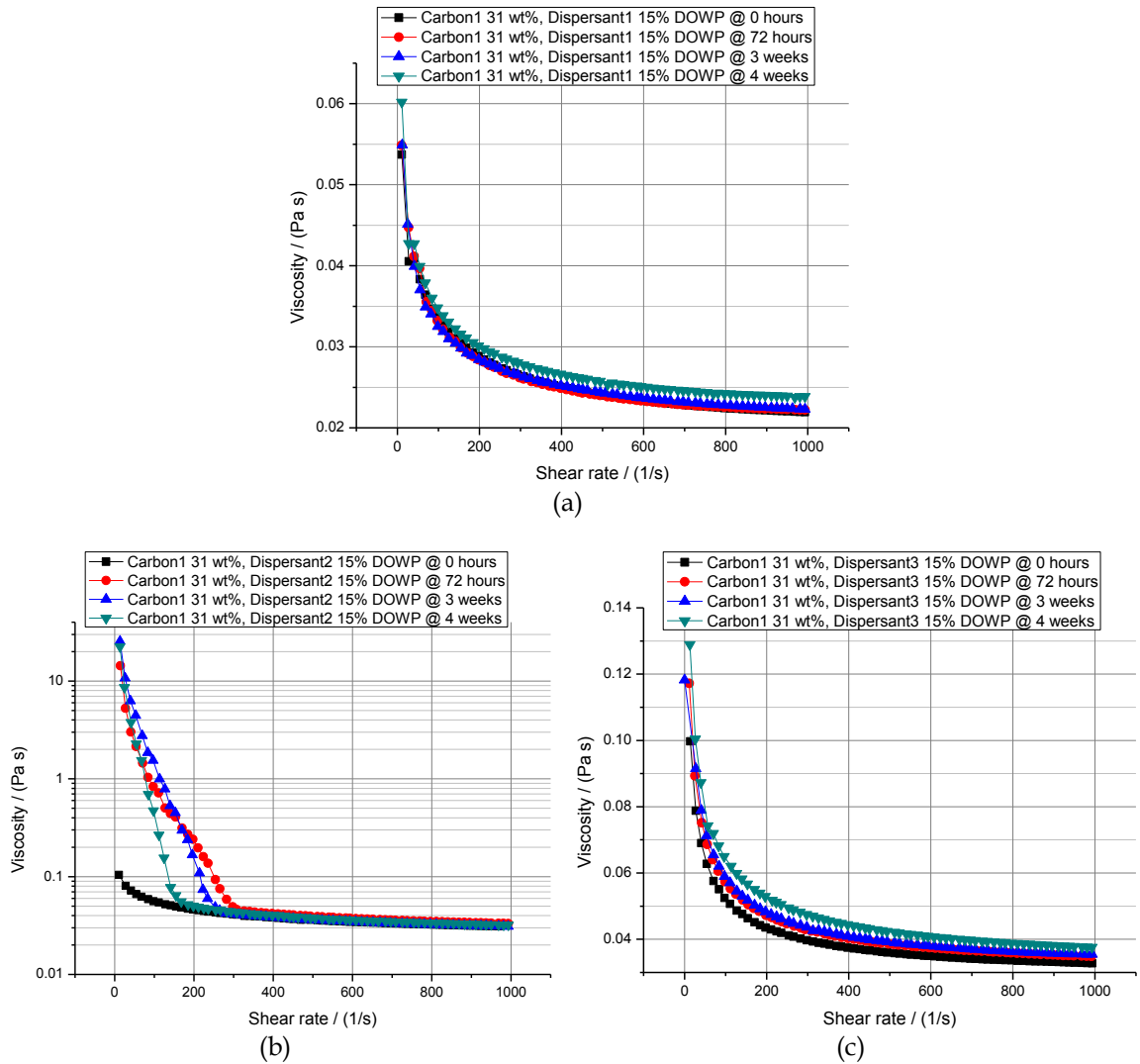


Figure 4-8: Stability of the viscosity of dispersions containing 31 wt% Carbon1 and 15% DOWP of (a) Dispersant1, (b) Dispersant2 and (c) Dispersant3.

The results of zeta potential measurements and particle size analyses of the dispersions of Carbon1, prepared in Step 4, are presented in Table 4-7. The particle size analysis of the dispersion prepared using Dispersant2 indicated that there was probably some aggregation of the pigment. During four weeks of storage, the average particle size varied in a broad range of 100 nm (approx.) and the extent of pigment aggregation became more pronounced as indicated by the appearance and increase in the area of a second peak (Peak 2) at above 4000 nm in the size distribution. In the dispersion prepared using Dispersant3, the average particle size remained relatively stable at around 220 nm. However, the consistent appearance of a second peak above 4500 nm in the size distribution indicated the development of structure in the dispersion. In comparison to Dispersant2 and Dispersant3, Dispersant1 produced a relatively more stable dispersion as indicated by fluctuation of the average particle size in a narrower

range of 195 nm – 226 nm. Peak 2 at 4500 nm (approx.) in the size distribution disappeared after 4 weeks of storage and the PDI also reduced.

The particle size analysis results of the dispersions of Carbon1 correlated fairly with the results of viscosity stability analyses which also indicated that the rheological character of the dispersions did not change considerably and/or irreversibly during storage.

Table 4-7: Zeta potential and particle size analysis results of dispersions containing 31 wt% Carbon1 and 15% DOWP of various dispersants.

Dispersion composition	Time	ζ (mV)	Z-Avg (nm)	PDI	Peak 1 (nm)	Peak 2 (nm)	Peak 1 Area (%)	Peak 2 Area (%)
Carbon1 31wt%, Dispersant1 15% DOWP	0 hrs	-13.2	195	0.12	224	0	100	0
	72 hrs	-23.8	222	0.24	265	4546	96.7	3.3
	3 weeks	-29.3	226	0.24	251	4629	95.9	4.1
	4 weeks	-41.8	194	0.14	227	0	100	0
Carbon1 31wt%, Dispersant2 15% DOWP	0 hrs	-29.0	286	0.26	399	0	100	0
	72 hrs	-15.2	189	0.09	210	0	100	0
	3 weeks	-16.0	232	0.24	297	4809	98	2
	4 weeks	-36.5	198	0.22	213	4047	94.4	5.6
Carbon1 31wt%, Dispersant3 15% DOWP	0 hrs	-12.8	218	0.13	251	0	100	0
	72 hrs	-11.0	222	0.16	253	0	100	0
	3 weeks	-25.2	275	0.25	330	4557	96	4
	4 weeks	-26.0	219	0.21	246	4606	96.9	3.1

As shown in Table 4-8, the electrical conductivity of the dispersion that was prepared using Dispersant1 was considerably greater than those of the other dispersions in the series. However, the surface resistivity of the K bar drawdowns of the dispersions was comparable. Thus, based on the combined results of particle size analyses, zeta potential measurements, viscosity stability studies and electrical conductivity evaluations, it was concluded that Dispersant1 was a more suitable dispersant than either Dispersant2 or Dispersant3 for the preparation of Carbon1 dispersions. Since the dispersion prepared using 15% DOWP of Dispersant3 did not clearly possess considerably inferior storage stability, it was also used to formulate finished inks. Despite the indication of flocculation in Carbon1-Dispersant2 dispersion, it was also considered for formulation of finished inks. This is because the viscosity profiles

recorded during storage indicated that the flocculates were easy to break. Furthermore, the surface resistivity of the drawdown of this dispersion was found to be comparable to that of the dispersions that were prepared using Dispersant1 and Dispersant3.

Table 4-8: Surface resistivity of K-bar 3 drawdowns of the optimised dispersions of Carbon1 pigment.

Dispersion composition	Surface resistivity (Ω/\square)
Carbon1 31 wt%, Dispersant1 15% DOWP	330
Carbon1 31 wt%, Dispersant2 15% DOWP	340
Carbon1 31 wt%, Dispersant3 15% DOWP	271

4.1.2 Optimisation of Carbon2 (Ensaco 250G) pigment dispersion

To perform the sinking test for the Carbon2 pigment, 0.150 g of the pigment powder was added to test tubes containing 5 wt% active matter dispersant solutions. Figure 4-9 shows the dispersion media that were isolated from the top of the test tubes after 72 hours of pigment addition. The Dispersant3 medium (760W) was the most opaque, followed by Dispersant1 medium (S44). Since the other low surface area pigment, i.e. Carbon1, was also optimised using Dispersant3, Carbon2 pigment dispersion was optimised using Dispersant1.

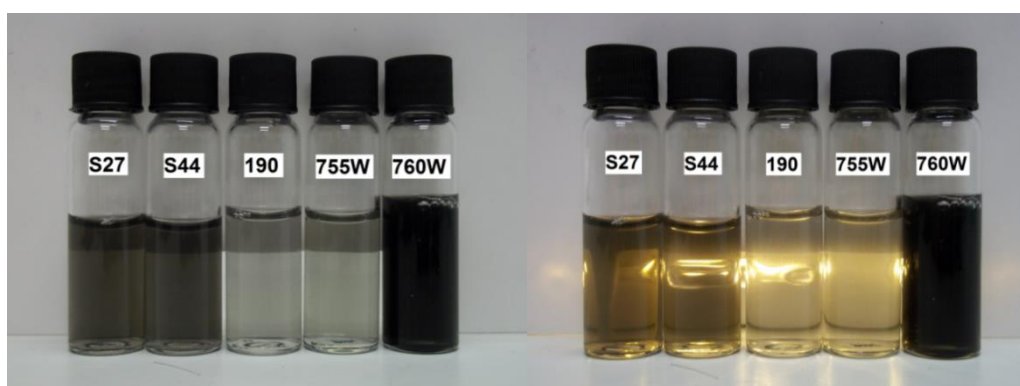


Figure 4-9: Dispersant solutions after 72 hours of addition of Carbon2.

Using Equation 16, the theoretical amount of Dispersant1 was calculated to be 12.5% DOWP (approx.). A series of dispersions, the composition of which is given in Table 4-9, was prepared with increasing amounts of Carbon2 and 12.5% DOWP of Dispersant1. Since Carbon1 and Carbon2 possessed very similar surface areas, the

formulation of control dispersion of Carbon2 was made the same as that of the control dispersion for Carbon1 pigment. It contained 15 wt% Carbon2 pigment and 10 wt% Glascol HN2 resin solids. Figure 4-10 shows that the viscosity profile of dispersion containing 28 wt% Carbon2 pigment matched the viscosity profile of the control dispersion.

Table 4-9: Composition of dispersions containing 12.5% DOWP of Dispersant1 and various amounts of Carbon2.

Dispersion composition	Carbon2 pigment (g)	Dispersant1 (50% active) (g)	Foamex 805 (g)	D.I. water (g)	Total (g)
Carbon2 14 wt%, Dispersant1 12.5% DOWP	14	3.5	1	81.5	100
Carbon2 22 wt%, Dispersant1 12.5% DOWP	22	5.5	1	71.5	100
Carbon2 28 wt%, Dispersant1 12.5% DOWP	28	7	1	64	100

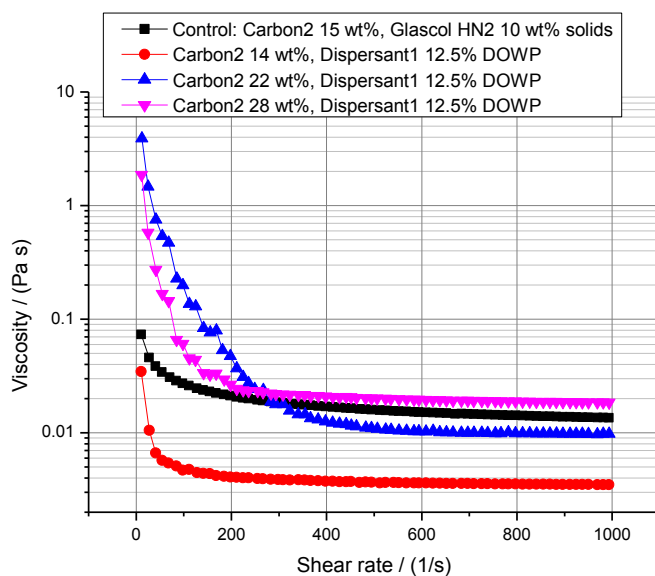


Figure 4-10: Viscosity profiles of dispersions of Carbon2 prepared in Step 2.

In the next step, which involved the attempted optimisation of the dispersant dosage, the amount of pigment in the ladder series of dispersions was kept at 28 wt% while the %DOWP of Dispersant1 was varied. Below 12.5% DOWP of Dispersant1, the viscosity of the pre-mixed dispersion was not low enough for proper bead milling. Thus a series of dispersions, the compositions of which are provided in Table 4-10, was prepared using 12.5%, 15%, 17.5% and 20% DOWP of Dispersant1.

Table 4-10: Composition of dispersions containing 28 wt% Carbon2 and various amounts of Dispersant1.

Dispersion composition	Carbon2 pigment (g)	Dispersant1 (50% active) (g)	Foamex 805 (g)	D.I. water (g)	Total (g)
Carbon2 28 wt%, Dispersant1 12.5% DOWP	28	7	1	64	100
Carbon2 28 wt%, Dispersant1 15% DOWP	28	8.4	1	62.6	100
Carbon2 28 wt%, Dispersant1 17.5% DOWP	28	9.8	1	61.2	100
Carbon2 28 wt%, Dispersant1 20% DOWP	28	11.2	1	59.8	100

The viscosity profiles of the dispersions, that were prepared in the attempt to optimise the dispersant dosage, are shown in Figure 4-11. The dispersion prepared using 17.5% DOWP of Dispersant1 possessed the lowest viscosity. It was noted that increasing the dispersant dosage beyond 17.5 % DOWP resulted in an increase in the dispersion viscosity. This effect can be attributed to the presence of excess free dispersant polymer in the dispersion.

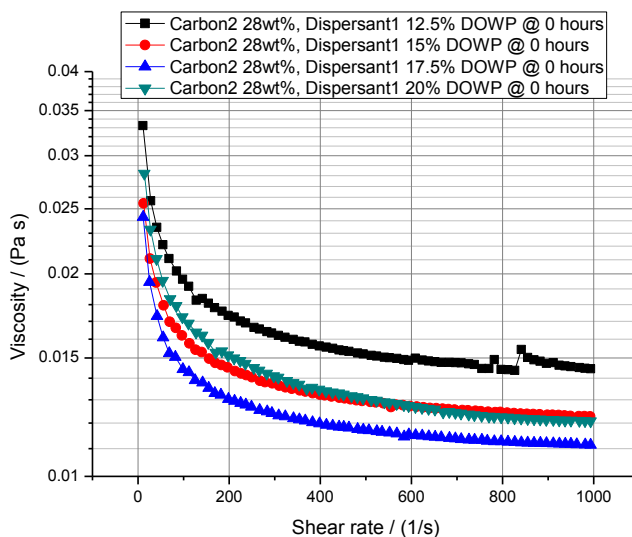


Figure 4-11: Viscosity profiles (after milling) of the dispersions containing 28 wt% Carbon2 and various amounts of Dispersant1.

The viscosity profiles (Figure 4-12) and particle size distribution (Table 4-11) of the dispersions that were prepared in Step 3 were also analysed during four weeks of storage. The viscosity profiles of dispersions containing 12.5% and 15% DOWP of

Dispersant1 showed a significant change in the rheological character of these dispersions after two weeks of storage. The considerable increase in the moderate-high shear rate viscosity clearly indicated that aggregation of the dispersed pigment occurred in these dispersions. In the dispersion containing 17.5% DOWP of Dispersant1, an increase in the low shear viscosity (up to shear rate of 200 s^{-1}) was observed. However, the viscosity profile at higher shear rates remained unchanged. In contrast to this, no significant change in the viscosity of the dispersion containing 20% DOWP of Dispersant1 was observed during four weeks of storage.

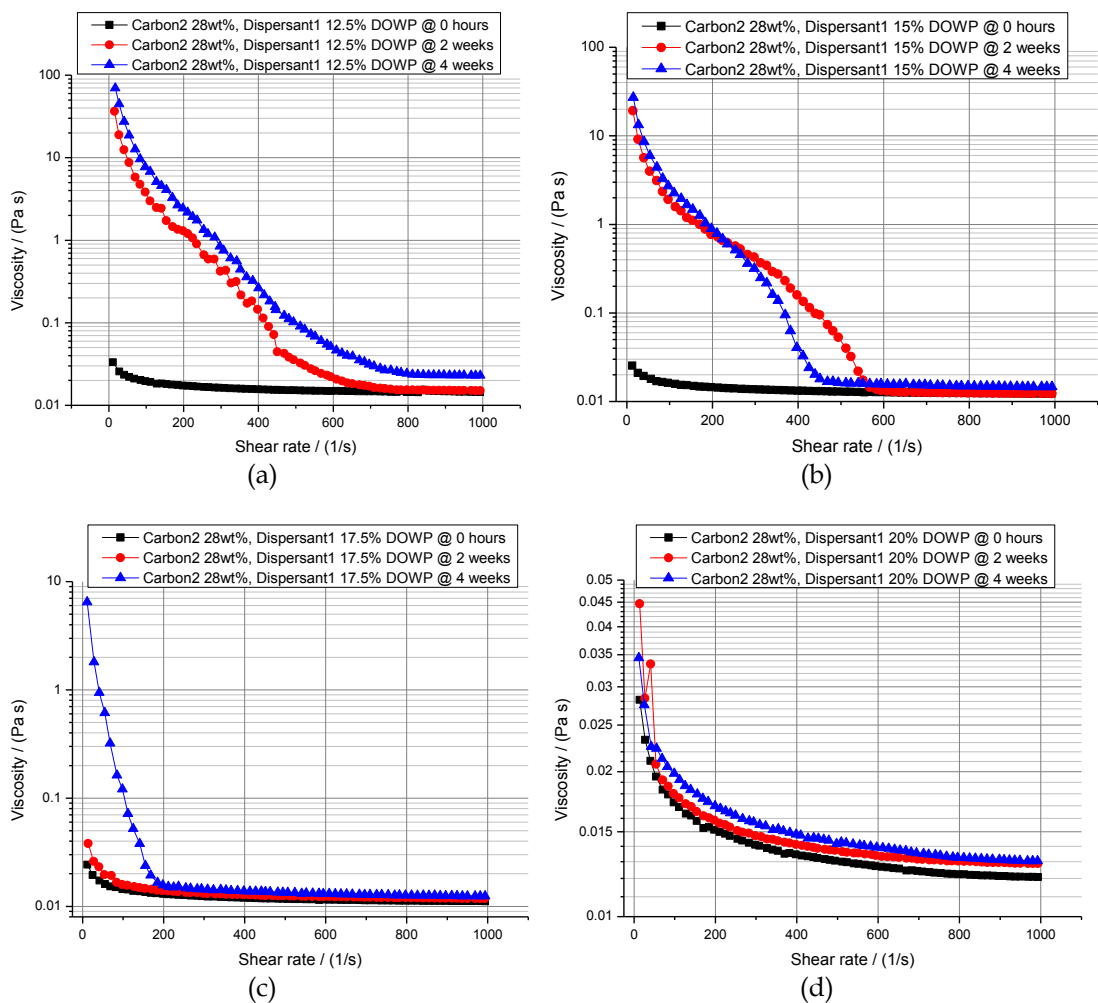


Figure 4-12: Stability of the viscosity profiles of dispersions of Carbon2 prepared using (a) 12.5%, (b) 15%, (c) 17.5% and (d) 20% DOWP of Dispersant1.

The results of particle size analyses carried out during storage indicated aggregation of pigment in the dispersion that contained 12.5% DOWP of Dispersant1, as evident from a consistent bi-modal size distribution, as shown in Table 4-11. This is in agreement with the results of viscosity stability analysis. However, in case of the dispersions that

were prepared using greater dosages of Dispersant1, the particle size analysis results were not in line with the results of rheological characterisation. The size analysis results indicated that there was virtually no aggregation in the dispersion that contained 15% DOWP of Dispersant1. Furthermore, this dispersion possessed the smallest average particle size at 182.8 nm and a uni-modal size distribution. However, the viscosity measurements indicated the possible occurrence of aggregation of the pigment. After four weeks of storage, a bi-modal size distribution was observed for the dispersions that contained either 17.5% or 20% DOWP of Dispersant1. It was noticed that the average particle size, in the dispersion containing 17.5% DOWP of Dispersant1, fluctuated within a narrower range (14 nm approximately) compared to the dispersion containing 20% DOWP of Dispersant1 in which the average particle size varied over a wider range (55 nm approximately).

Table 4-11: Results of zeta potential and particle size analysis of dispersions of Carbon2 prepared using various dosages of Dispersant1.

Dispersion composition	Time	ζ (mV)	Z-Avg (nm)	PDI	Peak 1 (nm)	Peak 2 (nm)	Peak 1 Area (%)	Peak 2 Area (%)
Carbon2 28 wt%, Dispersant1 12.5%	0 hours	-25.9	210	0.18	248	4738	98.8	1.2
	4 weeks	-28.3	229	0.26	257	3956	93.4	6.6
Carbon2 28 wt%, Dispersant1 15%	0 hours	-16.3	202	0.17	248	0	100	0
	4 weeks	-33.1	183	0.16	223	0	100	0
Carbon2 28 wt%, Dispersant1 17.5%	0 hours	-25.4	194	0.14	227	0	100	0
	4 weeks	-21.8	208	0.24	256	4451	97.3	2.7
Carbon2 28 wt%, Dispersant1 20%	0 hours	-16.4	190	0.15	228	0	100	0
	4 weeks	-33.9	246	0.29	328	5039	98.8	1.2

As shown in Table 4-12, the surface resistivity of dispersion containing 17.5% DOWP was lower than that of the dispersion containing 20% DOWP of Dispersant1. This can be attributed to the presence of excess free polymeric dispersant, which is also indicated by the slightly higher viscosity of the dispersion prepared using 20 %DOWP of Dispersant1, as shown in Figure 4-11.

Based on the analyses carried out on the dispersions prepared in attempts to determine the optimum dispersant dosage, it was concluded that the dispersions prepared using 17.5% and 20% DOWP of Dispersant1 were not significantly different from each other

in terms of storage stability and electrical characteristics. Thus, a lower dispersant dosage, i.e., 17.5% DOWP was selected for use as the optimal dispersant dosage in the next step.

Table 4-12: Surface resistivity of the drawdowns of dispersions of Carbon2 prepared using various amounts of Dispersant1.

Dispersion composition	Surface resistivity (Ω/\square)
Carbon2 28 wt%, Dispersant1 12.5%	289
Carbon2 28 wt%, Dispersant1 15%	368
Carbon2 28 wt%, Dispersant1 17.5%	345
Carbon2 28 wt%, Dispersant1 20%	451

In Step 4 of the Carbon2 dispersion optimisation, it was found during pre-mixing that the maximum possible loading of Carbon2 was 23 wt% of the total formulation when 17.5% DOWP of Dispersant3 was used. Thus, all the dispersions prepared in Step 4 were formulated to contain 23 wt% Carbon2. Table 4-13 provides the composition details, while Figure 4-13 shows the viscosity profiles of the dispersions that were prepared in this way.

Table 4-13: Composition of dispersions of Carbon2 prepared in Step 4.

Dispersion composition	Carbon2 pigment (g)	Dispersant (g)	Foamex 805 (g)	D.I. water (g)	Total (g)
Carbon2 23 wt%, Dispersant1 17.5% DOWP	18.4	6.44	0.5	54.66	80
Carbon2 23 wt%, Dispersant2 17.5% DOWP	24	10.5	0.5	69	104
Carbon2 23 wt%, Dispersant3 17.5% DOWP	18.4	9.2	0.5	51.9	80

As shown in Figure 4-14 and from the data provided in Table 4-14, the dispersion of the Carbon2 pigment, prepared using Dispersant2/Dispersant3, possessed very stable shear thinning rheology during storage. The increase in the low shear viscosity of the Carbon2-Dispersant1 dispersion, as shown in Figure 4-14(a), was regarded as an indication of formation of pigment flocculates that were easy to break by low shear mixing.

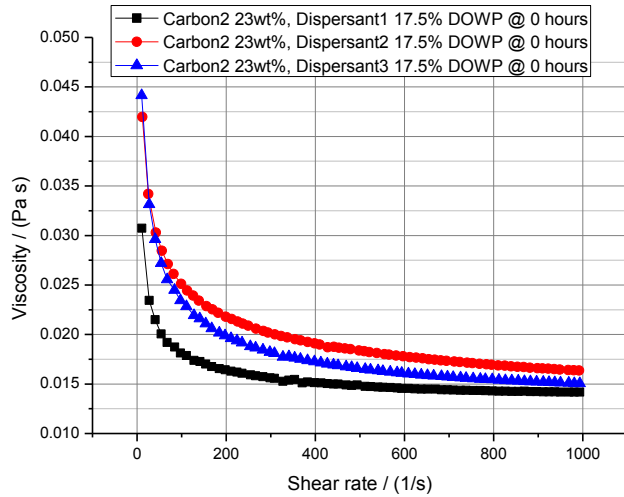


Figure 4-13: Viscosity profiles of dispersions containing 23 wt% Carbon2 and 17.5% DOWP of various dispersants.

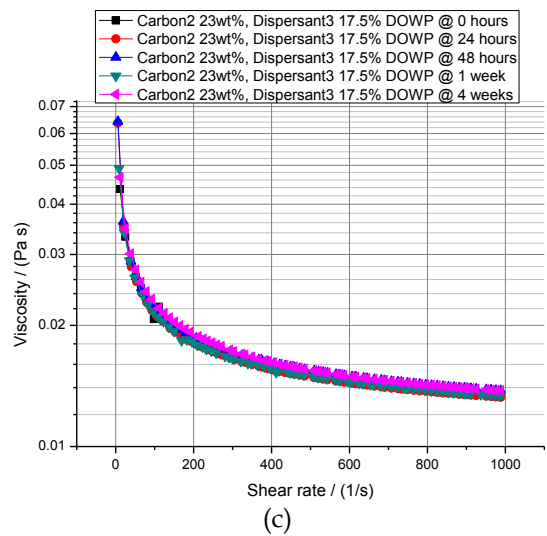
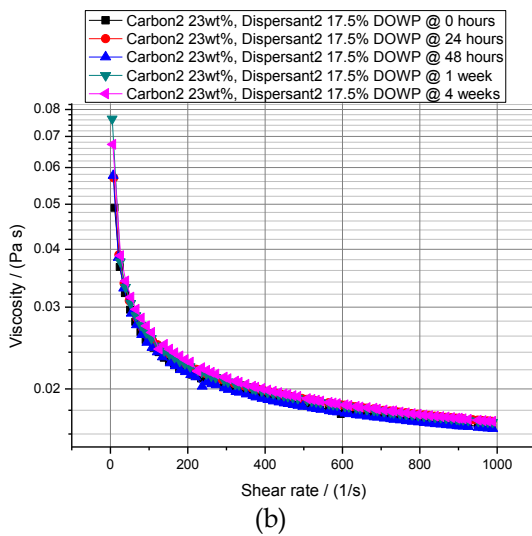
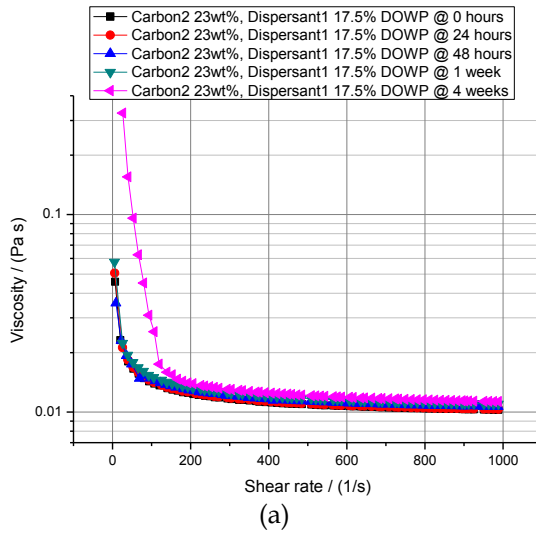


Figure 4-14: Viscosity profiles of dispersions containing 23 wt% Carbon2 and 17.5% DOWP of (a) Dispersant1, (b) Dispersant2 and (c) Dispersant3.

Table 4-14: Average increase in the viscosity of optimised dispersions of Carbon2.

Dispersion name	Average increase in viscosity (%)	St. Dev.
Carbon2-Dispersant1	11.11	0.88
Carbon2-Dispersant2	4.20	1.35
Carbon2-Dispersant3	2.43	0.88

The results of particle size analyses of the dispersions, which were prepared in the Step 4, are tabulated in Table 4-15. These results show that limited aggregation occurred in the dispersion that was prepared using Dispersant2, as indicated by the consistent appearance of a second peak in the size distribution. This result is not in line with the results of the rheological characterisations which indicated the presence of a very stable viscosity during storage. A second peak in the particle size distribution was recorded for the dispersions containing Dispersant1 and Dispersant3. However, the dispersion prepared using Dispersant3 appeared to be more stable than the dispersion prepared using Dispersant1. As shown in Table 4-16, the surface resistivity values of the K bar drawdowns of the optimised dispersions of Carbon2 pigment were similar.

Table 4-15: Results of particle size analyses of the dispersions of Carbon2 prepared in Step 4 of optimisation process.

Dispersion composition	Time	Z-Avg (nm)	PDI	Peak 1 (nm)	Peak 2 (nm)	Peak 1 Area (%)	Peak 2 Area (%)
Carbon2 23 wt%, Dispersant1 17.5% DOWP	0 hrs	240	0.28	342	4741	98.5	1.5
	24 hrs	270	0.30	580	0	100	0
	48 hrs	319	0.34	458	0	100	0
	1 week	221	0.24	239	3645	92.7	7.3
	4 weeks	203	0.20	221	4586	96.5	3.5
Carbon2 23 wt%, Dispersant2 17.5% DOWP	0 hrs	286	0.33	431	0	100	0
	24 hrs	203	0.15	243	55.95	98.4	1.6
	48 hrs	265	0.29	381	3771	94.7	5.3
	1 week	306	0.27	395	77.36	92.5	5.6
	4 weeks	248	0.35	218	989.4	67.4	32.6
Carbon2 23 wt%, Dispersant3 17.5% DOWP	0 hrs	246	0.26	326	4584	97.9	2.1
	24 hrs	226	0.25	267	3763	93.7	6.3
	48 hrs	275	0.29	454	0	100	0
	1 week	278	0.35	473	0	100	0
	4 weeks	216	0.22	238	4594	96.1	3.9

Table 4-16: Electrical characteristics of the optimised dispersions of Carbon2.

Dispersion composition	σ ($\mu\text{S}/\text{cm}$)	Surface resistivity (Ω/\square)
Carbon2 23 wt%, Dispersant1 17.5% DOWP	928	252
Carbon2 23 wt%, Dispersant2 17.5% DOWP	103.3	237
Carbon2 23 wt%, Dispersant3 17.5% DOWP	193.3	253

The analyses carried out on Carbon2-Dispersant1 and Carbon2-Dispersant3 dispersions indicated that these dispersions were stable. In case of the Carbon2-Dispersant2 dispersion, the results of particle size analysis were not in agreement with the results of other analyses that were carried out on this dispersion. However, the results of rheological and electrical characterisation, which were given more emphasis in this study, showed the observed differences in the characteristics were not significant enough to justify the exclusion of this dispersion from the let-down stage evaluations.

4.1.3 Optimisation of Carbon3 (Ensaco 350G) pigment dispersion

In order to select a dispersant for the study of the optimisation of the Carbon3 dispersion, the 'Sinking test' described in Section 2.2.2 was performed by adding 0.08g of Carbon3 to the various dispersant solutions. As shown in Figure 4-15, the opacity of the Dispersant3 solution (760W) after 72 hours of pigment addition was significantly greater than that of the other dispersant solutions. Thus, Dispersant3 was used in attempts at optimising the binder-free dispersion of Carbon3.

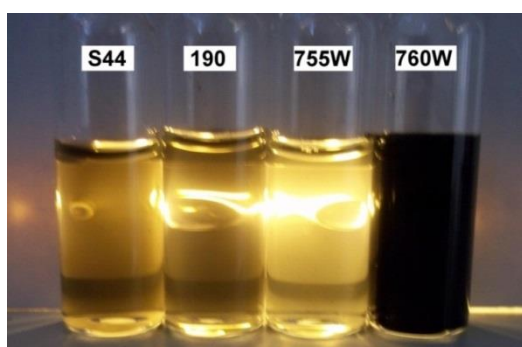


Figure 4-15: Dispersant solutions after 72 hours of addition of Carbon3.

Using Equation 16, the theoretical required amount of dispersant for Carbon3 was calculated to be approximately 170% DOWP. A control dispersion containing 6 wt% (of

the total formulation) of Carbon3 and 25 wt% (of the total formulation) of Glascol HN2 resin solids was prepared. In practice, the generally accepted viscosity of a control dispersion for equivalent systems is ≤ 1 Pa s at a shear rate of ≤ 50 s⁻¹. The Control dispersion of Carbon3, that was prepared as described above, met this criterion. Using the theoretical dispersant dosage, dispersions containing 8 wt% and 9.25 wt% Carbon3 were prepared and compared against the Control dispersion. The compositions of these dispersions are given in Table 4-17.

Table 4-17: Composition of dispersions of Carbon3 prepared in Step 2.

Dispersion composition	Carbon3 pigment (g)	Dispersant3 (35% active) (g)	Foamex 805 (g)	D.I. water (g)	Total (g)
Carbon3 8 wt%, Dispersant3 170% DOWP	6.4	31.08	1	41.51	80
Carbon3 9.25 wt%, Dispersant3 170% DOWP	8	38.78	1	38.70	86.5

As shown in Figure 4-16, the viscosities of both of the dispersions containing 8 wt% Carbon3 and 9.25 wt% Carbon3, were lower than that of the control dispersion. However, the pigment loading could not be increased beyond 9.25 wt% due to the very high viscosity of the pre-mixed dispersion which made it difficult to recirculate the dispersion in the bead mill properly. Thus, 9.25 wt% Carbon3 was considered to be the maximum achievable pigment loading when 170% DOWP of Dispersant3 was used.

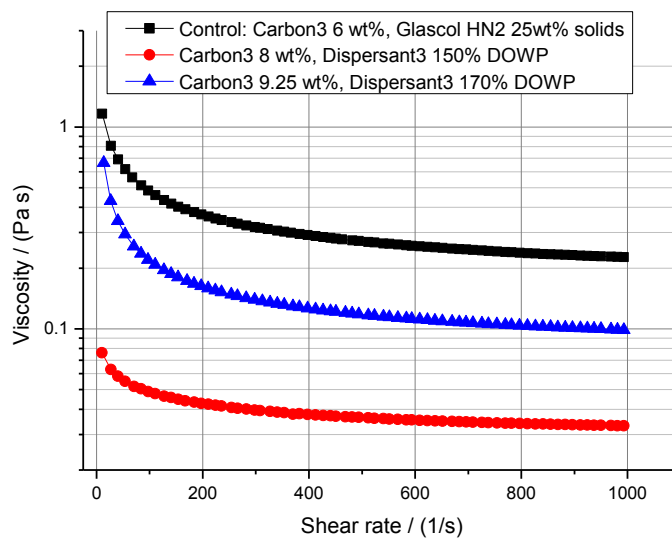


Figure 4-16: Viscosity profiles of dispersions of Carbon3 prepared in Step 2.

In Step 3 of the dispersion optimisation process, a series of dispersions containing 9.25 wt% Carbon3 and various amounts of Dispersant3 was prepared. The exact formulations are provided in Table 4-18. The least amount of Dispersant3 used was 140% DOWP because below this level the dispersant was likely to be well under-dosed, given the very high surface area of Carbon3. On the other hand, the maximum dispersant amount was 200% DOWP, chosen because upon further increasing the dispersant dosage, the pre-mixed dispersion possessed very high yield point which made it difficult to ensure effective recirculation in the bead mill.

Table 4-18: Composition of dispersions containing 9.25 wt% Carbon3 and various amounts of Dispersant3.

Dispersion Composition	Carbon3 pigment (g)	Dispersant3 (35% active) (g)	Foamex 805 (g)	D.I. water (g)	Total (g)
Carbon3 9.25wt%, Dispersant3 140% DOWP	7.4	29.6	0.5	42.5	80
Carbon3 9.25wt%, Dispersant3 155% DOWP	7.4	32.77	0.5	39.33	80
Carbon3 9.25wt%, Dispersant3 170% DOWP	7.4	35.94	0.5	36.16	80
Carbon3 9.25wt%, Dispersant3 200% DOWP	7.4	42.28	0.5	29.80	80

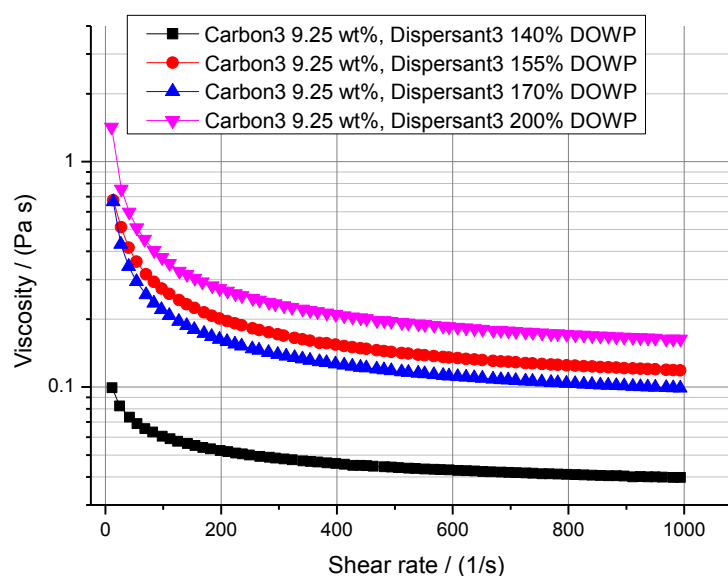


Figure 4-17: Viscosity profiles of dispersions of Carbon3, prepared in Step 3 of the optimisation process.

Generally, an increase in the dispersion viscosity was observed upon increasing the dispersant dosage, as shown in Figure 4-17. The initial particle size analysis results indicated that the use of 200% DOWP of Dispersant3 resulted in the smallest average particle size, at 205.5 nm. The average particle size in the dispersion of Carbon3, prepared using 155% DOWP was very close to that in the dispersion prepared using 200% DOWP of Dispersant3. Furthermore, a uni-modal size distribution and a narrow PDI were observed for both of these dispersions. As shown in Table 4-20, the surface resistivity of the dispersion containing 155% DOWP was less than that of the dispersion containing 200% DOWP of Dispersant3. In order to establish with some confidence that the optimal dispersant dosage that was needed to stabilise the Carbon3 dispersion was around 155% DOWP, the dispersions were assessed for their storage stability.

Table 4-19: Results of zeta potential and particle size analysis of the dispersions of Carbon3 prepared using various dosages of Dispersant3.

Dispersion composition	ζ (mV)	Z-Avg (nm)	PdI	Peak 1 (nm)	Peak 2 (nm)	Peak 1 Area (%)	Peak 2 Area (%)
Carbon3 9.25wt%, Dispersant3 140% DOWP	-25.8	271	0.332	338	5006	96.9	3.1
Carbon3 9.25wt%, Dispersant3 155% DOWP	-30.8	219	0.158	259	0	100	0
Carbon3 9.25wt%, Dispersant3 170% DOWP	-28.4	271	0.341	442	4571	98.3	1.7
Carbon3 9.25wt%, Dispersant3 200% DOWP	-6.23	205	0.180	259	0	100	0

Table 4-20: Electrical characteristics of dispersions of Carbon3 prepared using various dosages of Dispersant3.

Dispersion composition	Conductivity ($\mu\text{S/cm}$)	Surface resistivity (Ω/\square)
Carbon3 9.25 wt%, Dispersant3 140% DOWP	290	429
Carbon3 9.25 wt%, Dispersant3 155% DOWP	310	456
Carbon3 9.25 wt%, Dispersant3 170% DOWP	340	487
Carbon3 9.25 wt%, Dispersant3 200% DOWP	371	508

The viscosity profiles, presented in Figure 4-18, indicated that in all of the dispersions, shear thinning rheology was maintained upon storage, indicating that the state of dispersion of pigment probably did not change considerably. It was also noted that the viscosity of the dispersion containing 155 %DOWP decreased slightly during four weeks of storage.

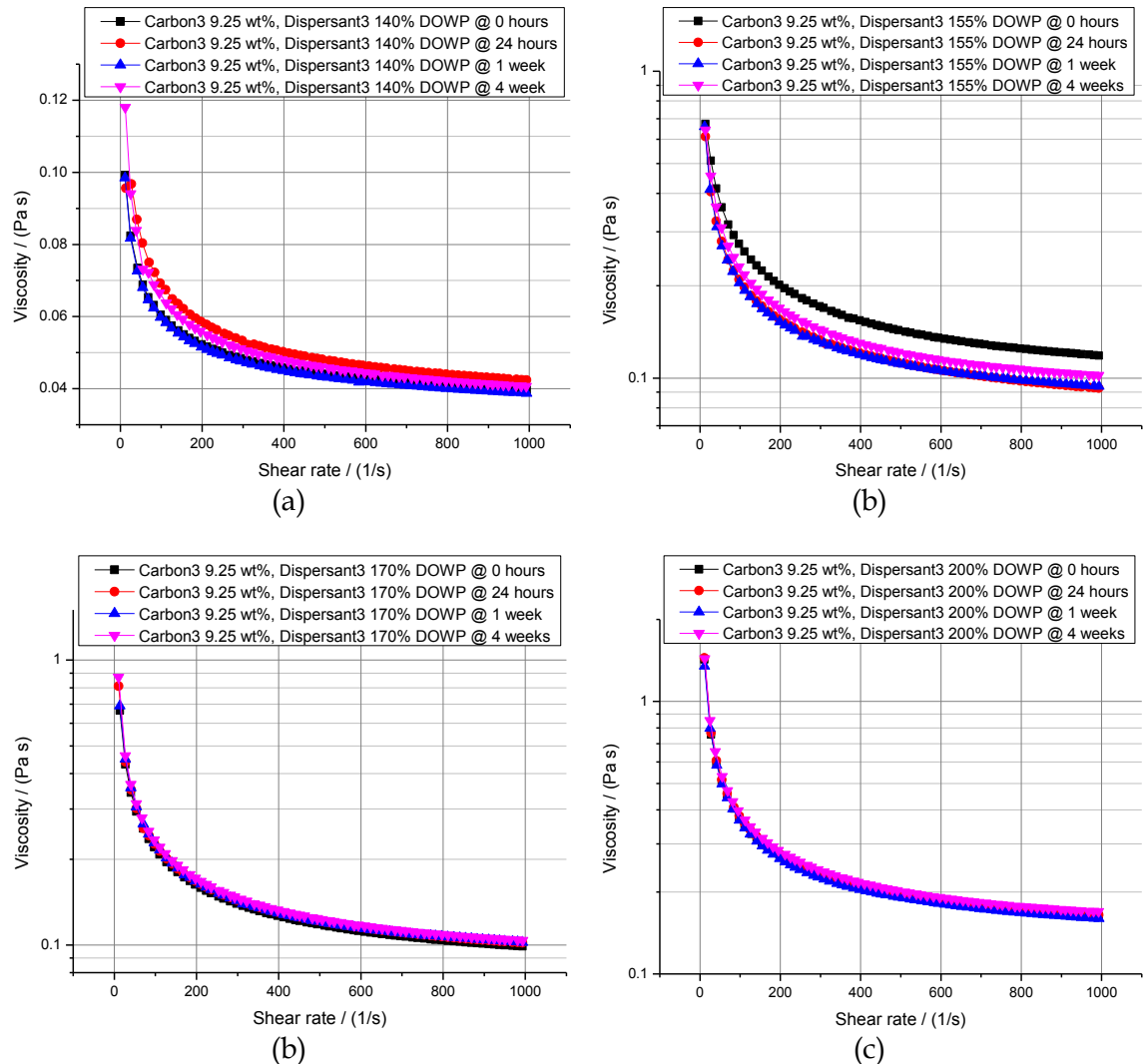


Figure 4-18: Viscosity stability analysis of the dispersions containing 9.25 wt% Carbon3 and (a) 140%, (b) 155%, (c) 170% and (d) 200% DOWP of Dispersant3.

The results of particle size analyses carried out on samples that had been stored are presented in Table 4-21. The average particle size as well as PDI of the dispersion containing 140% DOWP of Dispersant3 decreased considerably and unlike the other dispersions in the series, the particle size distribution remained consistently uni-modal. In the dispersions containing greater dispersant dosages, the average particle size decreased or fluctuated within a reasonably broad range. However, a second peak,

well above 4000 nm, was regularly observed in the particle size distribution. It was also noticed that in comparison to the dispersions containing 170% and 200% DOWP, the area of Peak 2 was generally smaller in the particle size distribution of the dispersion prepared using 155% DOWP of Dispersant3.

Table 4-21: Results of particle size analyses of the dispersions containing 9.25 wt% Carbon3 and various amounts of Dispersant3.

Dispersion composition	Time	Z-avg (nm)	PDI	Peak 1 (nm)	Peak 2 (nm)	Peak 1 Area (%)	Peak 2 Area (%)
Carbon3 9.25wt%, Dispersant3 140% DOWP	0 hours	271	0.33	338	5006	96.9	3.1
	24 hours	221	0.17	252	0	100	0
	1 week	226	0.21	336	0	100	0
	4 weeks	202	0.13	237	0	100	0
Carbon3 9.25wt% Dispersant3 155% DOWP	0 hours	219	0.16	259	0	100	0
	24 hours	314	0.36	466	4978	98.7	1.3
	1 week	226	0.22	269	4566	97.2	2.8
	4 weeks	226	0.15	253	0	100	0
Carbon3 9.25wt%, Dispersant3 170% DOWP	0 hours	271	0.34	442	4571	98.3	1.7
	24 hours	222	0.22	250	4569	96.7	3.3
	1 week	214	0.17	228	5047	98.4	1.6
	4 weeks	201	0.20	218	4192	95.6	4.4
Carbon3 9.25wt%, Dispersant3 200% DOWP	0 hours	205	0.18	259	0	100	0
	24 hours	244	0.26	333	4778	97.6	2.4
	1 week	226	0.22	248	4632	96.3	3.7
	4 weeks	224	0.26	292	4857	98.4	1.6

On the basis of the results of the rheological characterisations, particle size analyses and electrical characterisations, it was concluded that a dispersant dosage of greater than 155 %DOWP did not result in an improved dispersion of Carbon3. The dispersions that were prepared using 140% and 155% DOWP of Dispersant3 possessed fairly similar characteristics. Considering the fact that a slight increase was recorded in the viscosity of the dispersion that was prepared using 140% DOWP of Dispersant3, a greater dispersant dosage, i.e. 155% DOWP, was used to prepare the optimised dispersions of the pigment, in the next step.

During the preparation of the pre-mixed dispersions, in Step 4 of the optimisation process, it was found that the maximum amount of Carbon3 pigment that could be

dispersed using 155% DOWP of Dispersant3, while keeping the viscosity low enough for bead milling, was 11 wt% of the total formulation. Thus, pre-mixed dispersions containing 11 wt% of the Carbon3 pigment were prepared using 155% DOWP of Dispersant1 and Dispersant2, respectively. The viscosity profiles of the bead milled dispersions are presented in Figure 4-19 which clearly indicates that Dispersant3 limited the maximum amount of Carbon3 pigment that could be added in the dispersion under the prevailing conditions.

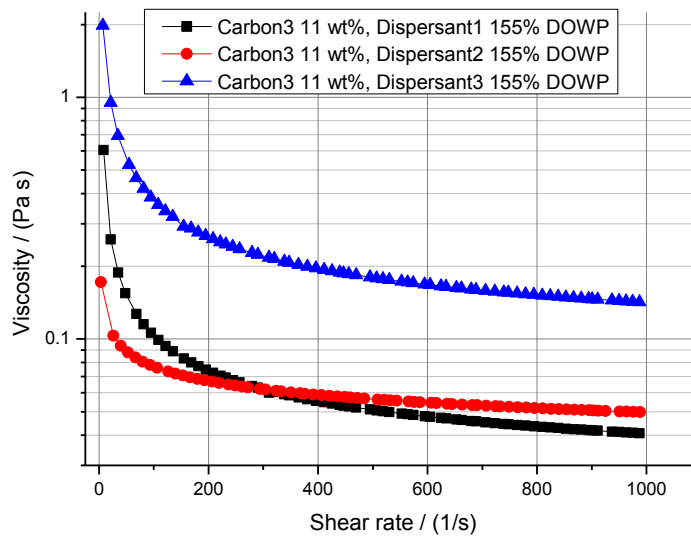


Figure 4-19: Viscosity profiles of dispersions of Carbon3 prepared in Step 4.

As in case of dispersions of other pigments, the stability of the Carbon3 pigment dispersions was analysed by recording the viscosity profiles during four weeks of storage. As shown in Figure 4-20(a-c), all of the dispersions possessed very stable shear thinning viscosity profiles. However, the average increase in viscosity was more pronounced in the case of Carbon3-Dispersant1 dispersion. The relevant data is provided in Table 4-22.

The results of particle size analyses carried out on Carbon3 pigment dispersions, prepared using optimum %DOWP of various dispersants, are presented in Table 4-23. It was observed that the extent of aggregation was more pronounced in the dispersion of Carbon3 prepared using Dispersant1. In contrast, the dispersions that were prepared using Dispersant2 or Dispersant3 possessed fairly stable particle size distribution during storage. These results correlate strongly with the results of viscosity stability analysis carried out on the different dispersions of Carbon3.

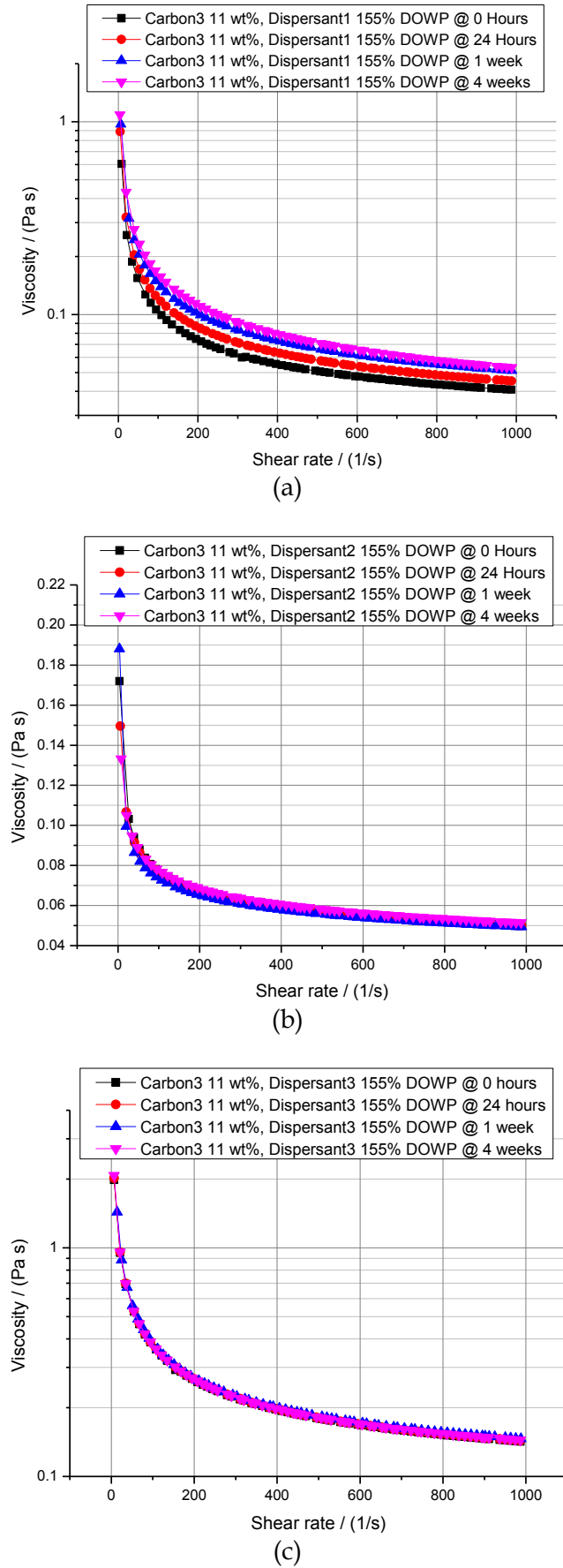


Figure 4-20: Viscosity stability of the dispersions of Carbon3 prepared using 155 %DOWP of (a) Dispersant1, (b) Dispersant2 and (c) Dispersant3.

Table 4-22: Average increase in viscosity of Carbon3 dispersions prepared in Step 3.

Dispersion name	Average increase in viscosity (%)	St. Dev.
Carbon3-Dispersant1	41.92	8.89
Carbon3-Dispersant2	2.79	0.87
Carbon3-Dispersant3	1.05	0.29

Table 4-23: Results of particle size analyses carried out on the optimised dispersions of Carbon3.

Dispersion composition	Time	Z-avg (nm)	PDI	Peak 1 (nm)	Peak 2 (nm)	Peak 1 Area (%)	Peak 2 Area (%)
Carbon3 11wt%, Dispersant1 155% DOWP	0 hours	203	0.28	243	2161	89.9	10.1
	24 hours	206	0.24	250	3650	95.7	4.3
	48 hours	215	0.24	250	4043	95.1	4.9
	1 week	300	0.28	422	4791	98.7	1.3
	4 weeks	210	0.20	247	4946	98.6	1.4
Carbon3 11wt%, Dispersant2 155% DOWP	0 hours	195	0.14	228	0	100	0
	24 hours	189	0.22	207	4672	96.5	3.5
	48 hours	250	0.28	384	0	100	0
	1 week	224	0.24	287	4593	98.2	1.8
	4 weeks	201	0.16	242	4592	98.4	1.6
Carbon3 11wt%, Dispersant3 155% DOWP	0 hours	202	0.22	248	4823	98.3	1.7
	24 hours	229	0.26	342	0	100	0
	48 hours	193	0.15	230	0	100	0
	1 week	204	0.19	258	0	100	0
	4 weeks	221	0.25	303	4385	98.7	1.3

The results of various analyses presented above, indicate that the optimised dispersion of Carbon3, which was prepared using Dispersant2 or Dispersant3, was very stable. In contrast, a considerable increase in the viscosity of the Carbon3-Dispersant1 dispersion was recorded. However, an instant shear thinning rheology was maintained. Furthermore, the surface resistivity of the drawdown of this dispersion was similar to that of the other dispersions of Carbon3 (The results of electrical characterisation are provided in Table 4-24). Consequently, it was decided to use all of the three optimised dispersions of Carbon3 in the let-down studies.

Table 4-24: Electrical characteristics of the optimised dispersions of Carbon3.

Dispersion composition	Conductivity ($\mu\text{S}/\text{cm}$)	Surface resistivity (Ω/\square)
Carbon3 11 wt%, Dispersant1 155% DOWP	2210	395
Carbon3 11 wt%, Dispersant2 155% DOWP	111	387
Carbon3 11 wt%, Dispersant3 155% DOWP	310	391

4.1.4 Optimisation of the Carbon4 (Printex XE2B) pigment dispersion

In the sinking test for Carbon4 pigment, approximately 0.05g of the pigment was added to the 5 wt% (active matter) solutions of various dispersants. It was observed that for all of the dispersant solutions, the pigment powder initially remained in a floating state on the surface of the solution. After approximately 1 minute of pigment addition, the pigment particles started to sink in the Dispersant3 solution. It was also observed that for Dispersant1 and Dispersant2 solutions, the sinking of pigment particles did not occur until at least 24 hours of pigment addition. Figure 4-21(a) shows the test tubes containing different dispersions after 72 hours of pigment addition, while Figure 4-21(b) shows the mixtures collected from the top of the test tubes. The Dispersant3 mixture (760W) was the most opaque followed by the Dispersant1 formulation (S44). Since Dispersant3 was also used in the optimisation of Carbon3 pigment, optimisation of dispersion of Carbon4 was carried out using Dispersant1 instead of Dispersant3.

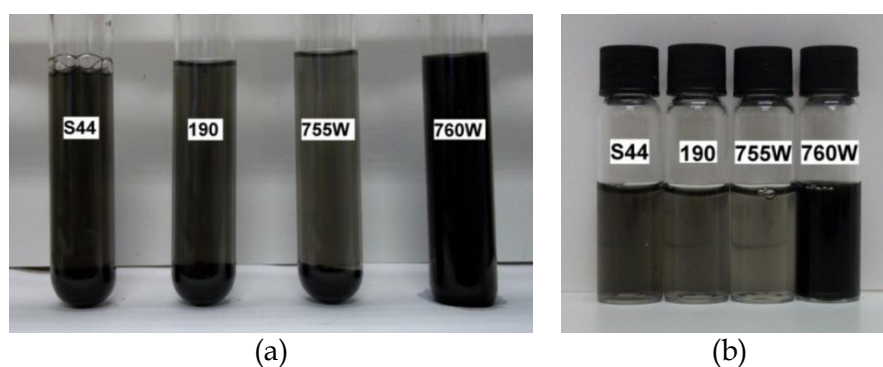


Figure 4-21: Dispersant solutions observed after 72 hours of addition of Carbon4.

The theoretically required amount of dispersant (from Equation 16) for Carbon4 pigment is 200% DOWP. To determine the maximum pigment loading, a series of dispersions was prepared using this %DOWP and increasing the amounts of the

Carbon4 pigment. The formulations of these dispersions are provided in Table 4-25. The control dispersion in this case contained 3.75 wt% of the Carbon4 and 25 wt% solids of the Glascol HN2 binder.

Table 4-25: Composition of dispersions of Carbon4 prepared in Step 2.

Dispersion composition	Carbon4 pigment (g)	Dispersant1 (50% active) (g)	Foamex 805 (g)	D.I. water (g)	Total (g)
Carbon4 6.3 wt%, Dispersant1 200% DOWP	5.17	20.66	0.5	55.67	82
Carbon4 9 wt%, Dispersant1 200% DOWP	7.2	28.8	0.5	43.5	80
Carbon4 10.75 wt%, Dispersant1 200% DOWP	8.8	35.2	0.5	37.3	81.8

As shown in Figure 4-22, the viscosity of the dispersion containing 10.75 wt% Carbon4 matched the viscosity of the control dispersion. Thus, in an attempt to determine the optimum dispersant dosage, a ladder series of dispersions containing 175% and 225 % DOWP of Dispersant1 was to be prepared. However, it was observed that if the pigment loading was maintained at 10.75 wt%, the viscosity of the pre-mixed dispersion that was prepared using 225 %DOWP of Dispersant1 was too high for effective bead milling. Thus in this step, the dispersant dosage was optimised for a lower (9.25 wt%) Carbon4 loading at which the pre-mixed dispersions recirculated properly in the bead mill.

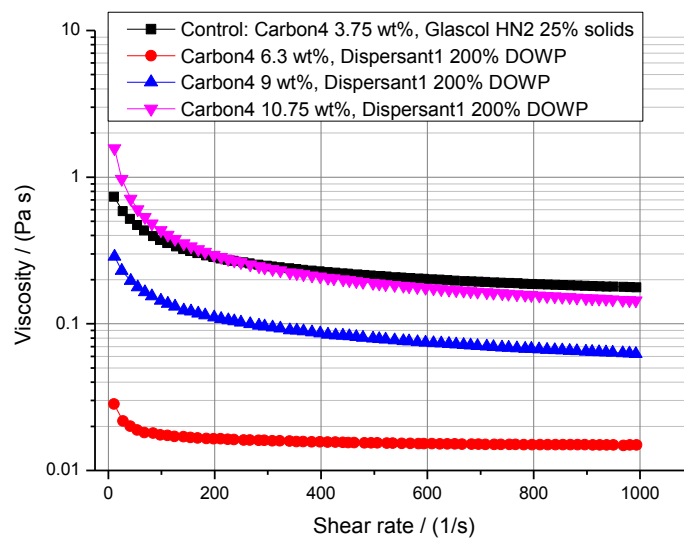


Figure 4-22: Viscosity profiles of dispersions of Carbon4 prepared in Step 2.

The composition of the dispersions that were used in the determination of optimum dispersant dosage is provided in Table 4-26 while the viscosity profiles of these dispersions are shown in Figure 4-23. Since the viscosity of Dispersant1 (as-supplied) was considerably lower than that of the dispersions containing 9.25 wt% Carbon4 pigment, the gradual increase in the viscosity upon increasing the amount of dispersant was attributed to improved dispersion of the pigment. In order to establish that higher dosage of Dispersant1 resulted in improved dispersion of Carbon4 pigment, the viscosity profiles and the particle size distribution of the dispersions were analysed during four weeks of storage.

Table 4-26: Composition of Carbon4 pigment dispersions prepared in Step 3 of the dispersion optimisation process.

Dispersion composition	Carbon4 pigment (g)	Dispersant1 (50% active) (g)	Foamex 805 (g)	D.I. water (g)	Total (g)
Carbon4 9.25 wt%, Dispersant1 175% DOWP	7.4	25.9	0.5	46.2	80
Carbon4 9.25 wt%, Dispersant1 200% DOWP	8.8	35.2	0.5	50.64	95.14
Carbon4 9.25 wt%, Dispersant1 225% DOWP	7.4	33.3	0.5	38.8	80

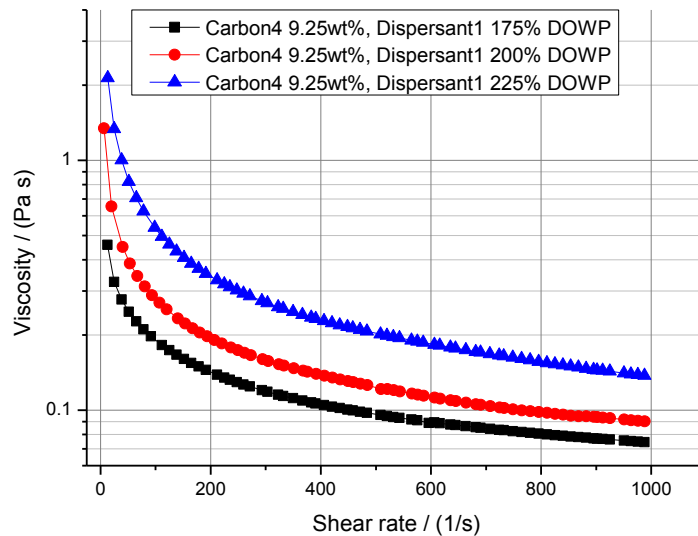


Figure 4-23: Viscosity profiles of dispersions containing 9.25 wt% Carbon4 and various amounts of Dispersant1.

A considerable increase in the viscosity of the dispersions that were prepared using various amounts of Dispersant1 was observed. However, shear thinning rheology was maintained in all cases. This is depicted in Figure 4-24.

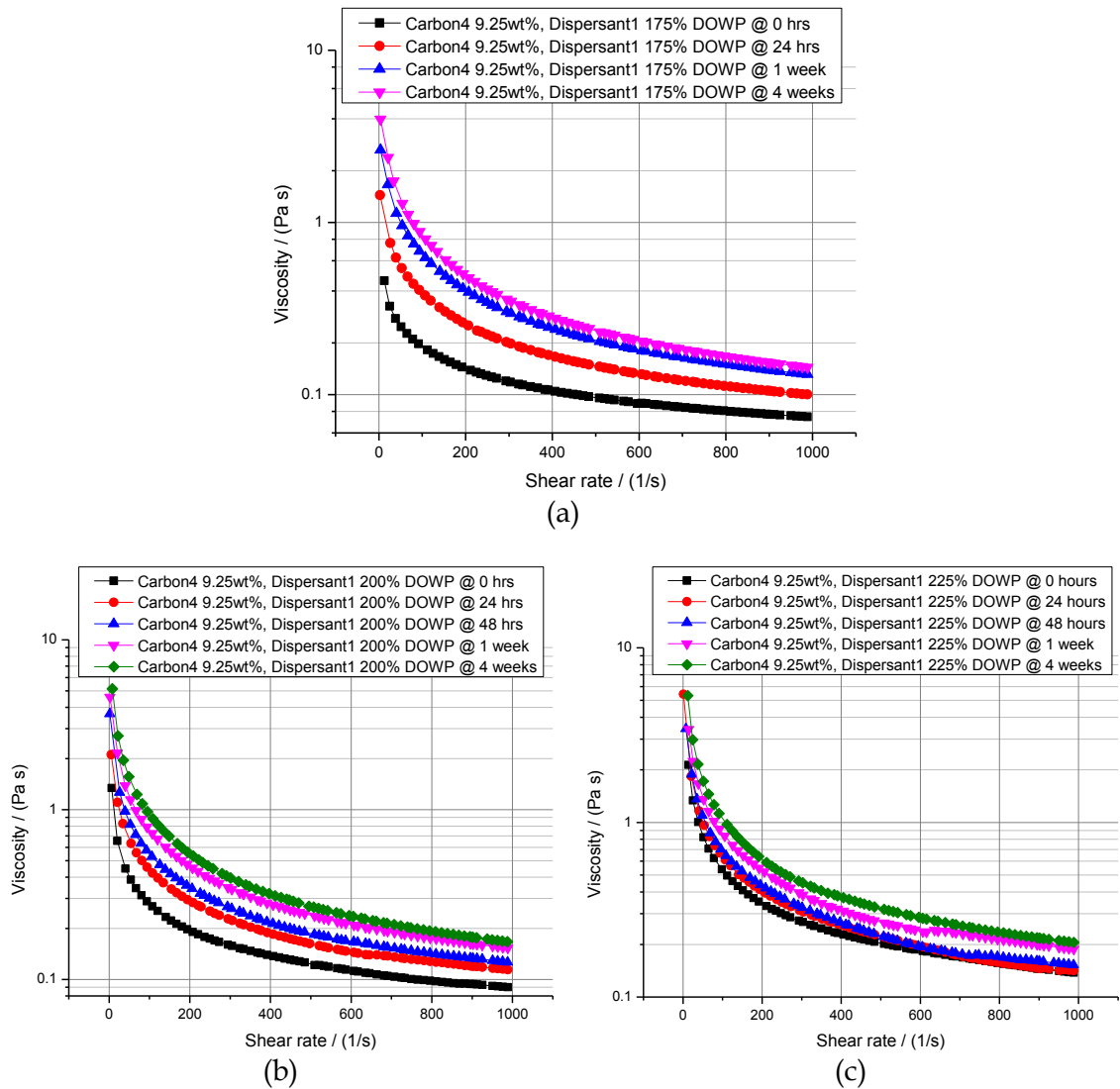


Figure 4-24: Viscosity stability of dispersions of Carbon4 prepared using (a) 175%, (b) 200% and (c) 225% DOWP of Dispersant1.

The zeta potential and particle size analysis results for the dispersions of Carbon4, prepared using various amounts of Dispersant1, are presented in Table 4-27. For all of the dispersions, the zeta potential recorded during four weeks of storage varied within a very broad range of approximately -40 mV. Since the dispersants are not expected to stabilise the pigment primarily by an electrostatic mechanism, large variations in the zeta potential values were not used as the primary indicator of stability/instability of the dispersions.

A consistent uni-modal size distribution was observed in the dispersion of Carbon4 prepared using 225% DOWP of Dispersant1. Furthermore, the average particle size in the dispersion varied within a relatively narrow range of approximately 84 nm over the four weeks of storage. In contrast, bimodal size distributions, with a second peak above 4000 nm, were frequently observed for the dispersions prepared using 175% and 200% DOWP of Dispersant1. The particle size analysis results clearly indicate that the better dispersant dosage for Carbon4 pigment was 225% DOWP. This finding is in line with the relatively smaller average increase in the viscosity profile of the dispersion prepared using 225% DOWP of Dispersant1. Thus, it was concluded that the appropriate %DOWP of Dispersant1 was 225% for Carbon4.

Table 4-27: Results of zeta potential and particle size analyses of the dispersions of Carbon4 prepared in Step 3.

Dispersion composition	Time	ζ (mV)	Z-avg (nm)	PDI	Peak 1 (nm)	Peak 2 (nm)	Peak 1 Area (%)	Peak 2 Area (%)
Carbon4 9.25 wt%, Dispersant1 175% DOWP	0 hours	-22.6	208	0.20	253	0	100	0
	24 hours	-16.4	192	0.19	220	4264	97.2	2.8
	48 hours	-14.8	251	0.32	312	4752	96	4
	1 week	-15.5	308	0.39	415	4132	92.7	7.3
	4 weeks	-58.5	260	0.24	297	4907	97.2	2.8
Carbon4 9.25 wt%, Dispersant1 200% DOWP	0 hours	-40.2	200	0.16	229	0	100	0
	24 hours	-18.0	263	0.29	386	4729	98.2	1.8
	48 hours	-17.0	192	0.20	222	4208	97	3
	1 week	-16.3	329	0.33	430	4583	96.5	3.5
	4 weeks	-57.2	228	0.19	286	0	100	0
Carbon4 9.25 wt%, Dispersant1 225% DOWP	0 hours	-35.3	192	0.12	222	0	100	0
	24 hours	-19.9	216	0.26	393	0	100	0
	1 week	-15.7	276	0.33	458	0	100	0
	4 weeks	-55.5	227	0.20	292	0	100	0

In Step 4 of dispersion optimisation, the Carbon4 pigment loading was to be maximised using 225% DOWP of the three dispersants used in this study. The results of the analyses carried out on the dispersion containing 9.25 wt% Carbon4 and 225 %DOWP of Dispersant1, which was prepared in Step 3, were also used in Step 4. The maximum amount of Carbon4 pigment that could be added in the pre-mixed dispersion was 9.5 wt% and 9 wt% for Dispersant2 and Dispersant3, respectively. The

formulations of these dispersions are provided in Table 4-28, while the viscosity profiles of the bead milled dispersions are shown in Figure 4-25.

In order to establish that the three dispersants produced stable dispersions of the Carbon4 pigment, the viscosity profiles were recorded and the particle size analyses carried out during four weeks of storage. As shown in Figure 4-26, all the three dispersants produced dispersions possessing very stable viscosity profiles during the four weeks of storage.

Table 4-28: Formulations of the dispersions prepared in Step 4 of optimisation of Carbon4 pigment dispersions.

Dispersion composition	Carbon4 pigment (g)	Dispersant (as-supplied) (g)	Foamex 805 (g)	D.I. water (g)	Total (g)
Carbon4 9.5 wt%, Dispersant2 225% DOWP	7.6	42.75	0.5	29.15	80
Carbon4 9 wt%, Dispersant3 225% DOWP	7.2	46.28	0.5	26.02	80

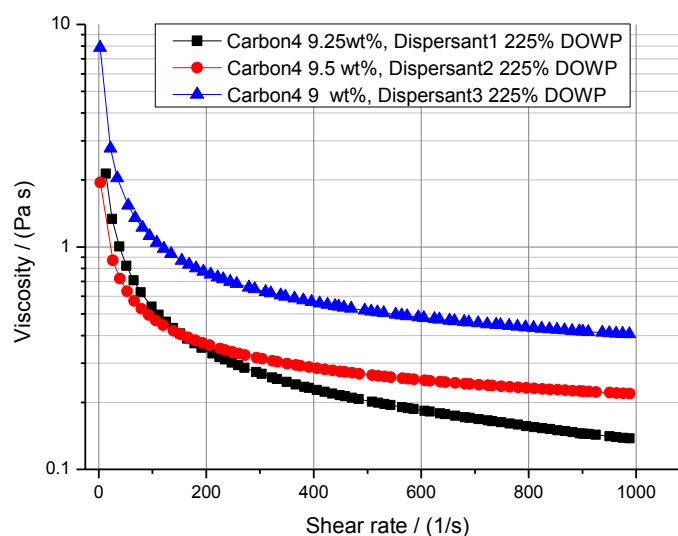
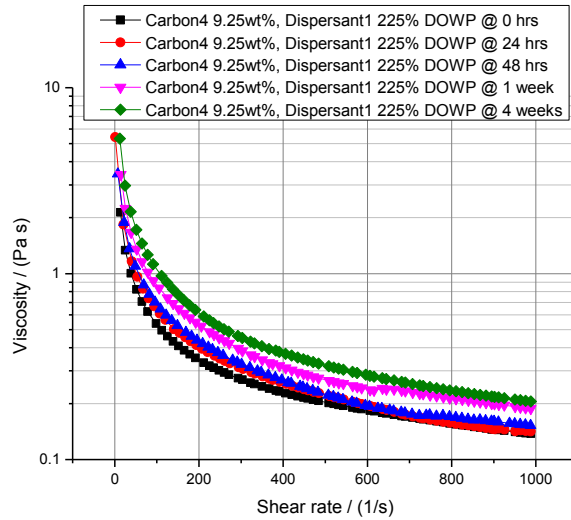
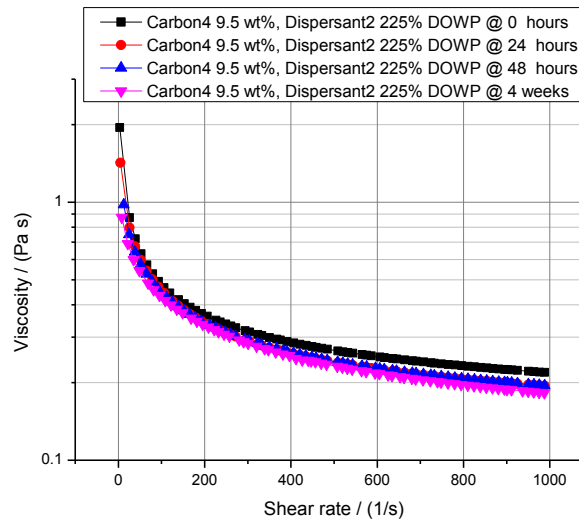


Figure 4-25: Viscosity profiles of dispersions of Carbon4 pigment prepared in Step 4.

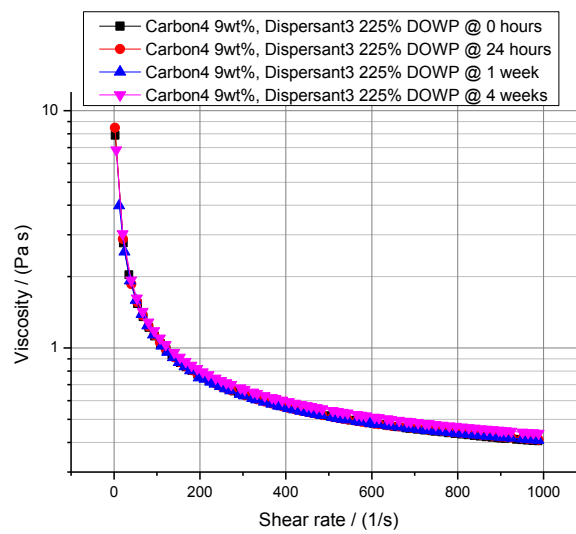
The average change in the viscosity after four weeks of storage was -13.35% (SD=3) and 6.39% (SD=1.21) for Carbon4-Dispersant2 and Carbon4-Dispersant3 dispersions, respectively. These changes are considerably smaller compared to the average increase of approximately 65% (SD=19.62) in the viscosity of Carbon4-Dispersant1 dispersion.



(a)



(b)



(c)

Figure 4-26: Viscosity profiles of optimised dispersions of Carbon4 pigment prepared using (a) Dispersant1, (b) Dispersant2 and (c) Dispersant3.

The particle size analysis of the Carbon4-Dispersant1 dispersion showed a consistent uni-modal PSD during four weeks of storage. This could not be related to the significant increase in the viscosity of this dispersion during storage. It is proposed that probably the size of aggregates that formed during storage was greater than 6 μm , which is the upper limit of particle size detection using Zetasizer Nano ZS. In contrast to the above, the particle size analysis results (Table 4-29), of the dispersions prepared using Dispersant2 and Dispersant3, indicated very limited flocculation of the pigment as depicted by the appearance of a second peak above 2000 nm in the particle size distribution. The area of this second peak was greater in case of dispersion prepared using Dispersant2. The average particle size, however, fluctuated in a range of approximately 43 nm which is narrower compared to that in the other two dispersions in the series.

Table 4-29: Particle size analysis results of the dispersions of Carbon4 pigment prepared using various dispersants.

Dispersion composition	Time	Z-avg (nm)	PDI	Peak 1 (nm)	Peak 2 (nm)	Peak 1 Area (%)	Peak 2 Area (%)
Carbon4 9.25wt%, Dispersant1 225% DOWP.	0 hours	192	0.12	221	0	100	0
	24 hours	216	0.26	393	0	100	0
	1 week	276	0.33	457	0	100	0
	4 weeks	227	0.20	292	0	100	0
Carbon4 9.5wt%, Dispersant2 225% DOWP.	0 hours	156	0.40	250	2073	94.8	5.2
	24 hours	147	0.38	196	2490	96.5	3.5
	48 hours	114	0.24	133	2312	96.7	3.3
	1 week	154	0.36	224	2126	94.9	5.1
	4 weeks	155	0.26	209	2445	98.5	1.5
Carbon4 9wt%, Dispersant3 225% DOWP.	0 hours	143	0.37	241	0	100	0
	24 hours	116	0.26	130	2327	95.1	4.9
	1 week	172	0.33	38	0	100	0
	4 weeks	109	0.19	118	2405	97.5	2.5

From the analyses presented above, it could not be concluded with certainty if one or more of the optimised dispersions of Carbon4 were considerably unstable. Furthermore, as shown in Table 4-30, the surface resistivity values of the drawdowns of these dispersions were also not significantly different from one another. Thus, the three optimised dispersions of Carbon4 that were prepared in Step 4 of the

optimisation process were tested for let-down stability and performance after formulation into inks.

Table 4-30: Electrical characteristics of optimised dispersions of Carbon4 pigment.

Dispersion composition	Conductivity ($\mu\text{S/cm}$)	Surface resistivity (Ω/\square)
Carbon4 9.25 wt%, Dispersant1 225% DOWP	1793	575
Carbon4 9.5 wt%, Dispersant2 225% DOWP	123	390
Carbon4 9 wt%, Dispersant3 225% DOWP	209	456

4.2 Shelf life/Stability of dispersions

In this study, rheological characterisation, particle size analysis and zeta potential measurements provided insight into the stability of the pigment dispersions. As discussed in Section 4.1, the results of these analyses were generally found to compliment each other and provided a rather clear indication that the dispersions prepared using the optimum %DOWP of various dispersants were stable for up to four weeks after preparation. In contrast to the techniques such as DLS, which are based on light scattering, centrifugation (or ultra centrifugation) can be employed to characterise a dispersion without diluting it. Thus, the dispersion properties are not modified during sample preparation (Weber et al. 2003). In this respect, analytical centrifugation, the underlying principles of which are described in Section 1.10.1.1, has significant potential and it is increasingly being used in the industry.

The data obtained from modern analytical centrifuges can be processed to characterise dispersion properties, such as particle size distribution, quantitatively. However in this study, the transmission profiles obtained during centrifugation of a dispersion were analysed to obtain qualitative description of the extent of sedimentation of pigment in the dispersion. For this purpose, a LUMiSizer® dispersion analyser was used. The transmission profiles of the undiluted dispersion samples were recorded following the procedure outlined in Section 3.4.1. In the sets of transmission lines presented in Figure 4-27 - Figure 4-29, the red lines show the transmission profiles recorded at the start of centrifugation while the green lines represent the transmission profiles recorded towards the end of test. At the start of the test, the dispersion/air phase

boundary in the cell was at the radial position in the range of 106-108 mm (approx.) from the centre of rotation.

The transmission profiles recorded during centrifugation of the dispersion of Carbon1 prepared using Dispersant1 are shown in Figure 4-27(a). Towards the end of the test that replicated six months storage, the light transmission through the upper 0.5 mm (approx.) of the dispersion increased to 30% (approx.). The maximum light transmission through the volume of dispersion present between a radial position of 107 - 108 mm was 10% (approx.). As shown in Figure 4-27(b), there was very little change in the light transmission through the Carbon1-Dispersant2 dispersion. A maximum transmission of 15% (approx.) was recorded. However, it occurred only through the upper 0.25 mm (approx.) of the dispersion. During centrifugation of the dispersion of Carbon1 pigment prepared using Dispersant3, the maximum light transmission through the upper 1 mm (approx.) of the dispersion was 30% (approx.). This is shown by the set of transmission profiles presented in Figure 4-27(c).

The transmission profiles recorded during centrifugation of the Carbon2 pigment dispersions are shown in Figure 4-28. As shown in Figure 4-28(a), the first recorded transmission profile of Carbon2-Dispersant1 is characterised by virtually no transmission while the transmission profiles recorded towards the end of the test show that the transmission through the upper 2 mm (approx.) of the dispersion was between 18% and 10% (approx.). A more or less similar pattern was observed in the transmission profile of the Carbon2-Dispersant2 dispersion. The transmission through the upper 2 mm (approx.) of the dispersion increased to 20 - 15% (approx.) towards the end of the test. During centrifugation, the movement of the solid(pigment)-liquid(dispersion medium) phase boundary was less pronounced in the Carbon2-Dispersant3 dispersion compared to that in the other two dispersions of the Carbon2 pigment. This is illustrated by the set of transmission profiles shown in Figure 4-28(c). The transmission was as high as up to 30 - 25% through the upper 0.5 mm (approx.) of the dispersion.

This space is deliberately left blank due to pagination.

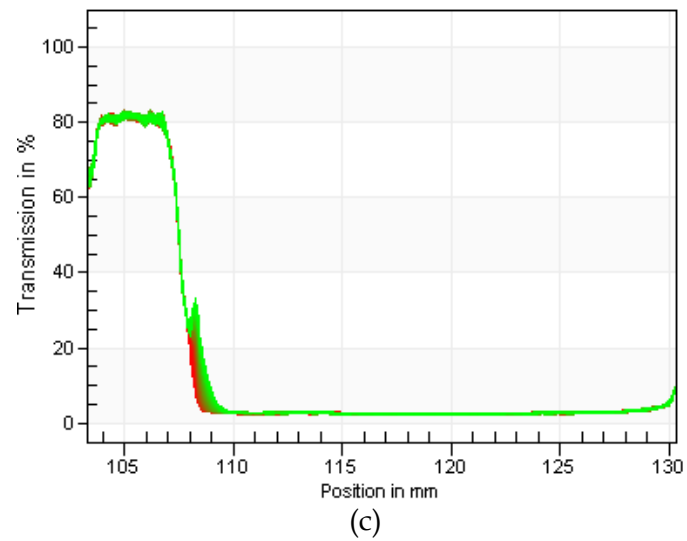
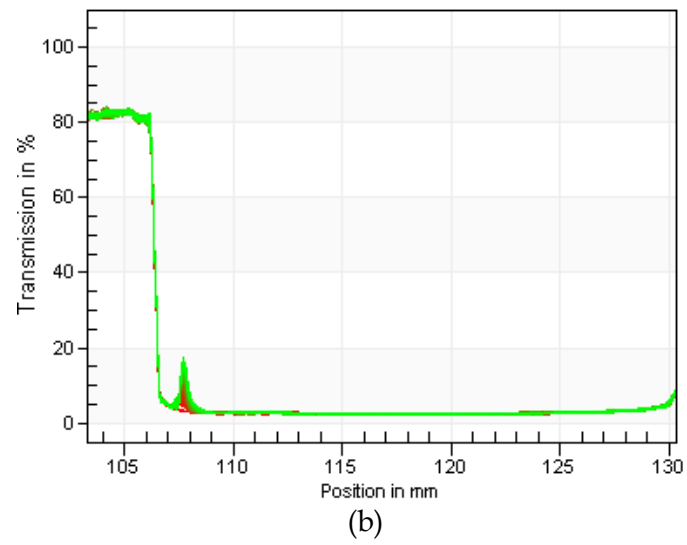
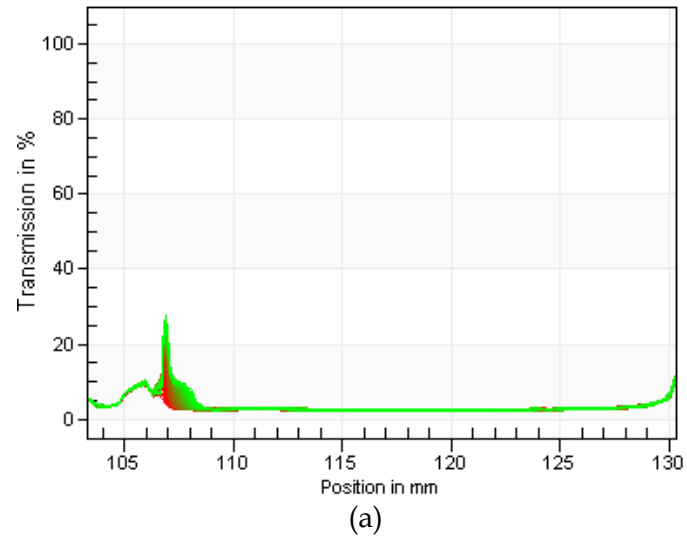


Figure 4-27: Transmission profiles recorded during centrifugation of Carbon1 dispersions prepared using (a) Dispersant1, (b) Dispersant2 and (c) Dispersant3.

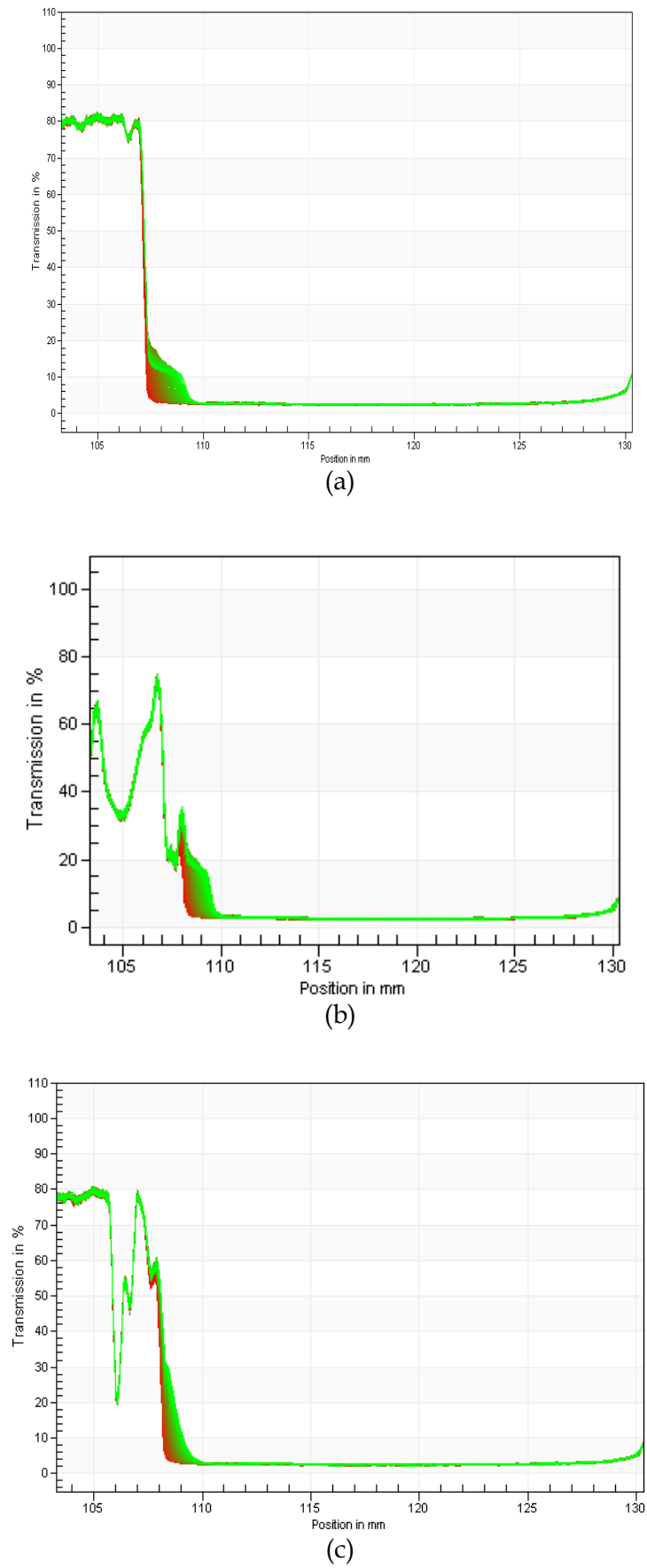


Figure 4-28: Transmission profiles recorded during centrifugation of Carbon2 dispersions prepared using (a) Dispersant1, (b) Dispersant2 and (c) Dispersant3.

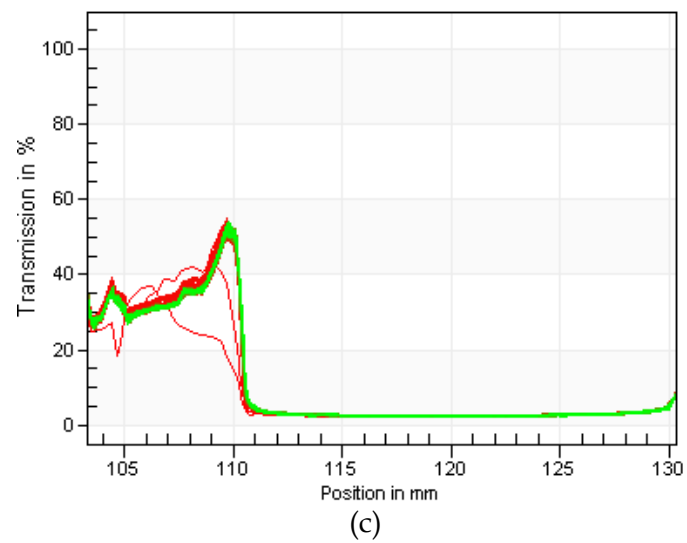
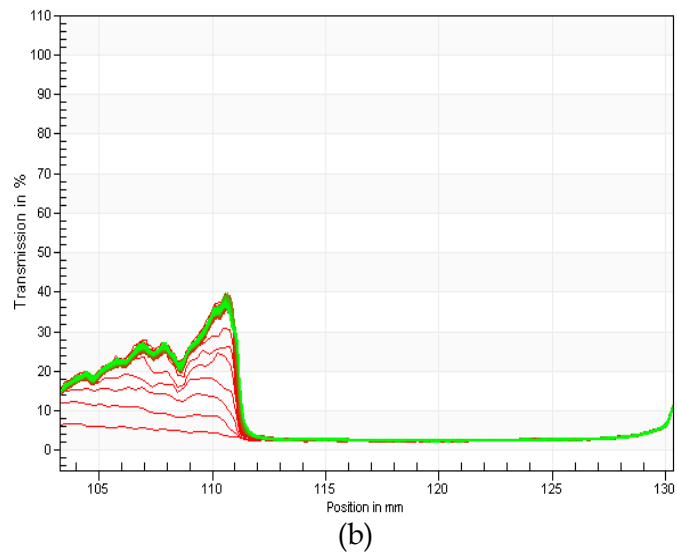
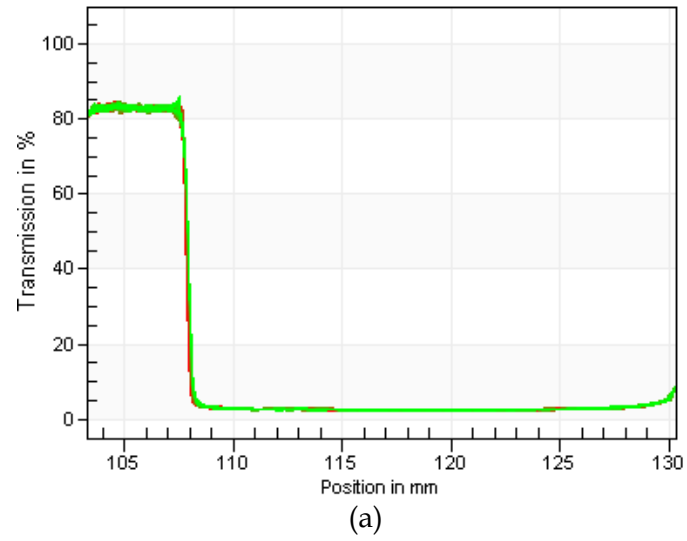


Figure 4-29: Transmission profiles recorded during centrifugation of Carbon3 dispersions prepared using (a) Dispersant1, (b) Dispersant2 and (c) Dispersant3.

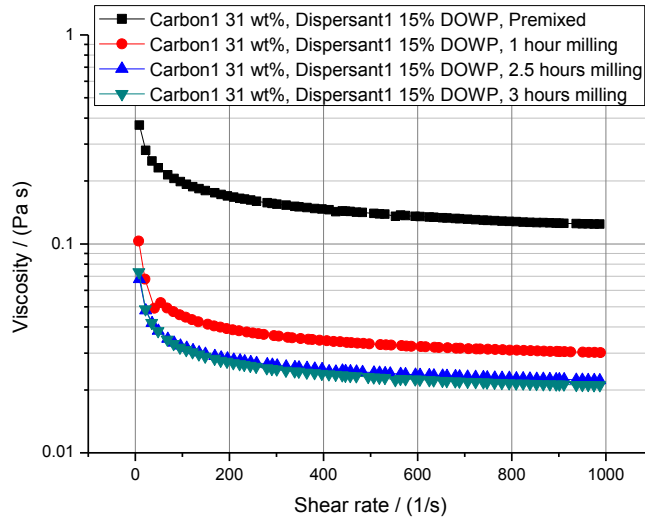
Figure 4-29 shows the transmission profiles recorded during centrifugation of the optimised dispersions of the Carbon3 pigment. There was no recordable increase in the light transmission through the Carbon3 pigment dispersions which were tested. As mentioned in Section 3.4.1, the dispersions of Carbon4 could not be analysed due to the very high viscosity of these dispersions.

In this study, the analytical centrifugation tests were not carried out to characterise the sedimentation of dispersed pigment quantitatively. However, the test results presented above clearly indicate that the optimised dispersions of Carbon1, Carbon2 and Carbon3 were very stable in terms of settling/sedimentation of the pigment particles during at least six months of storage.

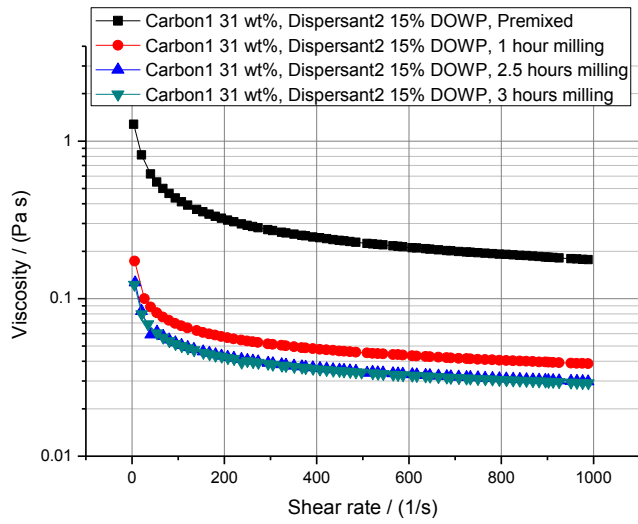
4.3 Optimisation of the bead milling process

The pigment dispersions produced in this study generally possessed high viscosity. Therefore, it was important to establish that the bead milling process parameters, as discussed in Section 2.2.4, resulted in the effective milling of the pigments. For this purpose, change in the viscosity of the dispersions, that were prepared in Step 4 of the optimisation process, was recorded at regular intervals during bead milling. The results of this study are considered in the following text.

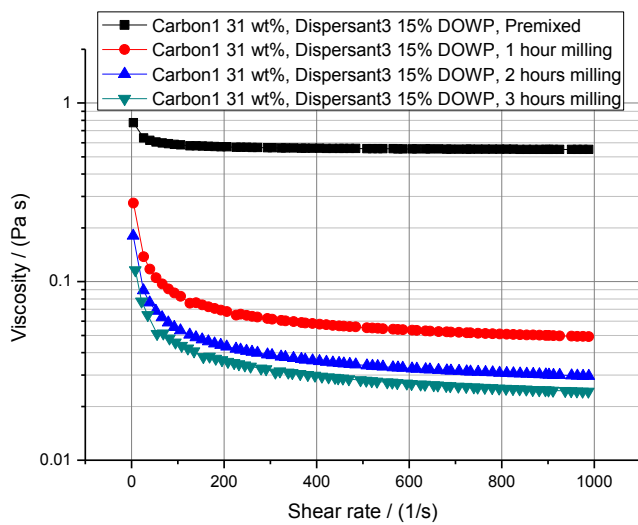
The most significant reduction in the viscosity of Carbon1 dispersions occurred during the initial one hour of bead milling, as shown in Figure 4-30. This was followed by only a slight reduction in the viscosity as the milling was continued for another 1 - 1.5 hours. Upon continuing the bead milling for another 30 minutes, a slight decrease in the viscosity of Carbon1-Dispersant3 dispersion was observed, while virtually no change in the viscosity of Carbon1-Dispersant1 and Carbon1-Dispersant2 dispersions was recorded. A more or less similar pattern of reduction in the viscosity was observed for the dispersions of Carbon2 and Carbon3 pigments, as depicted in Figure 4-31 and Figure 4-32, respectively. The initial 1 hour of milling resulted in the most pronounced reduction in the viscosity of the dispersions. As in case of dispersions of Carbon1, there was very small change or virtually no change in the viscosity of the dispersions of Carbon2 and Carbon3 pigments after 2 hours of milling.



(a)



(b)



(c)

Figure 4-30: Milling viscosity of dispersions of Carbon1 prepared using (a) Dispersant1, (b) Dispersant2 and (c) Dispersant3.

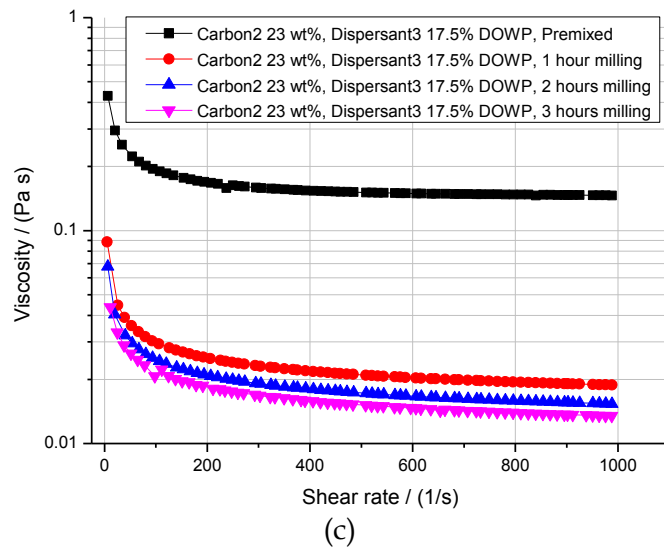
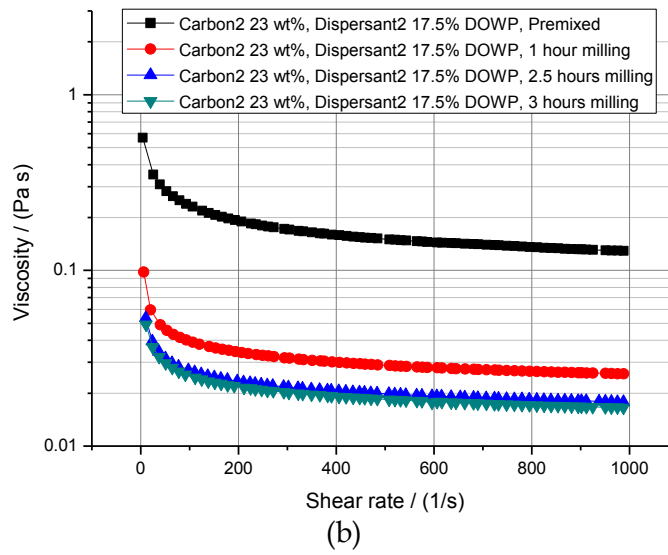
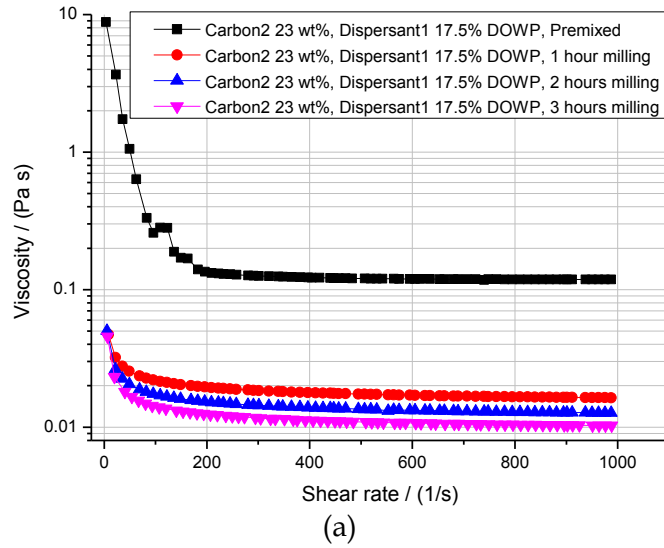


Figure 4-31: Milling viscosity of dispersions of Carbon2 prepared using (a) Dispersant1, (b) Dispersant2 and (c) Dispersant3

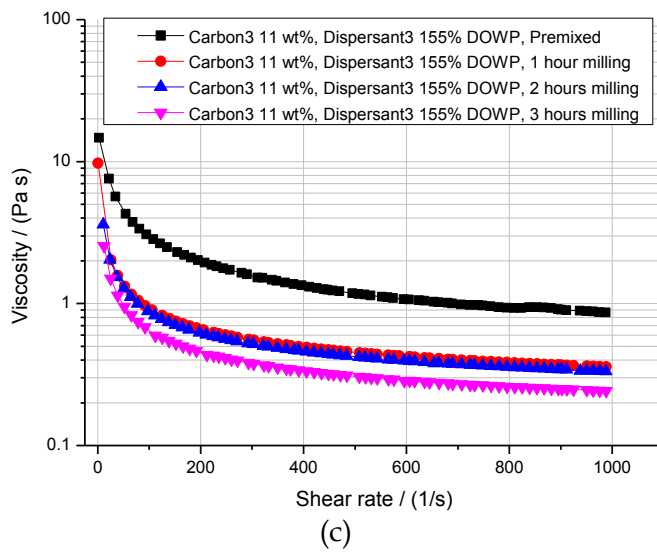
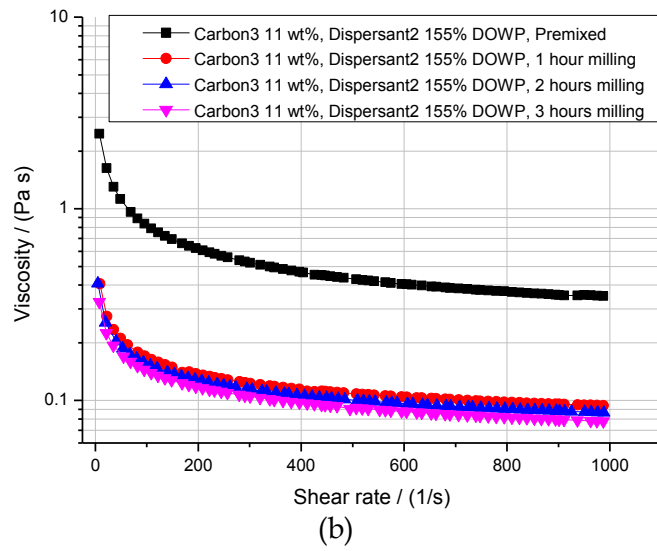
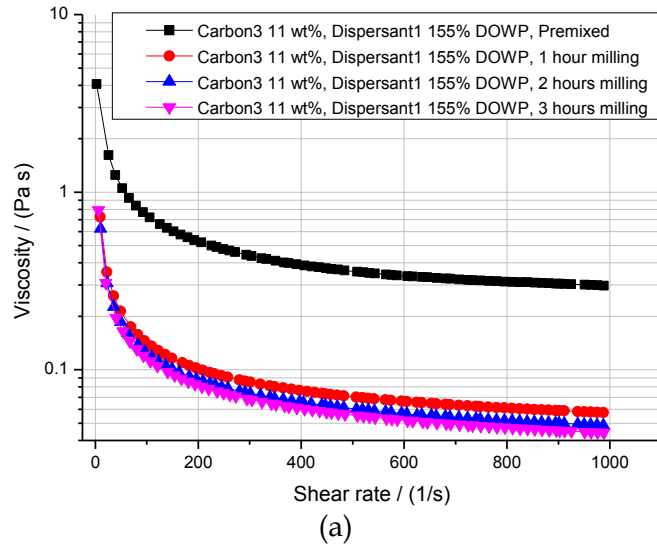


Figure 4-32: Milling viscosity of dispersions of Carbon3 prepared using (a) Dispersant1, (b) Dispersant2 and (c) Dispersant3.

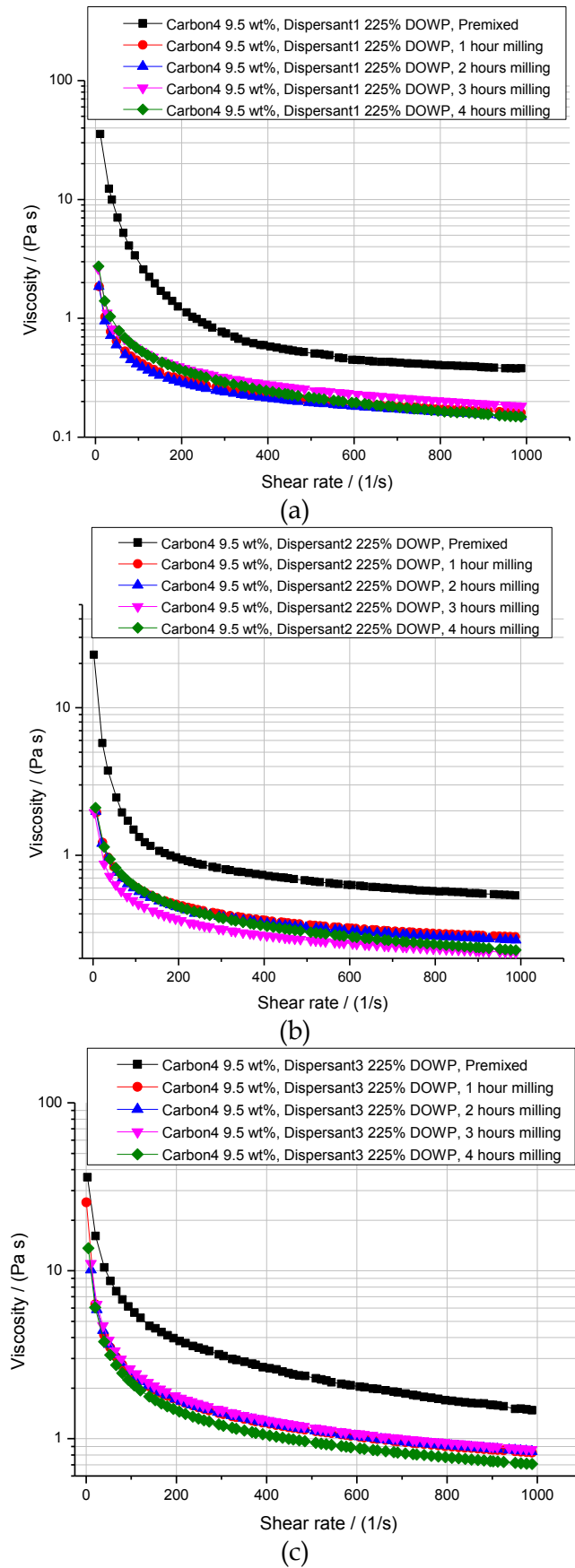


Figure 4-33: Milling viscosity of dispersions of Carbon4 prepared using (a) Dispersant1, (b) Dispersant2 and (c) Dispersant3.

The pre-mixed dispersions of Carbon4 pigment possessed very high viscosity and the recirculation rate through the milling chamber of the bead mill was very low, particularly during the initial several minutes of milling. Therefore, the dispersions of the Carbon4 pigment were bead milled for 4 hours instead of 3 hours, to ensure that the low recirculation rate was compensated for by longer duration of milling.

Figure 4-33 shows the viscosity profiles of dispersions of Carbon4 pigment, recorded along side the milling. The first hour of milling brought about the most significant decrease in the viscosity of all of the dispersions of Carbon4, followed by no recordable change in the viscosity during the second hour of milling. During the third hour of milling, a slight decrease in the viscosity of Carbon4-Dispersant2 dispersion was observed while there was no reduction in the viscosity of Carbon4-Dispersant3 dispersion. In contrast, an increase of 33% was observed in the viscosity of Carbon4-Dispersant1 dispersion. The viscosity of Carbon4-Dispersant1 and Carbon4-Dispersant2 dispersions, at the end of the fourth hour of milling, either remained unchanged or even slightly increased relative to the viscosity recorded after 3 hours of milling. The viscosity of Carbon4-Dispersant3 dispersion, however, decreased slightly during the fourth hour of milling. In summary, there was little or no change at all in the viscosity of all of the dispersions of Carbon4 pigment during the fourth hour of bead milling.

Based on the results of the rheological assessments presented above, it was concluded that three hours of milling at 3750 - 4000 RPM effectively dispersed the carbon black pigments that were used in this study.

4.4 Reliability and repeatability of the dispersion preparation process

As described in Section 2.2.5, it was considered to be important to establish the reliability and repeatability of the pigment dispersion preparation process and any acquired results. For this purpose, the following analyses were carried out on the different batches of each of the optimised pigment dispersions.

- To establish the reliability of the dispersion preparation process, thermogravimetric analysis of the optimised pigment dispersions was done, as

described in Section 3.7.3. In the context of this study, reliability of the milling process particularly refers to the amount of pigment that was present in different batches of a bead milled dispersion. Thus, the thermograms of different batches of a dispersion were compared for similarity in weight loss profile and final pigment loading. The pigment loading, as obtained from the thermogram of the dispersion, was also compared with the pigment loading in starting formulation to estimate the amount of pigment lost (if any) during bead milling.

- To assess the effectiveness of the bead milling process qualitatively, the viscosity profiles of the different batches of each of the optimised dispersions were compared with each other. Similarity in the viscosity profiles of the different batches of a dispersion was considered to be an indication of the fact that the bead milling process effectively furnished an appropriate degree of dispersion of the carbon black pigment.

During TGA, the production of carbon char or other decomposition products was possible as a result of the thermal decomposition of the polymeric dispersants present in a dispersion. Therefore, thermal analysis of the as-supplied dispersants was carried out to quantify the amount of residual matter. The thermograms showing the weight loss profiles of the dispersants are shown in Figure 4-34.

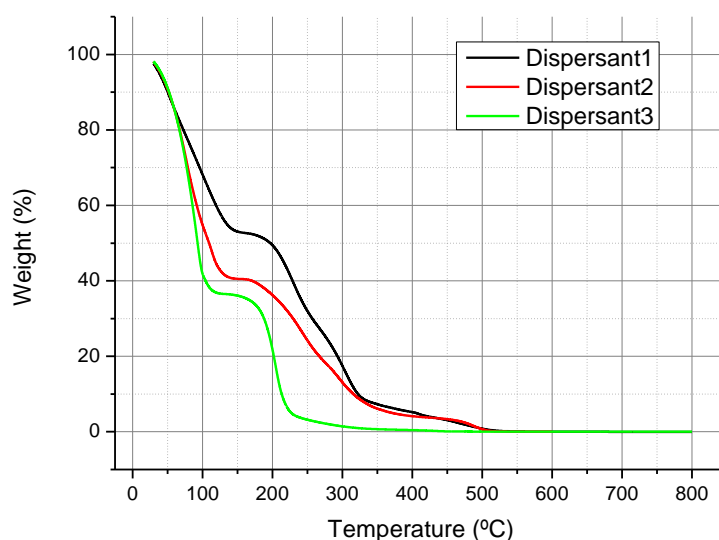


Figure 4-34: TGA thermograms of Dispersants (as-supplied form).

It is clear from the data presented in Table 4-31 that a considerable amount of residual matter was not present in any of the dispersants at a temperature of ≥ 600 °C. On the basis of this information, the thermal analysis of the formulated, bead milled dispersions was carried out at a temperature of up to 825 °C. Furthermore, the dispersion test specimen was held at 825 °C for 10 minutes to facilitate complete removal of the decomposition products (if present) of the respective dispersant. It is proposed that the residue from a dispersion sample at 825 °C (Table 4-32) or at a lower temperature at which the respective dispersant was completely removed can be regarded as the amount of carbon black pigment.

Table 4-31: Solids contents of dispersants at various temperatures in TGA.

	Residue (%wt) at different temperatures				
	400 °C	500 °C	600 °C	700 °C	800 °C
Dispersant1	5.20	0.82	0.03	0.01	0.00
Dispersant2	4.13	0.63	0.04	NA*	NA*
Dispersant3	0.45	0.06	0.05	0.03	0.02
*NA refers to 'solids content not measurable'					

Table 4-32: Pigment loading as obtained from the formulation calculations and TGA of the bead milled dispersions.

Dispersion name	Pigment loading (wt%)			
	Starting formulation	TGA of bead milled dispersion*		
		Batch 1	Batch 2	Batch 3
Carbon1-Dispersant1	31	35.16	34.24	-
Carbon1-Dispersant2	31	31.81	30.97	-
Carbon1-Dispersant3	31	31.74	31.29	-
Carbon2-Dispersant1	23	26.27	26.59	-
Carbon2-Dispersant2	23	26.99	24.97	-
Carbon2-Dispersant3	23	19.80	24.30	-
Carbon3-Dispersant1	11	10.25	12.14	-
Carbon3-Dispersant2	11	12.56	12.66	-
Carbon3-Dispersant3	11	11.81	9.20	-
Carbon4-Dispersant1	9.25	11.14	11.92	11.46
Carbon4-Dispersant2	9.5	11.50	11.92	-
Carbon4-Dispersant3	9	8.11	8.11	11.70
*Refers to the solids content in the dispersions at 825 °C.				

As shown in Figure 4-35 (a,b), the two batches of both Carbon1-Dispersant1 and Carbon1-Dispersant2 dispersions possessed very similar viscosity profiles after bead milling. In contrast, the viscosity of Batch 2 was lower compared to the viscosity of Batch 1 of the Carbon1-Dispersant3 dispersion. The difference in viscosity, as shown in Figure 4-35(c), was at least 30% (approx.) between a shear rate of 300 s^{-1} and 1000 s^{-1} . The thermogravimetric analyses showed that the weight loss profiles of the different batches of a dispersion of Carbon1 pigment were very similar, as shown in Figure 4-36. The solids content in the different batches of the dispersions of Carbon1 pigment are tabulated in Table 4-32. It was found that the pigment loading in both batches of Carbon1-Dispersant1 dispersion was similar, though it was above 34 wt% which is higher compared to that in the starting formulation. In contrast, in the dispersions of Carbon1 pigment that were prepared using Dispersant2 and Dispersant3, the amount of pigment was close to that in the starting formulations, which was 31 wt%. On the basis of the results of thermal analyses, the difference in the viscosity of the two batches of Carbon1-Dispersant3 dispersion was not regarded as a clear evidence of difference in the composition, particularly the pigment loading, after bead milling of these dispersions. This implied that there was probable some difference in the milling effect which resulted in a slightly different state of dispersion of pigment in the two batches of Carbon1-Dispersant3 dispersion.

As shown in Figure 4-37 (a), the viscosity of Batch 1 was approximately 40% greater than the viscosity of Batch 2 of the Carbon2-Dispersant1 dispersion. However, the amount of pigment, as estimated by TGA (Table 4-32), was 26 wt% (approx.) in both batches. Thus, the observed difference in the viscosity profiles was considered to be an indicator of difference in the extent of milling of the two batches. The different batches of the dispersions of Carbon2, prepared using Dispersant2 and Dispersant3, possessed very similar viscosity profiles, as shown in Figure 4-37(b) and Figure 4-37(c), respectively. The TGA analyses showed that, with the exception of Batch 1 of Carbon2-Dispersant3 dispersion, the amount of pigment in the bead milled dispersions of Carbon2 was in the range of 24 - 27 wt% which is greater than the pigment loading of 23 wt% in the starting formulation. It was observed, as shown in Figure 4-38(c), that the weight loss continued in Batch 1 of the Carbon2-Dispersant3 dispersion when the sample was heated above $500 \text{ }^{\circ}\text{C}$ and that the solids content at $825 \text{ }^{\circ}\text{C}$ was 19.80 wt%. However, the TGA data of this dispersion showed that the solids content at 500°C was

approximately 25 wt%. Since the TGA showed that the amount of residue of Dispersant3 was 0.06% at 500 °C, the decrease in solids content above 500 °C was attributed to loss of pigment as the dispersion sample was heated above this temperature.

As shown in Figure 4-39 (a), the batch-to-batch variation in terms of viscosity was not observed in the case of Carbon3-Dispersant1 dispersion. The thermal analysis showed that the two batches of the Carbon3-Dispersant1 dispersion possessed very similar weight loss profiles, as shown in Figure 4-40(a). The solids content at 825 °C was 10.25 wt% and 12.14 wt% in Batch 1 and Batch 2, respectively. However, the data points recorded during the thermal analysis of Batch 1 of the dispersion provided a solids content of 12 wt% (approx.) at 600 °C. Since Dispersant1 or a large proportion of its decomposition products were not likely to be present in the test specimen at 600 °C, the solids at this temperature was regarded as the pigment loading in the dispersion.

The viscosity profiles of the two batches of Carbon3-Dispersant2 dispersion (Figure 4-40(b)) were very similar so were the TGA thermograms (Figure 4-41(b)). The difference in pigment loading was 0.8% (approx.) at 825 °C, which clearly indicated that the batch-to-batch variation in terms of the composition was minimal in the batches of Carbon3-Dispersant2 dispersion.

The rheological analysis showed that the two batches of the Carbon3-Dispersant3 dispersion possessed different viscosity profiles, as shown in Figure 4-39(c). The difference in viscosity was as high as up to 40% (approx.) in the shear rate range used in the analysis. During the thermal analysis of the Batch 2 of Carbon3-Dispersant3 dispersion, it was observed that the solids content continued to decrease when the dispersion test specimen was heated above 500 °C. This is depicted by the thermogram of this dispersion sample, presented in Figure 4-40(c). As in case of other dispersions which showed a similar trend, the solids content at 500 °C was regarded as the pigment loading in this case as well. The recorded data points at 500 °C provided a pigment loading of 12 wt% (approx.). Thus, it was concluded that the two batches of the Carbon3-Dispersant3 dispersion were similar in terms of the pigment loading after bead milling. The difference in viscosity in this case was perhaps due to a difference in the milling action of the bead mill.

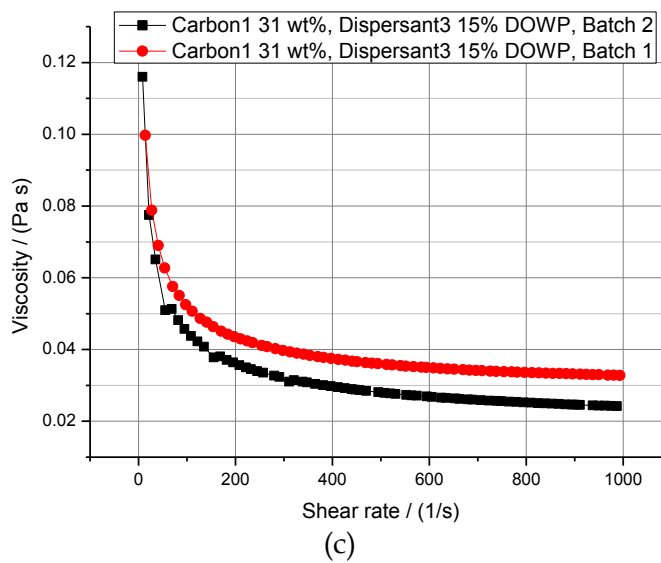
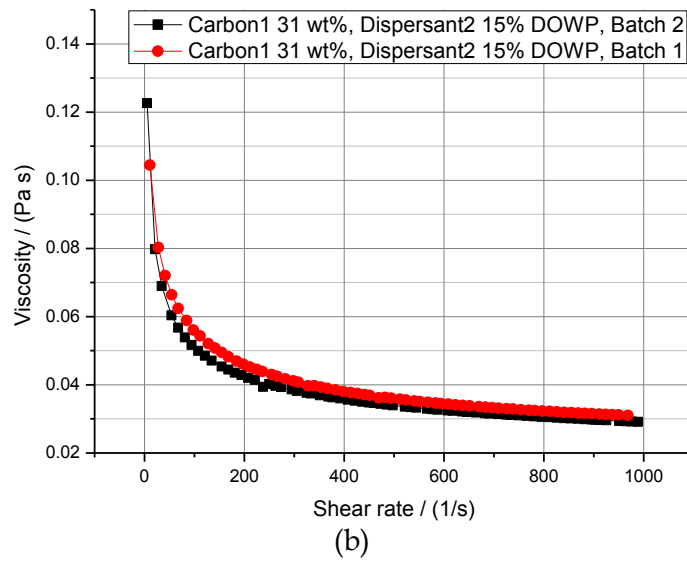
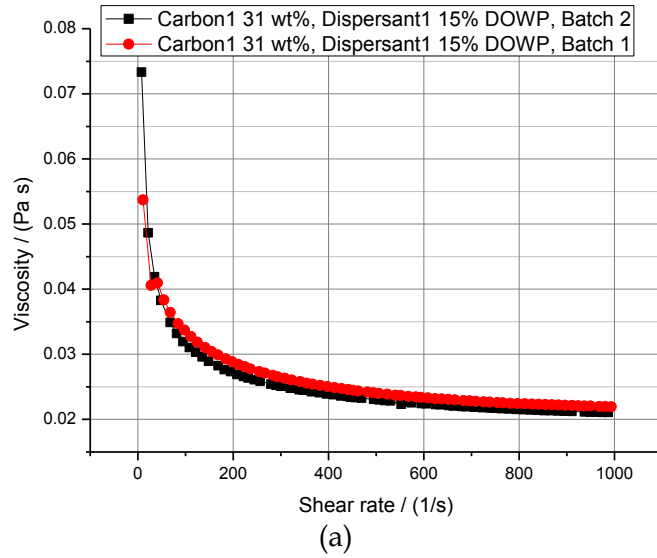
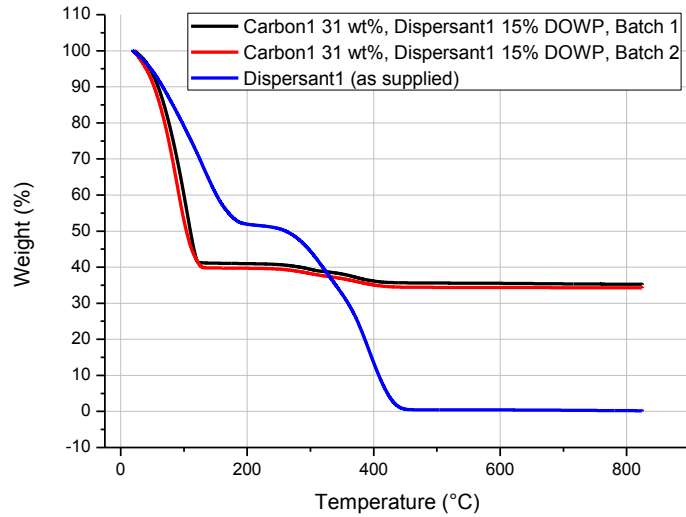
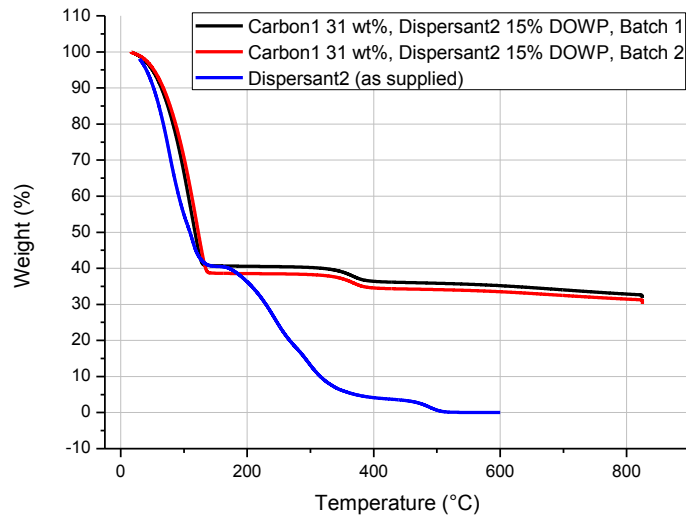


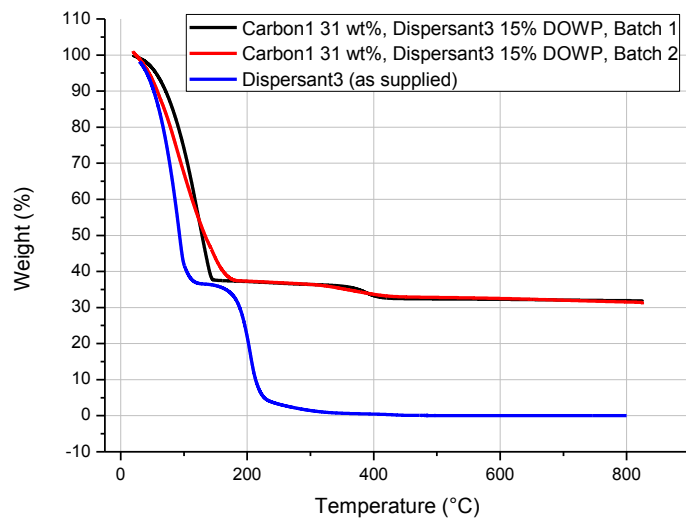
Figure 4-35: Viscosity profiles of different batches of Carbon1 dispersions prepared using (a) Dispersant1, (b) Dispersant2 and (c) Dispersant3.



(a)



(b)



(c)

Figure 4-36: TGA thermograms of different batches of dispersions of Carbon1 prepared using (a) Dispersant1, (b) Dispersant2 and (c) Dispersant3.

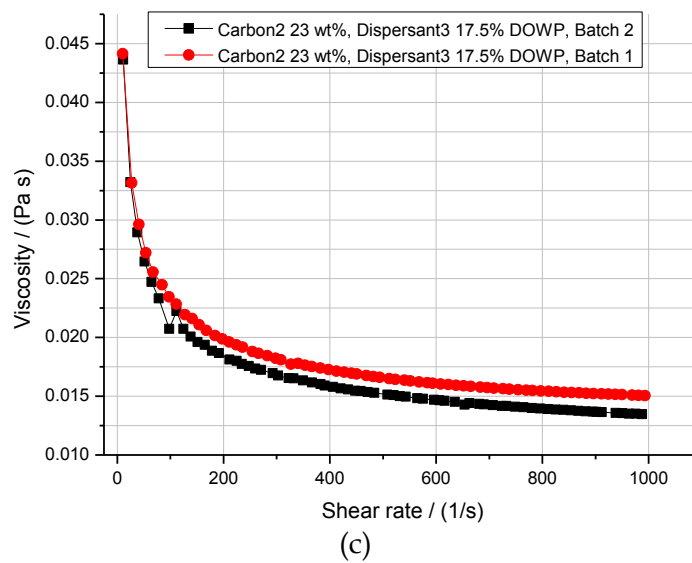
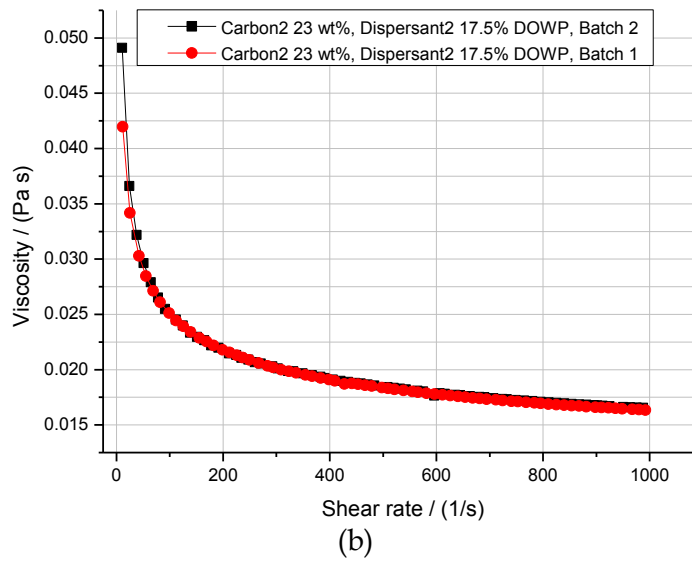
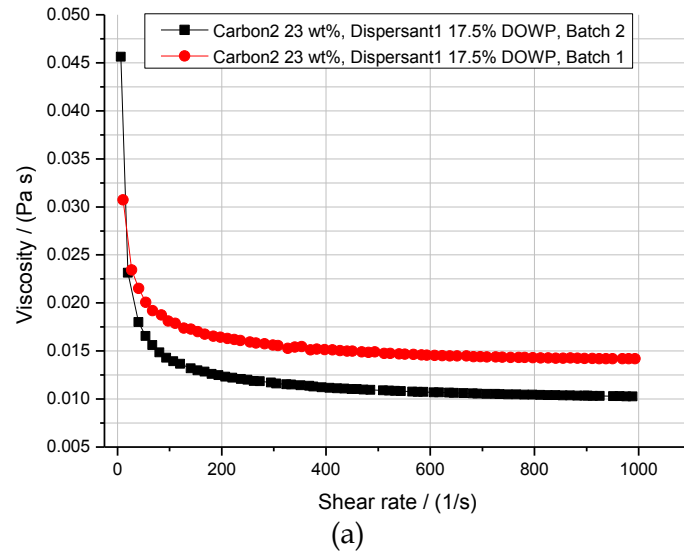
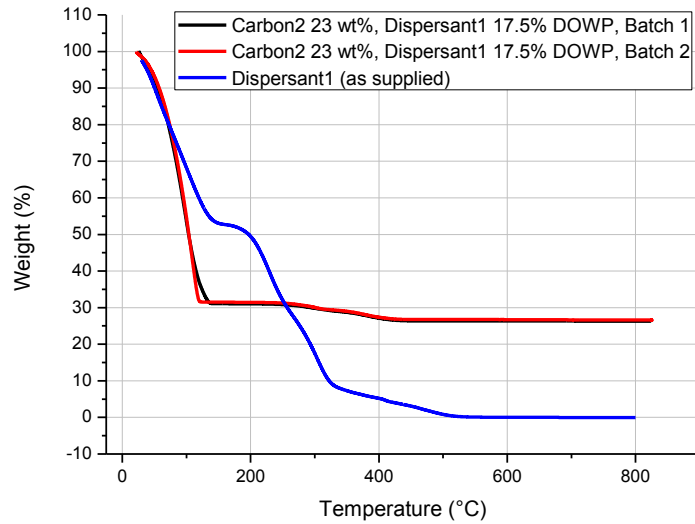
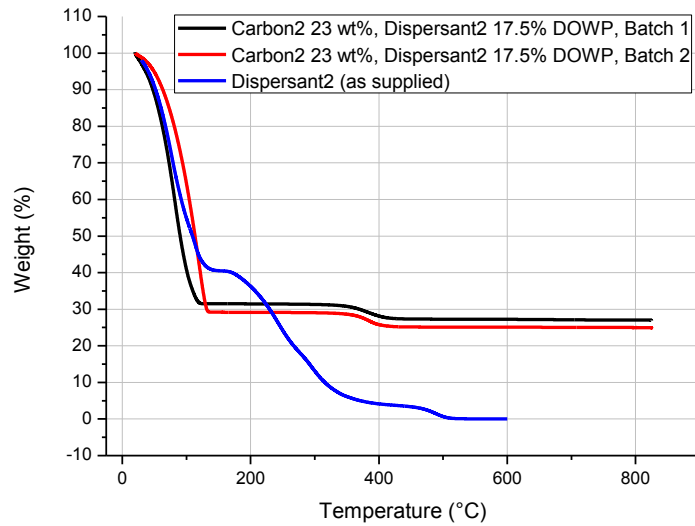


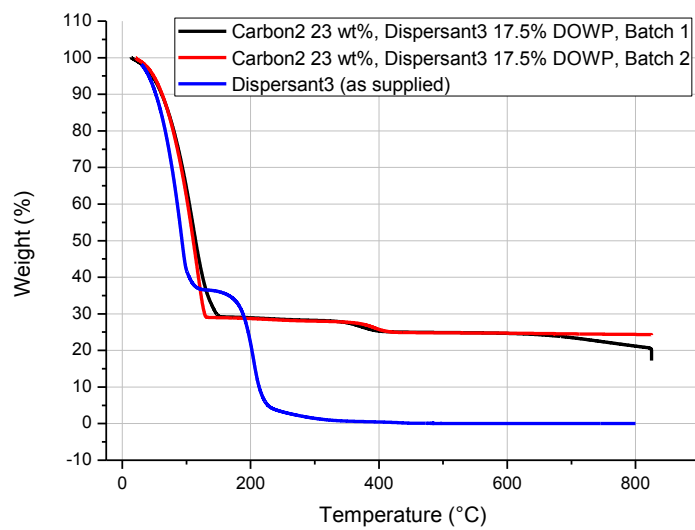
Figure 4-37: Viscosity profiles of different batches of Carbon2 dispersions prepared using (a) Dispersant1, (b) Dispersant2 and (c) Dispersant3.



(a)

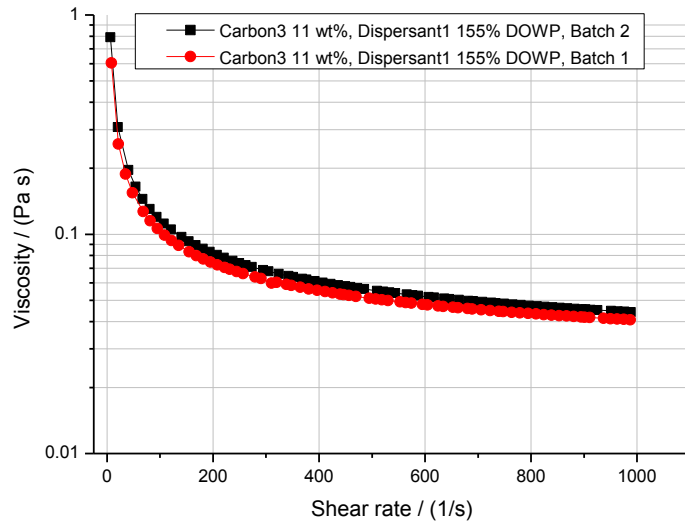


(b)

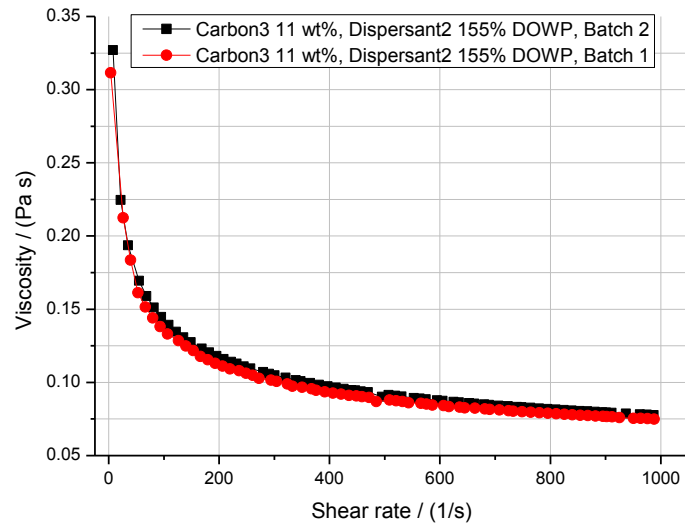


(c)

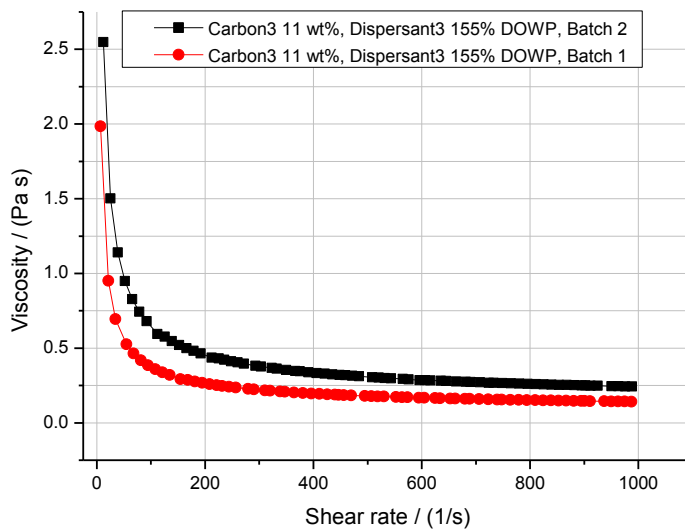
Figure 4-38: TGA thermograms of different batches of dispersions of Carbon2 prepared using (a) Dispersant1, (b) Dispersant2 and (c) Dispersant3.



(a)

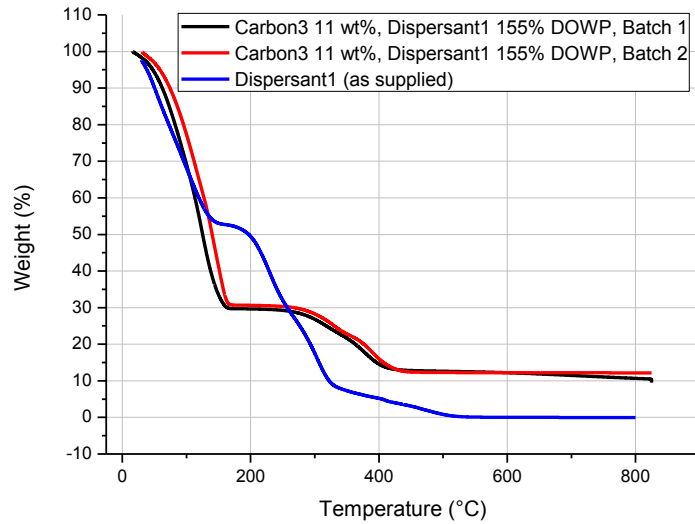


(b)

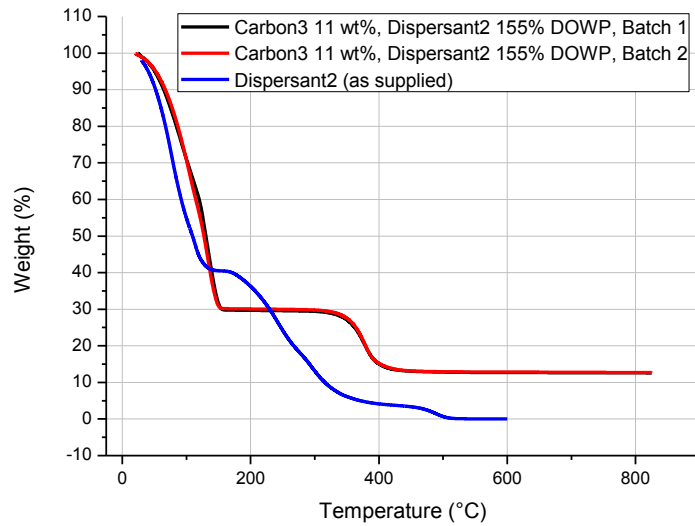


(c)

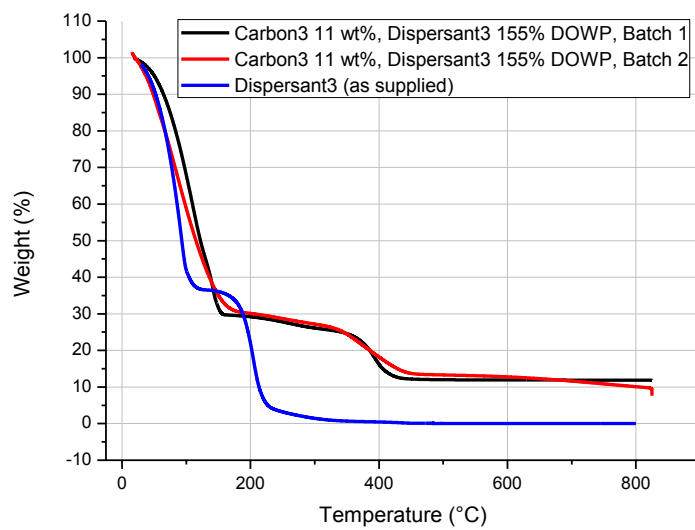
Figure 4-39: Viscosity profiles of different batches of Carbon3 dispersions prepared using (a) Dispersant1, (b) Dispersant2 and (c) Dispersant3.



(a)



(b)



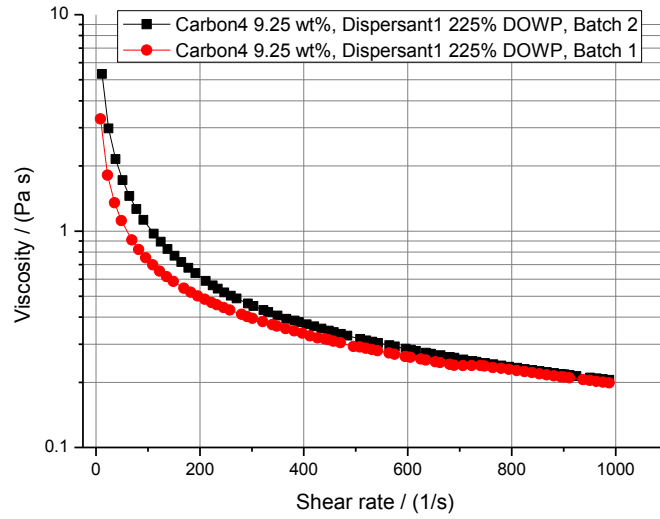
(c)

Figure 4-40: TGA thermograms of different batches of dispersions of Carbon3 prepared using (a) Dispersant1, (b) Dispersant2 and (c) Dispersant3.

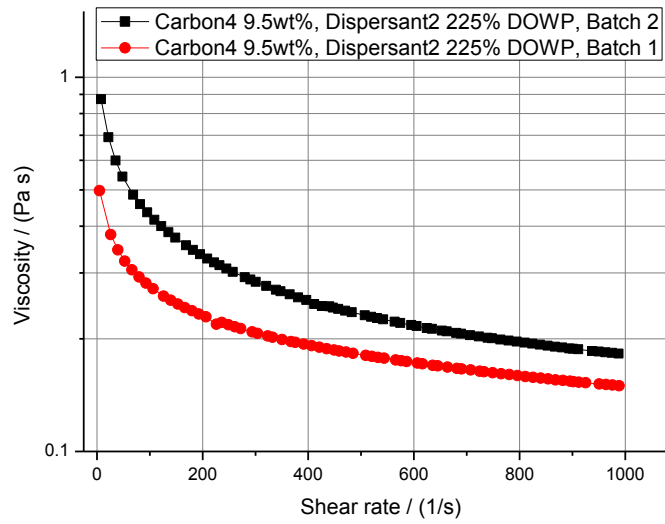
The viscosity profiles of the two batches of Carbon4-Dispersant1 dispersion were very similar, as shown in Figure 4-41(a). Three batches of the Carbon4-Dispersant1 dispersion were available for thermal analysis. The thermograms presented in Figure 4-42(a) showed similar weight loss profiles of these dispersions. The batch-to-batch variation in terms of pigment loading was minimal. However, the pigment loading was found to be in the range of 11 - 12 wt% which is higher than that in the starting formulations as tabulated in Table 4-32. This increase in pigment loading can be attributed to the evaporation of water which probably occurred due to the heating up of these viscous dispersions during bead milling.

As shown in Figure 4-41(b), the difference in viscosity of the two batches of Carbon4-Dispersant2 dispersion was smaller at greater shear rates with minimum being 15% (approx.) at 1000 s⁻¹. The pigment loadings in the bead milled Carbon4-Dispersant2 dispersions, as estimated from TGA, are presented in Table 4-32. The batch-to-batch in terms of pigment loading was 3.6% which can not be regarded as significant.

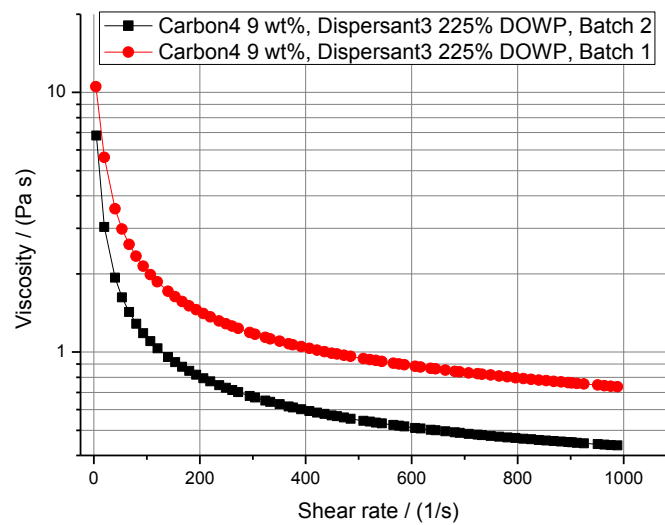
In case of dispersions of the Carbon4 pigment prepared using Dispersant3, the difference between the viscosity profiles of the two batches was considerable, particularly in the low shear rate region (up to 200 s⁻¹) in which the difference was at least 80%. The reason for this is likely to be the variation in the extent and effects of bead milling. This is because the pre-mixed Carbon4-Dispersant3 dispersions possessed the highest viscosity among all of the optimised pigment dispersions that were prepared in this study and it was extremely difficult to maintain a high recirculation rate during the bead milling. The TGA of Batch 1 and Batch 2 of Carbon4-Dispersant3 dispersions indicated that decrease in solids content continued to occur when the samples were heated above 500 °C and the solids content dropped to 8.11 wt% at 825 °C. However, the solids content was 11 wt% (approx.) at 500 °C. Since the solids content at 500 °C can be regarded as the pigment content, it was concluded that the three batches of the Carbon4-Dispersant3 dispersion were similar in terms of pigment loading after bead milling.



(a)

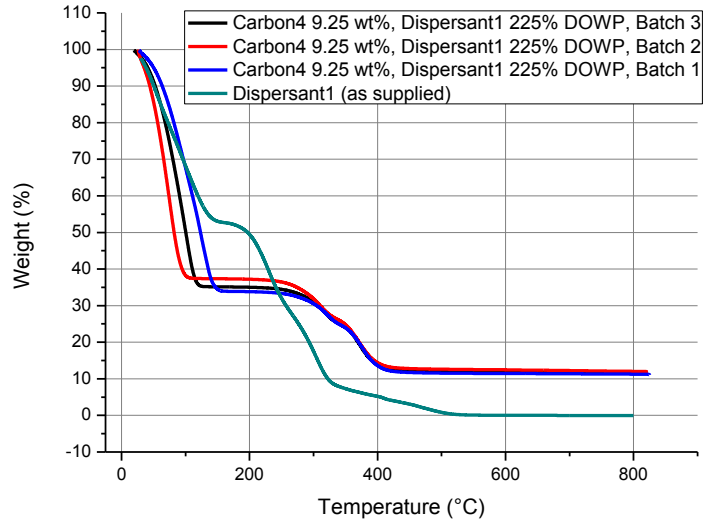


(b)

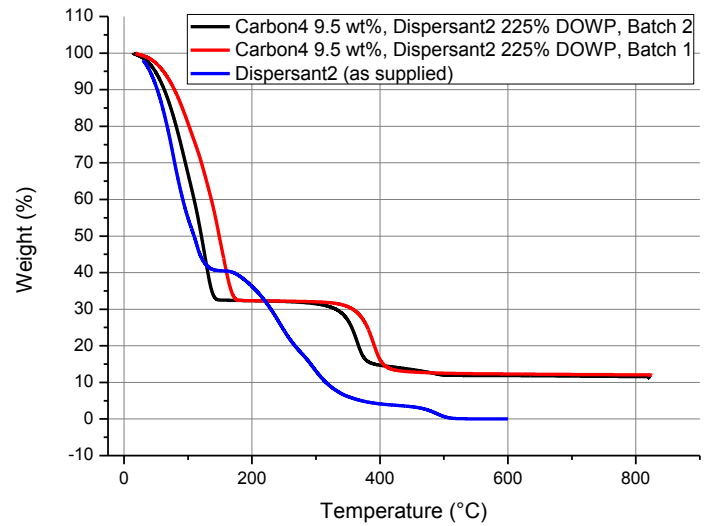


(c)

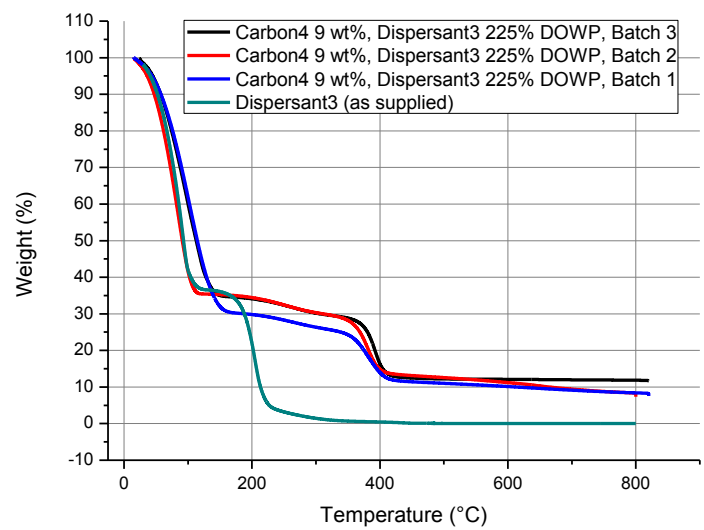
Figure 4-41: Viscosity profiles of different batches of Carbon4 dispersions prepared using (a) Dispersant1, (b) Dispersant2 and (c) Dispersant3.



(a)



(b)



(c)

Figure 4-42: TGA thermograms of different batches of dispersions of Carbon4 prepared using (a) Dispersant1, (b) Dispersant2 and (c) Dispersant3.

The batch-to-batch variation in terms of the viscosity and the pigment loading in the bead milled dispersions was generally very limited. For the dispersions prepared using Dispersant3, it was observed in a number of cases that decrease in the solids content continued to occur above 500 °C. Since the TGA data clearly show that Dispersant3 was completely decomposed at a temperature between 500 - 600 °C, the decrease in solids content that was recorded above 500 °C can be attributed to the loss of carbon black pigment at higher temperatures. In all such instances, the solids content at 500 °C was approximately the same as that in the starting formulation. This indicated that there was perhaps a difference in the milling effect in these cases. However, the thermal analyses indicated that pigment loss did not occur during milling. The comparative analyses carried out on the different batches of an optimised dispersion showed that the dispersion preparation procedure that was adopted during this study was repeatable. The analyses that were carried out on different batches of the optimised pigment dispersions proved to be helpful when the dispersions were used in the let-down stage. This point is considered in Section 4.5.3.

4.5 Preparation and characterisation of finished inks

In the first phase of this work, a number of “optimised” pigment dispersions were prepared and characterised, as discussed in Section 4.1 and Section 4.2. Since all of the optimised pigment dispersions met the stability criteria and other specified performance criteria and three binders were considered for use in the let-down of these dispersions, it was clear that a large number of inks would need to be prepared and tested. Furthermore, the requirement to test each ink on various textile substrates implied that the testing of hundreds of samples would be needed. Thus, various steps to screen out under-performing inks were followed, to keep the number of test samples within a manageable number without losing important data. These steps were:

- Determining the surface resistivity of the binder-free pigment dispersions. This was done in order to screen out the pigment dispersions which possessed high electrical resistivity.
- Screening tests to investigate whether or not the binders, listed in Table 2-3, would be suitable for use as let-down binders for all of the optimised dispersions selected after surface resistivity tests.

- Let-down stability testing of the finished inks to screen out unstable inks, before their printing and testing on textile substrates.
- Surface resistivity measurements of the inks containing known various amounts of binders. This was done to establish the required binder solid content in those inks that were prepared for textile printing.
- Printing of selected inks onto textile substrates followed by durability testing.

4.5.1 Selection of pigment dispersions for the let-down stage

Depending upon the viscosity of a dispersion, the amount of the dispersion recovered after bead milling varied between 50 g – 70 g. Since a number of tests were to be carried out on the finished inks formulated from the dispersions, it was estimated that approximately 140 g – 150 g of each of the optimised pigment dispersion was required for the let-down stage. Thus, at least two batches of each of the optimised dispersion were prepared and analysed for batch-to-batch variations in terms of their viscosity and their pigment loading, as discussed in the previous section. To eliminate batch-to-batch variations, different batches of a dispersion were mixed together in equal ratios to produce a single “homogenised” batch. As shown in Table 4-34, the homogenised dispersions in which the pigment loading was less than it was in the starting formulation were used in the let-down stage without making any adjustments to the composition. However, if the pigment loading in the homogenised batch was higher than that in the starting formulation, de-ionised water was added to adjust the pigment content. The dispersion was stirred at 2000 RPM for 10 minutes using a disk disperser (Figure 2-4) while the pigment loading was adjusted by adding the required amount of de-ionised water. Following the procedure described above, a single homogenised batch of each of the optimised dispersions was produced. In addition, the pigment loading in the dispersions of a pigment, that were prepared using various dispersants, was also made similar (where possible). This provided a basis for the comparison of the performance of inks that were formulated from the various dispersions of a pigment.

The electrical properties of the homogenised and adjusted dispersions were characterised following the procedures described in Section 3.5 and Section 3.6. It was observed that the dispersions containing Dispersant1 possessed high electrical

conductivity (as measured by a conductivity cell) compared to the dispersions of the same pigment prepared using Dispersant2 or Dispersant3. However, it was noted that the K-bar drawdowns of all of the pigment dispersions possessed comparable surface resistivity. Thus, the electrical conductivity of as supplied dispersants was measured, the results of which are provided in Table 4-33. It was found that high conductivity of the dispersions containing Dispersant1 could be attributed to the higher conductivity of the Dispersant1 in its solution form. Since in this study, surface resistivity was considered to be more important than the conductivity, measured using a conductivity cell, all of the twelve dispersions, listed in Table 4-34, were formulated into finished inks for further testing.

Table 4-33: Electrical conductivity of as-supplied dispersants.

Dispersant (As supplied solution)	Conductivity ($\mu\text{S}/\text{cm}$)
Dispersant1	1649
Dispersant2	116.2
Dispersant3	346

This space is deliberately left blank due to pagination.

Table 4-34: Pigment loading and electrical characteristics of the dispersions used in the let-down stage.

Dispersion name	Pigment loading (wt%)					Electrical characteristics		
	Starting formulation	Bead milled dispersions			Cumulative	Adjusted (Approx.)	Conductivity ($\mu\text{S/cm}$)	Surface resistivity (Ω/\square)
		Batch 1	Batch 2	Batch 3				
Carbon1-Dispersant1	31	35.16	34.24	-	34.70	31	890	321
Carbon1-Dispersant2	31	31.81	30.97	-	31.39	31	106.1	332
Carbon1-Dispersant3	31	31.74	31.29	-	31.52	31	181.7	265
Carbon2-Dispersant1	23	26.27	26.59	-	26.43	23	928	241
Carbon2-Dispersant2	23	26.99	24.97	-	25.98	23	103.3	234
Carbon2-Dispersant3	23	19.80	24.30	-	22.05	22	193.3	225
Carbon3-Dispersant1	11	10.25	12.14	-	11.19	11	2210	390
Carbon3-Dispersant2	11	12.56	12.66	-	12.61	11	111	378
Carbon3-Dispersant3	11	11.81	9.20	-	10.51	10.5	310	371
Carbon4-Dispersant1	9.25	11.14	11.92	11.46	11.51	9.5	1793	575
Carbon4-Dispersant2	9.5	11.50	11.92	-	11.71	9.5	123	390
Carbon4-Dispersant3	9	8.11	8.11	11.7	9.31	9.3	209	456

4.5.2 Binder-Dispersant compatibility tests

In this study, binder-free pigment dispersions were prepared to exploit the benefits of maximising the pigment loading, as discussed in Section 2.2.1. However, one of the major disadvantages of this two step process of ink preparation is that the presence of large amounts of pigment wetting and dispersing additives can pose potential compatibility problems and reduction in ink film properties (Hobisch and Tsang 2009). In the context of this study, it was important to anticipate such incompatibility issues because the pigment dispersion formulations, particularly those of the high surface area carbon black pigments, contained very large amounts of dispersants. Therefore, before the optimised pigment dispersions were formulated into finished inks, various relevant binder-dispersant combinations were tested for compatibility, following the procedure that was described in Section 2.3.1. The various binder-dispersant mixtures were deposited on to glass slides (Figure 4-43) and visually assessed for signs of incompatibility such as cloudiness of the film and precipitation of the mixture components. This qualitative assessment of the air dried and cured films showed no signs of incompatibility as all the mixtures produced clear films with no significant cracking or loss in adhesion. It was noticed, however, that the mixtures which contained large amount of dispersant and correspondingly a low amount of binder dried very slowly. This was expected because the binder solids content in these mixtures was very low.

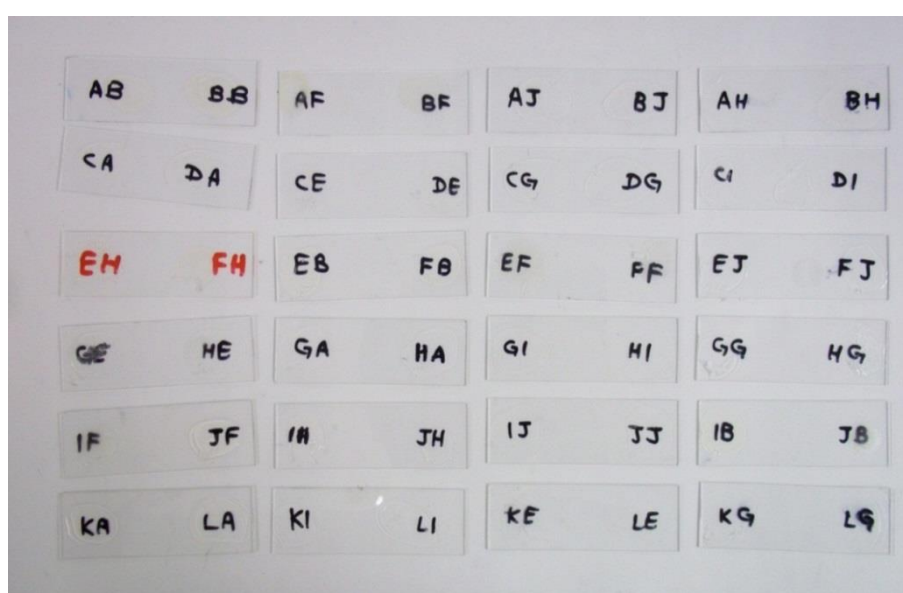


Figure 4-43: Glass slides deposited with various binder-dispersant mixtures.

The binder-dispersant mixtures were stored in air tight glass vials. After four weeks of storage at ambient temperature (20 °C – 25 °C), the mixtures were re-inspected visually and it was found that none of the mixtures showed increased turbidity/cloudiness or any visible signs of precipitation of the dispersant and/or the binder.

Based on the observations made in the above mentioned qualitative tests, it was concluded that all of the binder-dispersant mixtures were compatible at the loadings levels tested.

4.5.3 Let-down stability of pigment dispersions

Despite the optimal stabilisation of primary pigment particles, flocculation can occur in certain conditions, for instance, at relatively high temperatures which result in increased kinetic energy. Owing to this increased kinetic energy, the particles can approach close enough to allow the forces of attraction to overcome the effects of stabilising species. In preparation of pigment dispersions/concentrates, the aim is almost always to furnish an adequate amount of stabilising dispersant molecules. Furthermore, the dispersion formulation is designed to perform suitably on the dispersion preparation machinery with little or no direct consideration for the required properties in the finished ink. However, the finished ink is formulated to meet a completely different set of requirements such as printability, adhesion to the substrate, resistance to the action of water and/or chemicals and so on. Consequently, in the two step ink preparation process, the amount of binder solids that is incorporated in the let-down stage is significantly higher than that in the pigment dispersion. In an extreme case, as in the present study, the binder is not present at all in the pigment dispersion formulation. Thus in such cases, the amount of binder required to achieve the desired properties of the finished ink is added only in the let-down stage. This significant change in composition from the binder-free pigment dispersion to the let-down mixture can result in 'pigment shock'. Pigment shock can occur when a pigment dispersion containing no/low binder solids is formulated into an ink using a let-down mixture which has very high binder solids content. In this situation, a difference in osmotic pressure of the solvent exists in the dispersion and in the let-down mixture. Due to the difference in the binder-solvent ratio, the let-down mixture can draw

solvent molecules rapidly from the pigment dispersion, thus forcing the pigment particles to flocculate (Goldschmidt and Streitberger 2003).

Another problem commonly encountered during the two step production of a finished ink is 'solvent shock'. This occurs when the binder solids content in a pigment dispersion is high compared to that in the let-down mixture. In this situation, solvent molecules in the let-down mixture have high mobility and can quickly penetrate the pigment dispersion, thus displacing the stabilising binder/dispersant layer on the surface of stabilised particles. In this study, binder-free pigment dispersions were let-down with binder emulsions to produce finished inks. Thus, solvent shock was not anticipated as a potential cause of instability of the pigment dispersions.

Flocculation which occurs as a result of the phenomena described above, particularly pigment shock, results in an increase in the average particle size and accelerated sedimentation. Thus, particle size distribution analysis (Frimova et al. 2006) and sedimentation analysis (Tay and Edirisinghe 2002) can be used to estimate dispersion stability. Techniques based on multiple light scattering (MLS) can also be employed to optically detect any changes in the particle size during aging tests (*Stability of pigment inkjet inks* 2009). Since aging is an exothermic process, thermal analysis techniques, such as Differential Scanning Calorimetry (DSC) can be employed to predict the long term stability (aging properties) of an ink (*Long Term Stability Testing of Printing Inks by Differential Scanning Calorimetry*). Monitoring of rheological characteristics versus time can also provide insight into the stability of dispersion/ink. A stable viscosity profile over an extended time period can be regarded as an indication of the ink stability (Tay and Edirisinghe 2002).

In this study, after assessing the compatibility of various binder-dispersant mixtures, the optimised pigment dispersions were formulated into finished inks containing 100%, 150% and 200% BOWP. The procedure for this is described in detail in Section 2.3.2. In order to optimise the experimental effort, it was considered to be important to screen out unstable inks before electrical characterisation or durability performance testing. For this purpose, the viscosity profiles of the inks formulated from the "optimised" pigment dispersions were recorded and analysed to identify unstable inks.

4.5.3.1 Viscosity stability of the inks prepared from the dispersions of Carbon1.

The increase in the viscosity of inks that were prepared from Carbon1-Dispersant1 dispersion (Figure 4-45), was generally in-line with the average increase of 6.5% (SD=1.58) in the viscosity of the binder-free Carbon1-Dispersant1 dispersion. However, there are some exceptions. It is proposed that the significantly greater increase in the viscosity of Carbon1-Dispersant1-Binder3 inks, as shown in Figure 4-45(e,f), occurred due to the evaporation of ammonia from solution that was added in these inks to avoid premature polymerisation of Binder3. However, this could not be confirmed because the weight loss during storage was not recorded. In case of the ink prepared by adding 150% BOWP of Binder2 in the Carbon1-Dispersant1 dispersion, the increase in viscosity after four weeks of storage, as shown in Figure 4-45(c,d), was between 25 - 40 % (approx.) above a shear rate of 500 s^{-1} . Deviation from shear thinning rheology in this higher shear rate region was attributed to the drying of ink that was observed during viscosity measurement. Drying of Carbon1-Dispersant1-Binder2 inks, accompanied by an abrupt change in viscosity, was observed in all the repeat viscosity measurements. Furthermore, the average increase in the viscosity of inks that were formulated to contain 100% and 200% BOWP of Binder2 was 8% (SD=1.63) and -0.43% (SD=2.67), respectively. Therefore, the greater increase in the viscosity of the ink containing 150% BOWP of Binder2 was not regarded as an indication of Binder2-induced instability of the pigment dispersion.

In case of the inks prepared by incorporating various amounts of Binder1 in the Carbon1-Dispersant2 dispersion, the increase in viscosity after storage, as shown in Figure 4-46(a,b), was in-line with the average increase of 5.35% (SD=2.19) in the viscosity of Carbon1-Dispersant2 dispersion. From the viscosity profiles of Carbon1-Dispersant2-Binder2 inks, as presented in Figure 4-46(c,d), a general trend of increase or decrease in the viscosity could not be established. As in case of the Carbon1-Dispersant1-Binder3 inks, ammonia solution was also added in the Carbon1-Dispersant2-Binder3 inks. The viscosity of these inks considerably increased after four weeks of storage, as shown in Figure 4-46(e,f). However, smooth shear thinning rheology was maintained after storage. Therefore, the increase in viscosity was attributed to evaporation of ammonia from solution during storage of these inks.

As shown in Figure 4-47(a,b), the average increase in the viscosity of the ink prepared from Carbon1-Dispersant3 dispersion and 150 %BOWP of Binder1 was approximately 46% (SD=11.38) which is considerably greater compared to the average increase of 7.1% (SD=0.94) and 1.53% (SD=0.61) in the viscosity of the inks of the same dispersion but containing 100% or 200% BOWP of Binder1, respectively. It is proposed that if an ink was unstable due to any unfavourable pigment-dispersant-binder interaction(s), then a similar trend of change in the viscosity after storage should have been observed in all the inks prepared from a pigment dispersion but containing various amounts of a binder.

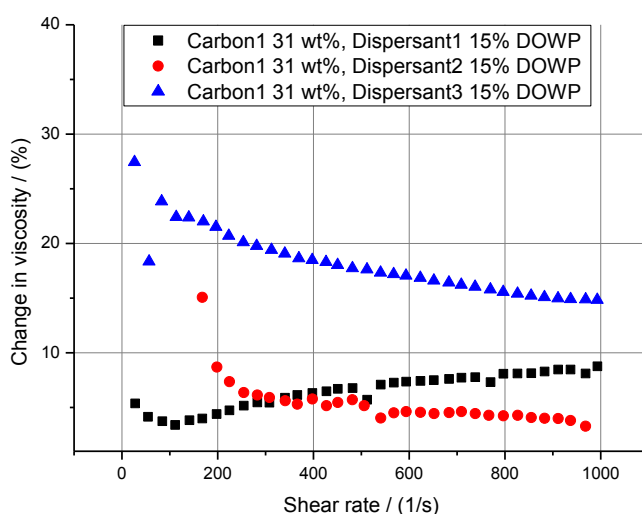


Figure 4-44: Change in viscosity during four weeks storage of the homogenised batch of the optimised dispersions of Carbon1 pigment.

The viscosity of binder-free Carbon1-Dispersant3 dispersion increased by 18% (SD=2.95) during storage. This is shown in Figure 4-44. However, the viscosity of inks that were prepared by incorporating Binder2 in this dispersion decreased considerably after four weeks of storage, as shown in Figure 4-47(c,d). This indicated that there was probably some degree of instability in this ink. In contrast to the above, the increase in the viscosity of inks prepared by incorporating Binder3 in the Carbon1-Dispersant3 dispersion was similar to that observed in the binder-free dispersion.

The viscosity stability analyses of inks indicated that incorporation of Binder2 probably induced destabilisation of the Carbon1 pigment dispersion. In contrast, the change in viscosity of Binder1-/Binder3-containing inks was generally in good agreement with the change in viscosity of the relevant binder-free dispersions.

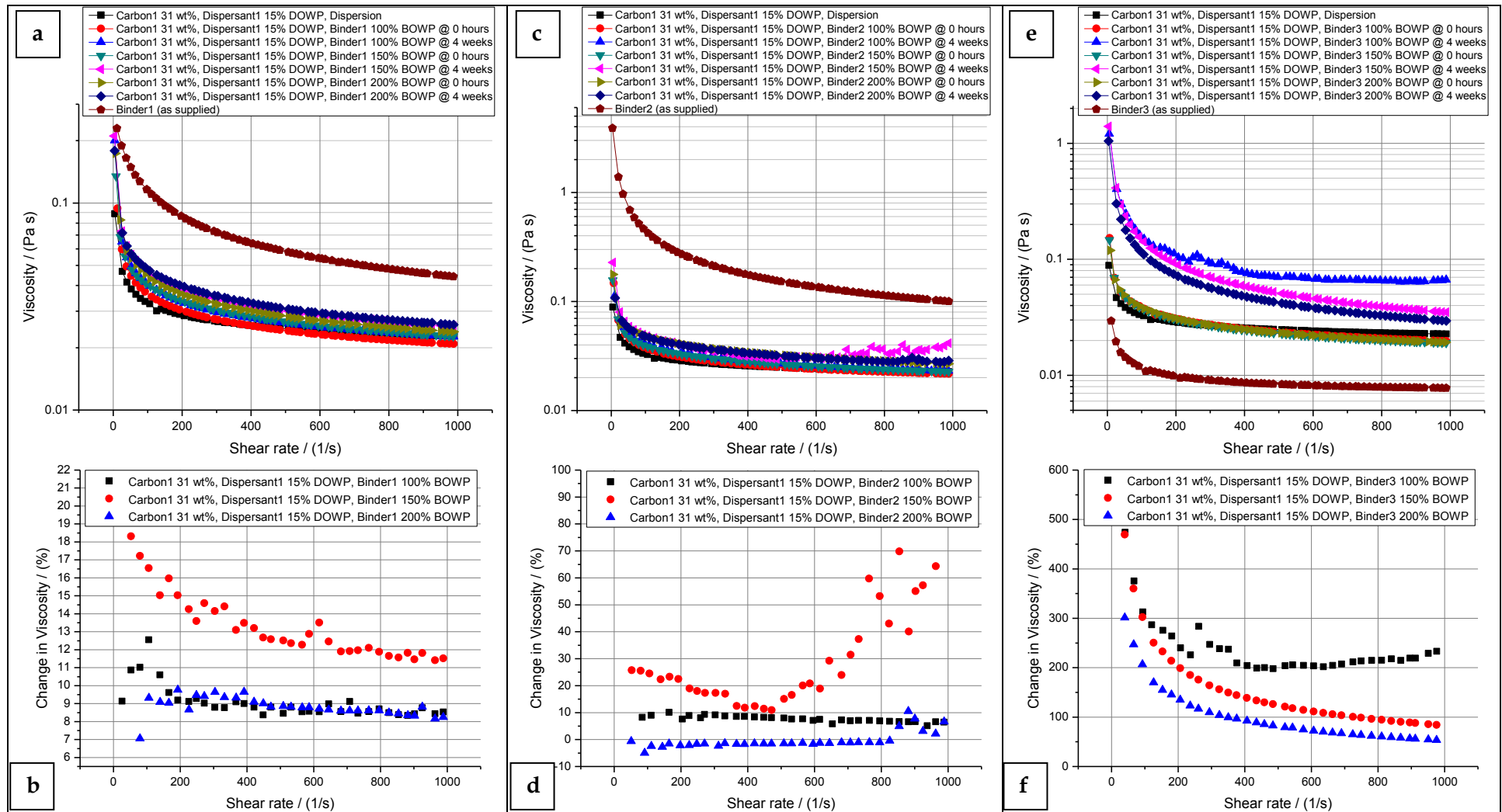


Figure 4-45: Viscosity stability of inks prepared by adding various amounts of Binder1/Binder2/Binder3 in Carbon1-Dispersant1 dispersion.

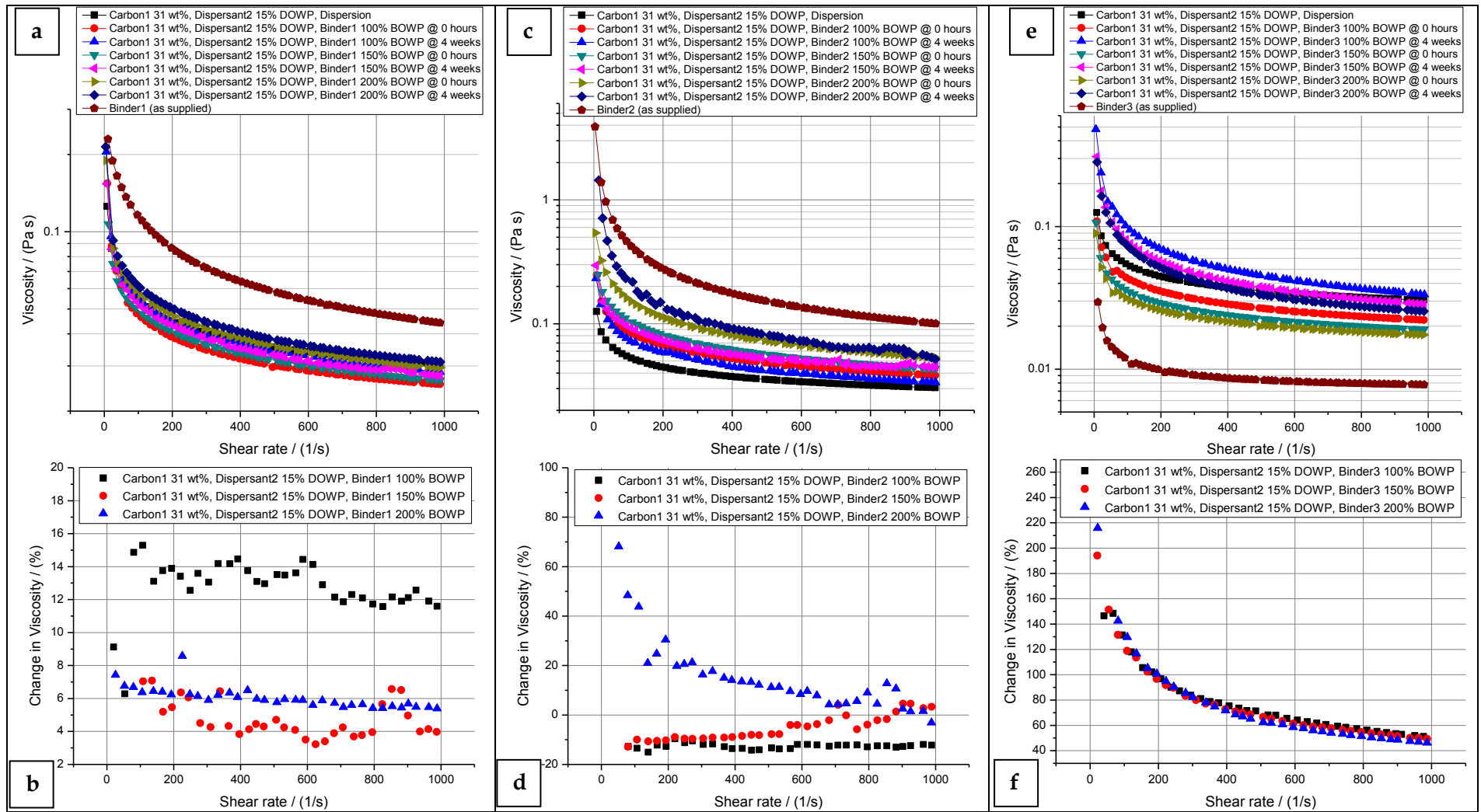


Figure 4-46: Viscosity stability of inks prepared by adding various amounts of Binder1/Binder2/Binder3 in Carbon1-Dispersant2 dispersion.

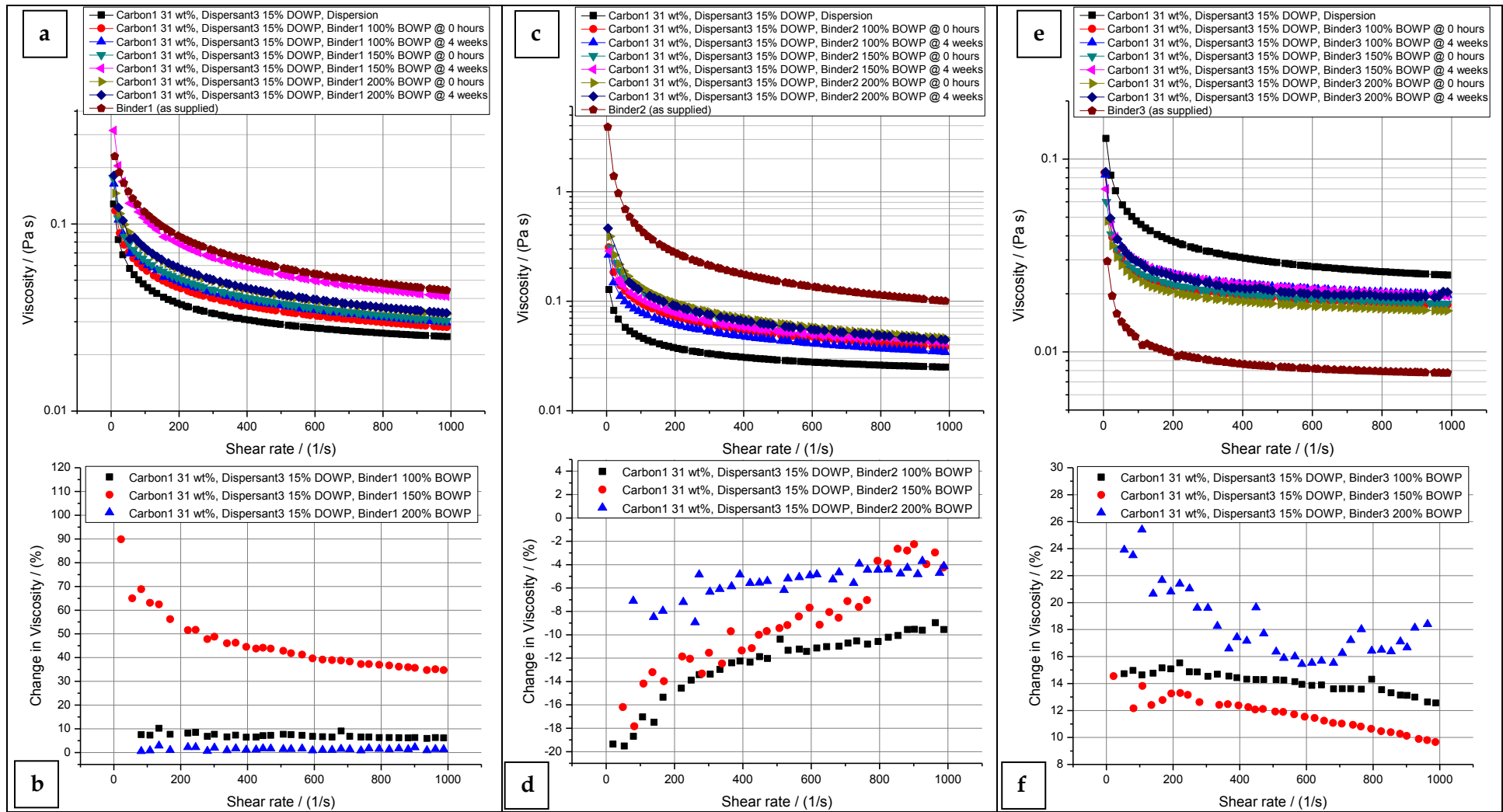


Figure 4-47: Viscosity stability of inks prepared by adding various amounts of Binder1/Binder2/Binder3 in Carbon1-Dispersant3 dispersion.

4.5.3.2 Viscosity stability of the inks prepared from the dispersions of Carbon2.

In this section, the results of viscosity stability analyses of the inks prepared from Carbon2 pigment dispersions are discussed with respect to the three binders that were used to formulate finished inks. As shown in Figure 4-49(c,d), a considerable change in the viscosity occurred in the inks prepared by adding Binder2 in the Carbon2-Dispersant1 dispersion. Furthermore, deviation from shear-thinning rheology was also recorded for these inks. The above mentioned changes in viscosity were more pronounced in the ink containing 200% BOWP of Binder2. Repeat viscosity measurements of these inks did not show a consistent trend. However, large variations in viscosity, which were not in-line with the average increase of 11.11% (SD=0.88) in the viscosity of binder-free Carbon2-Dispersant1 dispersion, were recorded in all the repeat measurements. The viscosity of inks prepared by adding Binder2 in the Carbon2-Dispersant2 and Carbon2-Dispersant3 dispersions decreased considerably after four weeks of storage, as shown in Figure 4-50(c,d) and Figure 4-51(c,d), respectively. The average decrease in the viscosity of Carbon2-Dispersant2-Binder2 and Carbon2-Dispersant3-Binder2 inks is tabulated in Table 4-35 below. It is evident that the change in viscosity of these inks is not in-line with the average increase of 4.20% (SD=1.35) and 2.43% (SD=0.88) in the viscosity of binder-free Carbon2-Dispersant2 and Carbon2-Dispersant3 dispersions, respectively.

Table 4-35: Average increase in the viscosity of Carbon1-Dispersant2-Binder2 and Carbon1-Dispersant3-Binder2 inks.

Ink composition		Increase in viscosity (%)	
		Average	SD
Carbon2 23wt%, Dispersant2 17.5% DOWP	100% BOWP Binder2	-18.81	1.81
	150% BOWP Binder2	-20.01	1.89
	200% BOWP Binder2	-16.27	2.50
Carbon2 23wt%, Dispersant3 17.5% DOWP	100% BOWP Binder2	-15.73	2.58
	150% BOWP Binder2	-16.02	2.63
	200% BOWP Binder2	-14.63	3.01

In contrast to the inks of Carbon2 pigment that were prepared using Binder2, the inks prepared using Binder1 and Binder3 were generally very stable as indicated by a small average change in the viscosity after four weeks of storage. The change in viscosity of most of these inks also correlated with the change in viscosity of the binder-free dispersions of Carbon2 pigment, as shown in Figure 4-48.

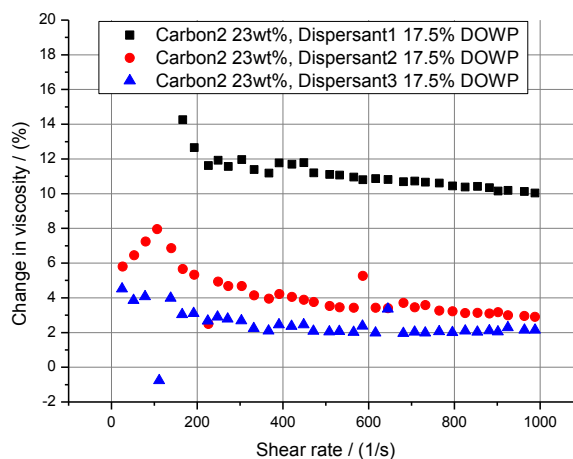


Figure 4-48: Change in viscosity during four weeks storage of the homogenised batch of the optimised dispersions of Carbon2 pigment.

The viscosity of Carbon2-Dispersant1 dispersion increased by approximately 11% (SD=0.88) while the increase in viscosity of Carbon2-Dispersant1-Binder1 inks was between 10-12% (approx.) as shown in Figure 4-49(a,b). The data shows a relatively weaker correlation between the increase in viscosity of Carbon2-Dispersant1-Binder3 and Carbon2-Dispersant1 dispersion. However, this difference is not significant enough to conclude that addition of Binder3 altered the state of dispersion of Carbon2 pigment. Similarly, as shown in Figure 4-50, small changes in the viscosity of Carbon2-Dispersant2-Binder1 and Carbon2-Dispersant2-Binder3 inks were recorded after four weeks of storage. This is in-line with the increase of 4.2% (SD=1.35) in the viscosity of binder-free Carbon2-Dispersant2 dispersion. The average increase of approximately 18% (SD=1.22) in the viscosity of ink prepared from Carbon2-Dispersant2 dispersion and 150% BOWP of Binder1 was not regarded as a clear indication of Binder1-induced changes in the state of dispersion of Carbon2 pigment. This is because the viscosity of the other two inks of this series virtually remained unchanged.

The results of viscosity stability analysis, presented in Figure 4-51, clearly indicated that in terms of viscosity the Carbon2-Dispersant3-Binder1 and Carbon2-Dispersant3-Binder3 inks were fairly stable, as was the binder-free Carbon2-Dispersant3 dispersion for which the average increase in viscosity was 2.4% (SD=0.88). In summary, the results of viscosity stability analysis of the binder-free dispersions of Carbon2 pigment and the finished inks prepared thereof from these dispersions were generally in good agreement and indicated that these formulations were very stable. The inks prepared by adding Binder2 are an exception.

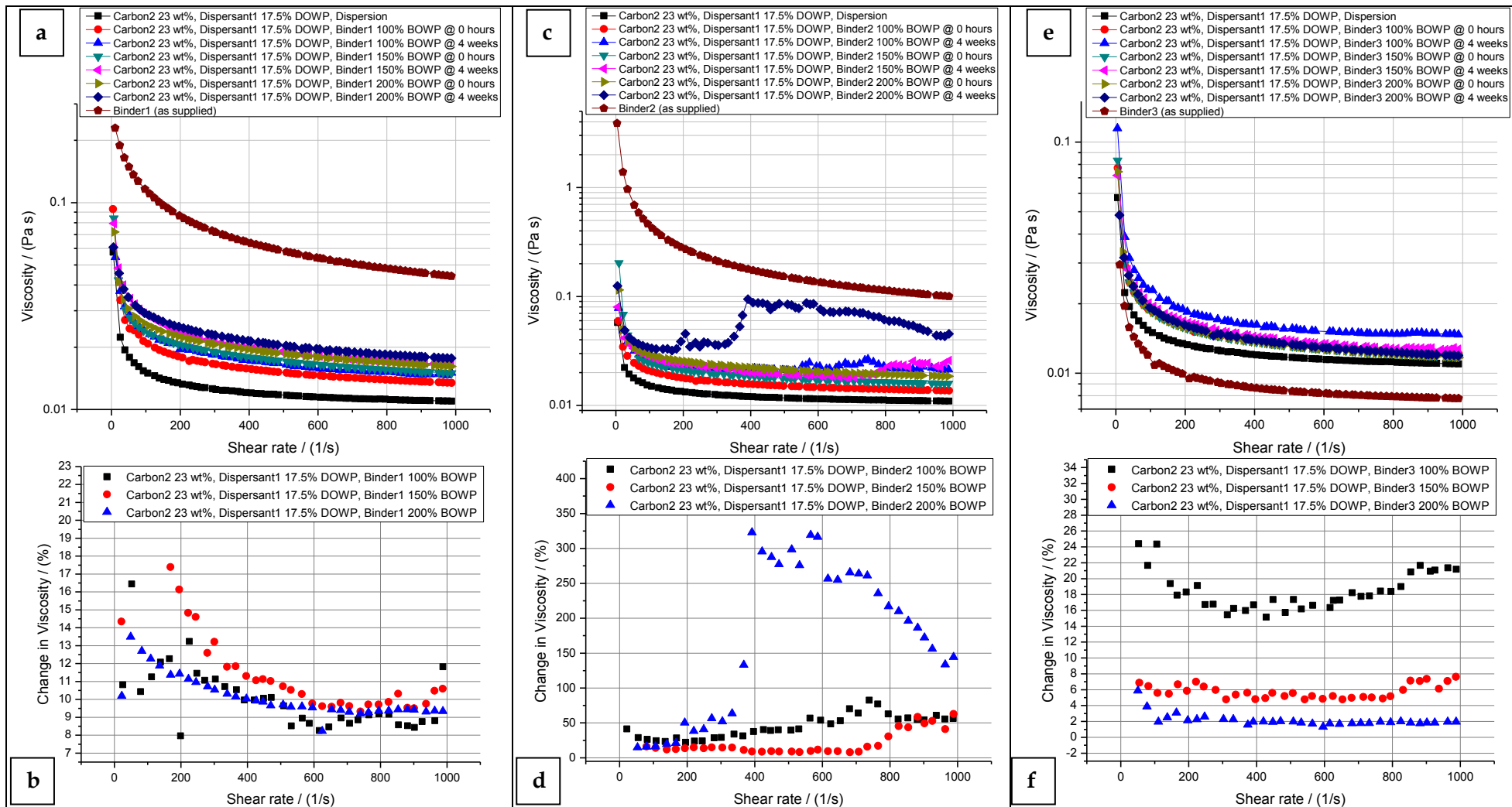


Figure 4-49: Viscosity stability of inks prepared by adding various amounts of (Binder1/Binder2/Binder3) in Carbon2-Dispersion1 dispersion.

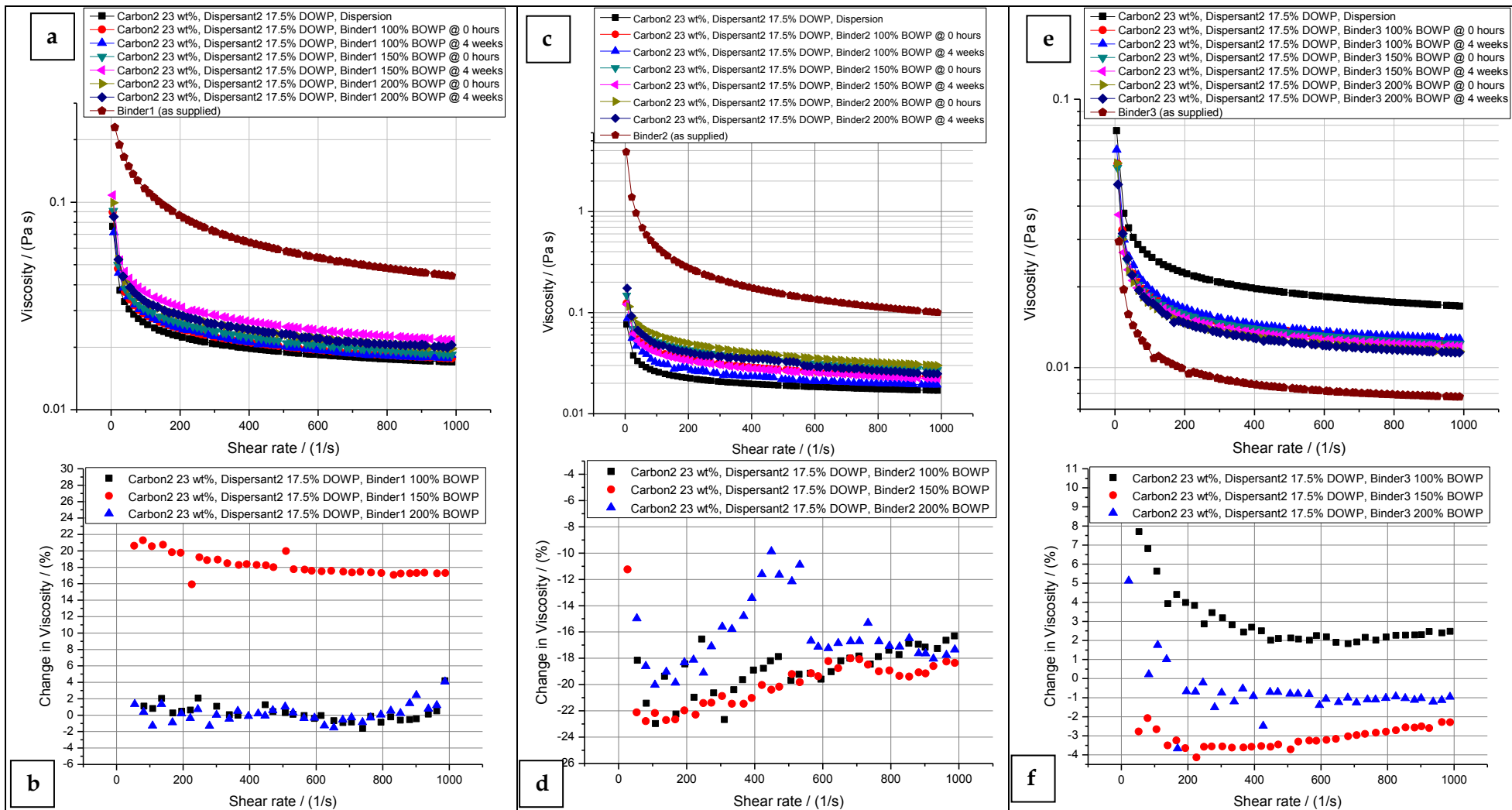


Figure 4-50: Viscosity stability of inks prepared by adding various amounts of Binder1/Binder2/Binder3 in Carbon2-Dispersant2 dispersion.

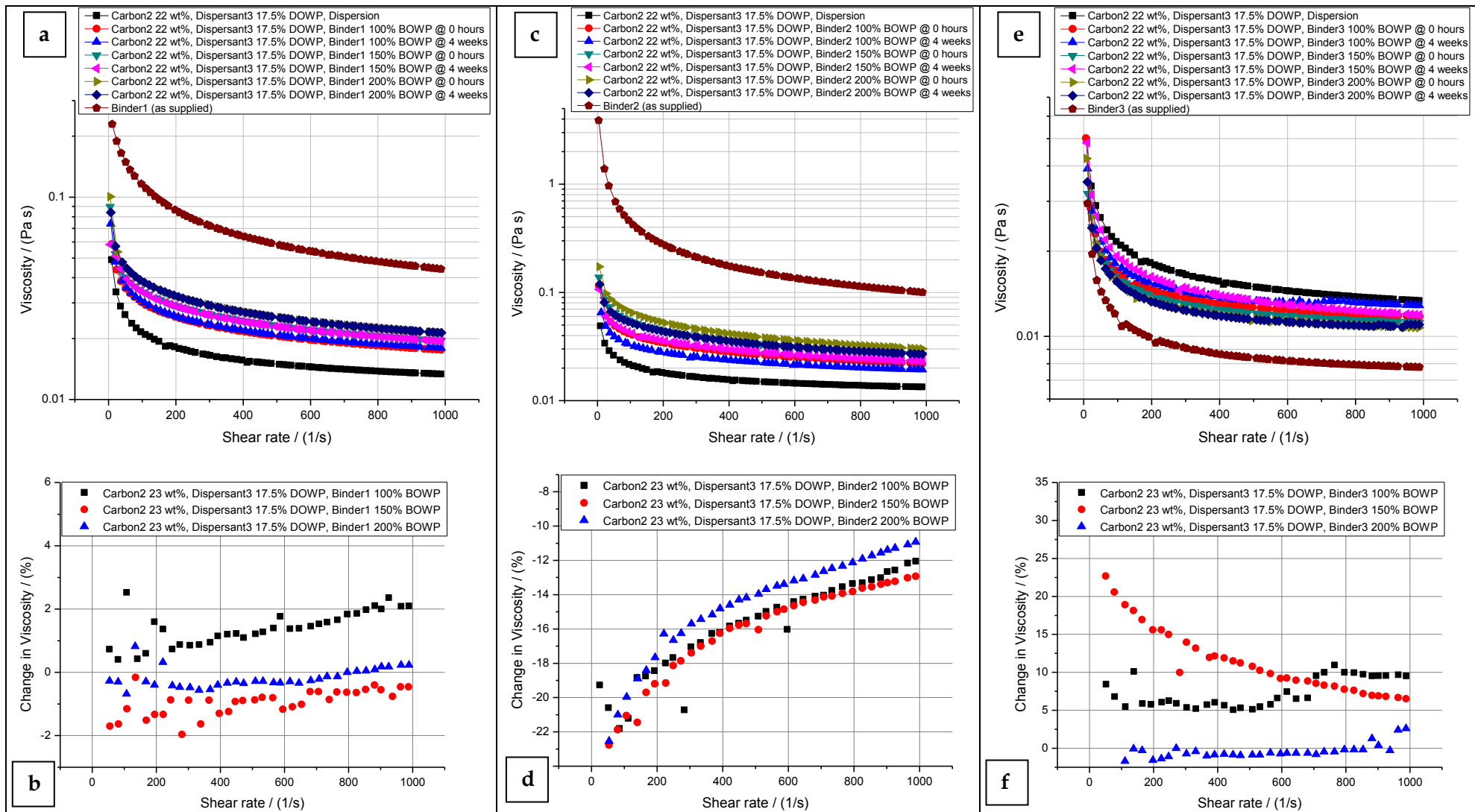


Figure 4-51: Viscosity stability of inks prepared by adding various amounts of Binder1/Binder2/Binder3 in Carbon2-Dispersant3 dispersion.

4.5.3.3 Viscosity stability of the inks prepared from the dispersions of Carbon3.

The viscosity of the inks prepared from Carbon3-Dispersant1 dispersion increased considerably after four weeks of storage (Figure 4-54). Generally, the increase in viscosity was smaller at higher shear rates. As depicted in Figure 4-52, a very similar trend of increase in the viscosity of binder-free Carbon3-Dispersant1 dispersion was recorded with the average increase being 42% (SD=8.89). This is in good agreement with the increase in the viscosity of the inks that were prepared from Carbon3-Dispersant1 dispersion (the exception is the ink prepared by adding 100% BOWP of Binder3). However, as in case of the inks prepared from dispersions of Carbon1 and Carbon2 pigments, the data did not provide a clear indication of a correlation between the amount of binder in the ink and the change in viscosity after storage.

In contrast to the inks prepared from Carbon3-Dispersant1 dispersions, the inks prepared from the Carbon3-Dispersant2 and Carbon3-Dispersant3 dispersions possessed considerably stable viscosity during storage, as shown in Figure 4-55 and Figure 4-56, respectively. This is in-line with the results of viscosity stability analysis of the Carbon3-Dispersant2 and Carbon3-Dispersant3 dispersions, which showed that virtually no change occurred in the viscosity of these dispersions after four weeks of storage. The average increase in the viscosity of the two dispersions is tabulated in Table 4-36. Little or no change in the viscosity or no deviation from shear thinning rheology was recorded, particularly for the inks prepared by adding Binder1/Binder3. The only exception was the ink containing Carbon3-Dispersant3 dispersion and 100% BOWP of Binder3, for which the average increase in the viscosity after storage was 46% (SD=1.17). This was not regarded as an indication of instability of the Carbon3-Dispersant3 dispersion after let-down with Binder3. This is because the viscosity of the other two inks of this pigment-dispersant-binder series virtually remained unchanged.

Table 4-36: Change in viscosity of Carbon3 pigment dispersions prepared using Dispersant2/Dispersant3.

Dispersion composition	Increase in viscosity (%)	
	Average	SD
Carbon3 11wt%, Dispersant2 155% DOWP	2.79	0.87
Carbon3 10.5wt%, Dispersant3 155% DOWP	1.05	0.29

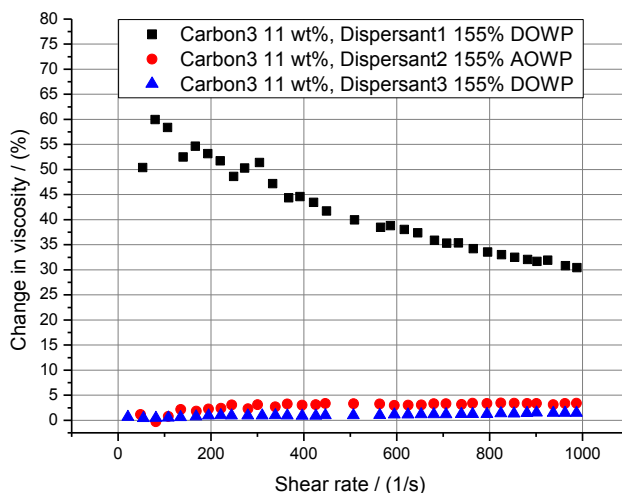


Figure 4-52: Change in viscosity during four weeks storage of the homogenised batch of the optimised dispersions of Carbon3 pigment.

The increase in viscosity of inks that were prepared by adding Binder2 in the Carbon3-Dispersant2 and Carbon3-Dispersant3, was relatively greater compared to the increase in the viscosity of the relevant binder-free dispersions. However, the difference is not large enough to establish that Binder2 altered the state of pigment dispersion in these formulations.

4.5.3.4 Viscosity stability of the inks prepared from the dispersions of Carbon4.

After four weeks of storage, a considerable increase in the viscosity of the inks prepared from Carbon4-Dispersant1 dispersions occurred, as shown in Figure 4-57. Generally, the magnitude of change in viscosity increased as the shear rate increased from 0 – 400 s⁻¹ (approx.). Above this range of the applied shear rate, the change in viscosity was relatively constant, generally. Except for the inks prepared by adding Binder3, the increase in viscosity of the inks prepared from Carbon4-Dispersant1 dispersion, particularly for the inks containing Binder2, was considerably greater compared to the average increase of 65% (SD=19.62) in the viscosity of binder-free Carbon4-Dispersant1 dispersion, as shown in Figure 4-53. The average increase in the viscosity of Binder3-containing inks was not significantly different from the increase in the viscosity of binder-free dispersion. However, the trend of change in viscosity of these inks could not be related to that in the binder-free dispersion. The data acquired in this study provided a rather clear indication that incorporation of binders, particularly Binder1/Binder2, resulted in a significant change in the viscosity of the Carbon4-Dispersant1 dispersion.

For the inks prepared by adding Binder1/Binder2 in the Carbon4-Dispersant2 dispersion, the results of viscosity stability analysis, which are presented in Figure 4-58, were found to correlate with the average change of -13.35% (SD=3) in the viscosity of the binder-free dispersion. The general trend was that the magnitude of change (reduction) in the viscosity of inks decreased as shear rate was increased from 0 - 200 s⁻¹ (approx.). As shear rate increased from 200 - 1000 s⁻¹, the viscosity again decreased by as much as 20% (approx.). The viscosity of Carbon4-Dispersant2-Binder3 inks did not decrease after storage. However, the trend of change in viscosity was in-line with that observed for the binder-free pigment dispersion.

The average increase in the viscosity of Carbon4-Dispersant3 dispersion after four weeks of storage, was 6.4% (SD=1.21). The viscosity profiles recorded after preparation and after four weeks of storage of the inks containing Carbon4-Dispersant3 dispersion are presented in Figure 4-59. Except for the inks containing Binder3, the average increase in the viscosity of these inks was generally much larger compared to the average increase in the viscosity of the binder-free Carbon4-Dispersant3 dispersion. However it was noticed that the inks maintained a smooth shear thinning rheology after storage, generally.

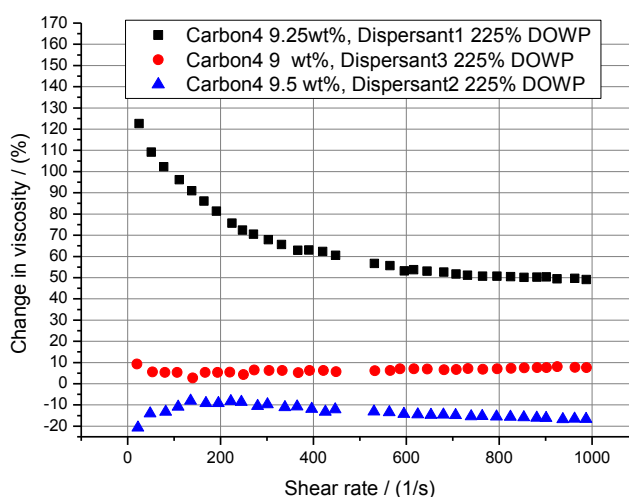


Figure 4-53: Change in viscosity during four weeks storage of the homogenised batch of the optimised dispersions of Carbon4 pigment.

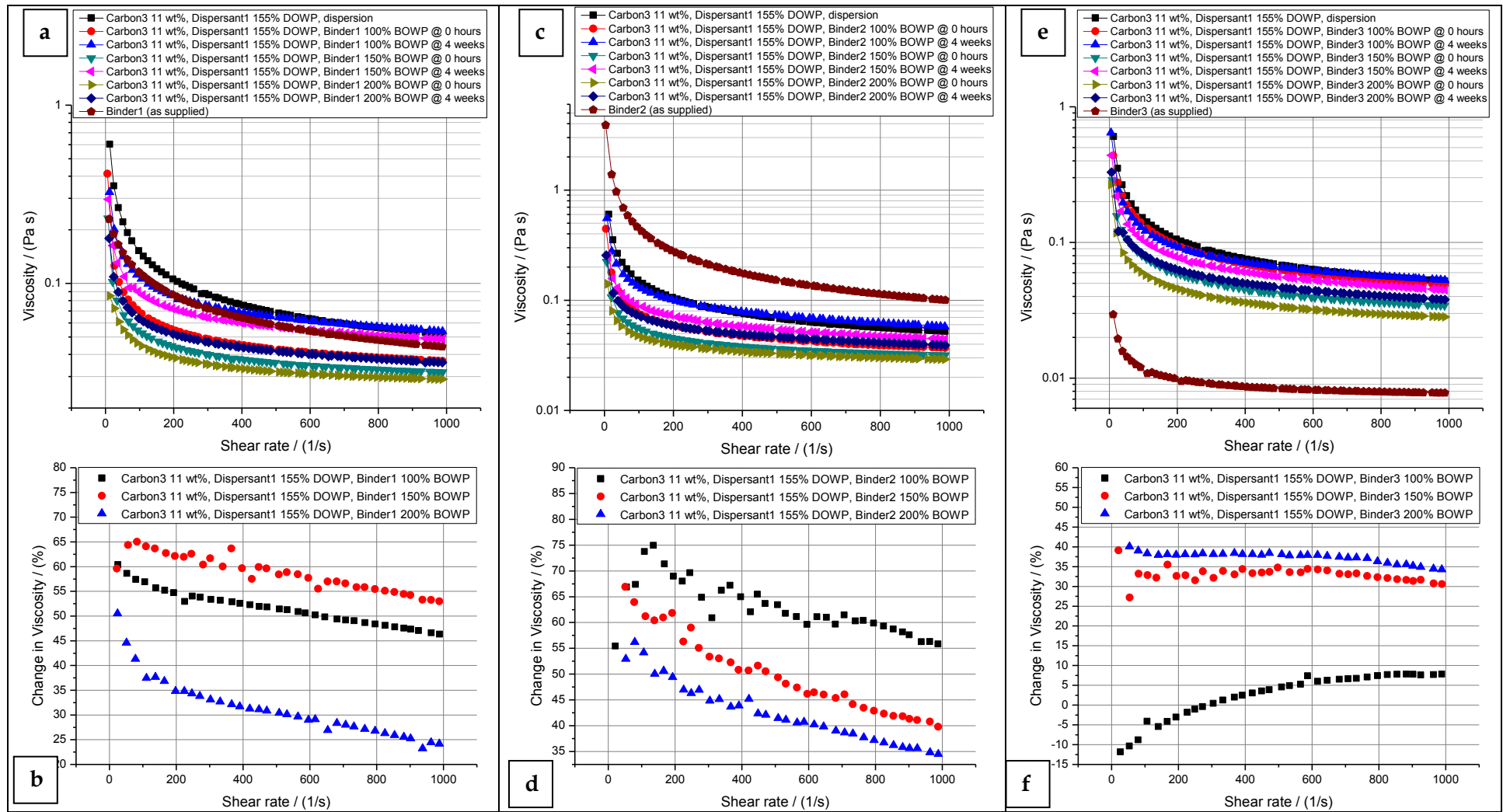


Figure 4-54: Viscosity stability of inks prepared by adding various amounts of Binder1/Binder2/Binder3 in Carbon3-Dispersant1 dispersion.

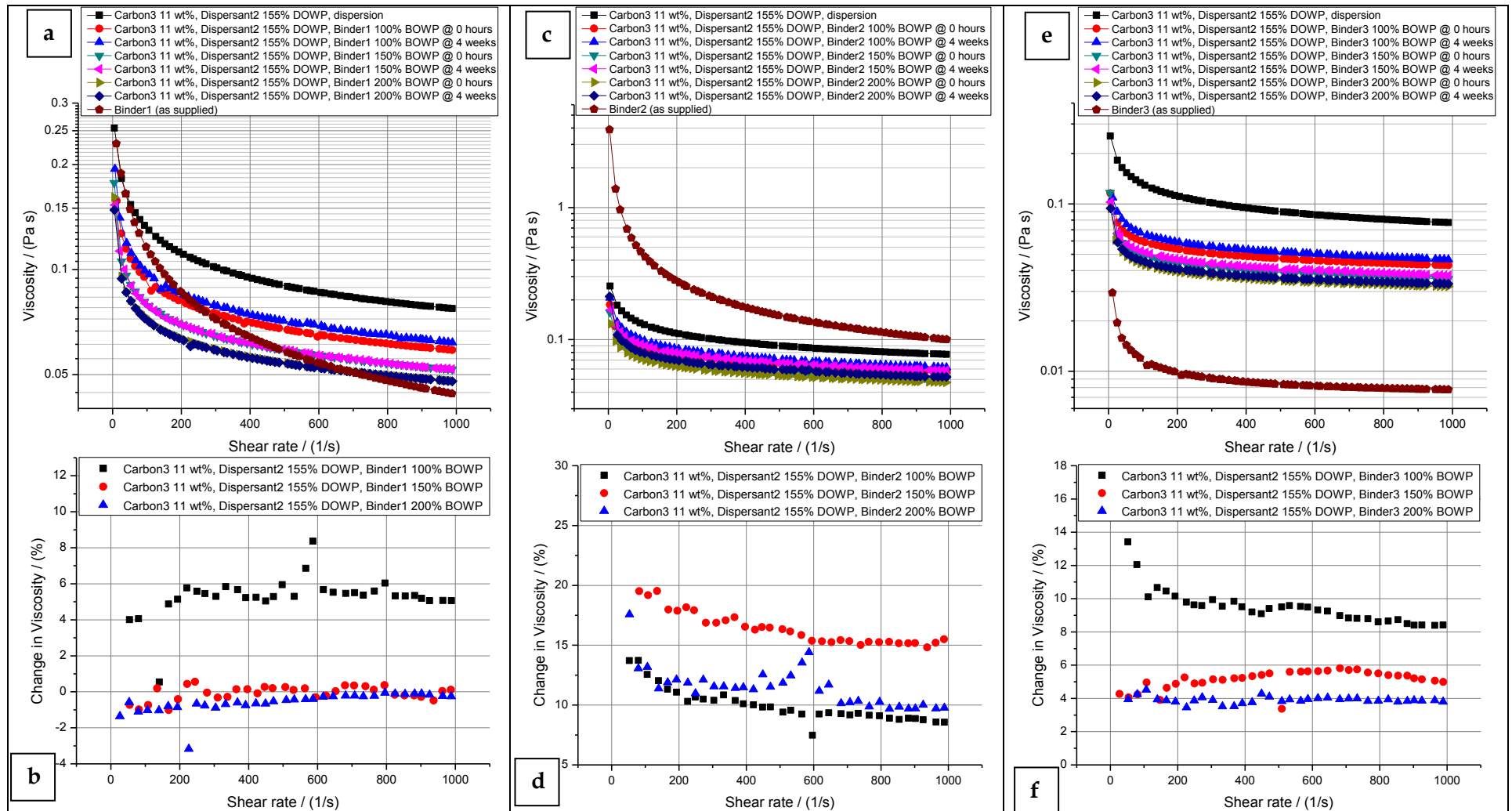


Figure 4-55: Viscosity stability of inks prepared by adding various amounts of Binder1/Binder2/Binder3 in Carbon3-Dispersant2 dispersion.

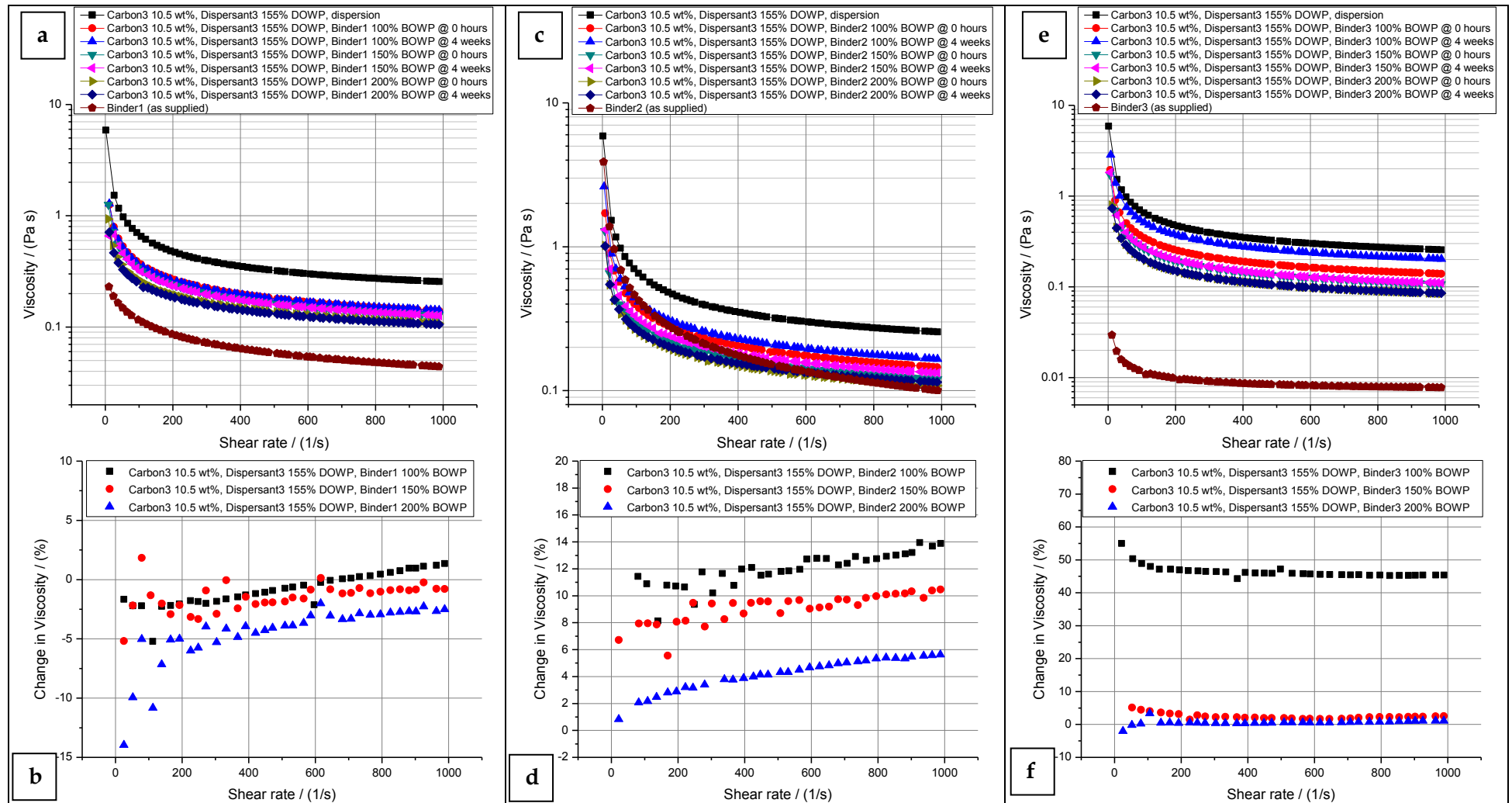


Figure 4-56: Viscosity stability of inks prepared by adding various amounts of Binder1/Binder2/Binder3 in Carbon3-Dispersant3 dispersion.

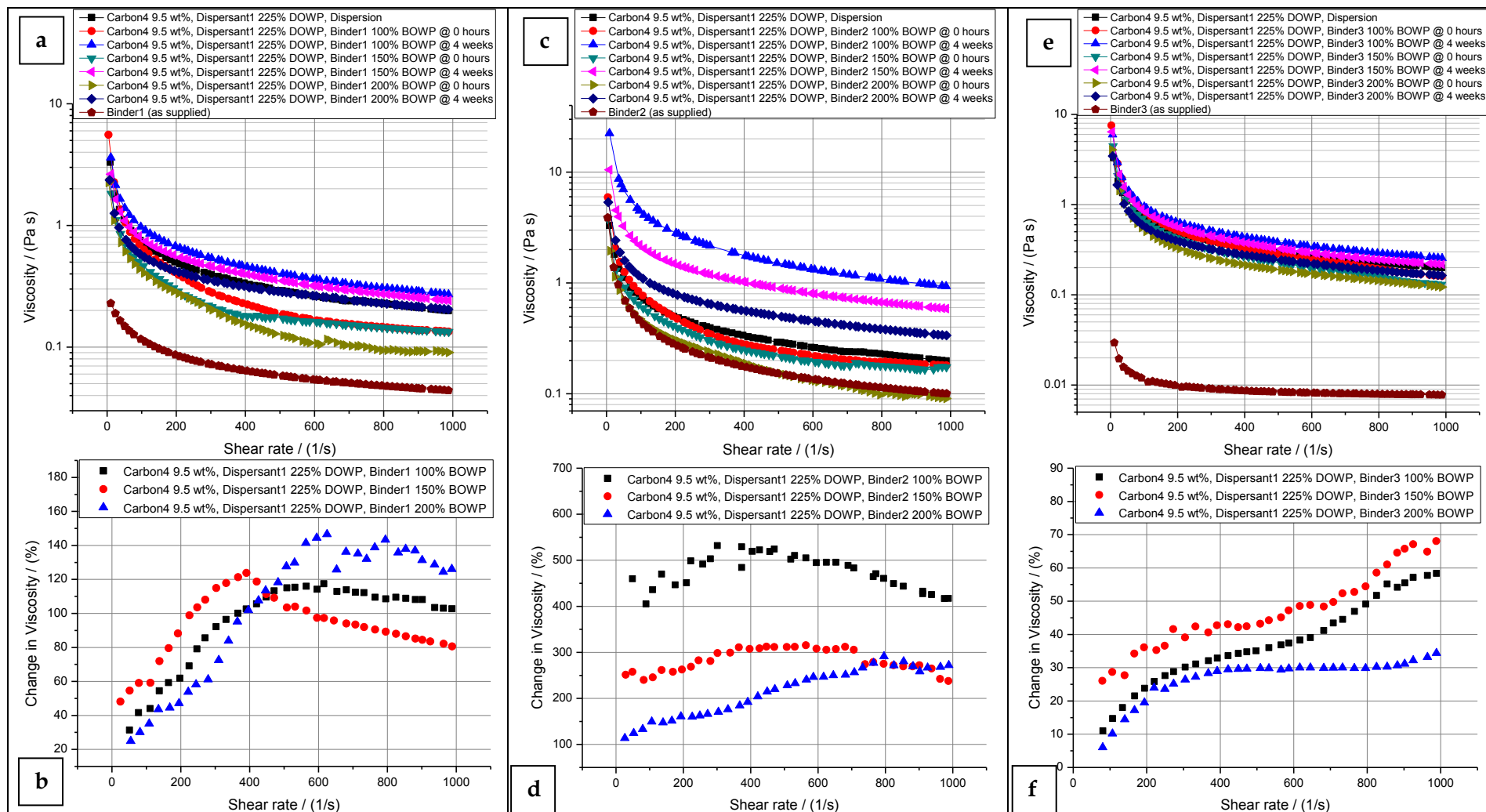


Figure 4-57: Viscosity stability of inks prepared by adding various amounts of Binder1/Binder2/Binder3 in Carbon4-Dispersant1 dispersion.

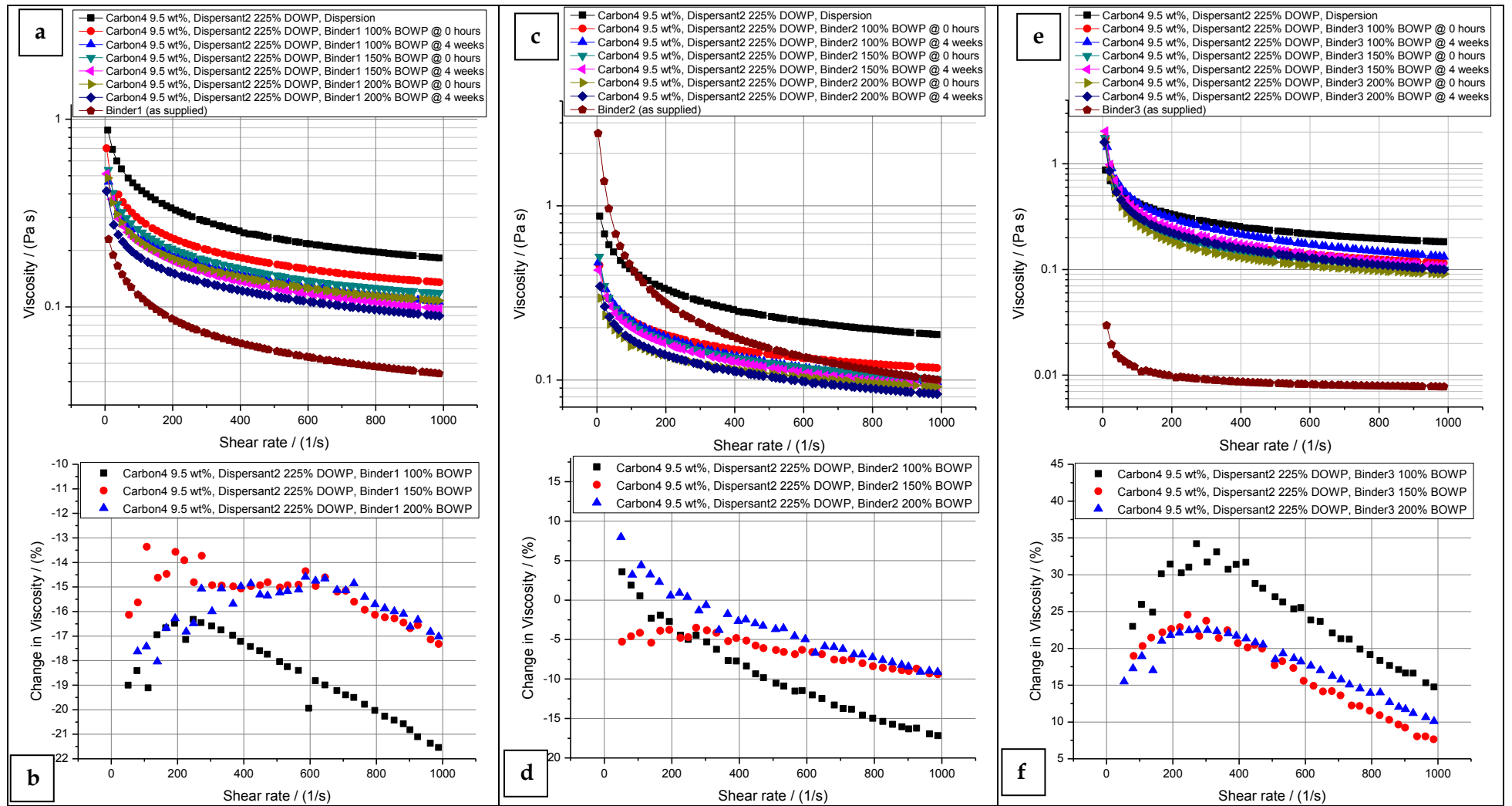


Figure 4-58: Viscosity stability of inks prepared by adding various amounts of Binder1/Binder2/Binder3 in Carbon4-Dispersant2 dispersion.

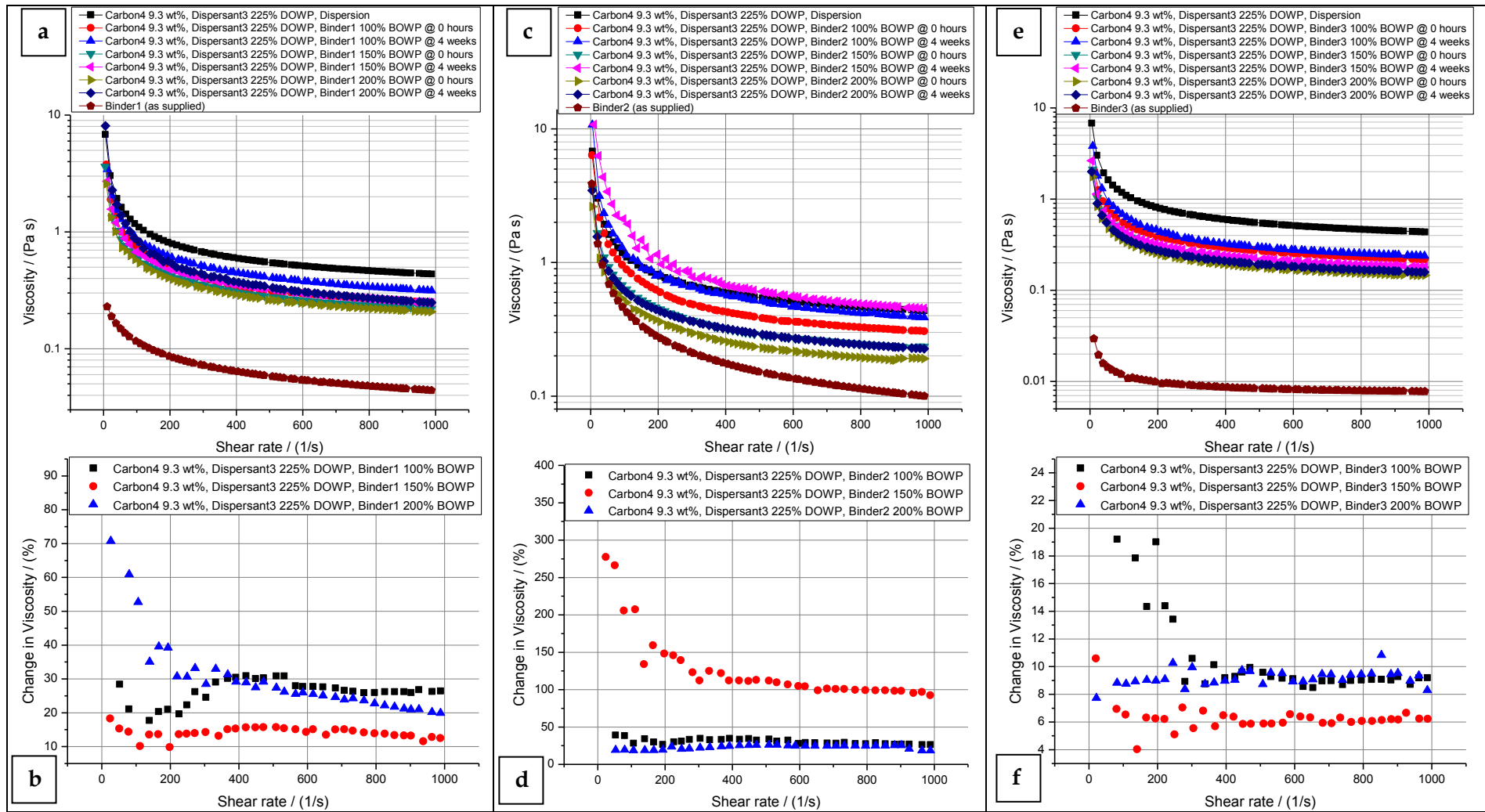


Figure 4-59: Viscosity stability of inks prepared by adding various amounts of Binder1/Binder2/Binder3 in Carbon4-Dispersant3 dispersion.

4.5.4 Electrical characteristics of finished inks

Following the let-down viscosity stability tests, the surface resistivity of ink films was recorded. The procedure for this is described in detail in Section 2.3.3.2. For surface resistivity measurements, the inks were printed onto paperboard substrate instead of textile fabrics. As described in Section 2.1.6.1, the paperboard substrate is designed by the manufacturer to provide uniform ink absorption. Thus, the use of this substrate facilitated the exclusion of the effects of substrate-dependent variations, such as non-uniform absorption/penetration of ink and a corresponding variation in the thickness of the dried ink layer. The objectives of this study can be summarised as follows.

- Identification of inks which possessed very high surface resistivity.
- Estimation of optimum binder solids content in the inks for printing onto textile substrates.
- Evaluation of the effects of increasing the thickness of ink deposit on the surface resistivity.

The following general patterns were observed among the data presented in Table 4-37 - Table 4-40.

- The surface resistivity of ink film increased as the binder solids content was increased in the formulation. This expected pattern was consistent in all of the inks formulated from both the low surface area and the high surface area pigments.
- In case of the low surface area pigments, the surface resistivity of the drawdowns of inks prepared by adding Binder3 was higher at any given binder solids content compared to that of the drawdowns of the inks of the same pigment dispersion but containing Binder1/Binder2.
- In case of the inks formulated from dispersions of high surface area pigments, no clear correlation between the surface resistivity and the binder used in let-down was observed.
- A significant decrease in the surface resistivity of ink film was observed as the number of ink layers was increased.

The solids content in each of the three binders that were used in the let-down stage was 40 wt%. Thus, as the binder solids content was increased in pigment dispersion, the amount of pigment in a given mass of the resulting ink decreased. The relevant calculations are provided in Appendix A. Since the electrical conductivity is heavily dependent on the amount of conductive pigment in an ink, a sharp increase in the surface resistivity was observed as the amount of binder was increased. This expected trend was consistent in all of the inks formulated from the dispersions of low surface area pigments and as well as the high surface area pigments.

At any given binder loading, the surface resistivity of the drawdowns of inks containing Binder3 was higher compared to that of the drawdowns of the inks containing Binder1/Binder2. This is valid only for the inks prepared from the dispersions of low surface area pigments. In contrast, in case of the inks formulated from the dispersions of high surface area pigments, a clear correlation between the surface resistivity and the binder used in let-down was not observed. In addition, the viscosity stability analyses that are presented in previous section did not indicate that the Binder3-containing inks prepared from a pigment dispersion was always less stable compared to the Binder1-/Binder2-containing inks prepared from the same pigment dispersion. Therefore, the inks containing Binder3 were not excluded from further testing. It was noticed that part of the observed difference between the surface resistivity of films of inks that were formulated by adding different binders in a pigment dispersion could be due to slightly different ink film thicknesses. However, characterisation of ink film thickness using SEM or other relevant analytical techniques was not carried out due to the high cost associated with such a large number of samples. Furthermore, such variations (if present), were not expected to be very significant. This is because the solids content was similar in the inks prepared by adding a certain amount of various binders in a pigment dispersion.

On the basis of the analysis presented in this section, all of the inks containing 100% binder solids on the weight of pigment were considered for further testing.

Table 4-37: Surface resistivity of the films of inks produced from Carbon1 pigment dispersions.

Ink composition		Surface resistivity (Ω/\square)			
		Air dried			Cured
		1 layer	2 layers	3 layers	3 layers
Carbon1 31 wt%, Dispersant1 15% DOWP	Binder1 100% BOWP	508	257	193	182
	Binder1 150% BOWP	814	432	302	313
	Binder1 200% BOWP	900	525	337	408
Carbon1 31 wt%, Dispersant1 15% DOWP	Binder2 100% BOWP	527	240	153	160
	Binder2 150% BOWP	882	372	228	241
	Binder2 200% BOWP	1051	450	330	359
Carbon1 31 wt%, Dispersant1 15% DOWP	Binder3 100% BOWP	700	441	281	291
	Binder3 150% BOWP	156	600	529	541
	Binder3 200% BOWP	3143	1634	1688	1600
Carbon1 31 wt%, Dispersant2 15% DOWP	Binder1 100% BOWP	580	327	225	227
	Binder1 150% BOWP	901	489	330	358
	Binder1 200% BOWP	1118	688	452	492
Carbon1 31 wt%, Dispersant2 15% DOWP	Binder2 100% BOWP	606	259	134	149
	Binder2 150% BOWP	843	338	241	252
	Binder2 200% BOWP	1238	584	436	473
Carbon1 31 wt%, Dispersant2 15% DOWP	Binder3 100% BOWP	584	347	297	295
	Binder3 150% BOWP	1970	1119	1065	1045
	Binder3 200% BOWP	4790	3615	4294	3840
Carbon1 31 wt%, Dispersant3 15% DOWP	Binder1 100% BOWP	650	380	245	224
	Binder1 150% BOWP	934	478	332	341
	Binder1 200% BOWP	1611	923	701	705
Carbon1 31 wt%, Dispersant3 15% DOWP	Binder2 100% BOWP	613	278	195	194
	Binder2 150% BOWP	904	457	333	367
	Binder2 200% BOWP	1940	1055	782	830
Carbon1 31 wt%, Dispersant3 15% DOWP	Binder3 100% BOWP	643	368	275	276
	Binder3 150% BOWP	1450	963	917	804
	Binder3 200% BOWP	3531	2065	2160	2026

Table 4-38: Surface resistivity of the films of inks produced from Carbon2 pigment dispersions.

Ink composition		Surface resistivity (Ω/\square)			
		Air dried			Cured
		1 layer	2 layers	3 layers	3 layers
Carbon2 23 wt%, Dispersant1 17.5% DOWP	Binder1 100% BOWP	745	349	210	210
	Binder1 150% BOWP	935	474	303	310
	Binder1 200% BOWP	1223	696	455	462
Carbon2 23 wt%, Dispersant1 17.5% DOWP	Binder2 100% BOWP	635	295	196	197
	Binder2 150% BOWP	873	402	282	265
	Binder2 200% BOWP	1143	577	358	405
Carbon2 23 wt%, Dispersant1 17.5% DOWP	Binder3 100% BOWP	1008	446	299	299
	Binder3 150% BOWP	1290	723	395	401
	Binder3 200% BOWP	2359	1255	986	1072
Carbon2 23 wt%, Dispersant2 17.5% DOWP	Binder1 100% BOWP	583	318	217	212
	Binder1 150% BOWP	811	406	275	284
	Binder1 200% BOWP	980	474	330	363
Carbon2 23 wt%, Dispersant2 17.5% DOWP	Binder2 100% BOWP	439	242	163	176
	Binder2 150% BOWP	554	305	205	220
	Binder2 200% BOWP	806	439	314	340
Carbon2 23 wt%, Dispersant2 17.5% DOWP	Binder3 100% BOWP	607	346	258	262
	Binder3 150% BOWP	946	562	403	455
	Binder3 200% BOWP	1798	1030	791	1006
Carbon2 22 wt%, Dispersant3 17.5% DOWP	Binder1 100% BOWP	578	318	223	199
	Binder1 150% BOWP	822	443	308	310
	Binder1 200% BOWP	1172	675	514	506
Carbon2 22 wt%, Dispersant3 17.5% DOWP	Binder2 100% BOWP	512	262	181	175
	Binder2 150% BOWP	1135	483	311	331
	Binder2 200% BOWP	1307	745	523	560
Carbon2 22 wt%, Dispersant3 17.5% DOWP	Binder3 100% BOWP	540	308	209	201
	Binder3 150% BOWP	1110	694	528	504
	Binder3 200% BOWP	2100	1165	881	907

Table 4-39: Surface resistivity of the films of inks produced from Carbon3 pigment dispersions.

Ink composition		Surface resistivity (Ω/\square)			
		Air dried			Cured
		1 layer	2 layers	3 layers	3 layers
Carbon3 11 wt%, Dispersant1 155% DOWP	Binder1 100% BOWP	742	397	262	252
	Binder1 150% BOWP	915	515	398	360
	Binder1 200% BOWP	1295	780	550	508
Carbon3 11 wt%, Dispersant1 155% DOWP	Binder2 100% BOWP	737	397	276	262
	Binder2 150% BOWP	1085	545	360	340
	Binder2 200% BOWP	1195	662	515	472
Carbon3 11 wt%, Dispersant1 155% DOWP	Binder3 100% BOWP	962	480	331	297
	Binder3 150% BOWP	1198	782	534	500
	Binder3 200% BOWP	1776	1168	885	789
Carbon3 11 wt%, Dispersant2 155% DOWP	Binder1 100% BOWP	567	318	242	221
	Binder1 150% BOWP	835	528	388	374
	Binder1 200% BOWP	1505	802	572	530
Carbon3 11 wt%, Dispersant2 155% DOWP	Binder2 100% BOWP	558	318	263	239
	Binder2 150% BOWP	770	482	378	337
	Binder2 200% BOWP	1034	632	494	440
Carbon3 11 wt%, Dispersant2 155% DOWP	Binder3 100% BOWP	702	380	317	298
	Binder3 150% BOWP	1070	655	530	464
	Binder3 200% BOWP	1327	914	691	572
Carbon3 10.5 wt%, Dispersant3 155% DOWP	Binder1 100% BOWP	620	368	268	252
	Binder1 150% BOWP	791	463	342	323
	Binder1 200% BOWP	1168	701	461	417
Carbon3 10.5 wt%, Dispersant3 155% DOWP	Binder2 100% BOWP	557	312	218	219
	Binder2 150% BOWP	855	510	346	332
	Binder2 200% BOWP	1040	627	435	414
Carbon3 10.5 wt%, Dispersant3 155% DOWP	Binder3 100% BOWP	487	294	209	206
	Binder3 150% BOWP	768	492	350	324
	Binder3 200% BOWP	1180	755	553	465

Table 4-40: Surface resistivity of the films of inks produced from Carbon4 pigment dispersions.

Ink composition		Surface resistivity (Ω/\square)			
		Air dried			Cured
		1 layer	2 layers	3 layers	3 layers
Carbon4 9.5 wt%, Dispersant1 225% DOWP	Binder1 100% BOWP	853	586	305	283
	Binder1 150% BOWP	988	514	366	320
	Binder1 200% BOWP	1062	640	435	341
Carbon4 9.5 wt%, Dispersant1 225% DOWP	Binder2 100% BOWP	610	332	286	276
	Binder2 150% BOWP	838	487	369	321
	Binder2 200% BOWP	1144	602	415	360
Carbon4 9.5 wt%, Dispersant1 225% DOWP	Binder3 100% BOWP	782	436	247	223
	Binder3 150% BOWP	976	477	338	225
	Binder3 200% BOWP	1216	662	417	353
Carbon4 9.5 wt%, Dispersant2 225% DOWP	Binder1 100% BOWP	650	316	253	250
	Binder1 150% BOWP	881	410	385	368
	Binder1 200% BOWP	1173	551	438	371
Carbon4 9.5 wt%, Dispersant2 225% DOWP	Binder2 100% BOWP	813	370	367	255
	Binder2 150% BOWP	836	395	302	270
	Binder2 200% BOWP	1213	580	450	424
Carbon4 9.5 wt%, Dispersant2 225% DOWP	Binder3 100% BOWP	628	324	268	246
	Binder3 150% BOWP	870	468	359	312
	Binder3 200% BOWP	1092	583	486	434
Carbon4 9.3 wt%, Dispersant3 225% DOWP	Binder1 100% BOWP	849	441	330	306
	Binder1 150% BOWP	930	601	426	392
	Binder1 200% BOWP	1197	804	500	474
Carbon4 9.3 wt%, Dispersant3 225% DOWP	Binder2 100% BOWP	680	466	323	285
	Binder2 150% BOWP	862	394	302	281
	Binder2 200% BOWP	1270	604	434	425
Carbon4 9.3 wt%, Dispersant3 225% DOWP	Binder3 100% BOWP	653	461	284	275
	Binder3 150% BOWP	863	554	404	381
	Binder3 200% BOWP	1222	790	580	506

4.6 Printing of formulated inks on textile substrates and subsequent testing

4.6.1 Selection of binders for the primer coating of textile substrates

Woven textile fabrics generally offer an uneven surface for the deposition of inks and coatings. Should there be any discontinuities and non-uniformities in the deposited ink layer, caused by the porous and uneven surface of the textile fabric, there can be a significant impairment of the electrical conductivity of the ink layer. Coating a fabric with a polymeric binder, to form a primer layer, results in a smoother fabric surface

which can considerably improve the desired functionality, i.e., electrical conductivity, of the ink deposit.

The characteristics of a binder primer layer depend on the properties of the binder and on the methods of its delivery and fixation. The primer layer application process can have significant influence on the properties of the primer layer. For instance, if the binder primer layer was applied by padding the fabric with a polymeric binder formulation, the padding pressure could considerably influence the wet pick-up by the fabric which in turn would affect the morphology and the performance of the final primer layer. For a particular fabric substrate, the effects of padding pressure can be summarised as follows.

- Increasing the padding pressure reduces the wet pick-up by the fabric. This is because higher padding pressure squeezes out a larger amount of binder from the fabric. Thus, the amount of binder left to cover the interstices in the fabric structure is reduced.
- In contrast, low padding pressure is more likely to produce a smooth primer layer because it leaves a large amount of binder in the fabric structure. However, if the pressure is insufficient to achieve optimum penetration of the binder into the fabric structure, it will result in a weakly adhering primer layer. This is because of the lack of mechanical bonding between the primer layer and the fabric.

The three binders (Table 2-3) used in this study for the let-down of pigment dispersions are claimed, by the producers of these binders, to be suitable for use as primer layer on textile substrates. In order to keep the number of test samples within a manageable range, experiments were conducted to select only one binder for primer coating of the fabric substrates. The selection of binder was made on the basis of the results of the following analyses carried out on the primer layers of the three binders.

- Morphology of the primer layers was analysed using SEM. The binder producing a smoother film and covering the capillaries and pores in the fabric structure to a greater extent compared to other binders was considered as a more suitable binder.

- The durability of the primer layers was tested by washing the primer coated fabrics. This test was considered important because a binder can produce a smooth but weak primer layer which is easily deteriorated, for instance, in a washing cycle. If binder primer layer is removed from the fabric surface, it carries away the ink film that adheres to it. Thus, a weakly bonded primer layer is likely to result in an under-performing ink layer.

To conduct the above mentioned analyses, both the 100% cotton and 100% polyester fabrics were padded with each of the three binders. The padding pressure was varied to alter the wet pick up of the fabrics, as tabulated in Table 4-41. The experimental procedure is described in detail in Section 2.4.1. As expected, the wet pick-up of both the cotton fabric and the polyester fabric decreased as the padding pressure was increased.

Table 4-41: Wet pick up of fabrics at different padding pressures.

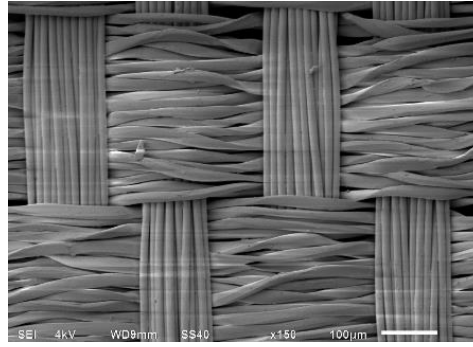
Binder	Substrate	Padding pressure (kPa)	Weight of fabric (g)		Wet pick up (%)
			Unpadded	Padded	
Binder1	Cotton	60	2.37	3.96	67.08
		100	2.34	3.89	66.24
		150	2.4	3.96	65.00
	Polyester	60	1.15	1.95	69.57
		100	1.11	1.68	51.35
		150	1.15	1.7	47.83
Binder2	Cotton	60	2.41	4.44	84.23
		100	2.43	4.25	74.90
		150	2.36	4.04	71.19
	Polyester	60	1.14	1.92	68.42
		100	1.13	1.72	52.21
		150	1.11	1.68	51.35
Binder3	Cotton	60	2.43	4.53	86.42
		100	2.4	4.2	75.00
		150	2.4	4	66.67
	Polyester	60	1.11	1.94	74.77
		100	1.13	1.76	55.75
		150	1.3	1.65	26.92

The padded fabrics were air dried and cured followed by washing as per the Test number C15 of the BS EN ISO 105:C06 standard method. In Figure 4-60 - Figure 4-65, SEM micrographs of the unwashed primer layers and washed primer layers of different binders are presented and the areas from which the primer layers detached after washing are highlighted. The analysis of the micrographs is summarised as follows.

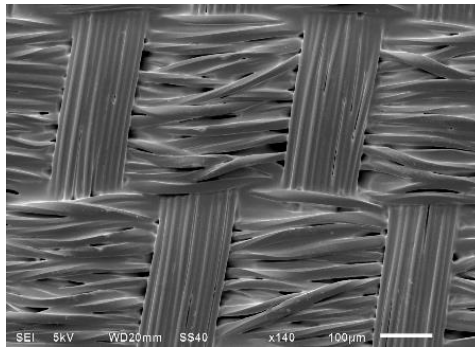
- Lower padding pressure resulted in deposition of a large amount of binder on the surface of the fabric substrates, thus covering the pores and interstices to a greater extent. It was also observed that in contrast to the primer layers on cotton fabric, the effects of changing the padding pressure were less pronounced in the primer layers produced on polyester fabric. This can be attributed to the generally low binder uptake of the Polyester fabric due to low absorbency, low density of the structure and low thickness of this fabric.
- The binders produced smooth primer layers, as observed in the micrographs of unwashed fabrics. The washing tests, however, indicated that Binder3 produced stronger primer layers compared to the primer layers produced by Binder1/Binder2. There was virtually no deterioration in the condition of the primer layers of Binder3 produced on both the cotton and polyester fabrics. In contrast, a considerable increase in the surface roughness and loss of adhesion was observed in the primer layers of Binder1 and Binder2 after only one wash cycle. The highlighted areas in Figure 4-60 - Figure 4-65 show that the Binder1/Binder2 primer layers were completely removed from large areas of both the cotton fabric and the polyester fabric.

Thus, on the basis of the analysis presented above, Binder3 was selected for primer coating of both the cotton and polyester fabrics. An intermediate padding pressure of 100 kPa, which gave sufficiently smooth primer layers on both cotton (Figure 4-65) and polyester (Figure 4-64) fabrics, was used for preparation of coated fabric substrates.

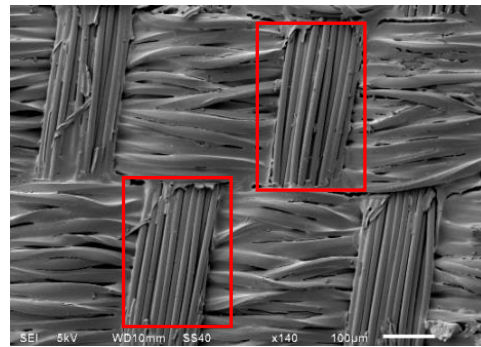
This space is deliberately left blank due to pagination.



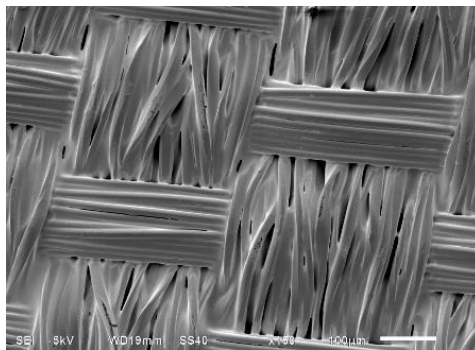
(a) Unpadded polyester fabric

Unwashed fabrics**Washed fabrics**

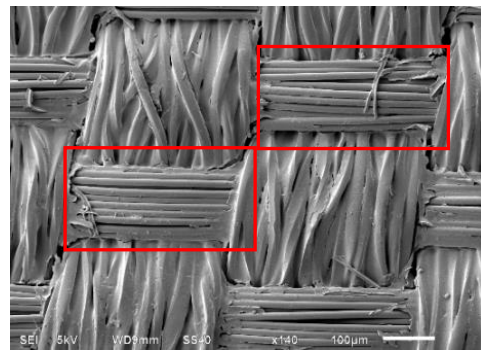
(b) 60 kPa



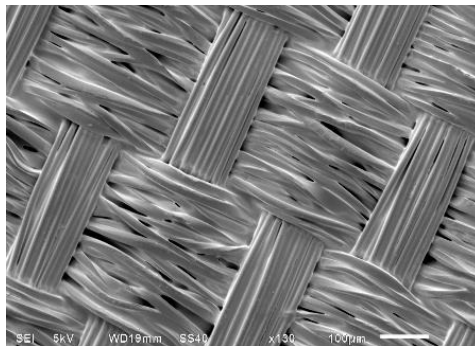
(c) 60 kPa



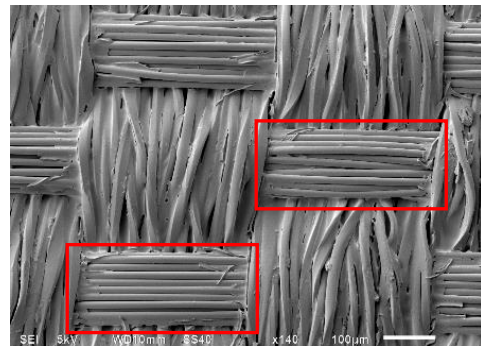
(d) 100 kPa



(e) 100 kPa

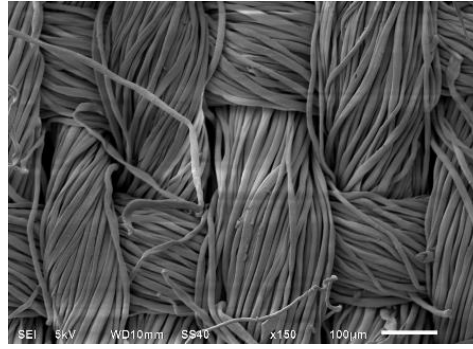


(f) 150 kPa

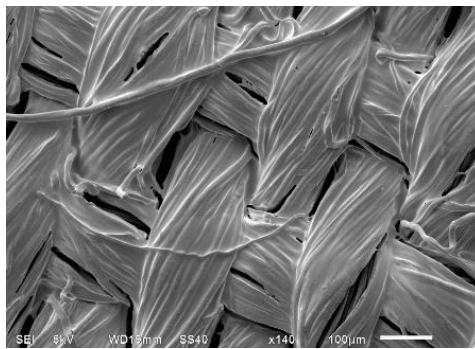


(g) 150 kPa

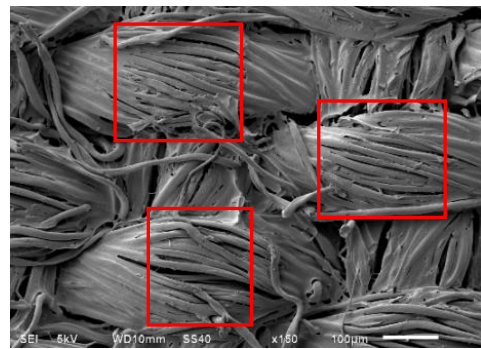
Figure 4-60: Micrographs of 100% polyester fabric padded with Binder1 at various padder pressure settings.



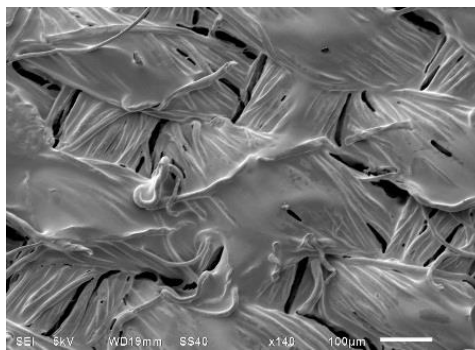
(a) Unpadded cotton fabric

Unwashed fabrics**Washed fabrics**

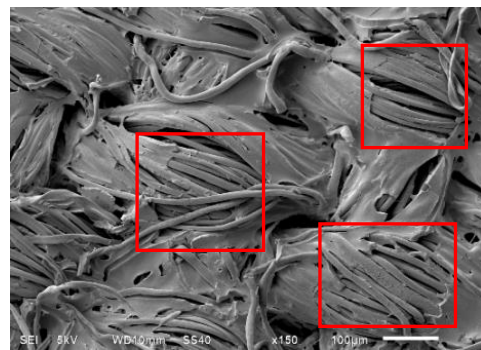
(b) 60 kPa



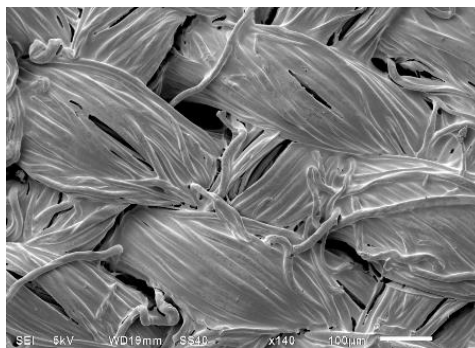
(c) 60 kPa



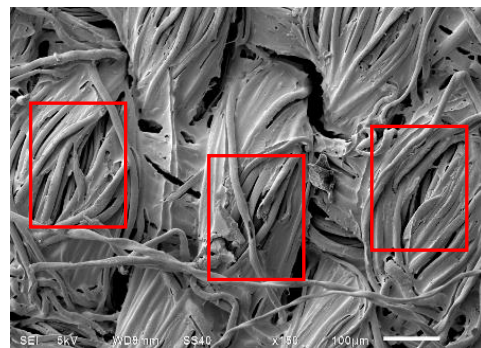
(d) 100 kPa



(e) 100 kPa

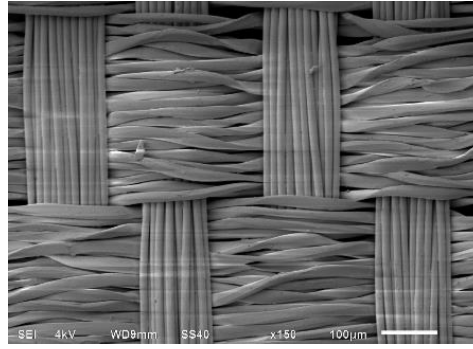


(f) 150 kPa



(g) 150 kPa

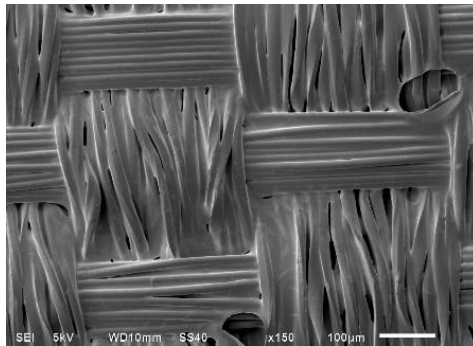
Figure 4-61: Micrographs of 100% cotton fabric padded with Binder1 at various padder pressure settings.



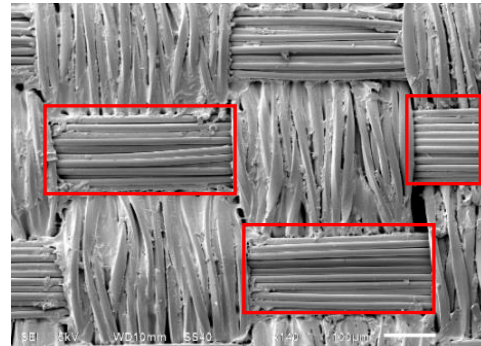
(a) Unpadded polyester fabric

Unwashed fabrics

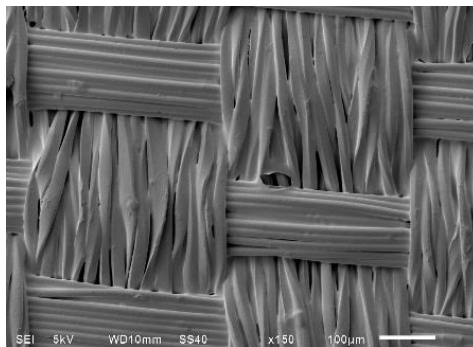
Washed fabrics



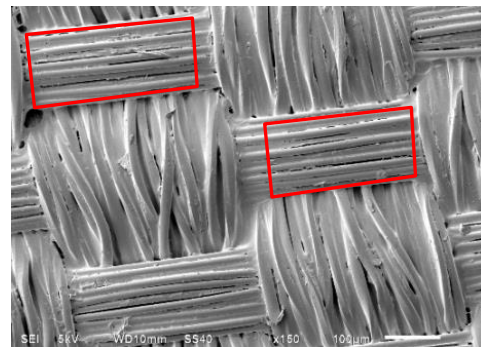
(b) 60 kPa



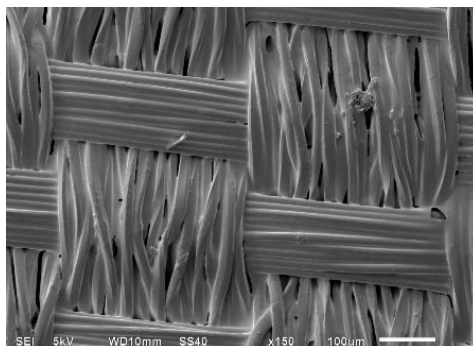
(c) 60 kPa



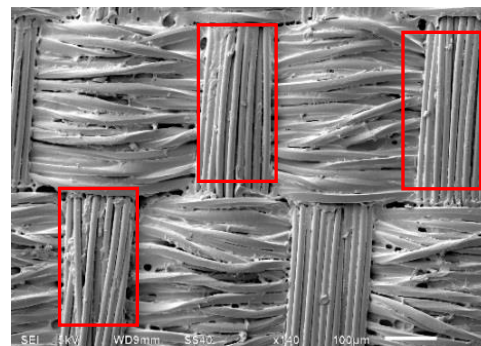
(d) 100 kPa



(e) 100 kPa

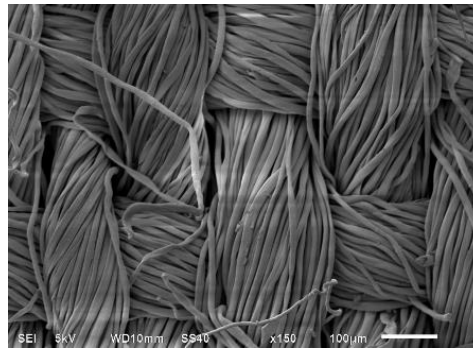


(f) 150 kPa



(g) 150 kPa

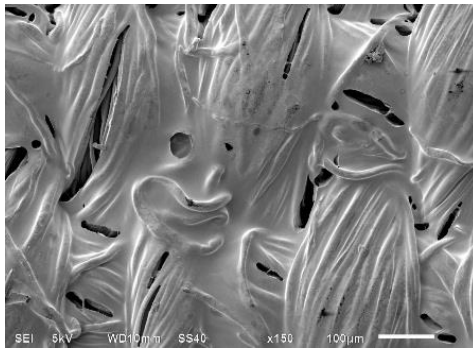
Figure 4-62: Micrographs of 100% polyester fabric padded with Binder2 at various padder pressure settings.



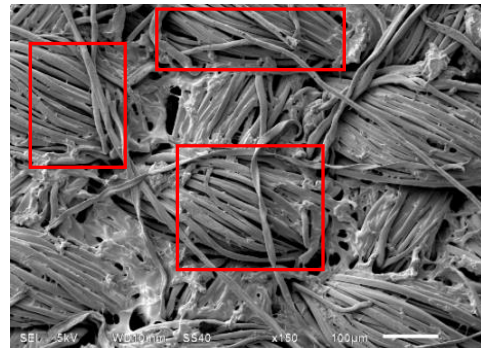
(a) Unpadded cotton fabric

Unwashed fabrics

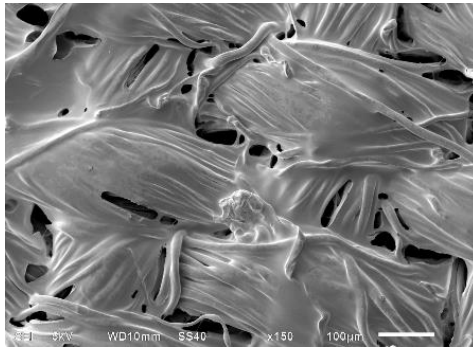
Washed fabrics



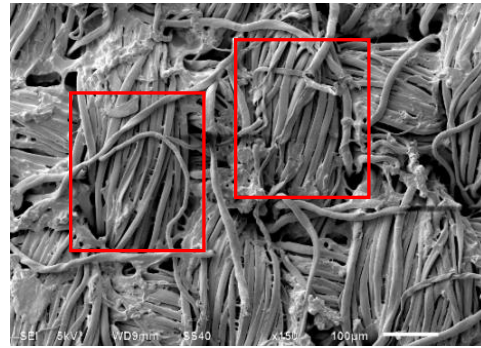
(b) 60 kPa



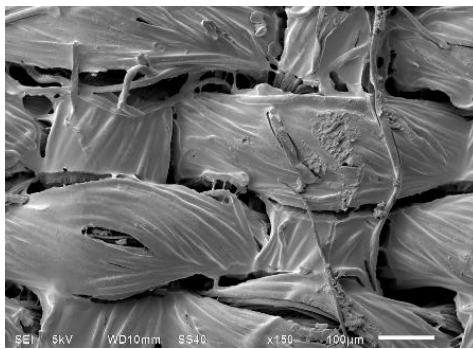
(c) 60 kPa



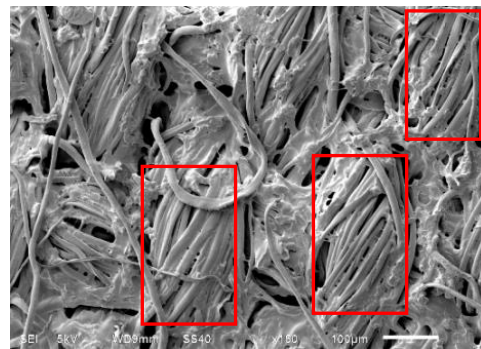
(d) 100 kPa



(e) 100 kPa

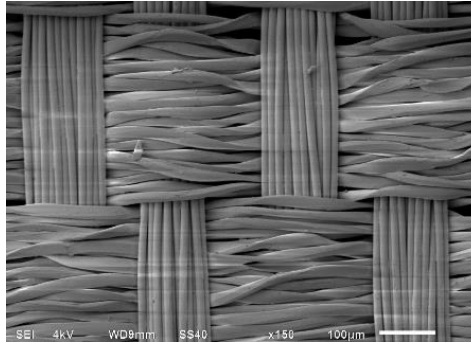


(e) 150 kPa

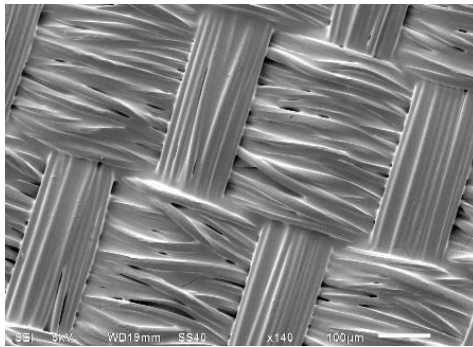


(f) 150 kPa

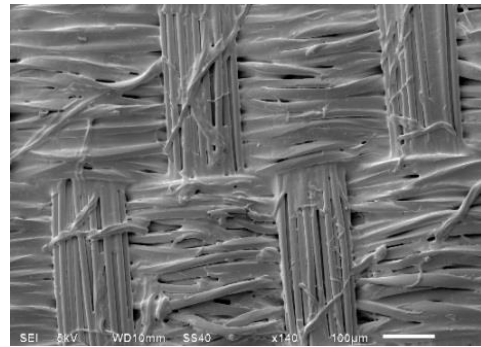
Figure 4-63: Micrographs of 100% cotton fabric padded with Binder2 at various padder pressure settings.



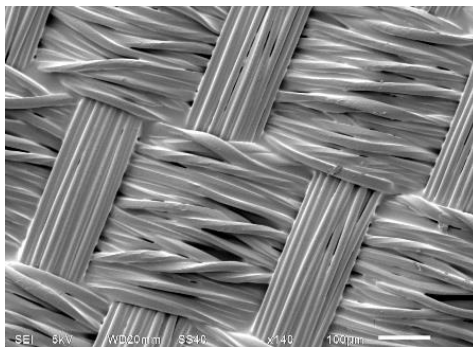
(a) Unpadded polyester fabric

Unwashed fabrics**Washed fabrics**

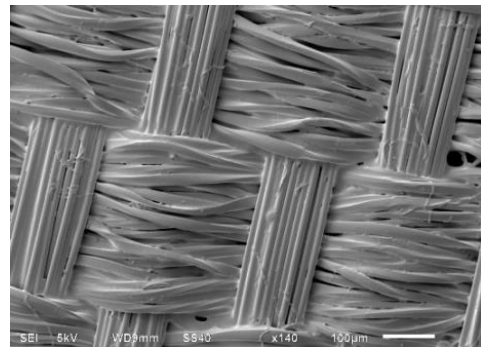
(b) 60 kPa



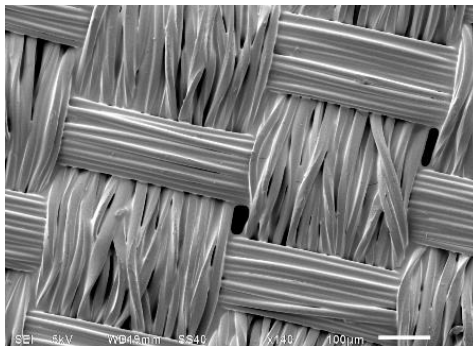
(c) 60 kPa



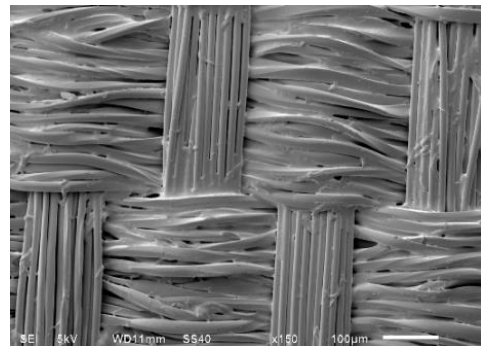
(d) 100 kPa



(e) 100 kPa

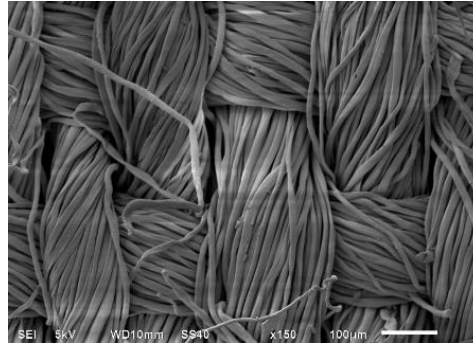


(f) 150 kPa

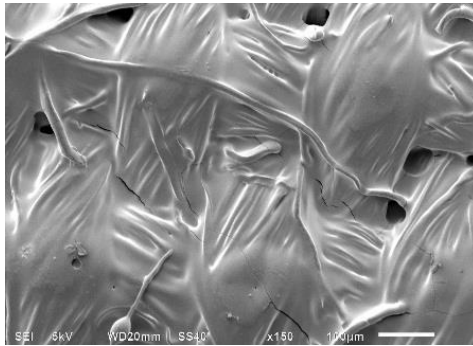


(g) 150 kPa

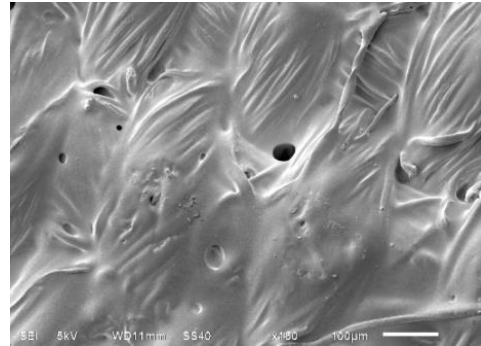
Figure 4-64: Micrographs of 100% polyester fabric padded with Binder3 at various padding pressure settings.



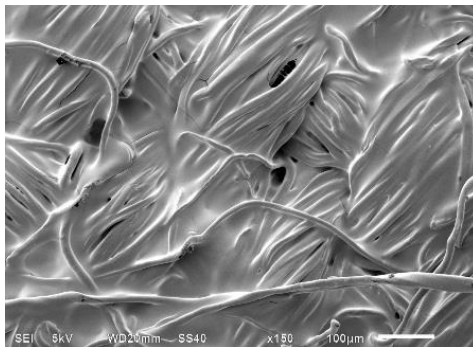
(a) Unpadded cotton fabric

Unwashed fabrics**Washed fabrics**

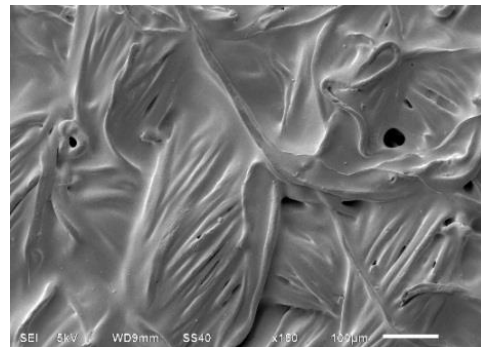
(b) 60 kPa



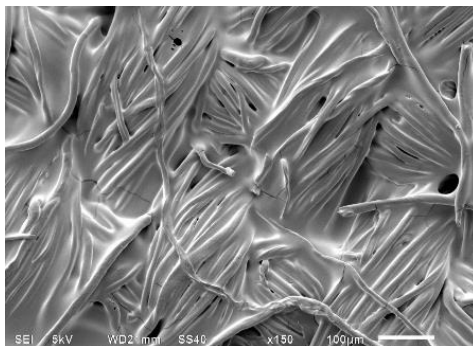
(c) 60 kPa



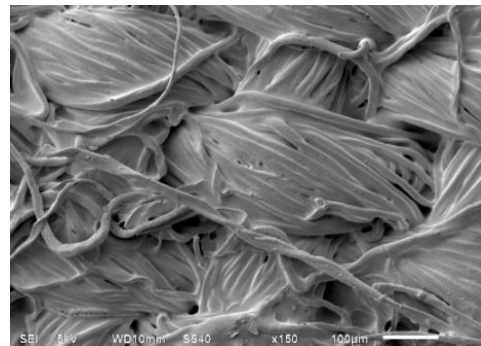
(d) 100 kPa



(e) 100 kPa



(f) 150 kPa



(g) 150 kPa

Figure 4-65: Micrographs of 100% cotton fabric padded with Binder3 at various padding pressure settings.

4.6.2 Electrical characteristics of ink films deposited on textile substrates

As discussed in Section 4.5.4, the surface resistivity of ink films containing 100% binder solids on the weight of pigment (%BOWP) was lower compared to that of the ink films containing 150% BOWP or 200% BOWP. Thus, only the inks that were formulated to contain 100% BOWP were initially considered for printing and testing onto textile substrates. Ink films were applied using a drawdown applicator (K bar 9) and the surface resistivity of was recorded after curing the films. The procedure is described in Section 2.4.2.

Table 4-42 and Table 4-43 contain the surface resistivity data of ink films containing 100% BOWP drawn on various substrates. It was observed that the surface resistivity varied within a very broad range when films of an ink were produced on different substrates. It is clear from the data that the surface resistivity of ink films containing Binder1 and Binder2 (particularly for the inks containing Binder1) was generally very high when deposited on Binder3-coated fabric substrates. The difference was less significant when ink films were produced on uncoated fabric substrates. It was noticed during preparation of drawdowns of inks that due to the very low GSM and thickness of uncoated polyester fabric, most of the deposited ink penetrated through the fabric. This resulted in large variations in the surface resistivity of the dried ink deposits on this substrate.

It was also noticed that on any given substrate, the surface resistivity of ink films containing Binder 3 was generally lower than that of the inks films containing Binder1 or Binder 2. The very high surface resistivity of ink films containing Binder1 and Binder2, on Binder3-coated cotton and coated polyester fabrics, was attributed to cracking of the ink layers. It was proposed the cracking of ink film occurred due to the difference in surface energies of the Binder3 primer layer and the Binder1-/Binder2-containing wet inks. However, the Binder1- and Binder2-containing ink layers, deposited on coated fabrics, visually appeared to be very smooth. Thus, the morphology of ink layers was analysed using high resolution optical microscopy, as described in Section 3.9.

The images obtained from the optical microscopy study are presented in Figure 4-66 - Figure 4-77. Analysis of these images revealed significant cracking of the ink films

containing Binder1/Binder2 deposited onto Binder3-coated fabrics. This resulted in the formation of isolated 'islands' of the deposited ink and consequently a significant decrease or even the complete loss of electrical conductivity. In contrast, the inks containing Binder3 formed very smooth and continuous films on both the coated fabrics and the uncoated fabrics. The images of Binder1- and Binder2- containing inks, deposited onto uncoated substrates, show that the dried ink films were smooth and continuous. In summary, the results of optical microscopy study confirmed that a major contributor in the very high surface resistivity of ink films containing Binder1/Binder2 was the cracking of these ink films when deposited onto Binder3-coated fabrics.

Following conclusions can be drawn from the analysis of data collated in this part of the present study.

- In terms of surface resistivity, the ink films containing Binder1 and Binder2 performed poorly on Binder3-coated cotton and polyester fabrics. However, the surface resistivity obtained on uncoated fabrics indicated that the intrinsic electrical conductivity was not low enough to exclude any of these inks from further testing.
- The surface resistivity of the ink films containing Binder3 was generally lower compared to the surface resistivity of ink films containing Binder1 or Binder2. This indicated that Binder3 was more suitable for fixation of the formulated conductive inks onto textile substrates.
- Uncoated cotton fabric and Binder3-coated coated polyester fabric were selected as substrates for further testing of the formulated inks. This is because the data presented Table 4-42 and Table 4-43 indicate that the uncoated cotton fabric was appropriate as a substrate for the estimation and comparison of intrinsic electrical conductivity and durability of the films produced from the formulated inks. On the other hand, the Binder3-coated polyester fabric was better as a substrate for the estimation of the lowest achievable surface resistivity of the films produced from selected inks.

This space is deliberately left blank due to pagination.

Table 4-42: Surface resistivity data of the films of inks prepared from the dispersions of low surface area carbon black pigments.

Ink composition		Surface resistivity (Ω/\square)			
		Cotton		Polyester	
		Coated	Uncoated	Coated	Uncoated
Carbon1 31 wt%, Dispersant1 15% DOWP	Binder1 100% BOWP	NR	484	26546	353
	Binder2 100% BOWP	493	367	357	242
	Binder3 100% BOWP	128	178	130	193
Carbon1 31 wt%, Dispersant2 15% DOWP	Binder1 100% BOWP	NR	463	NR	1649
	Binder2 100% BOWP	330	213	224	176
	Binder3 100% BOWP	121	101	153	206
Carbon1 31 wt%, Dispersant3 15% DOWP	Binder1 100% BOWP	NR	609	NR	650
	Binder2 100% BOWP	1184	230	428	174
	Binder3 100% BOWP	83	102	98	137
Carbon2 23 wt%, Dispersant1 17.5% DOWP	Binder1 100% BOWP	4900000	288	29751	273
	Binder2 100% BOWP	621	173	306	195
	Binder3 100% BOWP	76	149	93	220
Carbon2 23 wt%, Dispersant2 17.5% DOWP	Binder1 100% BOWP	NR	273	6902	202
	Binder2 100% BOWP	656	174	157	150
	Binder3 100% BOWP	98	152	91	236
Carbon2 22 wt%, Dispersant3 17.5% DOWP	Binder1 100% BOWP	13000000	379	640000	343
	Binder2 100% BOWP	791	163	282	136
	Binder3 100% BOWP	101	139	100	252
LEGEND:					
NR refers to 'no reading', i.e., the surface resistivity was greater than 100 M Ω .					

Table 4-43: Surface resistivity data of the films of inks prepared from the dispersions of high surface area carbon black pigments.

Ink composition		Surface resistivity (Ω/\square)			
		Cotton		Polyester	
		Coated	Uncoated	Coated	Uncoated
Carbon3 11 wt%, Dispersant1 155% DOWP	Binder1 100% BOWP	12262	549	5832	733
	Binder2 100% BOWP	1620	417	870	450
	Binder3 100% BOWP	216	282	166	274
Carbon3 11 wt%, Dispersant2 155% DOWP	Binder1 100% BOWP	4062	479	2082	358
	Binder2 100% BOWP	324	260	189	307
	Binder3 100% BOWP	159	180	133	175
Carbon3 10.5 wt%, Dispersant3 155% DOWP	Binder1 100% BOWP	52812	452	771	259
	Binder2 100% BOWP	177	233	115	138
	Binder3 100% BOWP	102	127	122	138
Carbon4 9.5 wt%, Dispersant1 225% DOWP	Binder1 100% BOWP	1071	1344	NR	1390
	Binder2 100% BOWP	353	903	NA	741
	Binder3 100% BOWP	187	392	113	407
Carbon4 9.5 wt%, Dispersant2 225% DOWP	Binder1 100% BOWP	90000000	788	11110000	969
	Binder2 100% BOWP	18077	639	363	504
	Binder3 100% BOWP	351	301	130	487
Carbon4 9.3 wt%, Dispersant3 225% DOWP	Binder1 100% BOWP	NR	985	NR	710
	Binder2 100% BOWP	1415	555	105	333
	Binder3 100% BOWP	241	230	114	135
LEGEND:					
NR refers to 'no reading', i.e., the surface resistivity was greater than 100 M Ω .					

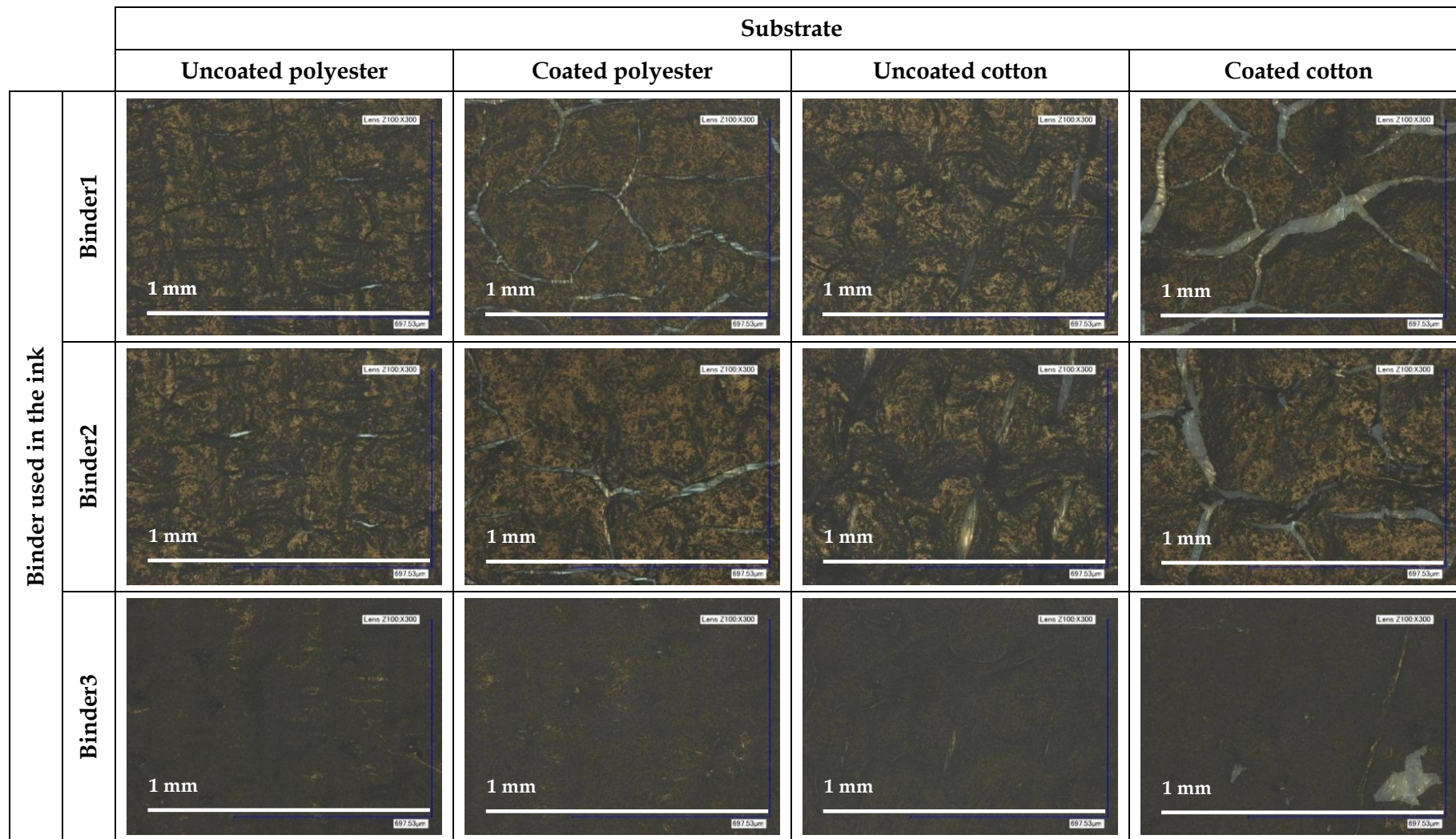


Figure 4-66: Optical microscope images (Magnification x 300) of drawdowns of inks prepared from Carbon1-Dispersant1 dispersion.

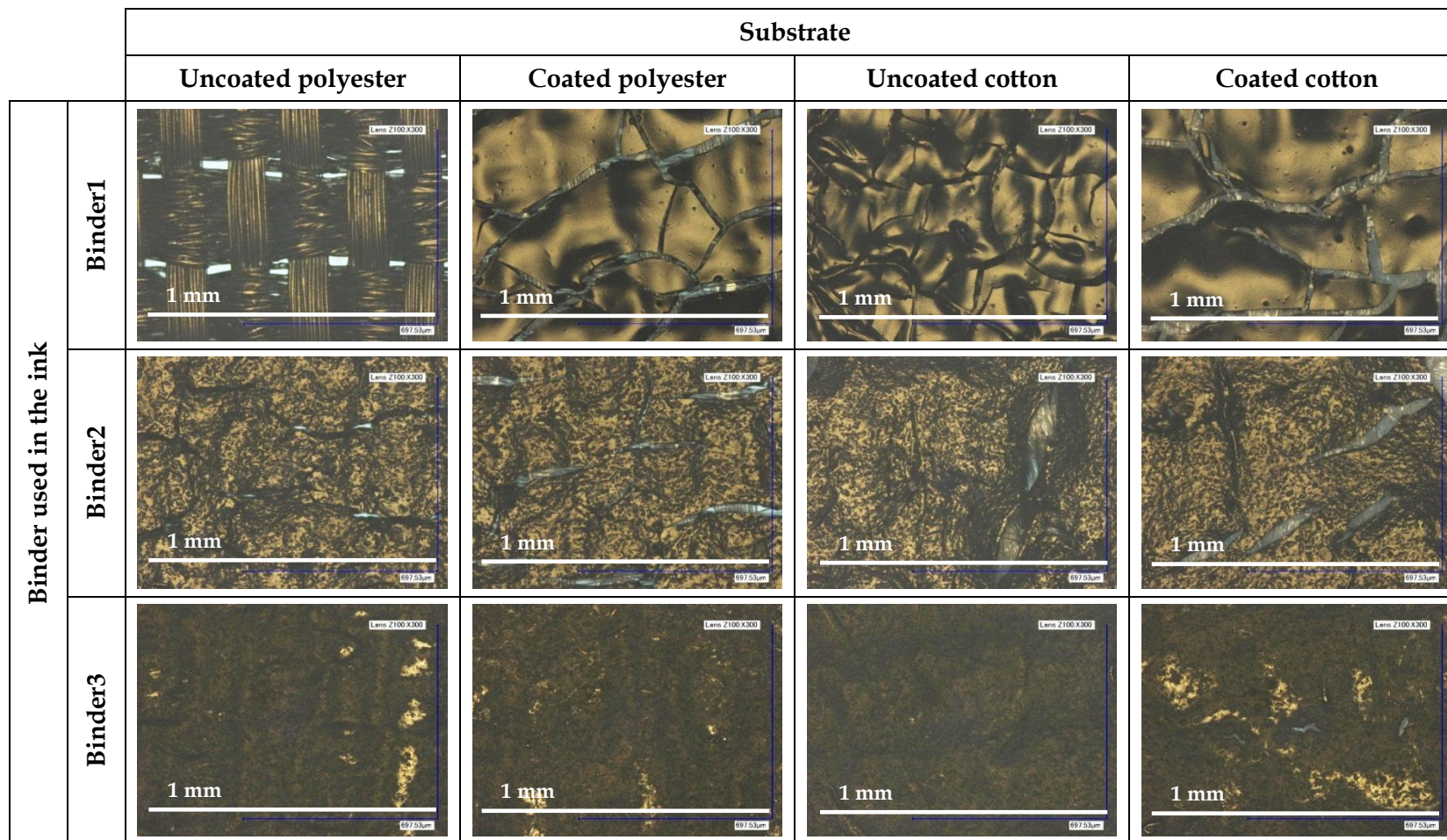


Figure 4-67: Optical microscope images (Magnification x 300) of drawdowns of inks prepared from Carbon1-Dispersant2 dispersion.

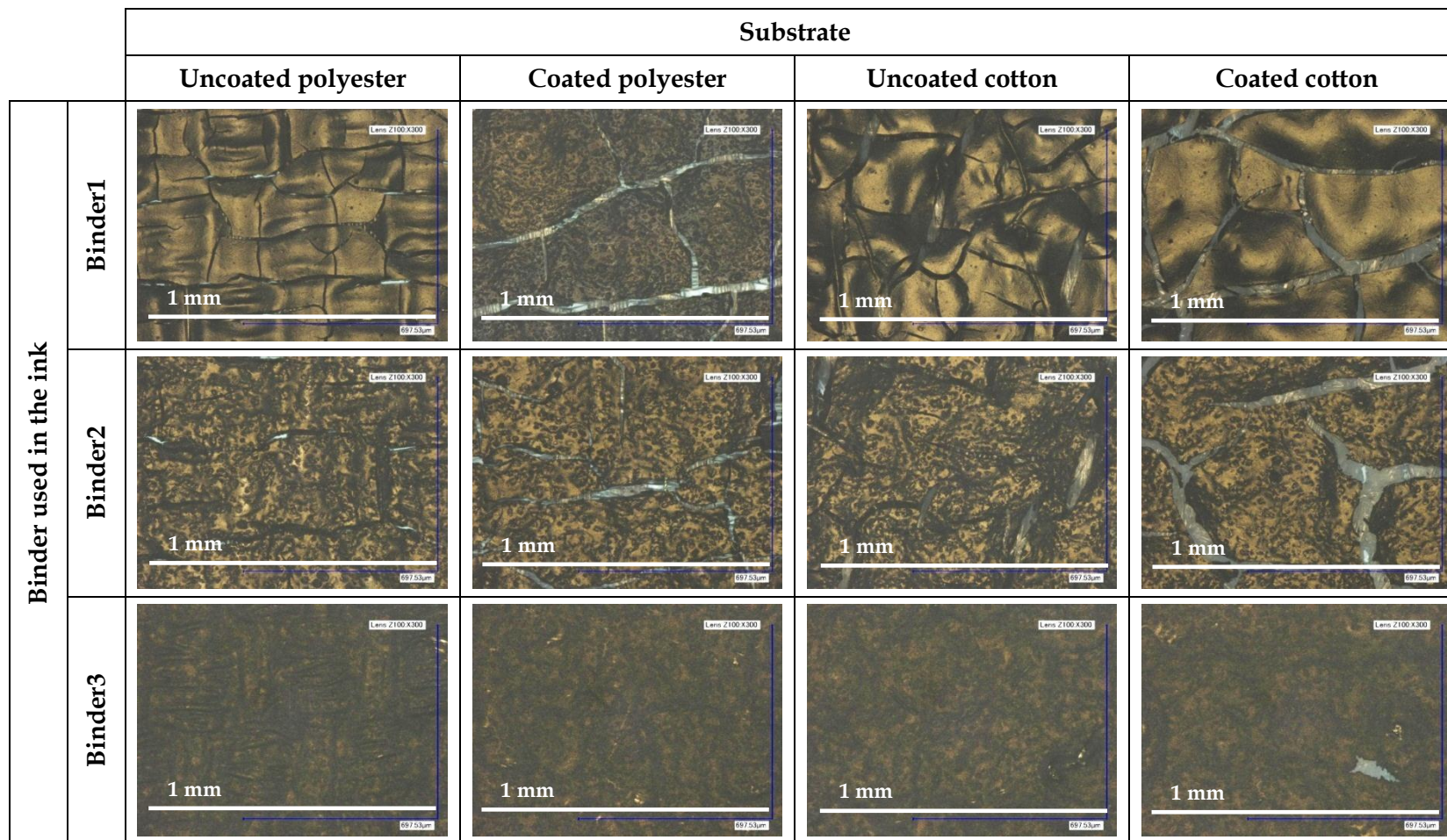


Figure 4-68: Optical microscope images (Magnification x 300) of drawdowns of inks prepared from Carbon1-Dispersant3 dispersion.

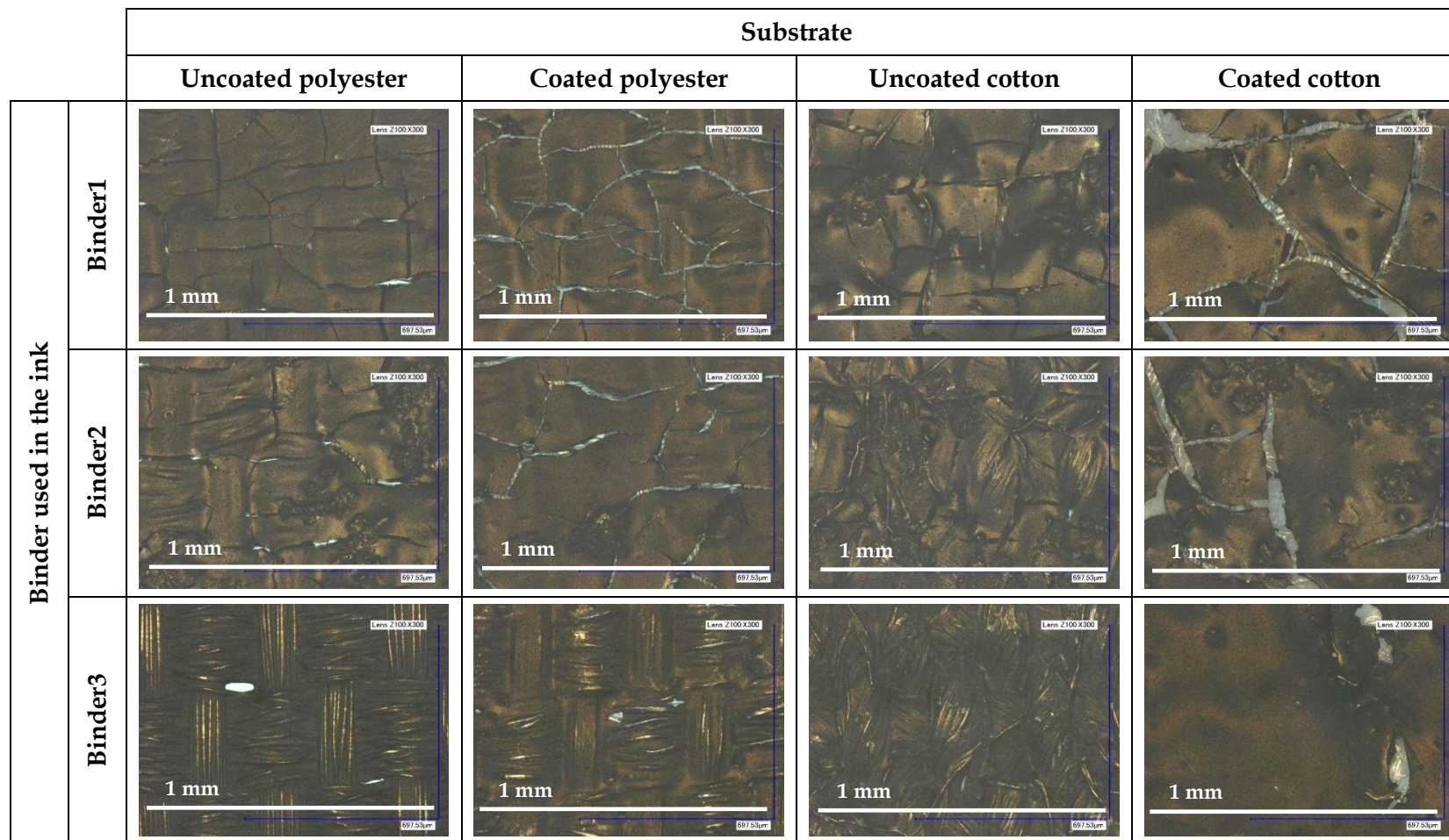


Figure 4-69: Optical microscope images (Magnification x 300) of drawdowns of inks prepared from Carbon2-Dispersant1 dispersion.

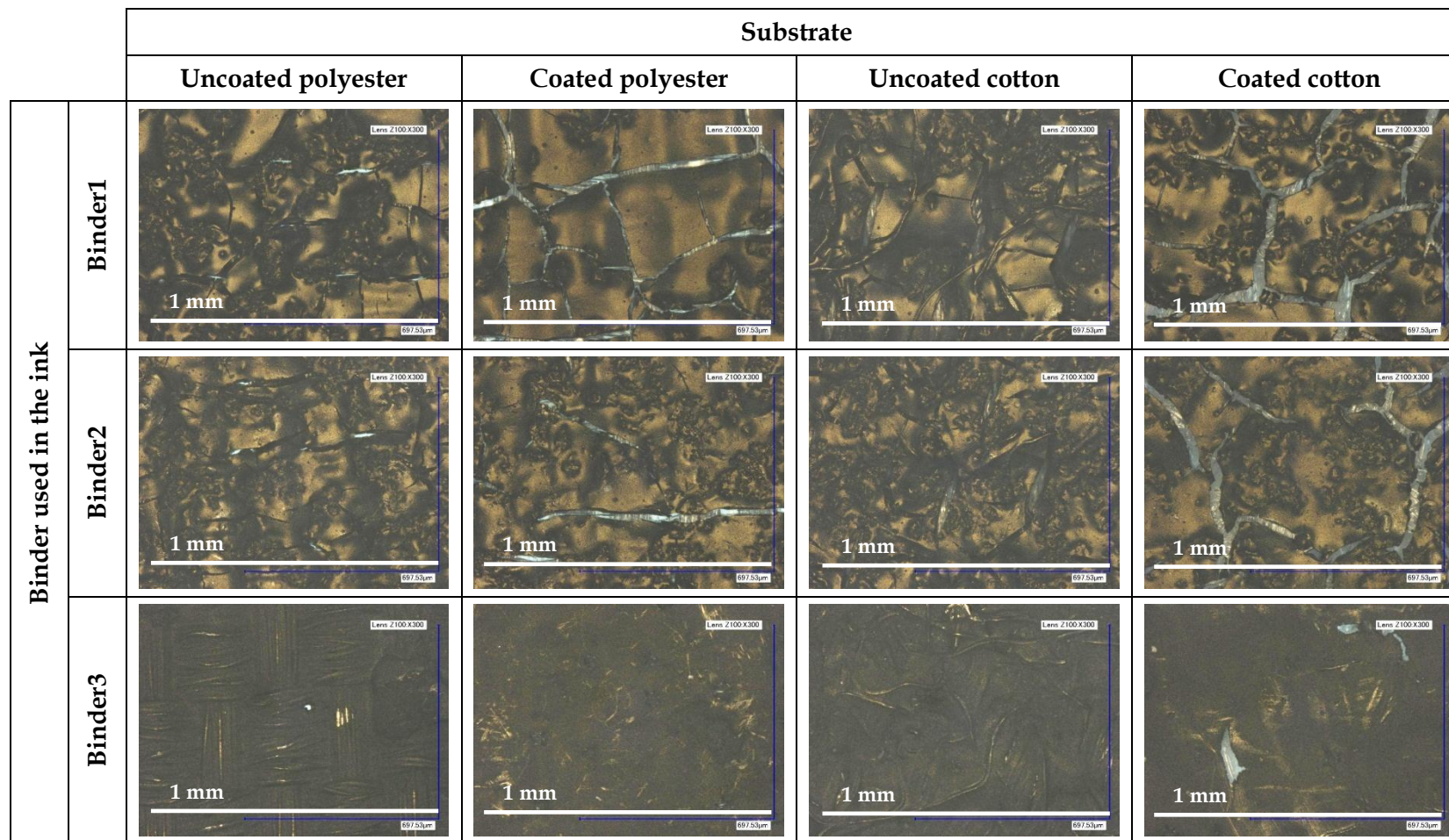


Figure 4-70: Optical microscope images (Magnification x 300) of drawdowns of inks prepared from Carbon2-Dispersant2 dispersion.

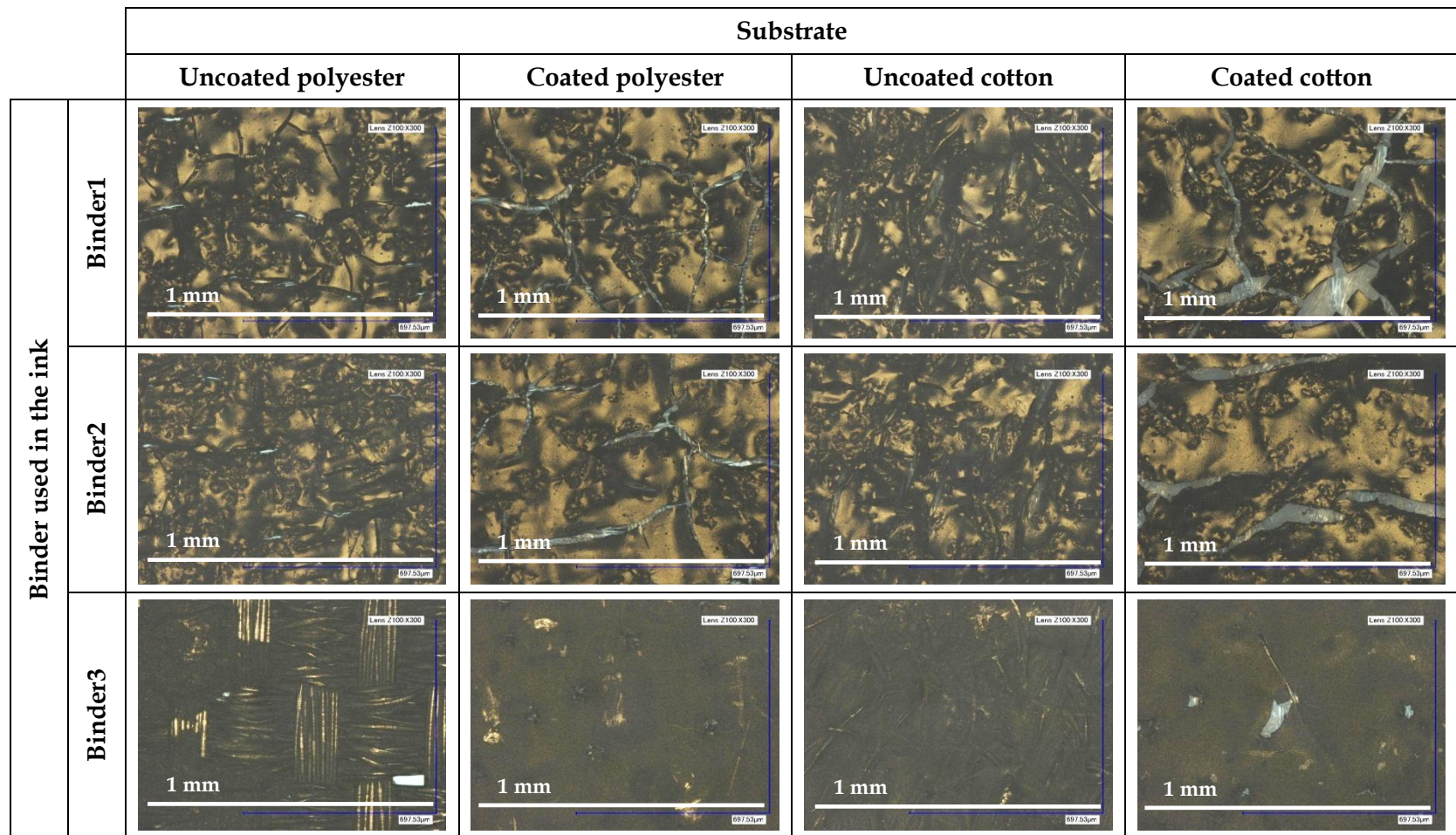


Figure 4-71: Optical microscope images (Magnification x 300) of drawdowns of inks prepared from Carbon2-Dispersant3 dispersion.

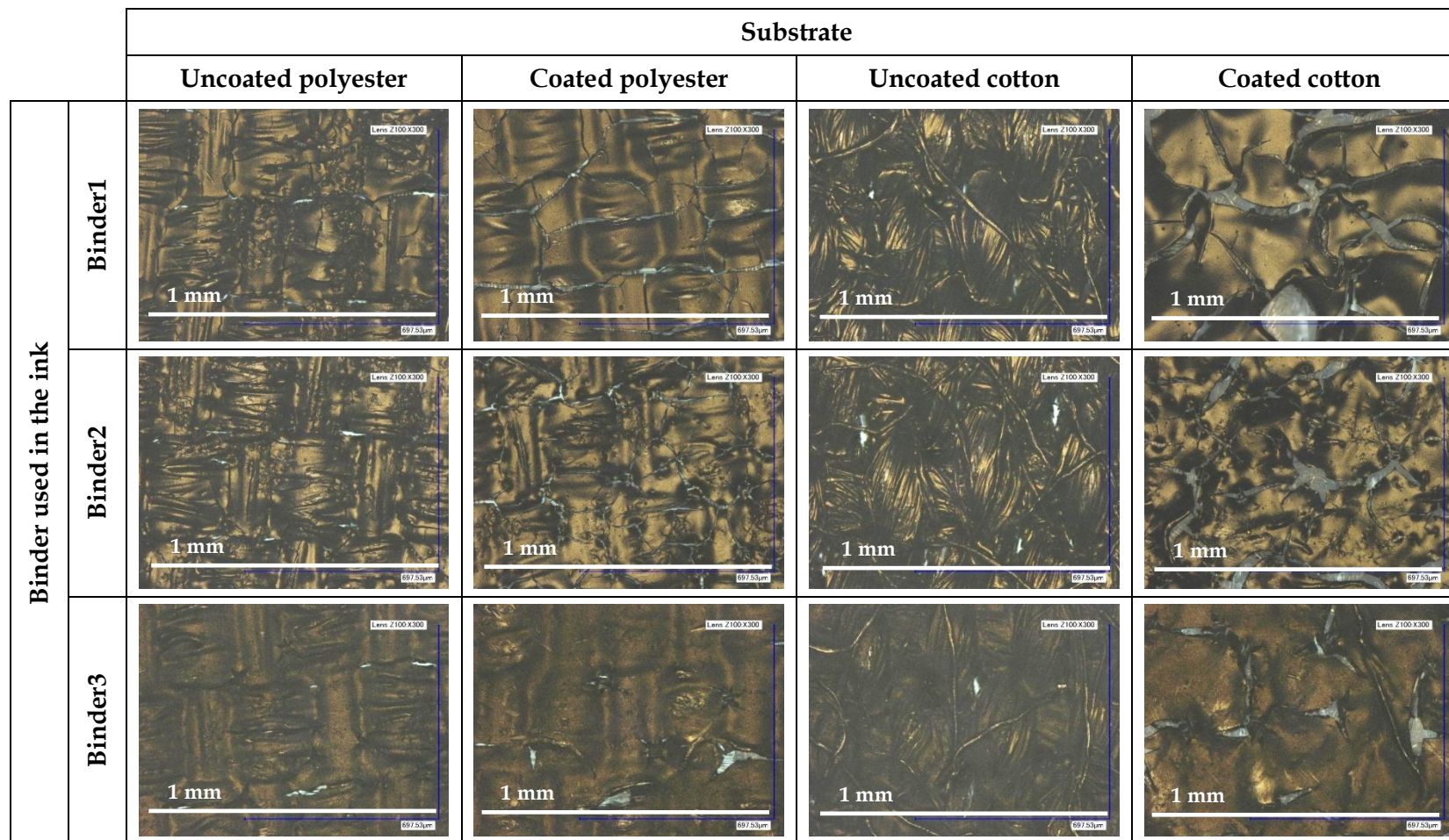


Figure 4-72: Optical microscope images (Magnification x 300) of drawdowns of inks prepared from Carbon3-Dispersant1 dispersion.

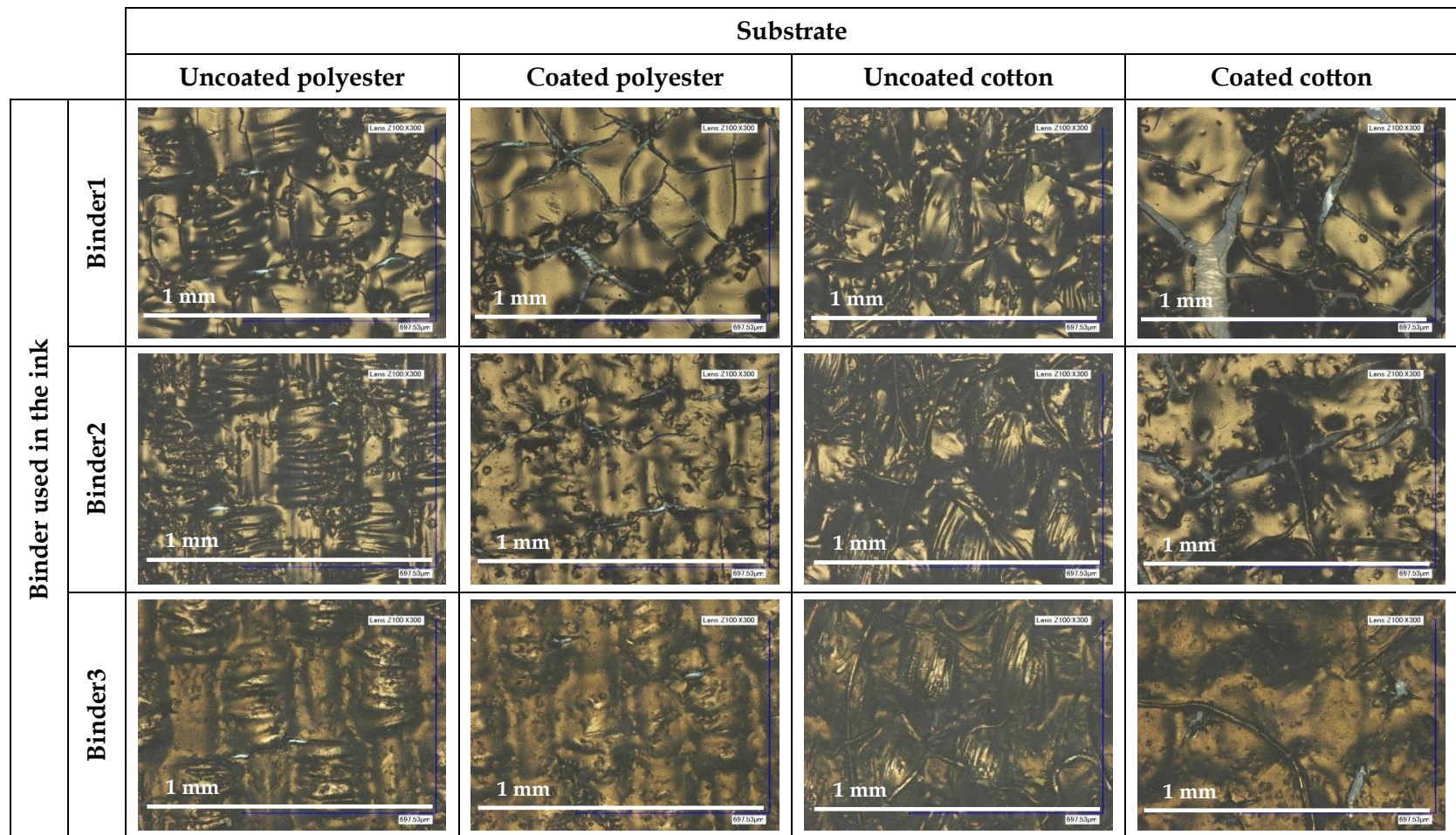


Figure 4-73: Optical microscope images (Magnification x 300) of drawdowns of inks prepared from Carbon3-Dispersant2 dispersion.

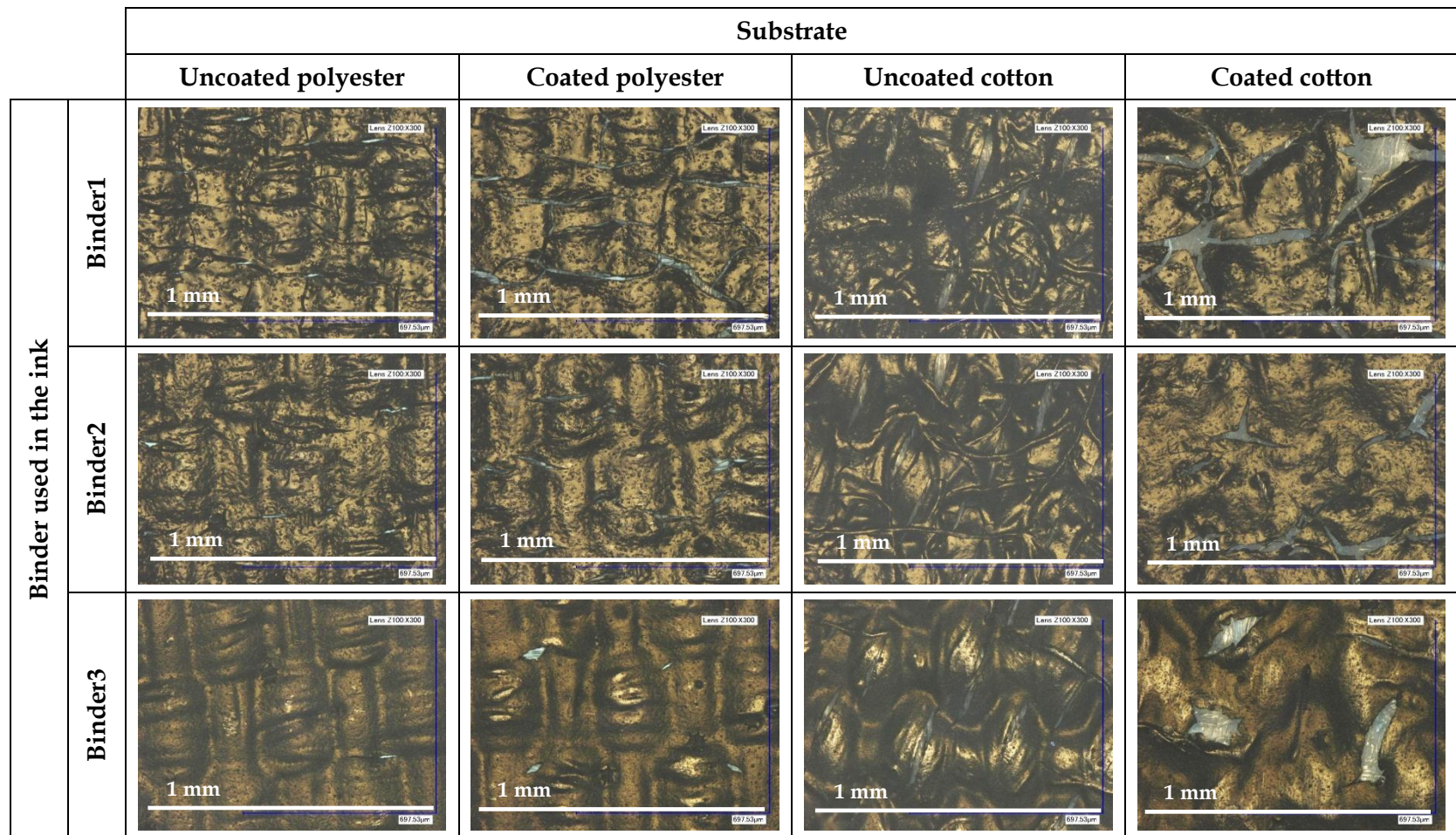


Figure 4-74: Optical microscope images (Magnification x 300) of drawdowns of inks prepared from Carbon3-Dispersant3 dispersion.

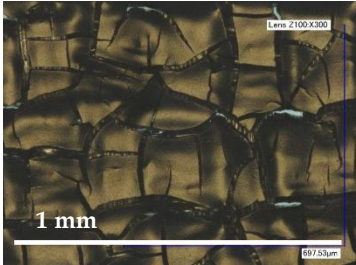
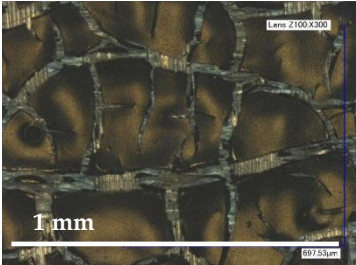
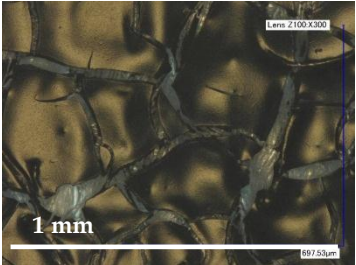
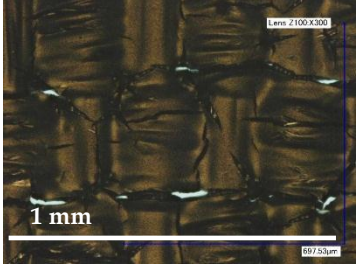
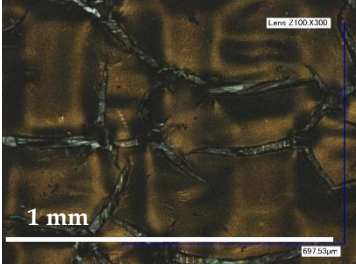
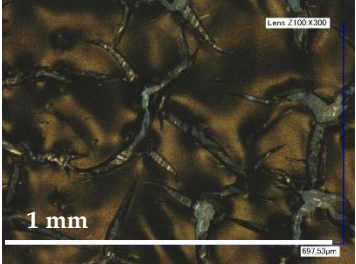
		Substrate			
		Uncoated polyester	Coated polyester	Uncoated cotton	Coated cotton
Binder used in the ink	Binder1				
	Binder2		Sample not available		
	Binder3				

Figure 4-75: Optical microscope images (Magnification x 300) of drawdowns of inks prepared from Carbon4-Dispersant1 dispersion.

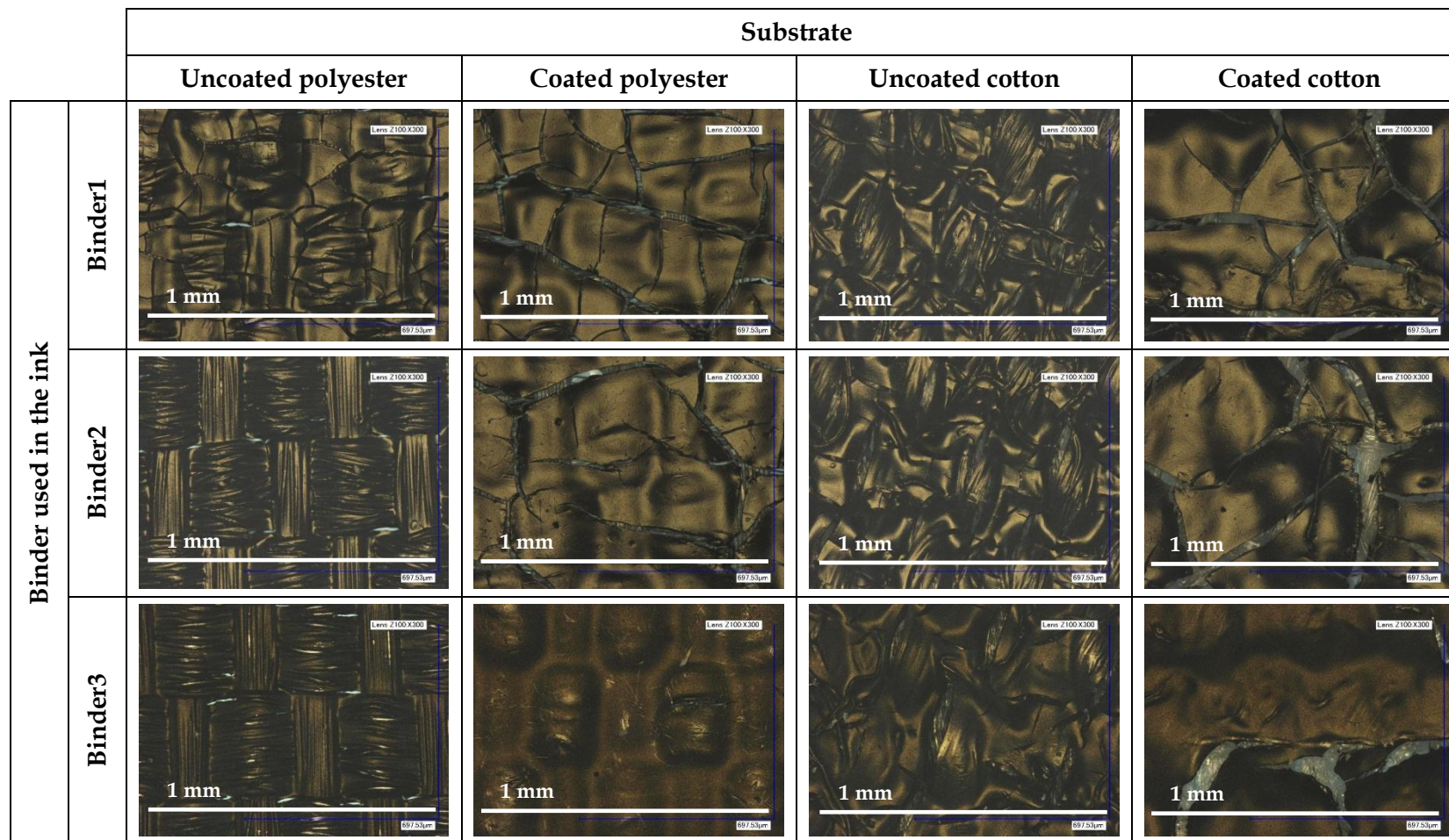


Figure 4-76: Optical microscope images (Magnification x 300) of drawdowns of inks prepared from Carbon4-Dispersant2 dispersion.

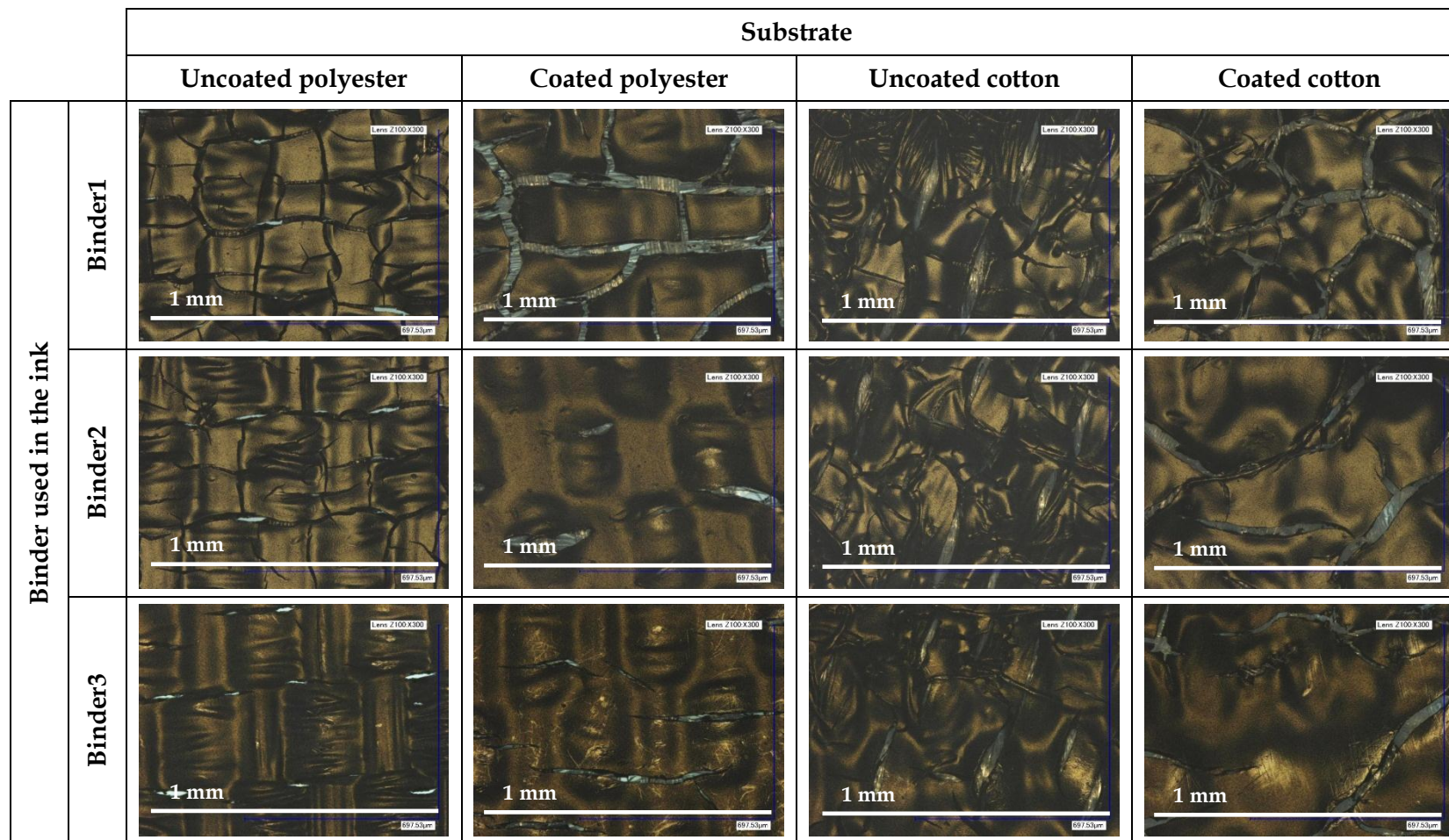


Figure 4-77: Optical microscope images (Magnification x 300) of drawdowns of inks prepared from Carbon4-Dispersant3 dispersion.

4.6.3 Performance testing of ink films

The presence of hydrophilic entities of the dispersants can result in a significant reduction in the water and chemical resistance of the dry ink film (Hobisch and Tsang 2009). This effect can be more pronounced if large amount of a dispersant is present in the formulation, as in the case of this study. In order to test the durability of films of inks formulated to contain 100% BOWP of various binders, fabrics were printed and tested as described in Section 2.4.3.

The results of washing tests are tabulated in Table 4-44 and Table 4-45. These indicate that none of the three binders was significantly inferior to others in terms of their resistance to washing. However, in most cases, the increase in surface resistivity was the least in those inks that were prepared using Binder3. Furthermore, the surface resistivity of ink films containing Binder3 was generally less (before and after the wash tests) compared to the surface resistivity of ink films containing Binder1 or Binder2.

The washing durability of ink films was also tested on Binder3-coated polyester fabric. The results presented in preceding section clearly indicated that the inks containing Binder1 or Binder2 were likely to under-perform on the coated polyester fabric. Thus, only the inks containing Binder3 were tested. The surface resistivity data, recorded before and after the washing tests, are presented in Table 4-46 and Table 4-47, along with the results of washing tests of ink films deposited onto uncoated cotton fabric. The results indicate that in a number of cases, the surface resistivity of an ink film was considerably lower when deposited on coated polyester fabric. Furthermore, in most cases, the increase in surface resistivity after washing was also significantly less than that recorded for the same ink printed onto uncoated cotton fabric.

This space is deliberately left due to pagination.

Table 4-44: Change in surface resistivity after washing of Carbon1-/Carbon2-containing ink films deposited onto cotton fabric.

Ink composition		Surface resistivity (Ω/\square)		
		Before wash	After wash	% Increase
Carbon1 31 wt%, Dispersant1 15% DOWP	Binder1 100% BOWP	442	536	21.26
	Binder2 100% BOWP	276	365	32.24
	Binder3 100% BOWP	287	311	8.36
Carbon1 31 wt%, Dispersant2 15% DOWP	Binder1 100% BOWP	558	690	23.65
	Binder2 100% BOWP	200	257	28.50
	Binder3 100% BOWP	139	169	21.58
Carbon1 31 wt%, Dispersant3 15% DOWP	Binder1 100% BOWP	725	737	1.65
	Binder2 100% BOWP	225	264	17.33
	Binder3 100% BOWP	99	123	24.24
Carbon2 23 wt%, Dispersant1 17.5% DOWP	Binder1 100% BOWP	220	320	45.45
	Binder2 100% BOWP	155	218	40.64
	Binder3 100% BOWP	127	166	30.71
Carbon2 23 wt%, Dispersant2 17.5% DOWP	Binder1 100% BOWP	270	383	41.85
	Binder2 100% BOWP	144	194	34.72
	Binder3 100% BOWP	140	188	34.28
Carbon2 22 wt%, Dispersant3 17.5% DOWP	Binder1 100% BOWP	307	361	17.59
	Binder2 100% BOWP	166	264	59.04
	Binder3 100% BOWP	151	201	33.11

Table 4-45: Change in surface resistivity after washing of Carbon3-/Carbon4-containing ink films deposited onto cotton fabric.

Ink composition		Surface resistivity (Ω/\square)		
		Before wash	After wash	% Increase
Carbon3 11 wt%, Dispersant1 155% DOWP	Binder1 100% BOWP	568	938	65.14
	Binder2 100% BOWP	441	1050	138.09
	Binder3 100% BOWP	324	573	76.85
Carbon3 11 wt%, Dispersant2 155% DOWP	Binder1 100% BOWP	422	896	112.32
	Binder2 100% BOWP	297	493	65.99
	Binder3 100% BOWP	188	350	86.17
Carbon3 10.5 wt%, Dispersant3 155% DOWP	Binder1 100% BOWP	461	1645	256.83
	Binder2 100% BOWP	216	462	113.88
	Binder3 100% BOWP	112	182	62.50
Carbon4 9.5 wt%, Dispersant1 225% DOWP	Binder1 100% BOWP	1321	2943	122.78
	Binder2 100% BOWP	784	1966	150.76
	Binder3 100% BOWP	376	987	162.50
Carbon4 9.5 wt%, Dispersant2 225% DOWP	Binder1 100% BOWP	647	2955	356.72
	Binder2 100% BOWP	411	1314	219.71
	Binder3 100% BOWP	277	582	110.11
Carbon4 9.3 wt%, Dispersant3 225% DOWP	Binder1 100% BOWP	721	1251	73.51
	Binder2 100% BOWP	241	410	70.12
	Binder3 100% BOWP	206	340	65.05

Table 4-46: Change in surface resistivity after washing of Carbon1-/Carbon2-containing ink films.

Ink composition	Substrate	Surface resistivity (Ω/\square)		
		Before wash	After wash	% Increase
Carbon1 31 wt%, Dispersant1 15% DOWP, Binder 3 100% BOWP.	Uncoated Cotton	287	311	8.36
	Coated Polyester	112	118	5.36
Carbon1 31 wt%, Dispersant2 15% DOWP, Binder3 100% BOWP	Uncoated Cotton	139	169	21.58
	Coated Polyester	101	99	-1.49
Carbon1 31 wt%, Dispersant3 15% DOWP, Binder3 100% BOWP	Uncoated Cotton	99	123	24.24
	Coated Polyester	129	157	21.58
Carbon2 23 wt%, Dispersant1 17.5% DOWP, Binder3 100% BOWP	Uncoated Cotton	127	166	30.71
	Coated Polyester	139	178	27.87
Carbon2 23 wt%, Dispersant2 17.5% DOWP, Binder3 100% BOWP	Uncoated Cotton	140	188	34.28
	Coated Polyester	153	183	19.63
Carbon2 22 wt%, Dispersant3 17.5% DOWP, Binder3 100% BOWP	Uncoated Cotton	151	201	33.11
	Coated Polyester	223	275	23.15

Table 4-47: Change in surface resistivity after washing of Carbon3-/Carbon4-containing ink films.

Ink composition	Substrate	Surface resistivity (Ω/\square)		
		Before wash	After wash	% Increase
Carbon3 11 wt%, Dispersant1 155% DOWP, Binder3 100% BOWP	Uncoated Cotton	324	573	76.85
	Coated Polyester	115	129	12.52
Carbon3 11 wt%, Dispersant2 155% DOWP, Binder3 100% BOWP	Uncoated Cotton	188	350	86.17
	Coated Polyester	128	145	12.44
Carbon3 10.5 wt%, Dispersant3 155% DOWP, Binder3 100% BOWP	Uncoated Cotton	112	182	62.50
	Coated Polyester	69	77	11.49
Carbon4 9.5 wt%, Dispersant1 225% DOWP, Binder3 100% BOWP	Uncoated Cotton	376	987	162.50
	Coated Polyester	739	1686	128.14
Carbon4 9.5 wt%, Dispersant2 225% DOWP, Binder3 100% BOWP	Uncoated Cotton	277	582	110.11
	Coated Polyester	116	238	105.17
Carbon4 9.3 wt%, Dispersant3 225% DOWP, Binder3 100% BOWP	Uncoated Cotton	206	340	65.05
	Coated Polyester	102	132	29.41

At this stage, the performance of selected inks was compared against that of the selected commercial conductive inks. For this purpose, the commercial inks were drawn on uncoated cotton and Binder3-coated polyester fabrics, followed by curing and washing the printed fabrics. The results of these washing tests are summarised in Table 4-48.

Table 4-48: Washing tests results of commercial inks

Ink name	Substrate	Surface resistivity (Ω/\square)		
		Before wash	After wash	% Increase
Gwent C2030519P4	Uncoated Cotton	20.83	81.9	293.18
Gwent C2030519P4	Coated Polyester	19.14	77.4	304.39
Peters SD 2843 HAL	Uncoated Cotton	59.96	NR	-
Peters SD 2843 HAL	Coated Polyester	42.5	307	622.35
NR refers to 'no reading', i.e., the surface resistivity was higher than 100 M Ω				

Prior to washing, the surface resistivity of the films produced from the commercial inks was generally lower than the surface resistivity of the films produced from the formulated inks. However, the films produced from the commercial inks were less durable, as indicated by a significantly greater increase in the surface resistivity after washing. Furthermore, as shown in Figure 4-78, the commercial inks were removed from large areas of the fabrics during washing. This showed that the commercial inks tested were not suitable for printing fine lines, a quality that is often required of prints when printing electrical interconnects.

The results obtained in the study presented above indicate that the ink films containing 100% BOWP of Binder3 possessed lower surface resistivity compared to the ink films containing 100% BOWP of Binder1/Binder2. Furthermore, the increase in the surface resistivity, when an ink film was deposited on Binder3-coated polyester fabric, was less than that in the surface resistivity of the film of same ink deposited onto uncoated cotton fabric. Thus, the creasing resistance of only the ink films produced on Binder3-coated polyester fabric was tested. For this purpose, the ASTM F 2749 - 09 test method was adopted, as described in Section 2.4.3.2. Durability of the ink films to withstand up to five creasing cycles was tested and the surface resistivity was recorded after each cycle. The results are tabulated in Table 4-49. The results of creasing tests indicate that

the overall increase in the surface resistivity of the films produced from the formulated inks was considerably lower compared to the increase in surface resistivity of films produced from the commercial inks. Furthermore, it was also noticed that the increase in surface resistivity was more pronounced in case of the inks that were prepared from the dispersions of high surface area pigments. As in the case of washing performance, this can be attributed to the very low binder solids content in the inks formulated from the dispersions of high surface area pigments.

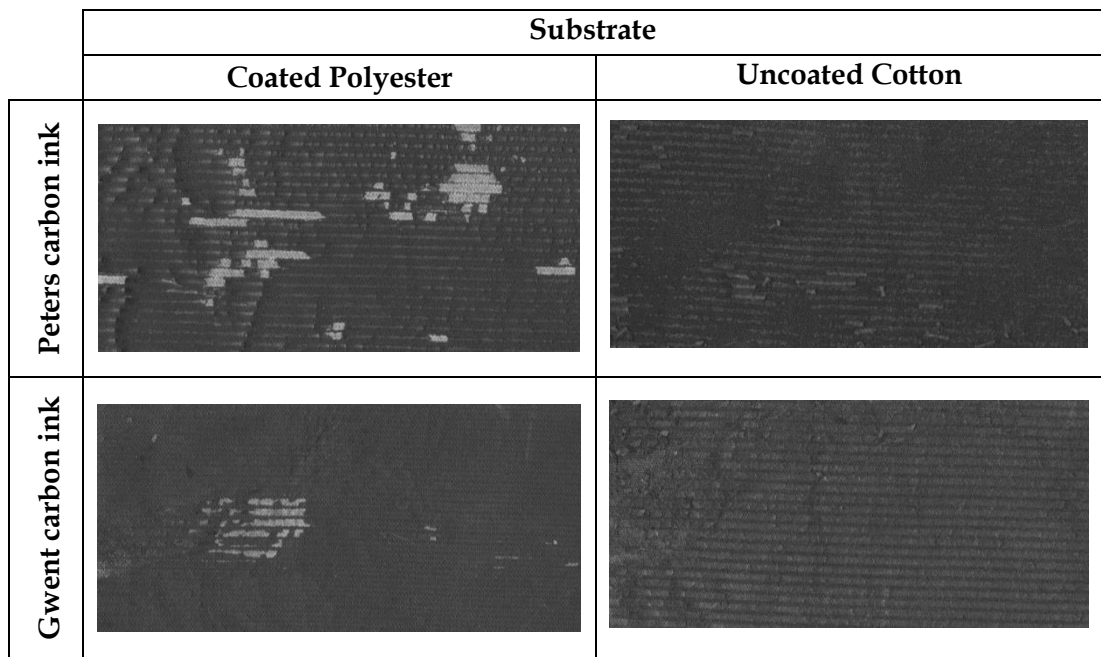


Figure 4-78: Images of commercial inks printed onto fabrics followed by washing.

This space is deliberately left blank due to pagination.

Table 4-49: Surface resistivity of inks recorded during crease testing of ink films.

Ink composition	Surface resistivity (Ω/\square)						
	Number of crease cycles						% Increase
	0	1	2	3	4	5	
Carbon1 31 wt%, Dispersant1 15% DOWP, Binder3 100% BOWP	112	121	125	128	127	128	14.29
Carbon1 31 wt%, Dispersant2 15% DOWP, Binder3 100% BOWP	143	165	170	174	175	181	26.57
Carbon1 31 wt%, Dispersant3 15% DOWP, Binder3 100% BOWP	90	96	99	103	102	104	15.56
Carbon2 23 wt%, Dispersant1 17.5% DOWP, Binder3 100% BOWP	102	106	111	108	113	113	10.78
Carbon2 23 wt%, Dispersant2 17.5% DOWP, Binder3 100% BOWP	92	101	103	103	104	106	15.22
Carbon2 22 wt%, Dispersant3 17.5% DOWP, Binder3 100% BOWP	86	87	87	90	91	91	5.81
Carbon3 11 wt%, Dispersant1 155% DOWP, Binder3 100% BOWP	134	146	155	157	162	162	20.90
Carbon3 11 wt%, Dispersant2 155% DOWP, Binder3 100% BOWP	120	139	149	151	156	158	31.67
Carbon3 10.5 wt%, Dispersant3 155% DOWP, Binder3 100% BOWP	108	113	123	125	134	141	30.56
Carbon4 9.5 wt%, Dispersant1 225% DOWP, Binder3 100% BOWP	248	289	314	338	364	386	55.65
Carbon4 9.5 wt%, Dispersant2 225% DOWP, Binder3 100% BOWP	120	147	159	186	207	226	88.33
Carbon4 9.3 wt%, Dispersant3 225% DOWP, Binder3 100% BOWP	91	123	163	230	408	538	491.21
Peters SD 2843 HAL carbon ink	28	63	98	157	196	411	311.00
Gwent C2030519P4 carbon ink	20	71	170	302	432	550	450.00

4.6.4 Screen printability of formulated inks

In comparison to the commercial inks and the other inks that were formulated in this work, the inks containing Binder3 gave more durable films on selected textile substrates. Optimisation of the binder solids content, to improve the durability of ink films, is proposed as potential future work.

At this stage, the inks which were tested for creasing performance were screen printed onto Binder3-coated polyester fabric. Rokuprint SD05 screen printer was used to establish the printability of these inks. The procedure and the screen printing process parameters employed in this study are described in detail in Section 2.4.4. A Keyence VHX-2000E digital optical microscope was used to analyse the print quality. The microscope software allowed real-time dimensioning of the features of interest in the focused area of the test specimen. Figure 4-79 shows the actual dimensions of the 1 mm wide line in the pattern (Figure 2-11) that was printed. The width of this 1 mm wide line, as obtained by screen printing the inks on coated polyester fabric, was measured while analysing the print quality using an optical microscope. The images of the prints are provided in Figure 4-80. Variation in the width of printed lines was considered to be within the acceptable range for such fine lines. The print resolution can be fine-tuned by adjusting the viscosity and/or the printing press settings. Thus, it was concluded that the screen printability of all of the selected inks was generally very good.

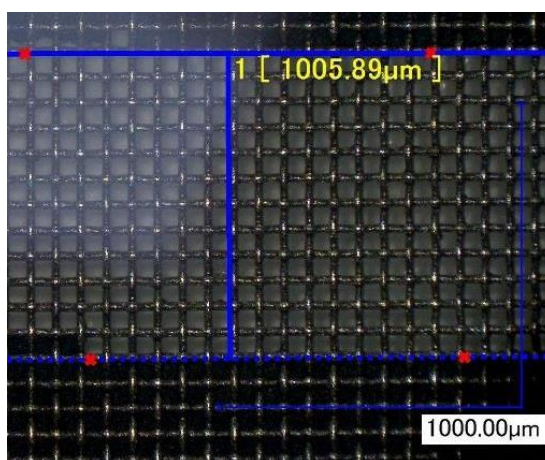


Figure 4-79: Optical micrograph (Magnification x100) of the stencil used to print 1 mm wide line on fabric substrate.

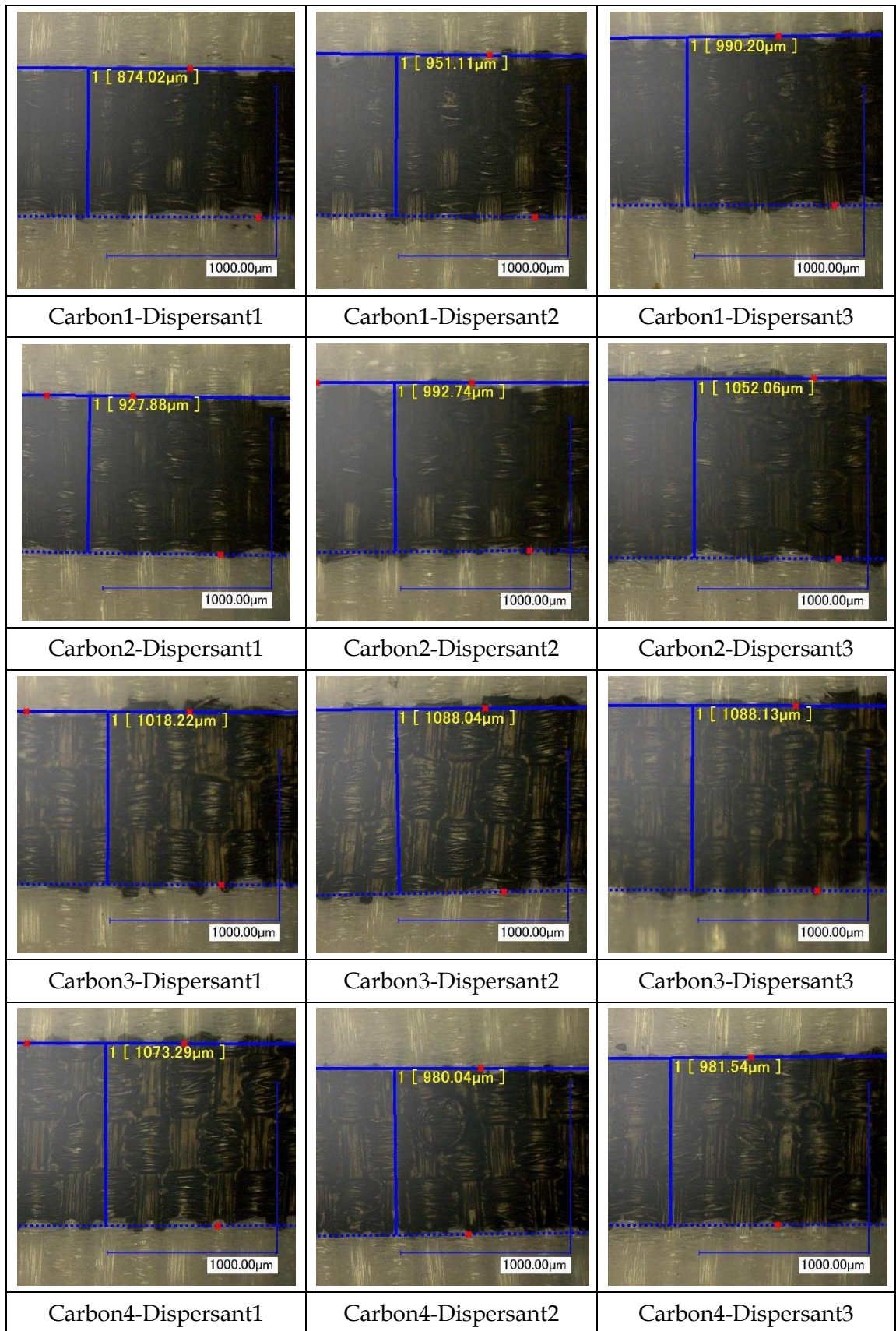


Figure 4-80: Images of Binder3-containing inks screen printed onto Binder3-coated polyester fabric.

4.6.5 Maximum conductivity of formulated inks

After establishing the screen printability, experiments were conducted to determine the lowest surface resistivity that could be achieved on textile substrates using selected inks from those formulated in this study.

For this purpose, those formulated inks that passed the creasing tests were drawn on Binder3-coated polyester fabric using K bar 9. The Binder3-coated polyester fabric was selected as a substrate on the basis of the results of aforementioned studies, which indicated that this substrate provided a very smooth surface for printing. Since screen printing can be employed to deposit relatively thick layers of inks onto textile substrates, two layers of an ink to be tested were deposited on top of each other with intermediate air drying for 1 hour between successive depositions. This was followed by air drying for 1 hour and then curing the ink deposit at 110 – 120 °C for 20 minutes. The cured specimens were conditioned at ambient temperature (22 – 25 °C) for 24 hours before measuring the surface resistivity and thickness of the ink deposit. The thickness of ink deposits was measured using a micrometre screw gauge of least count equal to 0.001 mm.

The pigment loading in finished inks is presented in Table 4-50 along with the surface resistivity and the thickness of cured ink layers. The following observations can be made from these data:

- The surface resistivity dropped significantly if two ink layers were deposited on top of each other with intermediate drying.
- The surface resistivity of the inks that contained low surface area carbon black pigments was generally less than that of the inks formulated from high surface area pigments. This was attributed to the very small amount of pigment in the finished inks that were prepared from the dispersions of high surface pigments.
- The final pigment loading in all of the formulated inks was significantly less than the pigment loading that is generally found in commercial conductive inks. In addition, the electrical conductivity after durability testing of the formulated inks was found to be comparable or even greater than that of the tested commercial conductive inks.

Table 4-50: Minimum surface resistivity achieved on Binder3-coated polyester fabric

Ink composition	Final pigment loading (wt%)	Surface resistivity (Ω/\square)		Thickness (microns)
		1 layer	2 layers	
Carbon1 31 wt%, Dispersant1 15% DOWP, Binder3 100% BOWP	17.46	89.4	50.72	50
Carbon1 31 wt%, Dispersant2 15% DOWP, Binder3 100% BOWP	17.46	115	68.65	50
Carbon1 31 wt%, Dispersant3 15% DOWP, Binder3 100% BOWP	17.46	80	43.68	50
Carbon2 23 wt%, Dispersant1 17.5% DOWP, Binder3 100% BOWP	14.60	111	53.74	50
Carbon2 23 wt%, Dispersant2 17.5% DOWP, Binder3 100% BOWP	14.60	106	49.96	50
Carbon2 22 wt%, Dispersant3 17.5% DOWP, Binder3 100% BOWP	14.19	87.4	46	65
Carbon3 11 wt%, Dispersant1 155% DOWP, Binder3 100% BOWP	8.63	162	103	45
Carbon3 11 wt%, Dispersant2 155% DOWP, Binder3 100% BOWP	8.63	140	92	40
Carbon3 10.5 wt%, Dispersant3 155% DOWP, Binder3 100% BOWP	8.32	152	85	40
Carbon4 9.5 wt%, Dispersant1 225% DOWP, Binder3 100% BOWP	7.68	530	435	55
Carbon4 9.5 wt%, Dispersant2 225% DOWP, Binder3 100% BOWP	7.68	180	149	70
Carbon4 9.3 wt%, Dispersant3 225% DOWP, Binder3 100% BOWP	7.54	157	101	40

Chapter 5. Conclusions

Advanced materials and novel fabrication methods are allowing concurrent developments in the technology of fabrication of generic components of an e-textile system; the power supply (e.g., flexible lithium polymer batteries), the circuitry (e.g., printed circuits produced using highly conductive inks) and the primary functional nodes (e.g., sensors, displays, light emitting devices, etc.). The focus of this study was the development of circuitry which is a common component of any simple or complex e-textile system. The means adopted for the realisation of such circuitry was printing of electrically conductive inks.

Review of literature revealed that inks that contained silver nano particles as the primary conductive filler met the requirement of high electrical conductivity. However, high cost and inferior washing and creasing performance of such inks were the major limitations. Other conductive fillers such as solution-processable conductive polymers are also expensive. Carbon black is widely used as black pigment in conventional printing inks. Carbon black is also used as conductive filler in electrically conductive inks for printing on flexible substrates such as polyimide films. On an equal weight basis, electrically conductive grades of carbon black are likely to result in higher electrical conductivity compared to the printing ink grades. However, due to the very low volatile matter content, generally high surface area and high structure, electrically conductive grades of carbon black are difficult to disperse and stabilise in aqueous media. Using effective dispersants and determining the optimum dispersant dosage are crucial in ensuring that the pigment dispersions remain stable throughout let-down and application stages. Rheological studies, particle size analysis, sedimentation analysis and electrical characterisation of the dispersions were carried out. Correlation of the results obtained from these different techniques gave credence to each other and indicated that the procedure devised in this study can be employed to prepare stable, waterborne dispersions of highly conductive grades of carbon black. The optimised, binder-free pigment dispersions were subsequently formulated into finished inks in the next step followed by thorough testing.

Reliability of the bead milling process was established on the basis of results of rheological and thermogravimetric analyses conducted on various batches of each of the optimised pigment dispersions. The results of these analyses indicated that the batch-to-batch variation in terms of viscosity and pigment loading was minimal, generally.

To formulate the optimised pigment dispersions into finished inks, different binders were used. The binder solids content was also varied in the formulations. It was observed, as expected, that increasing the binder solids content resulted in a sharp increase in the surface resistivity of finished inks. The stability of inks was assessed from rheological characterisation carried out after ink preparation and after four weeks of storage. It was found that most of the formulated finished inks possessed stable viscosity profiles. This gave credence to the results of analyses carried out on binder-free pigment dispersions and indicated that highly conductive grades of carbon black pigment were effectively dispersed and successfully stabilised following the devised procedure for dispersion optimisation and bead milling.

The design of experiments for formulation of finished inks was such that 108 inks were prepared and analysed for storage stability. All of the formulated inks were not considered for further testing because of practical limitations on the number of samples that could be tested. Since increasing the binder solids content resulted in a significant increase in the surface resistivity of inks, only the inks containing 100% BOWP were initially considered for performance testing on textile substrates. 100% cotton and 100% polyester plain woven fabrics were used as substrates on which the selected inks were tested for electrical performance and durability. The effects of primer coating of woven fabric substrates were also studied at this stage. The data obtained in these experiments indicated that the inks formulated from various binders possessed comparable surface resistivity on uncoated fabrics. However, the inks containing Binder1/Binder2 performed poorly on Binder3-coated fabrics. This was attributed to cracking of ink layers which was confirmed by the analysis of topography of ink deposits carried out using high resolution optical microscope.

Uncoated cotton fabric and Binder3-coated polyester fabrics were selected as substrates for performance testing and for the determination of maximum achievable

conductivity of ink deposits, respectively. The results of wash testing of inks drawn on uncoated cotton fabric indicated that none of the three binders was considerably inferior to others in terms of durability of ink deposits. However, the data showed that inks containing Binder3 generally possessed lower surface resistivity before and after wash tests.

Comparison of the percentage increase in surface resistivity of inks containing Binder3 drawn on uncoated cotton and Binder3-coated polyester showed that printing the inks on uncured Binder3 primer layer resulted in improved washing performance, as indicated by considerably smaller increase in the surface resistivity. Thus, the durability of inks containing 100% BOWP of Binder3 to withstand multiple creasing cycles was tested. The washing and creasing durability of two commercially available conductive carbon-based inks were also tested. The commercial inks possessed lower surface resistivity compared to most of the formulated inks, however, the increase in surface resistivity as a result of washing and creasing was considerably higher. This showed that the formulated inks were more suitable for the intended and other obvious applications in the fabrication of e-textiles.

The screen printability of the formulated inks was also found to be very good, as shown in the analysis of print quality carried out using a high resolution optical microscope. It was also shown that increasing the thickness resulted in a sharp decrease in the surface resistivity of an ink deposit. The surface resistivity was less than $100 \Omega/\square$ for a number of inks. Furthermore, such a high level of electrical conductivity was obtained at remarkably low pigment loadings as tabulated in Table 5-1. This is a considerable advantage in terms of the cost of the inks.

In conclusion, it was shown in this study that both low surface area and very high surface area electrically conductive grades of carbon black pigment can be used for formulation of stable, durable and highly conductive inks for printing of textile substrates. Such pigment grades imparted very high electrical conductivity at remarkably low pigment loading in the inks.

Table 5-1: Final pigment loading and surface resistivity of two layers of inks drawn on coated polyester fabric.

Ink composition	Final pigment loading (wt%)	Surface resistivity (Ω/\square)
Carbon1 31 wt%, Dispersant1 15% DOWP, Binder3 100% BOWP	17.46	50.72
Carbon1 31 wt%, Dispersant2 15% DOWP, Binder3 100% BOWP	17.46	68.65
Carbon1 31 wt%, Dispersant3 15% DOWP, Binder3 100% BOWP	17.46	43.68
Carbon2 23 wt%, Dispersant1 17.5% DOWP, Binder3 100% BOWP	14.60	53.74
Carbon2 23 wt%, Dispersant2 17.5% DOWP, Binder3 100% BOWP	14.60	49.96
Carbon2 22 wt%, Dispersant3 17.5% DOWP, Binder3 100% BOWP	14.19	46
Carbon3 11 wt%, Dispersant1 155% DOWP, Binder3 100% BOWP	8.63	103
Carbon3 11 wt%, Dispersant2 155% DOWP, Binder3 100% BOWP	8.63	92
Carbon3 10.5 wt%, Dispersant3 155% DOWP, Binder3 100% BOWP	8.32	85
Carbon4 9.5 wt%, Dispersant1 225% DOWP, Binder3 100% BOWP	7.68	435
Carbon4 9.5 wt%, Dispersant2 225% DOWP, Binder3 100% BOWP	7.68	149
Carbon4 9.3 wt%, Dispersant3 225% DOWP, Binder3 100% BOWP	7.54	101

Chapter 6. Suggestions for future work

Some other studies are suggested to compliment the outcomes and the following is proposed as future work in continuation of this research.

- Preparation of inks using moderate surface area (in the range of 200 – 300 m²/g) electrically conductive grades of carbon black pigment.
- Testing the suitability of non-woven textile fabrics as substrates for printing of electrical conductivity inks.
- Improving the durability by laminating or top coating the ink deposits with a polymeric film forming binder.
- Optimisation of the binder solids content in finished inks to improve the washing and creasing performance of inks.
- The binders used in this study contained only 40 wt% solids content and therefore incorporation in pigment dispersions to formulate finished inks decreased the final pigment loading. Thus, it is proposed to produce binder-containing pigment dispersions in order to maintain high pigment loading which is crucial for high electrical conductivity.
- DSC analysis of stability of inks.

Appendices

Appendix A: Let-down calculations

Table A-1: Let-down of pigment dispersions containing 31 wt% Carbon1.

	Formulae	Binder solids (%BOWP)		
		100%	150%	200%
Dispersion amount (g)	A	10	10	10
Pigment content (g)	$B = 0.31 \times A$	3.1	3.1	3.1
Binder, 100% solids (g)	C	3.1	4.65	6.2
Binder, 40% solids (g)	$D = (C \times 100)/40$	7.75	11.62	15.5
Amount of ink (g)	$E = A + D$	17.75	21.62	25.5
Pigment loading in ink (wt%)	$F = (B/E) \times 100$	17.46	14.33	12.15

Table A-2: Let-down of pigment dispersions containing 23 wt% Carbon2.

	Formulae	Binder solids (%BOWP)		
		100%	150%	200%
Dispersion amount (g)	A	10	10	10
Pigment content (g)	$B = 0.23 \times A$	2.3	2.3	2.3
Binder, 100% solids (g)	C	2.3	3.45	4.6
Binder, 40% solids (g)	$D = (C \times 100)/40$	5.75	8.625	11.5
Amount of ink (g)	$E = A + D$	15.75	18.625	21.5
Pigment loading in ink (wt%)	$F = (B/E) \times 100$	14.603	12.348	10.697

Table A-3: Let-down of pigment dispersions containing 22 wt% Carbon2.

	Formulae	Binder solids (%BOWP)		
		100%	150%	200%
Dispersion amount (g)	A	10	10	10
Pigment content (g)	$B = 0.23 \times A$	2.3	2.3	2.3
Binder, 100% solids (g)	C	2.3	3.45	4.6
Binder, 40% solids (g)	$D = (C \times 100)/40$	5.75	8.62	11.5
Amount of ink (g)	$E = A + D$	15.75	18.62	21.5
Pigment loading in ink (wt%)	$F = (B/E) \times 100$	14.603	12.35	10.69

Table A-4: Let-down of pigment dispersions containing 11 wt% Carbon3.

	Formulae	Binder solids (%BOWP)		
		100%	150%	200%
Dispersion amount (g)	A	10	10	10
Pigment content (g)	$B = 0.11 \times A$	1.1	1.1	1.1
Binder, 100% solids (g)	C	1.1	1.65	2.2
Binder, 40% solids (g)	$D = (C \times 100)/40$	2.75	4.125	5.5
Amount of ink (g)	$E = A + D$	12.75	14.125	15.5
Pigment loading in ink (wt%)	$F = (B/E) \times 100$	8.627	7.787	7.096

Table A-5: Let-down of pigment dispersions containing 10.5 wt% Carbon3.

	Formulae	Binder solids (%BOWP)		
		100%	150%	200%
Dispersion amount (g)	A	10	10	10
Pigment content (g)	$B = 0.105 \times A$	1.05	1.05	1.05
Binder, 100% solids (g)	C	1.05	1.58	2.1
Binder, 40% solids (g)	$D = (C \times 100)/40$	2.62	3.94	5.25
Amount of ink (g)	$E = A + D$	12.62	13.94	15.25
Pigment loading in ink (wt%)	$F = (B/E) \times 100$	8.32	7.53	6.88

Table A-6: Let-down of pigment dispersions containing 9.5 wt% Carbon4.

	Formulae	Binder solids (%BOWP)		
		100%	150%	200%
Dispersion amount (g)	A	10	10	10
Pigment content (g)	$B = 0.095 \times A$	0.95	0.95	0.95
Binder, 100% solids (g)	C	0.95	1.425	1.9
Binder, 40% solids (g)	$D = (C \times 100)/40$	2.38	3.56	4.75
Amount of ink (g)	$E = A + D$	12.38	13.56	14.75
Pigment loading in ink (wt%)	$F = (B/E) \times 100$	7.68	7.00	6.44

Table A-7: Let-down of pigment dispersions containing 9.3 wt% Carbon4.

	Formulae	Binder solids (%BOWP)		
		100%	150%	200%
Dispersion amount (g)	A	10	10	10
Pigment content (g)	$B = 0.093 \times A$	0.93	0.93	0.93
Binder, 100% solids (g)	C	0.93	1.39	1.86
Binder, 40% solids (g)	$D = (C \times 100) / 40$	2.33	3.48	4.65
Amount of ink (g)	$E = A + D$	12.33	13.56	14.75
Pigment loading in ink (wt%)	$F = (B/E) \times 100$	7.54	6.89	6.35

References

Abbott, S. 2008. The optional theory. In: S. Abbott, ed. *How to be a great screen printer*. MacDermid Autotype Ltd.

Adams, L. W., Gilpatrick M. W. and Gregory R. V. 1994. *Method for generating a conductive fabric and associated product*. Patent number: US5292573.

Allen, T. and Baudet M. G. 1977. The limits of gravitational sedimentation. *Powder Technology*, **18**(2), pp.131-138.

Ambrosetti, G. et al. 2009. Electron tunneling in conductor-insulator composites with spherical fillers. *Journal of Applied Physics*, **106**(1).

Andonovska, M. 2009. *E-textiles: The intersection of computation and traditional textiles*. Masters in Medialogy thesis, Aalborg University Copenhagen.

Azim, S. S., Satheesh A., Ramu K. K., Ramu S. and Venkatachari G. 2006. Studies on graphite based conductive paint coatings. *Progress in Organic Coatings*, **55**(1), pp.1-4.

Bao, Z., Feng Y., Dodabalapur A., Raju V. R. and Lovinger A. J. 1997. High-Performance Plastic Transistors Fabricated by Printing Techniques. *Chemistry of Materials*, **9**(6), pp.1299-1301.

Barker, M. J. 1993. Screen inks. In: R. H. Leach, R. J. Pierce, E. P. Hickman, M. J. Mackenzie and H. G. Smith, eds. *The Printing Ink Manual*. Springer, pp.599-635.

Barrett, K. E. J. 1973. Dispersion polymerisation in organic media. *British Polymer Journal*, **5**(4), pp.259-271.

Barringer, E. A., Novich B. E. and Ring T. A. 1984. Determination of colloid stability using photon correlation spectroscopy. *Journal of Colloid and Interface Science*, **100**(2), pp.584-586.

Bernhardt, C. 1988. Preparation of suspensions for particle size analysis. Methodical recommendations, liquids and dispersing agents. *Advances in Colloid and Interface Science*, **29**(1-2), pp.79-139.

Biddle, D., Walldal C. and Wall S. 1996. Characterisation of colloidal silica particles with respect to size and shape by means of viscosity and dynamic light scattering measurements. *Colloids and Surfaces A: Physicochemical and Engineering Aspects*, **118**(1-2), pp.89-95.

- Bidoki, S. M. et al. 2007. Ink-jet fabrication of electronic components. *Journal of Micromechanics and Microengineering*, **17**(5), p967.
- Bieleman, J. 2000. Basics. In: J. Bieleman, ed. *Additives for Coatings*. Wiley-VCH, pp.5-8.
- Bieleman, J., Heilen W., Silber S., Ortelt M. and Scholz W. 2000. Surface-Active Agents. In: J. Bieleman, ed. *Additives for Coatings*. Wiley-VCH, pp.65-138.
- Boehm, H. P. 1994. Some aspects of the surface chemistry of carbon blacks and other carbons. *Carbon*, **32**(5), pp.759-769.
- Bohren, C. F. and Huffman D. R. 2004. Absorption and Scattering by an Arbitrary Particle. *Absorption and Scattering of Light by Small Particles*. WILEY-VCH Verlag GmbH & Co, pp.57 - 81.
- Bourrat, X. 1993. Electrically conductive grades of carbon black: Structure and properties. *Carbon*, **31**(2), pp.287-302.
- Brenzikofer, F. 2002. The Global Market for Organic High Performance Pigments. In: H. M. Smith, ed. *High Performance Pigment*. Wiley-VCH, pp.127-134.
- Buxbaum, G. 2002. Introduction to Inorganic High Performance Pigments. In: H. M. Smith, ed. *High Performance Pigment*. Wiley-VCH, pp.3-6.
- Clayton, J. 1997. Pigment/Dispersant interactions in Waterbased Coatings. In: OCCA AGM symposium, 03-07-1997, The Science Museum, London. Oil and Colour Chemists' Association.
- Clayton, M. 1993. Raw Materials. In: R. H. Leach, R. J. Pierce, E. P. Hickman, M. J. Mackenzie and H. G. Smith, eds. *The Printing Ink Manual*. 5th ed. Springer, pp.187-188.
- Conley, R. F. 1996. Mechanical Assistance in Dispersion. *Practical Dispersion*. New York: Wiley-VCH, Inc, pp.213-255.
- Cowley, A. C. D. and Walsh T. 1997. Additives. In: P. Laden, ed. *Chemistry and Technology of Water-based Inks*. Blackie Academic and Professional, pp.208-219.
- Das, R. 2005. *Printed electronics white paper* [online]. [Accessed 04/02/2010]. Available from: http://www.idtechex.com/research/topics/printed_electronics_000089.asp
- Deangelis, A. R., Child A. D. and Green D. E. 1997. *Patterned conductive textiles*. Patent number: US5624736.
- Dhawan, A., Ghosh T. K., Seyam A. M. and Muth J. F. 2004a. Woven Fabric-Based Electrical Circuits: Part II: Yarn and Fabric Structures to Reduce Crosstalk Noise in Woven Fabric-Based Circuits. *Textile Research Journal*, **74**(11), pp.955-960.

Dhawan, A., Seyam A. M., Ghosh T. K. and Muth J. F. 2004b. Woven Fabric-Based Electrical Circuits: Part I: Evaluating Interconnect Methods. *Textile Research Journal*, **74**(10), pp.913-919.

Doheim, M. A., Abu-Ali M. H. and Mabrouk S. A. 1997. Investigation and modelling of sedimentation of mixed particles. *Powder Technology*, **91**(1), pp.43-47.

Ehrburger-Dolle, F., Lahaye J. and Misono S. 1994. Percolation in carbon black powders. *Carbon*, **32**(7), pp.1363-1368.

Frimova, A., Pekarovicova A., Fleming P. D. and Pekarovic J. 2006. Ink stability during printing. *TAGA Journal of Graphic Technology*, **Vol 2**.

Fuller, S. B., Wilhelm E. J. and Jacobson J. M. 2002. Ink-jet printed nanoparticle microelectromechanical systems. *Journal of Microelectromechanical Systems*, **11**(1), pp.54-60.

Ghosh, T. K., Dhawan A. and Muth J. F. 2006. Formation of electrical circuits in textile structures. In: H. Matilla, ed. *Intelligent Textiles and Clothing*. Cambridge: Woodhead Publishing.

Gimpel, S., Mohring U., Muller H., Neudeck A. and Scheibner W. 2004. Textile-Based Electronic Substrate Technology. *Journal of Industrial Textiles*, **33**(3), pp.179-189.

Goldschmidt, A. and Streitberger H.-J. 2003. Coating materials. *BASF Handbook on basics of coating technology*. Hannover, Germany: Vincentz Network, pp.27 - 318.

Goodwin, J. W. and Ottewill R. H. 1991. Properties of concentrated colloidal dispersions. *Journal of the Chemical Society, Faraday Transactions*, **87**(3), pp.357-369.

Gray, C., Wang J., Duthaler G., Ritenour A. and Drzaic P. S. 2001. Screen printed organic thin film transistors (OTFTs) on a flexible substrate. In: *Organic Field Effect Transistors*, San Diego, CA, USA. SPIE, pp.89-94.

Gregory, R. V., Kimbrell W. C. and Kuhn H. H. 1991. Electrically Conductive Non-Metallic Textile Coatings. *Journal of Industrial Textiles*, **20**(3), pp.167-175.

Harper, W. P. and Taylor J. 1983. *Conductive ink*. Patent number: US 4369269.

Hartschuh, H. J. et al. 1997. Emulsion and Solution Polymers. In: P. Laden, ed. *Chemistry and Technology of Water-Based Inks*. Blackie Academic and Professional, pp.190-207.

Hayes, D. J., Grove M. E., Wallace D. B., Chen T. and Cox W. R. 2002. Inkjet printing in the manufacture of electronics, photonics, and displays. In: *Nanoscale Optics and Applications*, Seattle, WA, USA. SPIE, pp.94-99.

Hobisch, G. and Tsang M. 2009. New Waterborne Pigment Grinding Resin for High-Performance Coatings. *Paint and Coatings Industry Magazine*.

Hostomský, J., Halász Z., Liszi I. and Nývlt J. 1986. Size analysis of non-spherical particles a correlation between the results of photosedimentation technique and microscopy. *Powder Technology*, **49**(1), pp.45-51.

Huebler, A., Hahn U., Beier W., Lasch N. and Fischer T. 2002. High volume printing technologies for the production of polymer electronic structures. In: *2nd International IEEE Conference on Polymers and Adhesives in Microelectronics and Photonics*, pp.172-176.

Hwang, Y. S., Son Y. and Lee Y. 2007. Printed Circuit Patterns of Conducting Polymer. *Molecular Crystals and Liquid Crystals*, **472**(1), pp.113/[503]-122/[512].

Inoue, M., Tada Y., Muta H., Hayashi Y. and Tokumaru T. 2012. Development of highly conductive inks for smart textiles. In: *14th International Conference on Electronic Materials and Packaging (EMAP)*, 13-16 Dec. 2012, pp.1-4.

Jackie, E. and Denise M. 1991. *Superconducting screen printing ink and process for producing a thick superconducting film using this ink*. Patent number: US5221662.

Jager, K. M., Mcqueen D. H., Tchmutin I. A., Ryvkina N. G. and Kluppel M. 2001. Electron transport and ac electrical properties of carbon black polymer composites. *Journal of Physics D-Applied Physics*, **34**(17), pp.2699-2707.

Jakubauskas, H. L. 1986. Use of A-B block polymers as dispersants for non-aqueous coating systems. *Journal of coatings technology*, **58**(736), pp.71-82.

Jang, B. Z. and Zhamu A. 2008. *Nano graphene platelet-based conductive inks*. Patent number: US 20100000441 A1.

Jansen, J. W., De Kruif C. G. and Vrij A. 1986. Attractions in sterically stabilized silica dispersions: IV. Sedimentation. *Journal of Colloid and Interface Science*, **114**(2), pp.501-504.

Jerome, R. 1992. Dispersion technology based on block and graft copolymers. *Farbe + Lack*, **98**(5), pp.325-329.

Jonas, F. and Guntermann U. 1998. *Screen printing paste for producing electrically conductive coatings*. Patent number: US 6358437.

Karaguzel, B. et al. 2009. Flexible, durable printed electrical circuits. *Journal of the Textile Institute*, **100**(1), pp.1 - 9.

Kawase, T., Sirringhaus H., Friend R. H. and Shimoda T. 2001. Inkjet Printed Via-Hole Interconnections and Resistors for All-Polymer Transistor Circuits. *Advanced Materials*, **13**(21), pp.1601-1605.

Kazani, I. et al. 2012. Electrical Conductive Textiles Obtained by Screen Printing. *Fibres & Textiles in Eastern Europe*, **20**(1), pp.57-63.

Kim, D., Jeong S., Lee S. H., Moon J. and Song J. K. 2009. Ink-jet printing of organic semiconductor for fabricating organic thin-film transistors: Film uniformity control by ink composition. *Synthetic Metals*, **159**(13), pp.1381-1385.

Kipphan, H. 2001. Fundamentals. In: H. Kipphan, ed. *Handbook of Print Media*. Heidelberg: Springer, pp.40 - 165.

Kirstein, T., Bonan J., Cottet D. and Troster G. 2002. Textiles for wearable computing systems. In: *Hightex 2002*, 23 April, Saint-Hyacinthe, Canada.

Kissa, E. 1999a. Electrochemical methods. *Dispersions characterization, testing and measurement*. New York: Marcel Dekker, Inc, p.550.

Kissa, E. 1999b. Preparation and Testing of Dispersions. *Dispersions characterization, testing and measurement*. New York: Marcel Dekker, Inc, pp.237 - 281.

Kissa, E. 1999c. Radiation scattering. *Dispersions characterization, testing and measurement*. New York: Marcel Dekker, Inc, pp.433 - 501.

Kissa, E. 1999d. Sedimentation. *Dispersions Characterization, Testing and Measurement*. Marcel Dekker Inc, p.345.

Kissa, E. 1999e. Stabilization with Dispersants and Dispersibility. *Dispersions: Characterization, Testing, and Measurements*. New York: Marcel Dekker, Inc, p.183.

Kosloff, A. 1981. Screen Printing Electronic Circuits. *Screen Printing Techniques*. 3 ed. Cincinnati: The Signs of the Times Publishing Co.

Krucińska, I., Skrzetuska E. and Urbaniak-Domagała W. 2011. The use of carbon nanotubes in textile printing. *Journal of Applied Polymer Science*, **121**(1), pp.483-490.

Kunjappu, J. 2003. Ink Chemistry. *Chemistry World*, (3).

Laden, P. J. and Fingerman S. 1997. Design and Formulation of Water-based Inks. In: P. Laden, ed. *Chemistry and Technology of Water-based Inks*. Blackie Academic & Professional, pp.224-226.

Lahaye, J. and Ehrburger-Dolle F. 1994. Mechanisms of carbon black formation. Correlation with the morphology of aggregates. *Carbon*, **32**(7), pp.1319-1324.

Laible, R. and Hamann K. 1980. Formation of chemically bound polymer layers on oxide surfaces and their role in colloidal stability. *Advances in Colloid and Interface Science*, **13**(1-2), pp.65-99.

Lange, H. 1995. Comparative Test of Methods to Determine Particle Size and Particle Size Distribution in the Submicron Range. *Particle & Particle Systems Characterization*, **12**(3), pp.148-157.

Leach, R. H. and Pierce R. J. 1993. The nature of printing ink. In: R. H. Leach, R. J. Pierce, E. P. Hickman, M. J. Mackenzie and H. G. Smith, eds. *The Printing Ink Manual*. 5th ed. Springer, pp.3-13.

Lebby, M. S. and Jachimowicz K. E. 1999. *Textile fabric with integrated electrically conductive fibers and clothing fabricated thereof*. Patent number: US5906004.

Lee, D. H., Choi J. S., Chae H., Chung C. H. and Cho S. M. 2009. Screen-printed white OLED based on polystyrene as a host polymer. *Current Applied Physics*, **9**(1), pp.161-164.

Li-Rong, B., Bin W. and Xiao A. Y. 2007. Conductive Coating Formulations with Low Silver Content. In: *Proceedings of the 57th Electronic Components and Technology Conference.*, May 29 2007-June 1 2007, pp.494-500.

Li, D., Sutton D., Burgess A., Graham D. and Calvert P. D. 2009. Conductive copper and nickel lines via reactive inkjet printing. *Journal of Materials Chemistry*, **19**(22), pp.3719-3724.

Liang, J. and Yang Q. Q. 2007. Aggregate structure and percolation behavior in polymer/carbon black conductive composites. *Journal of Applied Physics*, **102**(8).

Lin, L. 2003. Mechanisms of Pigment Dispersion. *Pigment & Resin Technology*, **32**(2), pp.78-88.

Locher, I. and Troster G. 2008. Enabling Technologies for Electrical Circuits on a Woven Monofilament Hybrid Fabric. *Textile Research Journal*, **78**(7), pp.583 - 594.

Locher, I. and Tröster G. 2007. Screen-printed Textile Transmission Lines. *Textile Research Journal*, **77**(11), pp.837-842.

Long Term Stability Testing of Printing Inks by Differential Scanning Calorimetry. [online]. [Accessed 05-08-2012]. Available from: http://www.tainstruments.com/main.aspx?n=2&id=181&main_id=461&siteid=11.

Lubrizol. 2011. *Hyperdispersants: Technology and Benefits* [online]. [Accessed 01-02-2012]. Available from: <http://www.lubrizol.com/Coatings/Literature/Hyperdispersants.html>.

Malvern. 2008. Man 0317. *Zetasizer Nano User Manual*.

- Mann, S. 2013. Wearable computing. In: S. Mads and D. Rikke Friis, eds. *The Encyclopedia of Human-Computer Interaction*. 2nd ed. Aarhus, Denmark: The Interaction Design Foundation.
- Marculescu, D. 2003. E-textiles: Toward computational clothing. *Pervasive Computing, IEEE*, **2**(1), pp.89-95.
- Marculescu, D. et al. 2003. Electronic textiles: A platform for pervasive computing. *Proceedings of the IEEE*, **91**(12), pp.1995-2018.
- Marmur, A. 1979. A kinetic theory approach to primary and secondary minimum coagulations and their combination. *Journal of Colloid and Interface Science*, **72**(1), pp.41-48.
- Martin, T., Jones M., Edmison J. and Shenoy R. 2003. Towards a design framework for wearable electronic textiles. In: *Wearable Computers, 2003. Proceedings. Seventh IEEE International Symposium on*, 18-21 Oct. 2005, pp.190-199.
- Mattana, G. et al. 2011. Organic electronics on natural cotton fibres. *Organic Electronics*, **12**(12), pp.2033-2039.
- McGown, D. N. L. and Parfitt G. D. 1966. Stability of non-aqueous dispersions. Part 4.-Rate of coagulation of rutile in aerosol OT + p-xylene solutions. *Discussions of the Faraday Society*, **42**, pp.225-231.
- Medalia, A. I., Rivin D. and Sanders D. R. 1983. A comparison of carbon black with soot. *Science of The Total Environment*, **31**(1), pp.1-22.
- Membrane Switch and Panel Inc. *Membrane switch technical information* [online]. [Accessed 05-06-2010]. Available from: http://www.membraneusa.com/technical_info.html.
- Merilampi, S., Laine-Ma T. and Ruuskanen P. 2009. The characterization of electrically conductive silver ink patterns on flexible substrates. *Microelectronics Reliability*, **49**(7), pp.782-790.
- Mewis, J. and Haene P. D. 1993. Prediction of rheological properties in polymer colloids. *Makromolekulare Chemie. Macromolecular Symposia*, **68**(1), pp.213-225.
- Michels, J. J., De Winter S. and Symonds L. H. G. 2009. Process optimization of gravure printed light-emitting polymer layers by a neural network approach. *Organic Electronics*, **10**(8), pp.1495-1504.
- Mills, G. D. 1995. Particle size measurements. In: J. V. Koleske, ed. *Paint and Coating Testing Manual*. 14 ed. Philadelphia: ASTM International.

Mustonen, T. 2009. *Inkjet printing of carbon nanotubes for electronic applications*. PhD thesis, University of Oulu.

Napper, D. H. 1970. Flocculation studies of sterically stabilized dispersions. *Journal of Colloid and Interface Science*, **32**(1), pp.106-114.

Nilsson, D., Kugler T., Svensson P.-O. and Berggren M. 2002. An all-organic sensor-transistor based on a novel electrochemical transducer concept printed electrochemical sensors on paper. *Sensors and Actuators B: Chemical*, **86**(2-3), pp.193-197.

Okazaki, M. and Tsubokawa N. 2000. Introduction of Cationic groups onto carbon black surface and their dispersibility in water. *Journal of Dispersion Science and Technology*, **21**(5), pp.511-524.

Osborne, R. 1996. *Textile braids for cables, flexible tubes and the like*. Patent number: US5485774.

Pantea, D., Darmstadt H., Kaliaguine S., Sümmchen L. and Roy C. 2001. Electrical conductivity of thermal carbon blacks: Influence of surface chemistry. *Carbon*, **39**(8), pp.1147-1158.

Papirer, E., Lacroix R. and Donnet J. B. 1996. Chemical modifications and surface properties of carbon blacks. *Carbon*, **34**(12), pp.1521-1529.

Paradiso, R. and Rossi D. D. 2006. Advances in textile technologies for unobtrusive monitoring of vital parameters and movements. *In: Engineering in Medicine and Biology Society, 2006. EMBS '06. 28th Annual International Conference of the IEEE, 30/08 - 03/09/2006*, pp.392-395.

Parashkov, R., Becker E., Riedl T., Johannes H. H. and Kowalsky W. 2005. Large Area Electronics Using Printing Methods. *Proceedings of the IEEE*, **93**(7), pp.1321-1329.

Park, S. M., Cho K. S. and Chung K. H. 2007. *Flexible printed conductive fabric and method of fabricating the same*. Patent number: WO 2008/060101.

Post, E. R., Orth M., Russo P. R. and Gershenfeld N. 2000. E-broidery: Design and fabrication of textile-based computing. *IBM Systems Journal*, **39**(3.4), pp.840-860.

Post, R. E. and Gershenfeld N. 2002. *Method of making flexible electronic circuitry*. Patent number: US 6493933.

Post, R. E., Orth M., Cooper E. and Smith J. R. 2001. *Electrically active textiles and articles made therefrom*. Patent number: US 6210771.

Rouse, J. H. and Klein D. 2011. *High conductive water-based silver ink*. Patent number: US20110155812.

- Russel, W. B., Saville D. A. and Schowalter W. R. 1989. Polymeric Stabilization. *Colloidal Dispersions*. Cambridge: Cambridge University Press, pp.310 - 312.
- Sambucetti, C. 1980. Magnetic ink for jet printing. *IEEE Transactions on Magnetics*, **16**(2), pp.364-367.
- Sang-Geun, C., Kwang-Won J., Jinbae K., Ki Hyeon K. and Jongryoul K. 2011. Synthesis and Ferromagnetic Properties of Magnetic Ink for Direct Printing. *IEEE Transactions on Magnetics*, **47**(10), pp.3157-3159.
- Savage, J. 1976. Screen Printing Materials and Procedures. In: P. J. Holmes and R. G. Loasby, eds. *Handbook of Thick Film Technology*. Ayr: Electrochemical Publications Ltd.
- Savitha, K. U. and Prabu H. G. 2013. Polyaniline-TiO₂ hybrid-coated cotton fabric for durable electrical conductivity. *Journal of Applied Polymer Science*, **127**(4), pp.3147-3151.
- Schak, J. A. 1997. Dispersion of low viscosity water-based inks. In: P. Laden, ed. *Chemistry and Technology of Water-Based Inks*. Blackie Academic and Professional, p.273.
- Schnablegger, H. and Glatter O. 1993. Simultaneous Determination of Size Distribution and Refractive Index of Colloidal Particles from Static Light-Scattering Experiments. *Journal of Colloid and Interface Science*, **158**(1), pp.228-242.
- Schofield, J. 1987. Polymeric dispersants. In: L. J. Calbo, ed. *Handbook of Coatings Additives*. New York: Marcel Dekker, p.105.
- Schumacher, W. 1997. Carbon Black. In: P. Laden, ed. *Chemistry and Technology of Water-based Inks*. Blackie Academic and Professional, pp.153-174.
- Shapiro, F. and Sagraves D. 1997. Introduction. In: P. Laden, ed. *Chemistry and Technology of Water-Based Inks*. Blackie Academic and Professional, pp.1-11.
- Shi, J. I. M. Science. 2002. *Steric stabilisation*. Ohio, USA: The Ohio State University.
- Shirakawa, H. 2001. The Discovery of Polyacetylene Film: The Dawning of an Era of Conducting Polymers (Nobel Lecture). *Angewandte Chemie International Edition*, **40**(14), pp.2574-2580.
- Sirringhaus, H. et al. 2000. High-Resolution Inkjet Printing of All-Polymer Transistor Circuits. *Science*, **290**(5499), pp.2123-2126.
- Slattery, J. C. 1961. Analysis of the cone-plate viscometer. *Journal of Colloid Science*, **16**(4), pp.431-437.

Stability of pigment inkjet inks. 2009. [online]. [Accessed 12-06-2012]. Available from: <http://www.formulaction.com/publication-stability.html>.

Stylios, G. K. 2004. An introduction to smart textiles. *International Journal of Clothing Science and Technology*, **16**(5).

Stylios, G. K. 2006. A survey on SMART fabrics and interactive textiles. *International Journal of Clothing Science and Technology*, **18**(3).

Subramanian, V. and Sung D. 2008. *Gravure as an Industrially Viable Process for Printed Electronics*. thesis, EECS Department, University of California, Berkeley.

Sung, D., De La Fuente Vornbrock A. and Subramanian V. 2010. Scaling and Optimization of Gravure-Printed Silver Nanoparticle Lines for Printed Electronics. *IEEE Transactions on Components and Packaging Technologies*, **33**(1), pp.105-114.

Svedberg, T. and Rinde H. 1924. The Ultra-centrifuge, a new instrument for the determination of size and distribution of size of particle in amicroscopic colloids. *Journal of the American Chemical Society*, **46**(12), pp.2677-2693.

Tanaka, K., Murashima M. and Yamabe T. 1988. Importance of the frontier orbital patterns in the molecular design of polymers with metallic properties. *Synthetic Metals*, **24**(4), pp.371-377.

Tao, X. ed. 2005. *Wearable electronics and photonics*. Cambridge: Woodhead Publishing.

Tay, B. Y. and Edirisinghe M. J. 2002. Dispersion and stability of silver inks. *Journal of Materials Science*, **37**(21), pp.4653-4661.

Todd, R. E. 1994a. Before Formulations. *Printing Inks Formulation Principles, Manufacture and Quality Control Testing Procedures*. Pira International, pp.13-70.

Todd, R. E. 1994b. Drying Mechanisms and ink formulations. *Printing Inks Formulation Principles, Manufacture and Quality Control Testing Procedures*. Pira International, pp.117-154.

Todd, R. E. 1994c. Formulations Principles and Raw Materials. *Printing Inks Formulation Principles, Manufacture and Quality Control Testing Procedures*. Pira International, pp.71-116.

Todd, R. E. 1994d. The Manufacturing Process. *Printing Inks Formulation Principles, Manufacture and Quality Control Testing Procedures*. Pira International, pp.165-193.

Todd, R. E. 1994e. The road to modern printing inks. *Printing Inks Formulation Principles, Manufacture and Quality Control Testing Procedures*. Pira International, pp.1-12.

Tracton, A. A. 2006. Coating Calculations. In: A. A. Tracton, ed. *Coatings Technology Handbook*. 3rd ed. CRC Press, pp.75-79.

Troster, G., Kirstein T. and Lukowicz P. 2003. Wearable computing: Packaging in textiles and clothes. In: *14th European Microelectronics and Packaging Conference & Exhibition, 23-25 June 2003, Friedrichshafen, Germany*. Wearble Computing Lab, ETH Zurich.

Tymecki, L., Glab S. and Koncki R. 2006. Miniaturized, Planar Ion-selective Electrodes Fabricated by Means of Thick-film Technology. *Sensors*, **6**(4), pp.390-396.

Van, L. L. and Hertleer C. 2004. Smart clothing: a new life. *International Journal of Clothing Science and Technology*, **16**(1/2), pp.63-72.

Vanheusden, K. et al. 2006. *Printable electrical conductors*. Patent number: WO2006/076603.

Vornbrock, A. D., Ding J. M., Sung D., Tseng H. Y. and Subramanian V. 2009. Printing and scaling of metallic traces and capacitors using a laboratory-scale rotogravure press. In: *Flexible Electronics & Displays Conference and Exhibition, 2-5 Feb., New York*. IEEE, pp.54-60.

Warnon, J. 2004. Present and future coatings legislation and the drive to compliance. In: A. Marrion, ed. *The Chemistry and Physics of Coatings*. The Royal Society of Chemistry, pp.8-25.

Weber, W. et al. 2003. Electronics in Textiles: The next stage in man machine interaction. In: *2nd CREST Workshop on Advanced Computing and Communicating Techniques for Wearable Information Playing, May 23-24, 2003, Nara Institute of Science Technology, Nara, Japan*.

Yoshioka, Y. and Jabbour G. E. 2006. Desktop inkjet printer as a tool to print conducting polymers. *Synthetic Metals*, **156**(11-13), pp.779-783.

Zhang, W., Dehghani-Sanij A. and Blackburn R. 2007. Carbon based conductive polymer composites. *Journal of Materials Science*, **42**(10), pp.3408-3418.

Zhao, Y.-P., Cai Z.-S. and Fu X.-L. 2011. Effect of polymeric additives on the formation and properties of polyaniline films on polyester fabrics. *Journal of the Textile Institute*, **103**(7), pp.724-732.

Zhiqing, X., Luhai L., Xiaojun T., Wen Z. and Peng D. 2010. The research of manufacture of flexible conductive tracks at room temperature. In: *3rd International Nanoelectronics Conference (INEC) 2010, 3-8 Jan. 2010*, pp.1276-1277.

Zysset, C., Kinkeldei T. W., Munzenrieder N., Cherenack K. and Troster G. 2012. Integration Method for Electronics in Woven Textiles. *IEEE Transactions on Components, Packaging and Manufacturing Technology*, **2**(7), pp.1107-1117.